

BIOFILM FORMATION BY *MORAXELLA CATARRHALIS*

APPROVED BY SUPERVISORY COMMITTEE

Eric J. Hansen, Ph.D. _____

Kevin S. McIver, Ph.D. _____

Michael V. Norgard, Ph.D. _____

Philip J. Thomas, Ph.D. _____

Nicolai S.C. van Oers, Ph.D. _____

BIOFILM FORMATION BY *MORAXELLA CATARRHALIS*

by

MELANIE MICHELLE PEARSON

DISSERTATION

Presented to the Faculty of the Graduate School of Biomedical Sciences

The University of Texas Southwestern Medical Center at Dallas

In Partial Fulfillment of the Requirements

For the Degree of

DOCTOR OF PHILOSOPHY

The University of Texas Southwestern Medical Center at Dallas

Dallas, Texas

March, 2004

Copyright

by

Melanie Michelle Pearson 2004

All Rights Reserved

Acknowledgements

As with any grand endeavor, there was a large supporting cast who guided me through the completion of my Ph.D. First and foremost, I would like to thank my mentor, Dr. Eric Hansen, for granting me the independence to pursue my ideas while helping me shape my work into a coherent story. I have seen that the time involved in supervising a graduate student is tremendous, and I am grateful for his advice and support. The members of my graduate committee (Drs. Michael Norgard, Kevin McIver, Phil Thomas, and Nicolai van Oers) have likewise given me a considerable investment of time and intellect. Many of the faculty, postdocs, students and staff of the Microbiology department have added to my education and made my experience here positive.

Many members of the Hansen laboratory contributed to my work. Dr. Eric Lafontaine gave me my first introduction to *M. catarrhalis*. I hope I have learned from his example of patience, good nature, and hard work. Dr. Christine Ward contributed many ideas and much encouragement to the early years of my project. Nikki Wagner and Sarah Guinn both conducted experiments that directly supported my work. Jo Latimer both delivered technical support and gave me a sense of what is truly involved in running a laboratory. The members of the “*M. cat* group”, including Dr. Wei Wang, Dr. Virginia Aragon, Dr. Tom Rosche, and Ahmed Attia, have all been invaluable sources of ideas and understanding. I thank all of the members of the Hansen lab for their friendship and hope that our paths will continue to cross.

My parents, Roy Pearson and Marcia Ellis, and Mary Pearson, instilled in me a love of learning, and have given unwavering support to me. Dan Naruta has seen the best and the worst of graduate school as I experienced it, yet was always there for me (including gently calming me while repairing my computer mishaps). And finally, the many musician friends I have met have made me feel that Dallas was home and not merely a stopover of a few years.

BIOFILM FORMATION BY *MORAXELLA CATARRHALIS*

Publication No. _____

Melanie Michelle Pearson, Ph.D.

The University of Texas Southwestern Medical Center at Dallas, 2004

Supervising Professor: Eric J. Hansen, Ph.D.

This is the first detailed study of biofilm formation *in vitro* by the Gram-negative bacterial pathogen *Moraxella catarrhalis*. Growth of *M. catarrhalis* in a continuous-culture biofilm system resulted in little detectable change in outer membrane protein production compared to broth-grown *M. catarrhalis*. Biofilm-grown *M. catarrhalis* may produce an extracellular polysaccharide and different colony phenotypes when grown in this continuous culture biofilm system. Transmission electron microscopy of biofilm-grown *M. catarrhalis* cells revealed abundant projections extending from the bacterial cell surface that were identified as the proteins UspA1, UspA2, and Hag, which are all putative members of the autotransporter protein family. The Hag protein of strain O35E was shown to be necessary for hemagglutination, autoagglutination, and binding of

human IgD. A crystal violet-based assay utilizing 24-well tissue culture plates was also used to evaluate biofilm formation by *M. catarrhalis*. The ability of *M. catarrhalis* strains to form biofilms in this crystal violet-based assay varied considerably, but most strains form little or no biofilm in this system. Screening of *M. catarrhalis* transposon insertion mutants using the crystal violet-based assay revealed that the UspA1 or the related UspA2H proteins play a strain-dependent, positive role in biofilm formation. Expression of the Hag protein prevented biofilm formation in tissue culture plates by several *M. catarrhalis* strains. In contrast, there appears to be a positive selection for Hag expression by strain O46E in the continuous-culture biofilm system. Proteins involved in cell wall recycling may also be involved in biofilm formation by *M. catarrhalis*. Nucleotide sequence analysis, site-directed mutagenesis, and domain swapping experiments indicated that the N-terminal region of UspA1 or UspA2H is likely involved in biofilm formation by *M. catarrhalis*.

TABLE OF CONTENTS

	Page
Acknowledgements	iv
Abstract	v
Previous Publications	xvii
List of Figures	xviii
List of Tables	xxiii
List of Abbreviations	xxiv
 CHAPTER 1. INTRODUCTION	 1
 CHAPTER 2. LITERATURE REVIEW	 3
I. Historical Perspective of <i>M. catarrhalis</i>	3
II. Classification of <i>M. catarrhalis</i>	4
III. Identification of <i>M. catarrhalis</i>	5
IV. Growth and Metabolism of <i>M. catarrhalis</i>	6
V. Genetic Transfer in <i>M. catarrhalis</i>	7
VI. <i>M. catarrhalis</i> Carriage	8
VII. <i>M. catarrhalis</i> Disease	9
A. Otitis media	9
B. Sinusitis	10
C. Exacerbations of chronic obstructive pulmonary disease	10

D. Pneumonia	11
E. Rare infections	11
VIII. Potential Virulence Factors	12
A. UspA1	12
B. UspA2/UspA2H	14
C. Hag (MID)	16
D. OMP CD	17
E. OMP E	19
F. McaP	20
G. TbpA and TbpB	20
H. LbpA and LbpB	22
I. CopB	23
J. Fur	24
K. LOS	25
L. Pili	26
IX. Animal Models of <i>M. catarrhalis</i> Disease	27
A. Mouse	27
B. SCID mouse	29
C. Chinchilla and gerbil models of otitis media	30
D. Rat	31
E. Macaque	32
X. Overview of Biofilm Research	33
XI. Biofilms in Infectious Disease	36

XII.	Methods for Growing Biofilms	38
CHAPTER 3. MATERIALS AND METHODS		41
I.	Bacterial Strains and Plasmids	41
	A. <i>M. catarrhalis</i> strains	41
	B. <i>E. coli</i> strains and plasmids	42
II.	Sorbarod Method for Biofilm Growth	51
III.	Crystal Violet-based Assay for Measuring Biofilm Formation	54
	A. <i>M. catarrhalis</i>	54
	B. <i>E. coli</i>	55
IV.	Electron Microscopy	55
	A. Transmission electron microscopy	55
	B. Scanning electron microscopy	56
	C. Cryoimmunogold electron microscopy	57
V.	Bacterial Antigen Preparation	58
	A. Whole cell lysates	58
	B. Preparation of extracts containing outer membrane vesicles	58
	C. LOS preparation	60
VI.	Sodium Dodecyl Sulfate-Polyacrylamide Gel Electrophoresis	60
VII.	Separation and Detection of Lipooligosaccharides and Polysaccharides	61
	A. Tricine SDS-PAGE	61
	B. Silver stain	62

VIII.	MAbs and Western Blot Analysis	63
IX.	DNA Preparation	64
	A. Preparation of <i>M. catarrhalis</i> chromosomal DNA	64
	B. Plasmid Isolation	65
X.	Polysaccharide Analysis	65
	A. Isolation of soluble polysaccharides from <i>M. catarrhalis</i> biofilms	65
	B. Characterization of <i>M. catarrhalis</i> polysaccharide	67
XI.	Transformation Protocols	68
	A. Electroporation of <i>M. catarrhalis</i>	68
	B. Electroporation of <i>E. coli</i>	68
	C. Chemical transformation of <i>E. coli</i>	69
	D. Natural transformation of <i>M. catarrhalis</i>	69
XII.	Transposon Mutagenesis	70
XIII.	Recombinant DNA Techniques	71
	A. DNA sequencing and analysis	71
	B. Southern blot analysis	71
XIV.	Identification of the Site of the Transposon Insertion in Mutant 20A3	73
XV.	Tissue Culture Protocols	74
XVI.	Attachment Assays	75
	A. <i>M. catarrhalis</i>	75
	B. <i>E. coli</i>	76

XVII. Hemagglutination Assays	76
XVIII. Autoagglutination Assays	77
XIX. Construction of and Enrichment for Biofilm-Forming Transformants	77
XX. Cell Surface Expression Assay	78
XXI. PCR	79
XXII. Analysis of Different Colony Phenotypes Arising from Sorbarod-Grown Biofilms	79
XXIII. Molecular Genetic Techniques	80
A. Construction of Isogenic Mutants	80
i. Construction of <i>uspA1</i> and <i>uspA2</i> mutants	80
ii. Construction of <i>hag</i> mutants	81
iii. Construction of a <i>corC</i> mutant	82
iv. Construction of an O35E strain expressing a hybrid UspA1 protein	80
v. Construction of a mutant unable to express a putative phosphotransferase	83
vi. Construction of an <i>ampD</i> mutant	84
vii. Construction of a mutant lacking the ability to express a putative lytic murein transglycosylase D	85
B. Enrichment for allelic exchange in <i>M. catarrhalis</i> by the use of conjugation	85
C. Insertional mutagenesis of <i>uspA2H</i>	87

D. Site-directed mutagenesis of <i>uspA2H</i> and <i>uspA1</i>	88
E. Cloning and expression of <i>uspA1</i> in <i>E. coli</i>	90
CHAPTER 4. THE SORBAROD CONTINUOUS-CULTURE	91
BIOFILM SYSTEM	
I. Introduction	91
II. Results	92
A. Growth dynamics	92
B. Outer membrane protein analysis	94
C. Isolation and characterization of a possible polysaccharide from <i>M. catarrhalis</i> biofilms	97
D. Identification of colony morphology variants derived from biofilms: “Lucky 4-leaf clovers”	99
III. Discussion	103
CHAPTER 5. CHARACTERIZATION OF STRUCTURES EXTENDING	108
FROM THE <i>M. CATARRHALIS</i> CELL SURFACE	
I. Introduction	108
II. Results	109
A. TEM analysis of <i>M. catarrhalis</i> grown in Sorbarod biofilms	109
B. Characterization of the <i>M. catarrhalis</i> strain O35E <i>hag</i> gene and its encoded protein product	111
C. Construction of mutants deficient in expression of	112

surface-exposed proteins	
D. Appearance of <i>M. catarrhalis</i> biofilms as revealed by SEM	116
E. Phenotype of the <i>M. catarrhalis</i> strain O35E <i>hag</i> mutant	118
i. effect of the <i>hag</i> mutation on hemagglutination ability	118
ii. autoagglutination ability of the <i>hag</i> mutant	119
iii. effect of the <i>hag</i> mutation on attachment ability	120
iv. the Hag protein has IgD-binding activity	122
F. Conservation of a Hag antigenic determinant	124
G. Phenotypes of <i>hag</i> mutants of other <i>M. catarrhalis</i> strains	126
i. Hemagglutination	126
ii. Autoagglutination	127
iii. IgD-binding	128
III. Discussion	128
 CHAPTER 6. USE OF THE CRYSTAL VIOLET-BASED ASSAY TO CHARACTERIZE BIOFILM FORMATION BY <i>M. CATARRHALIS</i>	 135
I. Introduction	135
II. Results	136
A. Elucidation of the optimal conditions for <i>M. catarrhalis</i> biofilm formation	136
B. <i>M. catarrhalis</i> strains vary in their ability to form biofilms	137
C. Time course for O46E biofilm formation	139

D. Biofilm formation in different growth media	140
E. Transposon mutagenesis of strain O35E	141
III. Discussion	143
 CHAPTER 7. USE OF THE CRYSTAL VIOLET-BASED ASSAY TO CHARACTERIZE BIOFILM FORMATION BY <i>M. CATARRHALIS</i> TRANSFORMANT STRAINS	 146
I. Introduction	146
II. Results	147
A. Transformation of biofilm formation ability into strain O35E	147
B. Isolation of biofilm-negative transposon insertion mutants	149
C. Transformant strains T13, T14, and T84 possess a hybrid <i>uspA1</i> gene	154
D. Characterization of mutant T14/27	155
E. Expression of Hag inhibits biofilm formation	157
F. Hag expression in ETSU-9 in relation to biofilm formation	161
G. Biofilm formation by strain O35E	163
H. Biofilm formation by recombinant <i>E. coli</i> expressing <i>uspA1</i>	165
III. Discussion	168
 CHAPTER 8. HAG EXPRESSION IN BIOFILMS	 173
I. Introduction	173
II. Results	173

A. Hag expression in Sorbarod biofilms	173
B. Hag expression in tissue culture plate biofilms	174
III. Discussion	176
 CHAPTER 9. ANALYSIS OF BIOFILM FORMATION BY	178
<i>M. CATARRHALIS</i> STRAIN O46E	
I. Introduction	178
II. Results	178
A. Attempts to analyze <i>M. catarrhalis</i> strain O46E transposon	178
insertion mutants	
B. Characterization of laboratory stocks of strain O46E	180
III. Discussion	181
 CHAPTER 10. ANALYSIS OF THE ABILITY OF <i>M. CATARRHALIS</i>	184
STRAIN ETSU-9 TO FORM BIOFILMS	
I. Introduction	184
II. Results	185
A. Screening for biofilm-negative transposon insertion mutants	185
of ETSU-9	
B. Insertional mutagenesis of the ETSU-9 <i>uspA2H</i> gene	189
C. Site-directed mutagenesis of the <i>uspA2H</i> gene	197
D. Site-directed mutagenesis of the O35E <i>uspA1</i> gene	197
E. Characterization of other biofilm-negative transposon mutants	198

III. Discussion	200
CHAPTER 11. SUMMARY AND CONCLUSIONS	206
REFERENCE LIST	214
VITA	245

PREVIOUS PUBLICATIONS

- Roszbach, S., M.L. Kukuk, T.L. Wilson, S.F. Feng, **M.M. Pearson**, and M.A. Fisher. 2000. Cadmium-regulated gene fusions in *Pseudomonas fluorescens*. Environ. Microbiol. **2**:373-382.
- Pearson, M.M.**, E.R. Lafontaine, N.J. Wagner, J.W. St. Geme, III, and E.J. Hansen. 2002. A *hag* mutant of *Moraxella catarrhalis* strain O35E is deficient in hemagglutination, autoagglutination, and immunoglobulin D-binding activities. Infect. Immun. **70**:4523-4533.
- Pearson, M.M.**, S.E. Guinn, and E.J. Hansen. Biofilm formation by *Moraxella catarrhalis*: roles of the UspA1 adhesin and the Hag hemagglutinin. **In Preparation.**
- Wang, W., **M.M. Pearson**, A. Attia, and E.J. Hansen. Effect of changes in a homopolymeric nucleotide tract on expression of the *Moraxella catarrhalis* *uspA2H* gene. **In Preparation.**

LIST OF FIGURES

Figure 1	General model of biofilm formation	36
Figure 2	The Sorbarod continuous culture biofilm system	52
Figure 3	Assembly of the Sorbarod biofilm apparatus	53
Figure 4	Growth of <i>M. catarrhalis</i> in the continuous culture biofilm system	93
Figure 5	SDS-PAGE comparison of outer membrane proteins	95
Figure 6	15% polyacrylamide gel analysis of broth- and biofilm-derived OMPs	96
Figure 7	Tricine SDS-PAGE comparison of silver and Coomassie stained putative polysaccharides	97
Figure 8	Comparison of ethidium bromide and Tsai-Frasch silver staining of the putative polysaccharide.	99
Figure 9	Colony morphologies of strain ATCC 43617 grown in the Sorbarod continuous-culture biofilm system	101
Figure 10	Colony morphologies of strain O46E grown in the Sorbarod continuous-culture biofilm system	103
Figure 11	TEM of biofilm-grown wild-type <i>M. catarrhalis</i> strains	110
Figure 12	TEM of <i>M. catarrhalis</i> packed within a cellulose fiber pocket of the Sorbarod filter	110
Figure 13	Expression of Hag, UspA1, and UspA2 by wild-type and mutant strains of <i>M. catarrhalis</i> O35E	113

Figure 14	Detection of projections on the surfaces of wild-type and mutant strains of <i>M. catarrhalis</i> by TEM	114
Figure 15	Use of cryoimmunoelectron microscopy to detect UspA1, UspA2, and Hag on the <i>M. catarrhalis</i> cell surface	115
Figure 16	SEM of wild-type O35E growing in a biofilm	117
Figure 17	SEM comparison of biofilm-grown O35E and its isogenic <i>uspA1 uspA2 hag</i> triple mutant O35E.ZCS	118
Figure 18	Hemagglutination ability of wild-type and mutant strains of <i>M. catarrhalis</i> O35E	119
Figure 19	Autoagglutination ability of wild-type and mutant strains of <i>M. catarrhalis</i> O35E	121
Figure 20	Attachment of strain O35E, the <i>uspA1</i> mutant O35E.118cat, the <i>uspA2</i> mutant O35E.2ZEO, and the <i>hag</i> mutant O35E.HG to several different epithelial cell lines	123
Figure 21	Binding of human IgD by wild-type and mutant strains of <i>M. catarrhalis</i>	124
Figure 22	Reactivity of 12 <i>M. catarrhalis</i> strains with Hag-specific MAb 5D2	126
Figure 23	Biofilm formation by wild-type <i>M. catarrhalis</i> strains	139
Figure 24	Strain O46E reaches maximal biofilm formation by 19 h in a 24-well tissue culture plate	140
Figure 25	Biofilm formation by transposon mutant 20A3	141
Figure 26	Metabolism of S-adenosyl homocysteine	144

Figure 27	Biofilm formation by wild-type and transformant strains of <i>M. catarrhalis</i>	148
Figure 28	Comparison of OMPs from strains O35E, O46E, and transformant strains	150
Figure 29	Comparison of LOS from strains O35E, O46E, and transformant strains	151
Figure 30	Biofilm formation by transposon insertion mutants and isogenic mutants	152
Figure 31	Attachment of transformant strains and isogenic mutants to Chang cells	152
Figure 32	Biofilm formation by strain O46E and its isogenic <i>uspA1</i> mutant O46E.1	154
Figure 33	Comparison of the nucleotide sequence of the <i>uspA1</i> ORFs from wild-type strain O46E, transformant T14, and wild-type strain O35E	156
Figure 34	Effect of Hag expression on biofilm formation by transformant T14	158
Figure 35	Alignment of the first 600 nt of the <i>hag</i> ORFs from strains O46E, T14, and O35E	160
Figure 36	Effect of Hag expression on biofilm formation by <i>M. catarrhalis</i> strain ETSU-9	162
Figure 37	Effect of UspA1 and Hag expression on biofilm formation by <i>M. catarrhalis</i> strain O35E and related strains	164

Figure 38	Biofilm formation by recombinant <i>E. coli</i> strains expressing UspA1 proteins	166
Figure 39	Biofilm formation by <i>E. coli</i> strains expressing <i>M. catarrhalis</i> UspA1	168
Figure 40	Hag expression by Sorbarod biofilm-grown strain O46E	175
Figure 41	UspA2H expression by biofilm-negative ETSU-9 transposon mutants	187
Figure 42	Biofilm formation by ETSU-9, the isogenic <i>uspA1</i> mutant ETSU-9.1, and the isogenic <i>uspA2H</i> mutant ETSU-9.2	188
Figure 43	Hag expression by biofilm-positive and biofilm-negative backcrossed transposon mutants	188
Figure 44	Position of 5 aa insertions in the ETSU-9 UspA2H protein	190
Figure 45	Biofilm formation by <i>uspA2H</i> insertion mutants	192
Figure 46	Expression of UspA2H by <i>uspA2H</i> insertion mutants	193
Figure 47	Expression of UspA2H by ETSU-9.mut92	194
Figure 48	Attachment of ETSU-9 <i>uspA2H</i> insertion mutants to Chang conjunctival epithelial cells	195
Figure 49	Cell surface expression assay for UspA2H	196
Figure 50	Alignment of the N-termini of ETSU-9 UspA2H, T14 UspA1, and O35E UspA1	196
Figure 51	Biofilm formation by ETSU-9 containing site-directed mutations in <i>uspA2H</i>	198

Figure 52	Biofilm formation by the isogenic mutants ETSU-9.222cat, ETSU-9.714cat, and ETSU-9.988cat	199
Figure 53	Growth curve of ETSU-9 and the three isogenic mutants	200
Figure 54	Model for biofilm formation by <i>M. catarrhalis</i>	210

LIST OF TABLES

Table 1	Bacterial strains used in these studies	43
Table 2	Plasmids used in these studies	48
Table 3	Glycosyl composition analysis	100
Table 4	Assessment of biofilm formation by 88 wild-type <i>M. catarrhalis</i> strains	138
Table 5	Characteristics of laboratory stocks of strain O46E	181

LIST OF ABBREVIATIONS

aa	amino acids
A	adenine
ATCC	American Type Culture Collection
AOM	acute otitis media
BHI	brain-heart infusion
bp	base pair
CEACAM	carcinoembryonic antigen-related cell adhesion molecule
CFU	colony-forming unit
CV	crystal violet
Da	Dalton
G	guanine
IEM	immunolectron microscopy
kb	kilobase
KDO	ketodeoxyoctonate
LB	Luria-Bertani
LOS	Lipooligosaccharide
mA	milliampere
MAb	monoclonal antibody
OME	otitis media with effusion
OMP	outer membrane protein
ORF	open reading frame

PAGE	polyacrylamide gel electrophoresis
PCR	polymerase chain reaction
PBS	phosphate-buffered saline
PBS-G	phosphate-buffered saline with 0.15% gelatin
RFLP	restriction fragment length polymorphism
SDS	sodium dodecyl sulfate
SEM	scanning electron microscopy
TEM	transmission electron microscopy
TH	Todd-Hewitt
UTR	untranslated region
V	volt

CHAPTER ONE

Introduction

Moraxella catarrhalis is now recognized as a common respiratory tract pathogen. This Gram-negative diplococcus is the third most common cause of otitis media in infants and young children, accounting for 15-20% of cases (160). It is also a frequent cause of sinusitis, occasionally causes pneumonia, and can exacerbate chronic obstructive pulmonary disease. In addition, *M. catarrhalis* rarely causes pericarditis, endocarditis, or meningitis. *M. catarrhalis* is also often found as a nasopharyngeal commensal, especially in young children (313).

Relatively little is known about the mechanisms *M. catarrhalis* employs to cause disease. Most studies to date have focused on the functions of cell surface-expressed molecules, including UspA1, UspA2/UspA2H, Hag, OMP CD, and LOS (204). Iron uptake by this pathogen has also been investigated; proteins involved in this process include TbpA/TbpB, LbpA/LbpB, and CopB (204). Direct determination of the roles each of these molecules play *in vivo* remains difficult, due to the lack of a relevant animal model that mimics human infection.

A biofilm is a community of microorganisms growing attached to a surface. Expression of genes by bacteria growing as a biofilm may be considerably different from gene expression by the same organisms growing in the planktonic state (i.e., in broth). Examples of differential gene expression include production of exopolysaccharides (68, 145) and novel outer membrane protein production (246, 266). Studies indicate that the majority of bacteria in their ecological niche are growing as biofilms (76), whether that

niche involves a rock in a stream or the gastrointestinal mucosa of our bodies. Biofilms are very difficult to remove and thus, they are a matter of great concern in medicine. An indwelling medical device that becomes colonized with a biofilm often has to be removed (76). More important to this dissertation is the increasing evidence that at least some diseases of the respiratory tract are biofilm-mediated, most notably *Pseudomonas aeruginosa* infections in cystic fibrosis patients (279).

This study comprises the first genetic analysis of biofilm formation by *M. catarrhalis*. The first few chapters detail the use of a continuous-culture biofilm system to study *M. catarrhalis* biofilms. These studies include the characterization of three proteins (UspA1, UspA2, and Hag) found to form projections extending from the bacterial cell surface; other experiments investigate growth dynamics, outer membrane protein expression, and polysaccharide production.

Later chapters describe the use of a crystal violet-based assay to examine biofilm formation. These studies revealed the roles of the UspA1, UspA2H, and Hag proteins in *M. catarrhalis* biofilm formation. Site-directed mutagenesis experiments were undertaken to identify the domain(s) of UspA2H and UspA1 that are involved in biofilm formation. Finally, the differential expression of the Hag protein in the continuous-culture and crystal violet methods for biofilm investigation were analyzed.

CHAPTER TWO

Review of the Literature

I. Historical Perspective of *M. catarrhalis*

M. catarrhalis was first isolated by Seifert in 1882 (referenced in (80)) from the sputum of bronchitis patients. Another early German report by Pfeiffer (referenced in (20)) gave the organism its first name, *Micrococcus catarrhalis* (catarrh: [Latin *catarrhus*, to flow down] inflammation of a mucous membrane, with a free discharge (1)). Ghon and Pfeiffer (referenced in (20)) proceeded to describe *M. catarrhalis* phenotypes such as pellicle formation in broth and the lack of pathogenicity in animal studies. *M. catarrhalis* was first isolated in England from nasopharyngeal secretions of patients. The authors detailed the first biochemical analyses of *M. catarrhalis* as a means of differential identification; they found that *M. catarrhalis* does not ferment the sugars glucose, galactose, maltose, or saccharose (80). This observation is still in use today for the definitive identification of *M. catarrhalis*. Unfortunately, in 1919, a study stated that *M. catarrhalis* is a cause of chronic colds (194). Responding to this assertion, Gordon (113) found that *M. catarrhalis* could also be isolated from the nasopharynx of healthy patients, and therefore he wrote that “the logical deduction is that its usual sphere is that of a harmless saprophyte”. Despite a subsequent paper in 1927 discussing the isolation of *M. catarrhalis* from patients with acute otitis media (125), reports describing *M. catarrhalis* as a pathogen were scarce for the next fifty years.

II. Classification of *M. catarrhalis*

Currently, *M. catarrhalis* is classified as subgenus *Branhamella*, genus *Moraxella*, family *Moraxellaceae*, order *Pseudomonadales*, within the γ -Proteobacteria (156). Until 1970, *M. catarrhalis* was designated *Neisseria catarrhalis* based on superficial similarities to other members of the *Neisseria* genus. However, several researchers (32, 33, 45, 48, 49) found that *M. catarrhalis* could be naturally transformed with DNA from several species of the genus *Moraxella* but not with DNA from *Neisseria* species. In addition, analysis of the GC content of its chromosomal DNA (33, 48) and cellular fatty acid analysis (176, 180) indicated that *M. catarrhalis* was not sufficiently related to *Neisseria* to warrant inclusion in that genus. Thus, Bøvre (137) suggested that *M. catarrhalis* should be reclassified as *Moraxella*. Other researchers agreed that the genus *Moraxella* should be included in the family *Neisseriaceae* but balked at the idea of placing *M. catarrhalis* cocci in the same genus with the rod-shaped *Moraxella* species (named for the Swiss ophthalmologist V. Morax, who described the original type strain; it should be noted that H. Axenfeld independently discovered the same species, which was known for a time as the “Morax-Axenfeld bacillus” (described in (156))). Therefore, Catlin (46) proposed that a new genus should be created for *M. catarrhalis*. Catlin named this new genus *Branhamella* after the late Sara Branham, a noted microbiologist in the *Neisseria* field. *Branhamella catarrhalis* was in usage until 1979, when *Branhamella* was reclassified as a subgenus of *Moraxella* (34). *Moraxella (Branhamella) catarrhalis* was so-named for a period of time until increasingly sophisticated molecular analyses indicated that there was not enough distinction between *M. catarrhalis*

and other *Moraxella* species to warrant a separate subgenus; thus, the organism is now simply named *Moraxella catarrhalis*. Ribosomal RNA sequence comparisons have now shown that *Moraxella* species are more closely related to the pseudomonads than they are to the *Neisseria*; therefore, *Moraxella* species were placed in a new family, *Moraxellaceae*, and reclassified as γ -Proteobacteria in the order *Pseudomonadales* (88, 238).

III. Identification of *M. catarrhalis*

M. catarrhalis is a Gram-negative diplococcus, similar in appearance in the Gram stain to *Neisseria* species. *M. catarrhalis* is nonhemolytic on blood agar; colonies are grayish-white, opaque, convex, and circular. This organism is distinguished by its inability to ferment carbohydrates, while it is positive for the reduction of both nitrate and nitrite. One of the hallmarks of *M. catarrhalis* is its production of DNase, which may be detected by growth on DNase test agar (incorporating methyl green). *M. catarrhalis* possesses esterase activity, which is usually evidenced by tributyrin hydrolysis; it is also catalase positive. An unusual characteristic of *M. catarrhalis* is the “hockey puck” phenotype of its colonies; that is, a colony of *M. catarrhalis* will easily slide across an agar surface and remain intact when nudged with a bacteriological loop (276). Catlin wrote that the combination of Gram stain and colony morphology with positive results for nitrate reduction, DNase, and tributyrin hydrolysis is definitive for *M. catarrhalis* (47).

Several methods of DNA typing have been employed in attempts to classify genetic lineages of *M. catarrhalis*. Some of the methods used include restriction fragment length

polymorphism (RFLP) with or without pulsed-field gel electrophoresis (PFGE) (30, 71, 127, 165, 317, 321), DNA-DNA hybridization dot blot (58) or Southern blot (321), and randomly amplified polymorphic DNA (RAPD) (317). One overall conclusion from these studies is that *M. catarrhalis* strains are genetically diverse and appear to acquire genes via horizontal transfer. However, some of the larger studies suggest that *M. catarrhalis* strains may be separated into two genetic lineages (30, 127, 321), which may be associated with complement resistance (30, 127) or the ability to attach to epithelial cells (30). More detailed molecular analyses need to be conducted to confirm these global observations, as both epithelial cell attachment and complement resistance are associated with genes that are known to be almost universally present in *M. catarrhalis* strains (207). DNA typing is probably most useful for distinguishing *M. catarrhalis* strains in a clinical setting.

Phenotypic traits have also been examined for their relationship to genetic typing of *M. catarrhalis*, with little success. A comparison of the outer membrane proteins from different *M. catarrhalis* strains revealed strong homogeneity in this species (18). Diversity of LOS has also been investigated; most strains of *M. catarrhalis* fell into three different LOS serotypes, although the LOS serotype could not distinguish clinical or geographic origin (311).

IV. Growth and Metabolism of *M. catarrhalis*

Generally, *M. catarrhalis* is cultured on rich, nutritionally complex media at 37°C under an atmosphere of 95% air-5% carbon dioxide, although *M. catarrhalis* is also able to

grow at room temperature. The medium used varies by laboratory; brain-heart infusion, blood, chocolate, Todd-Hewitt, Mueller-Hinton, and tryptic soy have all been published as growth media for *M. catarrhalis*. Juni and colleagues (157) formulated a chemically defined medium, named medium B4, for *M. catarrhalis*. The results of their study suggested that *M. catarrhalis* lacks the pathways for synthesis of α -amino acids, because *M. catarrhalis* has an absolute requirement for either glutamate, aspartate, or proline; this organism cannot utilize ammonium chloride as a nitrogen source. Most *M. catarrhalis* strains also require arginine, and need high levels of glycine (1 mg/ml) for optimal growth. Sodium lactate serves as a partial carbon source in medium B4.

V. Genetic Transfer in *M. catarrhalis*

It has long been known that most strains of *M. catarrhalis* are naturally competent for transformation (33). This ability has been used to determine genetic relatedness of *Moraxella* species; interspecies transformation efficiency was a major factor in the decision to move *M. catarrhalis* from the genus *Neisseria* to the genus *Moraxella* (137). Natural transformation remains a useful technique in the laboratory; details for this protocol are given in the “Materials and Methods” section of this dissertation. Electroporation has also been employed in *M. catarrhalis* research. First published by Helminen *et al* (131), this method will also be described later.

Because *M. catarrhalis* isolates apparently went from being predominantly penicillin-sensitive to predominantly penicillin-resistant within just a few years, Kamme *et al* (158)

suggested that *M. catarrhalis* β -lactamase production must be plasmid-mediated. The first evidence for this was the apparent presence of extrachromosomal DNA elements that seemed to be transferable between *M. catarrhalis* and *M. nonliquefaciens* (159). The authors were unable to characterize the extrachromosomal DNA, however, possibly due to the exonucleases produced by *M. catarrhalis*. Beaulieu *et al* (19) were the first (and only) group to describe the isolation of a plasmid from two clinical strains of *M. catarrhalis*. This plasmid, pLQ510, was later subjected to nucleotide sequence analysis and found to contain five putative ORFs, none of which appears to encode a β -lactamase (183). Derivatives of this plasmid are being evaluated for possible use as *M. catarrhalis* cloning vectors.

VI. *M. catarrhalis* Carriage

Studies of young children have shown that colonization rates with *M. catarrhalis* range from 39% to 58% (89, 211, 310, 312). A study of the nasopharyngeal flora of children found that 77.5% of children were colonized with *M. catarrhalis* at least once during their first two years of life (89). The carriage rate fell to 13-17% in children six to nine years of age (36, 190), and remained low throughout adulthood. Research indicates that about 1-5% of adults are carriers of *M. catarrhalis* (73, 154, 310). There is a correlation of *M. catarrhalis* carriage with winter months (73), which is also when *M. catarrhalis* disease peaks. Children with otitis media are much more likely to be colonized with *M. catarrhalis* than are healthy children (89); thus, colonization with *M. catarrhalis* is a likely prerequisite to *M. catarrhalis* disease.

VII. *M. catarrhalis* Disease

A. Otitis media

Otitis media, or infection of the middle ear, is the most common reason for health care visits by young children. This disease is most frequently found in infants and children less than 24 months old, and most (80%) children will have had at least one episode of acute otitis media (AOM) by three years of age (162). AOM is characterized by fever, irritability, or ear pain accompanied by redness or bulging of the tympanic membrane. Currently, otitis media accounts for the largest number (20 million) of antibiotic prescriptions in the U.S (236). Historically, AOM has been treated with amoxicillin or amoxicillin-clavulanate. However, approximately three-fourths of AOM cases will resolve within 48 hours without antibiotic treatment. For this reason, and due to rising concerns regarding increasing numbers of antibiotic-resistant bacteria, pediatricians are now given the option of observing certain AOM patients greater than two years of age without the administration of antibiotics. Even after antibiotic treatment and symptom resolution, fluid can persist in the middle ear. This phenomenon, called otitis media with effusion, or OME, often lasts for 30 days but may persist for up to three months (277). Persistent OME is associated with conductive hearing loss, which may result in language and cognitive delays in children. Patients who are susceptible to recurrent AOM may have tympanostomy performed, wherein a tube is inserted into the tympanic membrane to promote drainage; this procedure shortens the period of effusion. Approximately 60% of tympanocentesis cultures are positive for bacterial

pathogens (reviewed in (214)); however, PCR and RT-PCR data suggest that a far higher percentage of AOM cases have a bacterial cause (240, 254). The three most common causes of AOM are *Streptococcus pneumoniae*, *Haemophilus influenzae*, and *M. catarrhalis*. *M. catarrhalis* causes 15-25% of AOM cases, or approximately 3-4 million cases per year in the U.S. (160).

B. Sinusitis

Sinusitis is another very common childhood ailment, accounting for 5-10% of upper respiratory infections (URI) (320). Sinusitis occurs when the respiratory sinuses are not allowed to drain normally, resulting in the multiplication of bacteria within the sinus and subsequent inflammation. Usually this occurs as a complication of a viral URI. Generally, sinusitis is diagnosed when a URI persists without abatement of symptoms for more than 10 days. The same pathogens that cause AOM are also implicated in sinusitis (*S. pneumoniae*, *H. influenzae*, and *M. catarrhalis*), and sinusitis may be accompanied by otitis media. *M. catarrhalis* is responsible for about 20% of sinusitis cases, although it is possibly the major cause of both acute and chronic sinusitis in children with respiratory allergies (111).

C. Exacerbations of chronic obstructive pulmonary disease

Chronic obstructive pulmonary disease (COPD) is the presence of permanent or partially reversible obstruction of the airway in patients with chronic bronchitis or

emphysema. It is the fourth most common cause of death in the United States (2), and is usually a consequence of smoking. Acute exacerbations of COPD, often due to bacterial infection, may lead to death. It is also possible that repeated bacterial infections may cause inflammation and impairment of mucociliary clearance mechanisms, leading to the development of COPD. *M. catarrhalis* is the second most common cause of acute exacerbations of COPD, causing as many as 30% of these cases (reviewed in (274)).

D. Pneumonia

M. catarrhalis is a relatively uncommon cause of pneumonia, usually striking the elderly. Most cases of *M. catarrhalis* pneumonia occur in patients with preexisting pulmonary disease, such as COPD or end-stage malignancies (reviewed in (313)). Although bacteremia is rare, when it does occur, case-fatality rates can be as high as 30% (60, 150).

E. Rare infections

M. catarrhalis has sporadically been reported as a causative agent of endocarditis (150, 224, 291, 306), pericarditis (169), laryngitis (142, 267, 268), and keratitis (195). There is also evidence that *M. catarrhalis* may be responsible for some nosocomial infections (41, 212, 234, 258). Although it is extremely rare to find *M. catarrhalis* in these situations, the isolation of *M. catarrhalis* in pure culture from these sites underscores the pathogenic potential of this organism.

VIII. Potential Virulence Factors

A. UspA1

The Ubiquitous Surface Protein A, or UspA was originally described by two papers published in 1994. Klingman and Murphy (164) had noted that immunoblots of *M. catarrhalis* whole cell lysates probed with rabbit polyclonal antiserum raised against a high molecular weight antigen gel-purified from *M. catarrhalis* outer membrane vesicles showed a large antigen that migrated to a position near the top of the separating gels. They found that this large antigen, which they termed high-molecular-weight outer membrane protein (HMW-OMP) was indeed a protein that was present in most strains of *M. catarrhalis* that they tested. Furthermore, HMW-OMP was present in outer membrane protein preparations; the protein was detectable by both Coomassie staining and immunoblotting. Shortly after this publication, Helminen *et al* (130) wrote about the same antigen. By immunizing mice with *M. catarrhalis* outer membrane vesicles, this group produced a monoclonal antibody, 17C7, which recognized UspA. Western blot analysis and cell surface expression assays revealed that UspA was surface-expressed and also was expressed by 23 of 23 *M. catarrhalis* strains examined. In addition, convalescent sera from patients with *M. catarrhalis* pneumonia recognized UspA; acute phase sera did not. Furthermore, passive immunization of mice with MAb 17C7 enhanced pulmonary clearance of *M. catarrhalis* in a mouse model (130). Building upon these data, Chen *et al* found that MAb 17C7 had bactericidal activity

against *M. catarrhalis*, and that active immunization of mice with purified UspA also resulted in more rapid clearance of *M. catarrhalis* from mouse lungs after challenge (54).

These data indicated that UspA would be a promising component of a *M. catarrhalis* vaccine. What all these researchers did not realize at the time was that *M. catarrhalis* produces two different proteins with an identical epitope; these proteins were subsequently designated UspA1 and UspA2 (6). However, the data derived when studying both proteins simultaneously also held true when UspA1 and UspA2 were studied individually: both proteins are localized to the outer membrane and are surface-expressed (5), humans possess normal serum antibodies against these proteins (53, 201), and active immunization of mice with either of these proteins results in enhanced pulmonary clearance of *M. catarrhalis* following a challenge (205). A screen of 108 *M. catarrhalis* isolates revealed that the *uspA1* and *uspA2* genes are present in 99% or 100% of those strains, respectively (207); thus, these proteins truly deserve their “ubiquitous” title.

The UspA1 protein is an adhesin which is necessary for *M. catarrhalis* to attach to some cell lines *in vitro*, including Chang conjunctival epithelial cells and HEp-2 cells (5). Purified UspA1 has been shown to bind human plasma fibronectin (205), indicating that it could be a possible receptor for UspA1 binding *in vivo*. Hill and Virji (138) have reported that UspA1 recognizes the N-domain of carcinoembryonic antigen-related cell adhesion molecule-1 (CEACAM1); however, Chang cells may not express significant levels of CEACAMs (316). It is possible that UspA1 binds more than one receptor on eukaryotic cells. UspA1 was shown by Lafontaine *et al* (136) to undergo phase variation involving a homopolymeric polynucleotide (poly(G)) tract located in the 5' UTR of the *uspA1* gene,

probably due to a slipped-strand mispairing mechanism. The presence of 10 G residues in this poly(G) tract resulted in a relatively high level of expression, while 9 G resulted in a much lower level of expression (175). Although predicted to have a mass of approximately 88,000 Da, the UspA1 protein actually has an apparent mass on SDS-PAGE of about 120,000 Da (6). The reason for this discrepancy remains unknown; however, expression of these proteins in a *H. influenzae* background still resulted in the same protein migration patterns in SDS-PAGE (174). The N-terminus of the mature protein was determined by Cope *et al* (62) following treatment of UspA1 from strain O35E with pyroglutamate aminopeptidase to remove a pyroglutamyl residue that was blocking Edman degradation. This study revealed that UspA1 has an unusually long signal peptide of 48 aa, leaving a mature protein of 83,364 Da. Comparison of different strains of *M. catarrhalis* indicated that the UspA1 protein has about 70% identity with UspA1 from other strains (174). BLAST analysis (12) shows that UspA1 is most similar to other bacterial adhesins, including Hsf (287, 289) and Hia (17) from *H. influenzae*.

B. UspA2/UspA2H

The UspA2 protein is a factor proposed to be involved in the resistance of *M. catarrhalis* to killing by normal human serum (5, 26) (many bacteria are readily killed by the complement and antibodies that are present in normal human serum). In addition, McMichael *et al* (205) found that UspA2 binds vitronectin. Some evidence has been presented indicating that the presence of UspA2 correlates with serum resistance (26);

however, this group's conclusions were based solely on the use of a monoclonal antibody that was deliberately chosen for its ability to bind complement-resistant strains but not complement-sensitive strains. Other researchers have shown that UspA2 is expressed by virtually all isolates of *M. catarrhalis* (130, 164, 207). This raises the possibility that the UspA2 proteins from serum-sensitive strains of *M. catarrhalis* are structurally different from UspA2 from serum-resistant strains, and that these differences could be distinguished by comparison of their primary amino acid sequences. Indeed, Verduin *et al* have proposed that complement-resistant and complement-sensitive strains form separate genetic lineages based on RFLP data (314). As is the case for UspA1, the predicted mass of UspA2 and its apparent mass in SDS-PAGE do not match. Western blot analysis of *M. catarrhalis* whole cell lysates showed UspA2 migrating as a large aggregate near the top of the separating gel (6). When outer membrane vesicles were analyzed, a probable UspA2 monomer is visible with an apparent mass of 85,000 Da (6). However, the predicted mass of UspA2 is around 62,000 Da. UspA2 resembles both DsrA, a serum resistance factor in *Haemophilus ducreyi* (86), and the *Yersinia enterocolitica* protein YadA. UspA2 and YadA possess the most sequence homology and this is found in the C-terminal region of these proteins; however, a second region of homology is also located in the middle of each protein. Interestingly, YadA also migrates in SDS-PAGE as a complex much larger than its predicted size (128, 280), comprised of several YadA monomers (193). YadA has been implicated in both serum resistance (239) and attachment to HEp-2 cells (25).

Approximately 20% of *M. catarrhalis* strains express a UspA2H protein instead of UspA2. This UspA2H protein has homology to both UspA1 and UspA2, and accordingly is

both an adhesin as well as a serum resistance factor. Sequence alignment of UspA2H with UspA1 and UspA2 shows that much of the N-terminal half of UspA2H is homologous to the N-terminal half of UspA1 while the C-terminal region is homologous to the C-terminal half of UspA2 (174). In most *M. catarrhalis* strains expressing a UspA2H protein, both the UspA1 and UspA2H proteins independently mediate attachment to Chang cells (174).

C. Hag (MID)

It has been recognized since 1971 that *M. catarrhalis* can mediate agglutination of mouse and rabbit red blood cells *in vitro* (334). Others have since observed agglutination of human erythrocytes (10, 11, 94, 161, 213, 260, 285) and sometimes animal erythrocytes (9, 94, 161, 260) by *M. catarrhalis*, although the hemagglutination ability of *M. catarrhalis* varies from strain to strain. Some of these groups differed on whether or not the presence of fimbriae, detectable by TEM, correlated with hemagglutination (10, 94, 260) or the ability to attach to mammalian cells (161, 260). Several of these groups noted that hemagglutination did not occur if *M. catarrhalis* was first treated with trypsin or heated to 70°C, indicating that the molecule mediating hemagglutination was likely a protein (94, 161, 260). Scott and colleagues (92) subsequently noted that the presence of a 200 kDa protein, visible either by Coomassie staining of whole cell extracts or by immunoblotting with polyclonal rabbit antiserum raised against whole cells of one *M. catarrhalis* strain, correlated with hemagglutination ability. A later study using the same antiserum that had been pre-absorbed with non-hemagglutinating *M. catarrhalis* for IEM analysis indicated that the protein

involved in hemagglutination formed a fibrillar layer extending from the surface of the bacterial outer membrane (93). Meanwhile, Sasaki *et al* had cloned and sequenced a gene encoding a 200 kDa protein from *M. catarrhalis* (264). They found that although not all strains of *M. catarrhalis* expressed the 200 kDa protein, all strains included in their study possessed the entire gene (265). Furthermore, this group isolated a spontaneous mutant that had lost the ability to produce the 200 kDa protein; the only difference between the mutant and its parent was the number of G residues in a poly(G) tract located within the ORF. Sasaki *et al* concluded that the poly(G) tract acts as a phenotypic switch to turn the gene on and off (265). It should be noted that slipped-strand mispairing which involves homopolymeric nucleotide repeats is a well-known mechanism for allowing phase variation in prokaryotes (reviewed in (136, 308)). My own studies detailing the hemagglutination, autoagglutination, IgD-binding activity, and eukaryotic cell attachment ability of isogenic mutants of the 200 kDa protein, hereafter called “Hag”, are discussed in the Results section of this dissertation; also see (235). Subsequent publications by other groups on these same topics (99, 100, 144, 210, 226, 332) will be analyzed in the discussion following my Hag results.

D. OMP CD

Originally identified as two separate proteins, OMP C and OMP D (18), OMP CD was found to migrate as a doublet on SDS-PAGE when heated prior to SDS-PAGE but as a single band when processed without heating (221). Subsequent cloning and expression of

ompCD in *E. coli* revealed that OMP C and OMP D are actually the same protein, now designated OMP CD (219). Holm *et al* (143) have recently found that OMP CD is an adhesin for human lung cells. These data are compatible with an earlier report by Reddy *et al* (255) in which it was shown that OMP CD binds human middle ear mucin. Holm *et al* (143) have also indicated that an *ompCD* mutant lacks serum resistance. Although the serum resistance data are weakened by the fact that their isogenic *ompCD* mutant grew more slowly than the corresponding wild-type strain (possibly due to membrane perturbation or decreased nutrient uptake) (143), it has been reported that the OMP CD homolog OmpA, found in *E. coli*, contributes to serum resistance in that organism by binding the complement C4b binding protein (241). OMP CD also shares sequence similarity with the porin OprF, found in *Pseudomonas aeruginosa* (219, 338), indicating that OMP CD is possibly a porin involved with nutrient uptake. Interestingly, OprF has also been shown to be an adhesin (15).

As is the case with UspA1 and UspA2, OMP CD is widely expressed (263, 336) and is localized to the bacterial cell surface; one study found that all 51 strains of *M. catarrhalis* screened were positive for OMP CD (263). Nucleotide sequence analysis of the gene encoding OMP CD indicated that this gene is highly conserved among different isolates (146). Injection of purified OMP CD into guinea pigs and mice resulted in antibodies that were bactericidal to *M. catarrhalis* in an *in vitro* assay (336). In addition, either mucosal or intramuscular immunization of mice with purified OMP CD resulted in improved pulmonary clearance of *M. catarrhalis* following intratracheal challenge (220). Furthermore, antibodies reactive with OMP CD are present in convalescent sera from otitis media patients (123, 336).

E. OMP E

OMP E, like OMP CD above, was originally identified as a protein detectable by Coomassie blue staining in outer membrane preparations of *M. catarrhalis* (18). Antiserum absorption experiments indicated that this protein is surface-expressed and displays antigenic conservation across diverse strains (215). The latter finding was strengthened with the observations that the *ompE* gene shows little variation between strains using RFLP analysis (22) and that the nucleotide sequence of *ompE* is highly conserved (217); furthermore, at least one surface epitope of OMP E is conserved (23). Taken together, these data suggested that OMP E might be useful in a *M. catarrhalis* vaccine (217). However, it is not yet known whether antibody responses to OMP E are protective. Although OMP E is immunogenic in rabbits, adult humans who are infected with *M. catarrhalis* exhibit low or undetectable antibody titers to OMP E (23). Bhushan *et al* (23) contend that this protein may still have vaccinogenic potential when administered in a purified form. Mutant analysis showed that *ompE* mutants were more sensitive to killing by normal human serum; however, these mutants also have a modest growth defect compared to the corresponding wild-type strains (216). OMP E has homology to *E. coli* FadL, which is involved in uptake of long-chain fatty acids (22, 24). Unfortunately, no experiments have yet been conducted to address whether OMP E is involved with nutrient uptake.

F. McaP

Although the UspA1, UspA2H, and Hag proteins appear to be the primary adhesins for *M. catarrhalis* attachment to Chang or A549 cells (discussed above), *M. catarrhalis* still exhibited low levels of attachment to these cell lines when a *uspA1 uspA2 hag* triple mutant was evaluated. In a recent publication, Timpe *et al* (300) analyzed *E. coli* expressing a library of *M. catarrhalis* chromosomal DNA fragments and found one isolate expressing a previously unidentified adhesin capable of attaching to several cell lines. They went on to determine that this protein, which they named McaP (*M. catarrhalis* adhesin protein), has homology to *Moraxella bovis* phospholipase B. Further experimentation revealed that *M. catarrhalis* expressing McaP exhibited esterase activity and that McaP is a phospholipase B (as evidenced by its ability to cleave phosphatidylcholine; see (300)); the corresponding *mcaP* isogenic mutant lacked this activity. The authors noted that phospholipases may contribute to pathogenesis by several different mechanisms, including host tissue colonization (77) and destruction of lung surfactant (97). More study of this novel protein to elucidate its possible role in pathogenicity is warranted.

G. TbpA and TbpB (OMP B1)

A pathogen such as *M. catarrhalis* encounters conditions of extremely low free iron when growing in the human body. Most of the iron in our bodies is intracellular; the small amount of extracellular iron is sequestered by the iron-binding proteins transferrin (localized

primarily to the serum) (reviewed in (326)) and lactoferrin (localized primarily to mucosal surfaces) (200). Pathogenic species of *Neisseria*, *Moraxella*, and several other bacteria address iron starvation by producing proteins that directly bind transferrin and lactoferrin. The molecules responsible for the ability to bind transferrin are called transferrin binding proteins, or Tbps. Tbp proteins recognize a very narrow host range of transferrin (*M. catarrhalis* only recognizes transferrin from humans and certain primates); this is believed to contribute to the host-specificity of *M. catarrhalis* (116). Unlike enteric pathogens, *M. catarrhalis* does not employ siderophores for iron uptake (43). Originally found in *N. meningitidis* (14), Tbp was first detected in *M. catarrhalis* by Schryvers and Lee (272). This report also noted that more than one *M. catarrhalis* protein is capable of binding human transferrin; two of these, homologous to Tbps from *Neisseria* species, are designated TbpA and TbpB (the third protein, CopB, is described below). TbpA is essential for *M. catarrhalis* to utilize transferrin as its sole iron source, while *tbpB* mutants display a diminished capacity to bind transferrin (186). There are conflicting reports as to whether the *M. catarrhalis* TbpB protein is unique relative to other transferrin binding proteins in that it preferentially recognizes iron-saturated transferrin over apotransferrin (257, 341). TbpB, also called OMP B1, is known to induce the synthesis of antibodies in patients with either otitis media (42, 201) or lower respiratory tract disease (273, 339). Antibodies to an 84-kDa OMP that binds transferrin, and is likely TbpB, have also been detected in pooled serum from apparently healthy adults (202). In addition, guinea pigs immunized with purified recombinant TbpB produce antibodies that were bactericidal for *M. catarrhalis*; TbpA antibodies were not bactericidal (222). Furthermore, Luke *et al* (187) isolated a bactericidal MAb which

recognizes TbpB from approximately one-third of *M. catarrhalis* strains. The domains of TbpB and transferrin that bind each other have been identified (257, 278). With these data, it may be possible to create a vaccine incorporating TbpB or develop a therapeutic treatment that will prevent TbpB from binding transferrin.

A 74-kDa transferrin-binding protein has also been found in *M. catarrhalis*. Vaccination of mice with this unnamed protein resulted in enhanced pulmonary clearance following challenge by *M. catarrhalis*. Although this protein exhibits several of the same characteristics of TbpB, including some internal peptide sequences, it is not apparent whether the 74-kDa protein and TbpB are the same protein (55). BLAST analysis (12) of the 74-kDa protein internal peptide sequences against the incomplete *M. catarrhalis* genome only produces alignments to TbpB, indicating that the 74-kDa protein is in fact TbpB. If these proteins are indeed the same, the vaccine potential of TbpB would be strengthened. Sequencing of the gene encoding the 74-kDa protein would definitively answer this question.

H. LbpA and LbpB

Lactoferrin binding proteins A and B (LbpA and LbpB) allow *M. catarrhalis* to use human lactoferrin as an iron source (43). LbpA and LbpB both bind lactoferrin (28, 29, 272) and are homologous to TbpA and TbpB. LbpA is essential for *M. catarrhalis* growth on lactoferrin as a sole iron source, while a *lbpB* mutant can still utilize lactoferrin (27). The regions of human lactoferrin that recognize LbpA have been identified (335, 340). As is the case for Tbp, immunization of animals with LbpB results in bactericidal antibodies, while

immunization with LbpA does not (79, 339). In addition, sera from convalescent patients recognizes LbpB but not LbpA (28). Thus, LbpB is being investigated as a possible vaccine component.

I. CopB

M. catarrhalis outer membrane protein B, or CopB, was originally identified by use of a MAb targeted against the outer membrane of *M. catarrhalis* (129). It is possibly the same protein labeled OMP B in the study by Bartos and Murphy of conserved outer membrane proteins of *M. catarrhalis* (18); it has also been called OMP B2 (273). This protein, homologous to the iron-regulated protein FrpB of *Neisseria* species (21, 237), was shown by Aebi *et al* (7) to be necessary for acquisition of iron from transferrin or lactoferrin but not from ferric citrate. In addition, expression of CopB is increased under iron starvation conditions (7, 43). On the other hand, a *copB* mutant was still able to bind transferrin and lactoferrin (7); thus, CopB is distinct from the Tbp and Lbp proteins described above. Helminen *et al* (131) found that a *copB* mutant was sensitive to killing by normal human serum, and that this defect could be repaired by expressing wild-type CopB in the mutant strain. However, it is possible that the serum resistance defect is not directly due to the absence of CopB; expression of CopB in a heterologous background such as *E. coli* or *H. influenzae* would address this question. Helminen *et al* also reported that the *copB* mutant is cleared more readily than the isogenic wild-type strain from mouse lungs in the pulmonary challenge model (131). To investigate the potential of CopB as a vaccine candidate, the

amino acid sequence and antigenic heterogeneity of CopB were analyzed. Two independent groups found that CopB has greater than 90% identity at the amino acid level across strains (4, 275). Regions of identity were separated by several variable regions, which are presumably surface-expressed. Low titers of CopB antibody have also been found in bronchiectasis patients (273). Unfortunately, MAbs generated against CopB only react with 60-70% of *M. catarrhalis* strains, indicating antigenic heterogeneity (129, 275). If CopB is to be included in a vaccine, it appears that it will be necessary to incorporate CopB from more than one strain. Further studies elucidating the role of CopB in iron uptake would also prove useful.

J. Fur

The ferric uptake regulator Fur is a well-characterized negative regulator of expression of iron-regulated proteins (reviewed in (253)). Recently, Fur was identified in *M. catarrhalis*. As expected, a *fur* mutation resulted in constitutive expression of iron-regulated proteins. Furthermore, this mutant has a defect in growth under iron-replete conditions. Surprisingly, the *fur* mutant also has increased susceptibility to killing by normal human serum (104). However, this study was conducted using bacteria grown under iron-replete conditions, and it is possible that the growth defect of the *fur* mutant somehow leads to cell death in the presence of serum. The authors proposed that the *fur* mutant may be useful as a vaccine strain, as it produces all the proteins described above yet may not be able to cause disease (104).

K. Lipooligosaccharide

Lipopolysaccharide is perhaps the most extensively studied molecule of *M. catarrhalis*, with preliminary observations occurring in the 1960s and 1970s. These early reports utilized fractionation to analyze the components of *M. catarrhalis* LPS (3, 152). More recently, a study of 302 strains found that greater than 90% of *M. catarrhalis* isolates can be divided into one of three LPS serotypes, designated A, B, and C (311). Several other reports noted the presence of a short chain oligosaccharide attached to the lipid A moiety in place of the long O chain characteristic of most Gram-negative bacteria; thus, the lipopolysaccharide of *M. catarrhalis* is now usually referred to as lipooligosaccharide (LOS) (98, 199).

Most recent research on *M. catarrhalis* LOS has progressed along two fronts: continuing structural studies of LOS (82-84, 199), and investigation of the vaccine potential of this molecule. Although *M. catarrhalis* LOS induces serotype-specific responses in rabbits (250), the same result was not seen during lower respiratory tract infections in humans (251). A MAb has been produced that appears to recognize LOS from all *M. catarrhalis* serotypes (230); however, no data were published regarding the protective or bactericidal activity of this MAb. Gu *et al* (119) detoxified *M. catarrhalis* LOS, linked this LOS to tetanus toxoid, and showed that this conjugate induced bactericidal antibodies when administered to rabbits and enhanced clearance of *M. catarrhalis* from mouse lungs in the pulmonary clearance model (147). Gu and colleagues also described a MAb that recognizes both serotypes A and C LOS and which is bactericidal. Passive immunization with this MAb

is protective in the mouse pulmonary clearance model; this MAb can also block adherence of *M. catarrhalis* to an epithelial cell line (148).

LOS has also been implicated in serum resistance; a mutation in an LOS epitope designated P^k caused a serum-resistant *M. catarrhalis* strain to become serum sensitive (342). The authors hypothesized that P^k mimics a human antigen and loss of this epitope exposes an antigen on the bacterium that allows complement-mediated lysis. However, it is not clear whether all *M. catarrhalis* strains, or even all serum-resistant strains, possess the P^k epitope.

Recently, Luke *et al* (185) created a *kdsA* mutant defective in production of the LOS inner core component KDO. This mutant possesses only the lipid A portion of its LOS. Intriguingly, KDO is believed to be essential for viability in most Gram-negative bacteria, although a similar mutant has been constructed in *N. meningitidis* (290). The *kdsA* mutant, not surprisingly, displayed very slow growth and has compromised outer membrane integrity (185).

L. Pili

Pili are protein filaments that extend from the bacterial cell surface and are comprised of primarily pilin subunits, often with a separate adhesin molecule on the tip (reviewed in (295)). There have been several reports in the *M. catarrhalis* literature of pili (8, 10, 196, 260, 334), usually referring to cell surface projections that are visible by TEM. However, at least some of these projections are now known to be comprised of proteins other than pilins; descriptions of these non-pilus surface structures of *M. catarrhalis* will be provided in the

Results section of this dissertation. Nevertheless, it is possible that some strains of *M. catarrhalis* possess pili that have not yet been isolated. Wistreich and Baker (334) published TEM photos of *M. catarrhalis* displaying very long structures on the cell surface. Marrs and Weir (196), who have also detected similar projections using TEM, found that at least one *M. catarrhalis* strain possesses a homolog to the gene encoding type IV pilin of *Moraxella bovis* as detected by Southern blot analysis, although expression of this gene has not been reported in *M. catarrhalis*. *M. catarrhalis* does have several characteristics of type IV pilus-positive strains, including autoagglutination, pellicle formation, and colony morphology (196), but these phenotypes may be attributable to the expression of other proteins. There are also no reports of *M. catarrhalis* exhibiting twitching motility, another characteristic of type IV pili. It is important to note that one study of *Campylobacter jejuni* found that long, filamentous structures visible by TEM on this organism were actually bacteria-independent culture medium artifacts (107). Clearly, more rigorous molecular studies need to be conducted to determine whether or not *M. catarrhalis* strains actually express functional type IV pili.

IX. Animal Models of *M. catarrhalis* Disease

A. Mouse

There have been several attempts to develop models of *M. catarrhalis* infection that utilize mice. The initial study by Onofrio *et al* (231) reported the use of an aerosol exposure chamber and a nebulizer to introduce *M. catarrhalis* into the lungs. This publication

indicated that most of the bacteria were cleared from the lungs of infected mice within a few hours, although they did not examine bacterial load beyond 4 hours post-infection. It was also noted that granulocytes were recruited to the lungs following aerosol exposure, but that alveolar macrophages were not. The clearing of bacteria from the lungs was used to model the removal of normal nasopharyngeal flora that are routinely aspirated, as the authors believed that *M. catarrhalis* was nonpathogenic. Gu and colleagues (149) employed a similar aerosol model and found that more than 99% of a *M. catarrhalis* challenge was cleared from mouse lungs within 24 hours. The same study also reported that passive immunization of mice with rabbit anti-*M. catarrhalis* serum before challenge with *M. catarrhalis* resulted in enhanced pulmonary clearance. The aerosol model has since been used to evaluate potential vaccine candidates (147, 148).

A related approach to the aerosol challenge is the endotracheal bolus challenge, wherein a dose of *M. catarrhalis* is introduced into the lungs of an anesthetized mouse via a catheter. This method of inoculation possibly more closely resembles the *in vivo* aspiration of oropharyngeal fluids which is presumably the route by which *M. catarrhalis* gains access to the lower respiratory tract. However, as with the aerosol model, bacteria are almost completely cleared from the lungs within 24 hours, accompanied by an influx of granulocytes (307, 315). Even so, researchers using this model have found that there is a strain-to-strain variation in the rate of clearance (307). Furthermore, either active immunization of mice with *M. catarrhalis* outer membrane vesicles or passive immunization with *M. catarrhalis* immune serum resulted in enhanced pulmonary clearance (191). Thus, this model was used

in many of the studies described above in “Potential Virulence Factors” (55, 129, 130, 220), and also to investigate clearance following mucosal immunization (172).

B. SCID mouse

The severe combined immunodeficient mouse (SCID) lacks functional T and B lymphocytes (reviewed in (31)). In addition, SCID/beige mice also lack natural killer cells. Because *M. catarrhalis* does not establish an infection in any rodents tested to date, and because *M. catarrhalis* disease in humans is occasionally associated with immune incompetence (reviewed in (47)), SCID mice have been investigated as a possible model for *M. catarrhalis* infection (124). Unfortunately, few SCID mice challenged either intravenously or intranasally with *M. catarrhalis* displayed any clinical symptoms. These researchers also administered iron-loaded human transferrin to SCID/beige mice before IV challenge with *M. catarrhalis*, but still did not establish infection. However, one strain of *M. catarrhalis* caused mortality in SCID/beige mice that were 7 days old, while 12-day-old mice survived; a different *M. catarrhalis* strain did not cause mortality with either age group. In this aspect, the SCID model resembles human infection in that most *M. catarrhalis* infections occur in infants. Postmortem examination of these *M. catarrhalis*-challenged SCID/beige mice revealed that these animals frequently had organ lesions, especially in the liver. However, these lesions were not associated with clinical symptoms, nor was live *M. catarrhalis* ever recovered from the blood or organs of infected mice. It is not clear how

relevant the SCID/beige model of infection might be, but investigation of the mechanism behind the observed age-related mortality following infection might prove useful.

C. Chinchilla and gerbil models of otitis media

The chinchilla (*Chinchilla laniger*) is often used as a model for studying otitis media caused by *H. influenzae* and *S. pneumoniae* (109, 297). Unlike these pathogens, *M. catarrhalis* did not persist in the middle ear of chinchillas following intrabullar inoculation (78, 103), and no viable organisms were recovered by 24 hours post-infection. However, inoculation of the chinchilla middle ear with either heat-killed or viable *M. catarrhalis* resulted in inflammation or effusion (59, 78). It is known that challenge of the chinchilla middle ear with *H. influenzae* endotoxin also results in inflammation and effusion (70); thus, it seems likely that the inflammation observed following challenge with *M. catarrhalis* is due to a similar mechanism. Bakeletz *et al* (16) made another attempt at using the chinchilla model by intranasally infecting chinchillas with both adenovirus type I and *M. catarrhalis*. A previous report had shown synergistic infection with *H. influenzae* and adenovirus in the chinchilla (297). Nevertheless, chinchillas infected with *M. catarrhalis* failed to develop otitis media, even though these animals were positive for nasopharyngeal colonization with *M. catarrhalis* for at least two weeks (16).

Fulghum and Marrow (103) employed a very similar approach using gerbils (*Meriones unguiculatus*). They reported essentially the same results, with inflammation

occurring regardless of whether live or dead *M. catarrhalis* was used. However, the inflammation was more severe in animals exposed to live *M. catarrhalis*.

D. Rat

Sprague-Dawley rats have also been investigated as a possible model for *M. catarrhalis*-induced otitis media (327). In this report, intrabullar inoculation of *M. catarrhalis* resulted otitis media that cleared within 8 days. Unlike experiments in other animal models, the rats developed opaque effusions and were culture-positive for *M. catarrhalis* through at least day 4. In contrast, rats inoculated with heat-killed bacteria produced only a transparent effusion. Either subcutaneous or intrabullar immunization with formalin-fixed *M. catarrhalis* did not prevent the development of acute otitis media, although the rate of resolution was faster. A more recent study using the rat model found that experimental *M. catarrhalis* infection caused an increase in goblet (mucus-producing) cells within the Eustachian tube, although this change was milder and more transient than goblet cell increases triggered by *S. pneumoniae* or *H. influenzae* infections (50). Overall, this approach seems promising, and it is surprising that there have not been additional studies published using the rat model for *M. catarrhalis* otitis media.

E. Macaque

Bacterial screening of quarantined cynomolgus macaques (*Macaca fascicularis*) revealed that *M. catarrhalis* was often present in the nasopharynx during episodes of nasal discharge, sneezing, and epistaxis (nosebleed) (309). Furthermore, of the macaques presenting with “bloody-nose syndrome”, characterized by mucohemorrhagic nasal discharge, 94% were culture-positive for *M. catarrhalis*. In order to confirm whether or not *M. catarrhalis* infection was causing the respiratory symptoms of these macaques, the authors of this study (309) proceeded to intranasally inoculate healthy macaques with *M. catarrhalis*. Sixty-three percent of these animals developed mild disease, including spontaneous nasal bleeding. These macaques remained positive for *M. catarrhalis* by culture for 4 weeks; following antibiotic therapy, symptoms resolved and the macaques were culture-negative for *M. catarrhalis*. A more recent report from Philipp and colleagues (35) found that rhesus macaques (*Macaca mulatta*) with bloody-nose syndrome were infected with *M. catarrhalis*. Furthermore, a survey of 50 healthy macaques found that none of these animals was colonized with *M. catarrhalis*. The authors of both of these studies (35, 309) state that macaque infection with *M. catarrhalis* might prove useful as a model of human infection. Of course, the high cost and lack of accessibility associated with primate research makes use of this model difficult for most researchers.

X. Overview of Biofilm Research

The first evidence that bacteria in nature preferentially grow attached to a surface was found over a century ago, when it was noted that water in flasks with more surface area accumulated biomass more quickly than flasks with more volume but less surface area (328). ZoBell, who has been credited with the first description of a biofilm, observed that when a slide is submerged in seawater, bacteria attached to the surface wash away easily at first but form tenacious attachments within a few hours (344, 345). He also described a film that appeared to be secreted by attached bacteria that increased with the length of time that a slide was submerged. Despite these early experiments, biofilms were not studied extensively until the last 25 years or so. This likely occurred because many experiments are much easier to conduct on a flask of planktonically-grown cells: bacteria in broth grow rapidly at defined rates to high densities, and the cells are much more easily harvested for analysis. However, extensive surveys indicate that the vast majority of bacteria in aquatic environments are growing as biofilms (reviewed in (64)). Our understanding of biofilms has advanced considerably with the development of new research techniques, such as scanning confocal laser microscopy (SCLM) (178), reporter constructs (145), and specialized devices for growing biofilms (described below). Historically, industry conducted much of the research into biofilms, which are more frequently termed “biofouling” in this setting, as these organizations are eager to develop methods for removing or preventing biofilms that clog filters and corrode pipes (64). Similarly, pathogens may form biofilms on indwelling medical devices, on the surfaces of our teeth, or on host tissues (reviewed in (65)).

It is important to investigate bacteria growing as biofilms because they have been shown repeatedly to differ from their planktonic counterparts. Perhaps the most notable feature of biofilms is their notorious resistance to killing by antibiotics. Studies have found that planktonic bacteria can be as much as four orders of magnitude more sensitive to a given antibiotic than biofilm-grown bacteria of the same species (13, 51, 225). The reason for these differing susceptibilities to antibiotics remains unknown, although several mechanisms have been proposed (reviewed in (76, 81)). Biofilms are often characterized as having thick exopolysaccharide “slime” layers, and researchers have found that production of the exopolymer alginate is upregulated in biofilm-grown *P. aeruginosa* (68, 145). On the other hand, *Escherichia coli* has been found to downregulate flagellin expression in biofilms (246). Analysis of global gene expression patterns indicates that 38% of *E. coli* genes are differentially regulated in biofilms (246). There are conflicting reports on *P. aeruginosa* biofilm formation; Davies *et al* (266) found, using two-dimensional SDS-PAGE, that as many as 50% of *P. aeruginosa* genes have differential expression in biofilms while Greenberg and colleagues (331) found only a 1% difference using microarrays. These discrepancies are possibly due to either the method of investigation or the method for biofilm growth. The signals that trigger differential gene expression are still being elucidated, but global regulators have been implicated in *P. aeruginosa* (σ^E) (198), *E. coli* (CsrA) (151), *Staphylococcus epidermidis* (RsbU) (166), and *Staphylococcus aureus* (*agr*) (318).

A number of gene products are necessary for biofilm formation, although the exact requirements vary from species-to-species, and even within the same species growing under different conditions. For example, *P. fluorescens* requires flagellar motility for biofilm

formation in minimal media, but nonmotile mutants can form biofilms when grown in the same minimal media supplemented with citrate, glutamate, or iron (229). In addition to flagella, *P. aeruginosa* needs twitching motility (mediated by type IV pili) (228) and quorum sensing (69) to form mature biofilms. Similarly, *Vibrio cholerae* requires flagella, type IV pili, and exopolysaccharide secretion (325), while flagella, type I pili, curli, and colanic acid play roles in *E. coli* biofilm development or maturation (242, 245). In contrast, the nonmotile bacterium *H. influenzae* has been shown to require pili for biofilm formation, but has little detectable differential protein expression (218). Transposon-mediated mutagenesis of *S. epidermidis* shows that the polysaccharide intercellular adhesin (PIA) is involved in cell accumulation during biofilm formation (192); the locus encoding PIA (*icaADBC*) has also been found in *S. aureus* and appears to play a similar role in this organism (66). A fascinating example of a multispecies system is biofilm formation by *Porphyromonas gingivalis* on top of *Streptococcus gordonii* (61). In this case, both the streptococcal SspA or SspB proteins and the *P. gingivalis* Mfa1 protein are required for *P. gingivalis* biofilm development (177).

Several authors have proposed models of biofilm formation, all of which have certain similarities (65, 81, 294, 323) (Fig. 1). First, a planktonic bacterial cell has transient, reversible interactions with a surface. Next, the cell becomes irreversibly attached to the surface by any of several means such as pili or other adhesins. At this point, the attached bacterium multiplies to form a microcolony. Then, a biofilm is born as an extracellular matrix is formed and characteristic structures develop. The biofilm may propagate itself by signaling some cells to revert to the planktonic phenotype so that these cells can repeat the

process elsewhere. Alternatively, a piece of the biofilm might simply break off and seed a new site with a pre-formed biofilm.

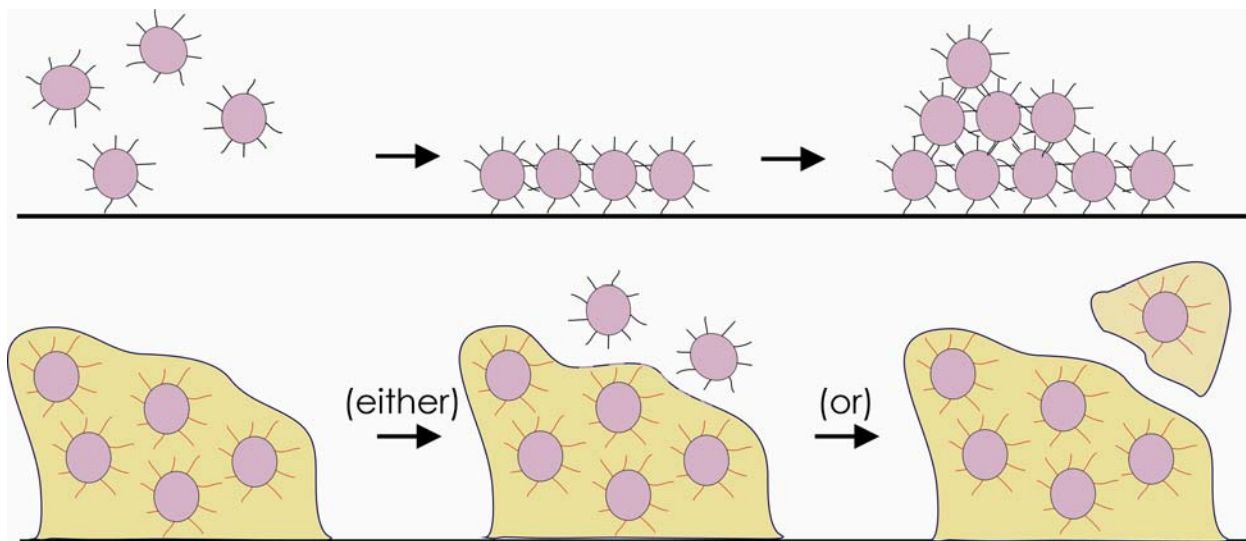


Fig. 1. General model of biofilm formation. Top row, from left to right: planktonic bacteria form transient interactions with a surface. Once bacteria are permanently attached to a surface, growth or some types of motility may cause accumulation of the bacteria. Simultaneously, attached bacteria can divide to form a microcolony. Bottom row, left to right: various changes in attached bacteria lead to the formation of a mature biofilm, including differential expression of surface molecules and extracellular polysaccharides. Bacteria may either leave the biofilm by returning to the planktonic state or by breaking away as an intact biofilm.

XI. Biofilms in Infectious Disease

Although biofilms were initially characterized in rivers and oceans, the evidence for medically relevant biofilms is considerable. The most thoroughly studied single-species

biofilms are those formed by *P. aeruginosa*. This organism, an opportunistic pathogen of humans, is isolated from the lungs of up to 80% of cystic fibrosis (CF) patients (115). At some point after colonization, *P. aeruginosa* shifts to a mucoid phenotype characterized by the overproduction of alginate (167); mucoid strains are less readily cleared from the lungs compared to nonmucoid strains (261). *Burkholderia cepacia* is often co-cultured from CF patients; thus, there have been studies examining the ability of *P. aeruginosa* and *B. cepacia* to form mixed biofilms (259, 302).

Indwelling medical devices are frequently colonized by bacterial biofilms. One study found, using TEM and SEM, that central venous catheters are almost universally colonized (249). Patients with long-term (greater than 28 days) urinary tract catheterization almost always experience urinary tract infections; several studies have traced these infections to biofilm formation on the catheter (reviewed in (76)). Other devices that may develop biofilms include tympanostomy tubes, intrauterine devices, prosthetic heart valves, and contact lenses (76). Organisms that have been found colonizing the surfaces of these devices include but are not limited to *S. epidermidis*, *S. aureus*, *E. faecalis*, *E. coli*, *Proteus mirabilis*, and *P. aeruginosa* (76). A well-characterized multispecies biofilm is dental plaque (reviewed in (168)). Finally, most relevant to this dissertation is the recent visualization by SEM of *H. influenzae* biofilms in the middle ear of experimentally infected chinchillas (85).

XII. Methods for Growing Biofilms

One challenge of working with biofilms is choosing an appropriate method for growing them. Researchers have developed several different strategies for accomplishing this aim. One of the first *in vitro* methods used for growing biofilms was the Robbins device (203). This device consists of circular tubing with inlets for bacterial inoculum, fresh growth media, or other substances, and an outlet for the effluent. Within the circuit is the Robbins sampler, which has evenly spaced ports into which test surfaces may be inserted or removed during biofilm growth. Perhaps the method most often employed for biofilm growth is the flow cell. A flow cell is basically an open channel(s) with inoculated media flowing through, supplied by a peristaltic pump. A glass cover (i.e., microscope slide) is placed over the flow cell for sterility, but the slide can be placed under a microscope for real-time imaging of biofilm structure and development (87, 171, 178, 293). Another method that has been used to study biofilms is the constant-depth film fermentor (CDFF) (243, 244). In this system, bacteria are grown on plugs inside the fermentor; air and media are supplied to the fermentor through ports, and effluent flows out through a different port. The biofilm-coated plugs may be removed for more detailed analyses. A more simplistic version of biofilm growth on plugs of test material has been devised in which an inoculated plug is placed in a Petri dish containing broth media and incubated without aeration or flow (247). The plug may be removed at any point for microscopy or determination of viability. Gilbert and colleagues (105, 110) have grown biofilms by pressure filtration of a culture onto a membrane, and then perfusion of the inverted membrane with growth medium; the filtered bacteria form a biofilm

on the side of the membrane opposite the flow of the fresh medium. Hodgson *et al* (140) devised a simpler version of the perfused biofilm fermentor that negated the need to purchase expensive chemostats for control experiments. This technique uses a cellulose filter housed inside tubing; the filter is inoculated with a bacterial culture, and fresh medium is supplied to the filter at a constant rate. My work with a derivative of this biofilm reactor will be described in later sections of this dissertation.

One drawback to the devices listed above is the lack of conformity from laboratory to laboratory. That is, many of these biofilm reactors are homemade constructs and require some skill (and some measure of creativity) to build. It is now possible to purchase mass-produced flow cells (Stovall, Greensboro, NC); therefore, biofilm research may become more accessible for investigators. Another problem with these methods is that they are time-consuming; furthermore, it is not possible to screen many samples simultaneously. For this reason, Ceri *et al* (51) developed the Calgary Biofilm Device (CBD) for testing the amount of antibiotic necessary to eradicate a biofilm (the “biofilm eradication concentration”, or BEC). The CBD consists of a 96-well plate fitted with a lid with 96 pegs, which is placed on a tilt platform. Viable counts can be enumerated by sonicating the biofilms from each peg and dilution plating. The CBD is potentially useful in a clinical setting, and is commercially available as the MBEC Assay system (MBEC Biofilms Technology Ltd., Calgary, Alberta, Canada).

The time, volume, and consistency barriers greatly limited work on the molecular genetics of biofilm formation. The answer to this bottleneck was the development of the crystal violet assay for measuring biofilm formation. Fletcher (96) had noted in 1977 that

bacterial attachment to a polystyrene surface could be visualized by the addition of crystal violet. O'Toole and Kolter (229) extended this idea to use microtiter plates for measuring biofilm formation by different isolates. Furthermore, the amount of biofilm formation was quantifiable by the addition of ethanol to extract the crystal violet from adherent bacteria. Using this high-throughput method, these authors (229) measured the biofilm formation ability of 14,000 *P. fluorescens* transposon mutants. Since this initial report, there has been an explosion of papers employing the crystal violet-based assay (44, 75, 182, 228, 242, 292, 325). This assay will be discussed in greater detail in the "Materials and Methods" section of this dissertation.

CHAPTER THREE

Materials and Methods

I. Bacterial Strains and Plasmids

A. *M. catarrhalis* Strains

All of the *M. catarrhalis* strains used in these studies were clinical isolates. Strains O35E and O46E, which were the wild-type strains used in most of the early experiments in this dissertation, were isolated in Dallas, TX, from middle ear fluid of children with otitis media and were obtained from Dr. John D. Nelson, Department of Pediatrics, UT Southwestern. Wild-type strain ETSU-9, used in later chapters of this dissertation, was obtained from Dr. Steven Berk, James H. Quillen School of Medicine, East Tennessee State University, Johnson City, TN. Strains with a designation beginning with “V” were obtained from Dr. Frederick W. Henderson, University of North Carolina at Chapel Hill. Strains with designations beginning with ATCC were purchased from the American Type Culture Collection. All *M. catarrhalis* strains used in these studies are listed in Table 1. *M. catarrhalis* was routinely grown on either brain-heart infusion (BHI) or Todd-Hewitt (TH) medium (Difco/Becton Dickinson, Sparks, MD) supplemented with 1.5% (w/v) agar. Cultures were grown at 37°C in an atmosphere of 95% air-5% CO₂. Broth cultures were aerated using a gyratory water bath maintained at 37°C. When required, antibiotic supplementation involved the use of chloramphenicol (0.6 µg/ml), kanamycin (15 µg/ml),

spectinomycin (15 $\mu\text{g/ml}$), Zeocin (5 $\mu\text{g/ml}$) (Invitrogen, Carlsbad, CA), or dihydrostreptomycin sulfate (750 $\mu\text{g/ml}$). Stock cultures of *M. catarrhalis* were stored at -70°C in BHI or TH containing 50% (v/v) glycerol.

B. *E. coli* Strains and Plasmids

E. coli strains used in these studies were obtained commercially and are listed in Table 1. All plasmids utilized in this study are listed in Table 2. Plasmid pCC1 (Epicentre, Madison, WI) is a plasmid that, when used with the host strain EPI 300, can be controlled with respect to plasmid copy number. Antibiotics were added as necessary at the following concentrations: chloramphenicol (20 $\mu\text{g/ml}$) (15 $\mu\text{g/ml}$ for experiments using pCC1), kanamycin (50 $\mu\text{g/ml}$), ampicillin (100 $\mu\text{g/ml}$), or spectinomycin (150 $\mu\text{g/ml}$).

Table 1. Bacterial strains used in this study

Strain	Genotype or Description	Source or Reference
<i>M. catarrhalis</i>		
O35E	Wild-type isolate	(6)
O35E.118CAT	<i>uspA1::cat</i> reporter strain; chloramphenicol-resistant	(175)
O35E.2ZEO	Isogenic <i>uspA2</i> mutant of strain O35E with a Zeocin resistance cartridge inserted into the <i>uspA2</i> gene	This study; (235)
O35E.HG	Isogenic <i>hag</i> mutant of strain O35E with a spectinomycin resistance cartridge inserted into the <i>hag</i> gene	This study; (235)
O35E.ZCS	<i>uspA1 uspA2 hag</i> mutant of strain O35E; resistant to chloramphenicol, Zeocin, and spectinomycin	This study; (235)
O35E.ZC	<i>uspA1 uspA2</i> mutant of strain O35E; expresses Hag; resistant to chloramphenicol and Zeocin	This study; (235)
O35E.1HG	<i>uspA1 hag</i> mutant of strain O35E; resistant to chloramphenicol and spectinomycin	This study; (235)
O35E.2HG	<i>uspA2 hag</i> mutant of strain O35E; resistant to Zeocin and spectinomycin	This study; (235)
O12E	Wild-type isolate	(4)
4223	Wild-type isolate	(173)
O46E	Wild-type isolate	(174)

ATCC 25238	Wild-type isolate	ATCC
ATCC 25240	Wild-type isolate	ATCC
P44	Wild-type isolate	(153)
TTA24	Wild-type isolate	(62)
TTA37	Wild-type isolate	(174)
E22	Wild-type isolate	(19)
V1171	Wild-type isolate from the nasopharynx of a healthy child	F. Henderson
ETSU-13	Serum-resistant wild-type strain	S. Berk
ETSU-25	Serum-sensitive wild-type strain	S. Berk
ETSU-9	Wild-type isolate	S. Berk
ATCC 43617	Wild-type isolate	ATCC
V1119	Wild-type isolate	F. Henderson
7169	Wild-type isolate	(186)
T13	O35E transformant expressing a hybrid UspA1 protein	This study
T14	O35E transformant expressing a hybrid UspA1 protein	This study
T84	O35E transformant expressing a hybrid UspA1 protein	This study
T13/38	T13 with a transposon insertion in <i>uspA1</i> ; kanamycin-resistant	This study
T13/54	T13 with a transposon insertion in <i>uspA</i> ; kanamycin-resistant	This study
T14/27	T14 with a transposon insertion in <i>corC</i> ; kanamycin-resistant	This study

T13.1	Isogenic <i>uspA1</i> mutant of T13; chloramphenicol-resistant	This study
T14.1	Isogenic <i>uspA1</i> mutant of T14; chloramphenicol-resistant	This study
T14.COR	Isogenic <i>corC</i> mutant of T14; chloramphenicol-resistant	This study
O35E.1	Isogenic <i>uspA1</i> mutant of O35E; kanamycin-resistant	(5)
O35E.14U1	O35E with hybrid <i>uspA1</i> gene from T14	This study
O35E.14U1.HG	Isogenic <i>hag</i> mutant of of O35E.14U1; spectinomycin- resistant	This study
T14.HG	T14 with a spectinomycin- resistance cartridge inserted into the <i>hag</i> gene	This study
T14.O35EHG1-5	T14 transformed with a <i>hag</i> gene from O35E; strains vary in expression of Hag; streptomycin- resistant	This study
ETSU-9.HG	ETSU-9 with a spectinomycin- resistance cartridge inserted into the <i>hag</i> gene	This study
ETSU-9.O35EHG1-5	ETSU-9 transformed with a <i>hag</i> gene from O35E; strains vary in expression of Hag; streptomycin- resistant	This study
ETSU-9.222	ETSU-9 with a transposon insertion in a putative lytic murein transglycosylase D gene; kanamycin-resistant	This study

ETSU-9.222cat	Isogenic putative lytic murein transglycosylase D gene mutant of ETSU-9; chloramphenicol-resistant	This study
ETSU-9.698	ETSU-9 with a transposon insertion in the <i>uspA2H</i> gene; kanamycin-resistant	This study
ETSU-9.714	ETSU-9 with a transposon insertion in a putative phosphotransferase gene; kanamycin-resistant	This study
ETSU-9.714cat	Isogenic predicted phosphotransferase gene mutant of ETSU-9; chloramphenicol-resistant	This study
ETSU-9.724	ETSU-9 with a transposon insertion in the <i>uspA2H</i> gene; kanamycin-resistant	This study
ETSU-9.988	ETSU-9 with a transposon insertion in the <i>ampD</i> gene; kanamycin-resistant	This study
ETSU-9.988cat	Isogenic <i>ampD</i> mutant of ETSU-9; chloramphenicol-resistant	This study
ETSU-9.2311	ETSU-9 with a transposon insertion in the <i>uspA2H</i> gene; kanamycin-resistant	This study
ETSU-9.1	Isogenic <i>uspA1</i> mutant of ETSU-9; kanamycin-resistant	This study
ETSU-9.2H	Isogenic <i>uspA2H</i> mutant of ETSU-9 spectinomycin-resistant	This study
ETSU-9 str ^R	Streptomycin-resistant isolate of ETSU-9	This study
ETSU-9.K34E	ETSU-9 with the K34E mutation in <i>UspA2H</i> ; streptomycin-resistant	This study

ETSU-9.K34A	ETSU-9 with the K34A mutation in UspA2H; streptomycin-resistant	This study
O35E.E66K	O35E with the E66K mutation in UspA1	This study
O35E.E66K str ^R	O35E with the E66K mutation in UspA1; streptomycin-resistant	This study

E. coli

DH5 α	Host strain	(262)
XL1-Blue	Host strain	Stratagene
XL10-Gold	Host strain	Stratagene
INV α F'	Host strain	Invitrogen
EPI300	Copy-control host strain	Epicentre

Table 2. Plasmids used in this study

Plasmid	Description	Source or Reference
pCR-Blunt II-TOPO	Cloning vector for blunt-ended insertions; has kanamycin and Zeocin resistance genes	Invitrogen
pCR2.1 TOPO	Cloning vector for TA overhang insertions; has kanamycin and ampicillin resistance genes	Invitrogen
pACYC184	Cloning vector; has chloramphenicol and tetracycline resistance genes	(52)
pCC1	Copy-control plasmid; has chloramphenicol resistance gene	Epicentre
pCC1kan	pCC1 containing a kanamycin resistance gene; confers resistance to chloramphenicol and kanamycin	This study
pMP35U1	pCC1 containing the O35E <i>uspA1</i> gene; confers resistance to chloramphenicol	This study
pMP46U1	pCC1 containing the O46E <i>uspA1</i> gene; confers resistance to chloramphenicol	This study
pMP14U1	pCC1 containing the T14 hybrid <i>uspA1</i> gene; confers resistance to chloramphenicol	This study
pMPGTG3	pCR-Blunt II-TOPO containing the majority of the <i>uspA2H</i> ORF from strain ETSU-9; confers resistance to kanamycin and Zeocin	This study

pMPUspA1	pCR-Blunt II-TOPO containing the majority of the <i>uspA1</i> ORF from strain O35E; confers resistance to kanamycin and Zeocin	This study
pMP222	pCR2.1 containing a putative lytic murein transglycosylase D gene; confers resistance to kanamycin and ampicillin	This study
pMP222cat	pMP222 with a promoterless <i>cat</i> cartridge inserted into the <i>NdeI</i> site of the putative lytic murein transglycosylase D gene; confers resistance to kanamycin, ampicillin, and chloramphenicol	This study
pMP714	pCR2.1 containing the putative phosphotransferase gene; confers resistance to kanamycin and ampicillin	This study
pMP714cat	pMP714 with a promoterless <i>cat</i> cartridge inserted into the <i>AccI</i> site of the putative phosphotransferase gene; confers resistance to kanamycin, ampicillin, and chloramphenicol	This study
pMP988	pCR2.1 containing the <i>ampD</i> gene; confers resistance to kanamycin and ampicillin	This study
pMP988cat	pMP988 with a promoterless <i>cat</i> cartridge inserted into the <i>AccI</i> site of the <i>ampD</i> gene; confers resistance to kanamycin, ampicillin, and chloramphenicol	This study
pUSPAKAN	Has kanamycin-resistance gene inserted into the <i>uspA1</i> ORF	(5)
pELU1CAT	Has a promoterless <i>cat</i> cartridge inserted into the <i>uspA1</i> ORF	(175)

pELU244ZEO	Has Zeocin resistance gene inserted into the <i>uspA2</i> ORF	(235)
pELU244SPEC	Has spectinomycin resistance gene inserted into the <i>uspA2</i> ORF	(174)
pELHGSPEC	Has spectinomycin resistance gene inserted into the <i>hag</i> ORF	(235)

II. Sorbarod Method for Biofilm Growth

This method was adapted from that described by Budhani and Struthers (38). A 3-ml portion of an overnight culture was used to inoculate a sterile Sorbarod filter (diameter, 10 mm; length, 20 mm; Ilacon, Kent, United Kingdom) contained within a short piece (length, 3 in.; inside diameter, 3/8 in.) of silicone tubing. After inoculation, sterile BHI broth was dripped through silicone tubing onto this Sorbarod filter at a rate of 0.1 ml/min with a multichannel peristaltic pump (Watson Marlow, Wilmington, MA). The entire biofilm apparatus was housed in a 37°C environmental room. Cells were routinely harvested after 3 days of growth on the filter. A photograph of the biofilm apparatus is shown in Figure 2A, and a photograph of a Sorbarod filter inside the silicone tubing is shown in Figure 2B.

Fig. 3 shows how to construct the Sorbarod biofilm apparatus. A 1 L screw-cap Erlenmeyer flask was used as the sterile medium reservoir (A). Two $\frac{3}{8}$ in. diameter holes were drilled into the cap to allow insertion of silicone tubing (1/32 in. interior diameter by 3/32 in. exterior diameter by 1/32 in. thick) (B). This tubing was inserted into a size 000 silicone stopper (C) with a hole drilled through the center (a $\frac{1}{4}$ in. diameter drill bit results in a hole of the appropriate size). The silicone tubing was connected to 0.89 mm interior diameter peristaltic pump tubing (“orange-orange”, Watson Marlow) (E) by a P-200 pipette tip (D). The peristaltic pump tubing was inserted into the peristaltic pump (F) and connected via another P-200 pipette tip to another length of silicone tubing. The terminal end of this silicone tubing was inserted into a second stopper, which was connected to the piece of silicone tubing that housed the Sorbarod filter (G). A 1.3 cm length was removed from one

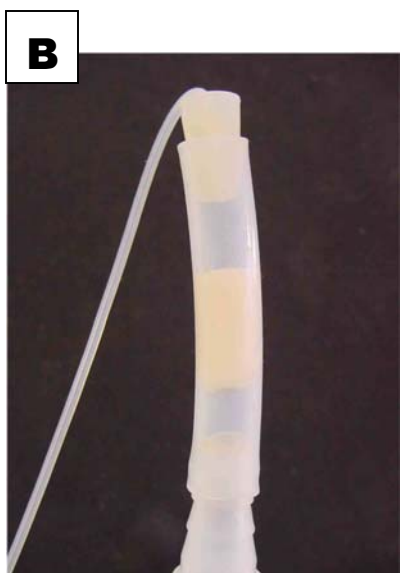


Fig. 2. The Sorbarod continuous culture biofilm system. Panel A, photograph of the entire apparatus; Panel B, close-up of the Sorbarod filter within the silicone tubing.

end of a 5-in-1 plastic tubing connector (Secure Medical Products, Kalamazoo, MI) (H), which was used to connect the Sorbarod tubing to a P-1000 pipet tip (also with approximately 5-8 mm removed from the tip) (I). A portion of the nozzle of an autoclavable squeeze bottle (Nalge Nunc, Rochester, NY) was removed (J); the P-1000 pipette tip was used to connect this effluent bottle to the remainder of the apparatus. The entire apparatus (except for the peristaltic pump, F) was autoclaved before the addition of media to the reservoir flask or the addition of broth culture to the Sorbarod filter.

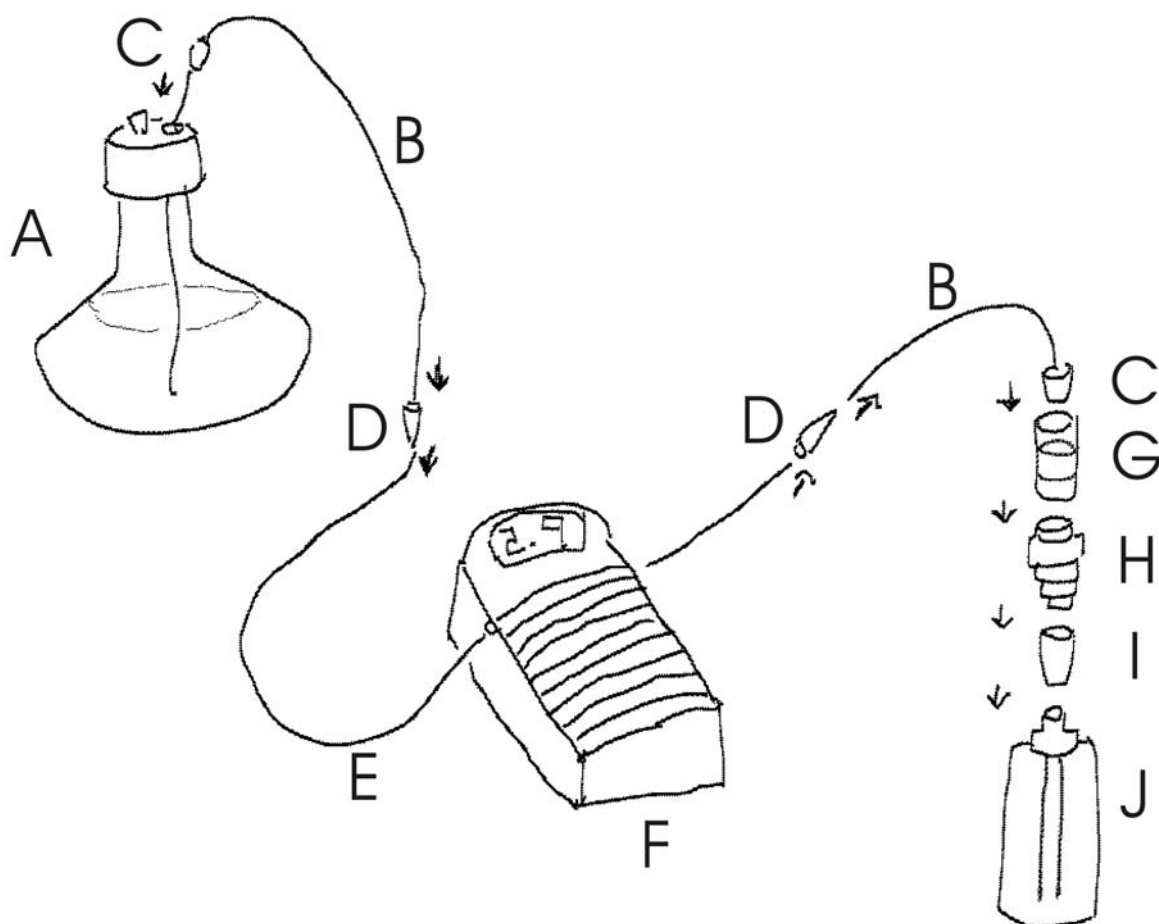


Fig. 3. Assembly of the Sorbarod biofilm apparatus.

III. Crystal Violet-based Assay for Measuring Biofilm Formation

A. *M. catarrhalis*

This method was adapted from the protocol published by O'Toole and Kolter (229) for use with *P. fluorescens*. Polystyrene plastic tubes (17 x 100 mm) (Fisher Scientific Company, Pittsburgh, PA) containing 5 ml BHI or TH broth were inoculated with *M. catarrhalis*. These cultures were incubated at 37°C with aeration until the bacterial density reached at least $2\text{--}4 \times 10^8$ colony-forming units (cfu)/ml, corresponding to a reading of 125 Klett units as determined by the use of a Klett-Summerson colorimeter (Klett Manufacturing Company, New York, NY). These cultures were diluted 1:100 in BHI or TH and 2 ml portions of this suspension were loaded, in triplicate, into a 24-well tissue culture plate (Corning Incorporated, Corning, NY), and incubated at 37°C for 19 h without aeration. The broth was then removed from each well and replaced with 2 ml of Medium 199 tissue culture medium containing Earle's balanced salt solution, L-glutamine, and HEPES (BioWhittaker/Fisher Scientific, Pittsburgh, PA) plus 100 μ l 0.7% (w/v) crystal violet (Sigma, St. Louis, MO). After a 15 min incubation at room temperature, the fluid contents of each well were decanted and the well washed three times with deionized water. To determine the extent of biofilm formation, 2 ml of 95% ethanol was added to each well, and the plate was rocked gently for 15 min. A 1.5 ml portion of this ethanol solution was then transferred to a new 24-well tissue culture plate, and the absorbance at 600 or 570 nm was measured using a SPECTRAFluor Plus fluorometer (Tecan, Research Triangle Park, NC).

B. *E. coli*

E. coli strains were grown overnight in 5 ml LB broth, supplemented with chloramphenicol as appropriate. A 0.5 ml portion of the overnight culture was used to inoculate 4.5 ml LB (with chloramphenicol as necessary) containing 5 µl CopyControl induction solution. Cultures were induced with vigorous agitation for 5 hr, after which all cultures were adjusted to the same density by addition of LB broth. A 20 µl portion of each induced culture was used to inoculate 2 ml LB broth containing 2 µl induction solution in a 24-well tissue culture plate. The remainder of the crystal violet-based assay was conducted as described above for *M. catarrhalis*.

IV. Electron Microscopy

A. Transmission Electron Microscopy

After *M. catarrhalis* cells were grown for 3 days on the Sorbarod filter, the BHI growth medium was replaced by TEM prefixative consisting of 75 mM lysine monohydrochloride (Sigma), 2% (v/v) paraformaldehyde (Electron Microscopy Sciences, Fort Washington, PA), and 2.5% (v/v) glutaraldehyde (Sigma) in 0.1 M sodium cacodylate buffer (Electron Microscopy Sciences). Prefixative was pumped onto the filter at 0.1 ml/min for 1 h at 37°C. Then, TEM fixative consisting of 2% paraformaldehyde and 2.5% (v/v)

glutaraldehyde in 0.1 M sodium cacodylate was pumped onto the filters for 2 h at a rate of 0.1 ml/min at 37°C. The filter was then rinsed three times for 10 min in 0.1 M. sodium cacodylate buffer at room temperature after which 1% osmium tetroxide in this buffer (Electron Microscopy Sciences) was added and the filter was rocked gently for 90 min. The filter was then washed with distilled water, dehydrated with ethanol, and embedded in Spurr resin (Polysciences, Warrington, PA), which was polymerized at 60°C overnight. Sections for TEM were cut at 80 nm with a diamond knife (Micro Star, Huntsville, TX) and picked up on copper 200-mesh thin-bar grids (Electron Microscopy Sciences). The grids were stained with uranyl acetate and lead citrate and observed with a JEOL 1200EX II transmission electron microscope. TEM was performed by Dennis Bellotto, Molecular and Cellular Imaging Facility, UT Southwestern.

B. Scanning Electron Microscopy

Samples were fixed, postfixed with osmium tetroxide, and dehydrated as for TEM, then dried in a Tousimis Samdri-795 critical point drier. The samples were then coated with gold using a Denton 502A sputter coat and examined using a JEOL 840A scanning electron microscope. SEM was performed by George Lawton, Molecular and Cellular Imaging Facility, UT Southwestern.

C. Cryoimmunoelectron Microscopy

Biofilm-grown *M. catarrhalis* cells in the Sorbarod filter were pre-fixed as described above except that the prefixative was composed of 2% (v/v) paraformaldehyde, 0.2% (v/v) glutaraldehyde, and 75 mM lysine monohydrochloride in PBS, pH 7.3. The cells on the filter were then fixed with 2% (v/v) paraformaldehyde and 0.2% (v/v) glutaraldehyde in PBS, pH 7.3, at 37°C for 2 h as described above. Subsequently, they were embedded in 10% (w/v) gelatin as described previously (281) except that the gelatin was not fixed. After centrifugation, the gelatin was solidified on ice and the blocks were prepared for ultramicrotomy and infused with 2.3 M sucrose. Ultrathin sections were obtained and immunolabeled as described previously (282) with minor modifications. In particular, 10% (v/v) goat serum was used in the blocking buffer in place of 1% (w/v) bovine serum albumin and immunolabeling was carried out with a 1:1 dilution of MAb 5D2 or a 1:10 dilution of MAb 17C7 for 2 h and a 1:15 dilution of goat anti-mouse IgG-18-nm colloidal gold (Jackson ImmunoResearch Laboratories, West Grove, PA) for 1 h. Sections were stained with uranyl acetate and embedded in methyl cellulose according to a modification of the method of Tokuyasu (301) introduced by Griffiths *et al.* (117). Samples were viewed and photographed with a Zeiss 902 electron microscope. Cryoimmunoelectron microscopy was performed in collaboration with Dr. Joseph St. Geme and Marilyn Levy, Department of Molecular Microbiology, Washington University School of Medicine.

V. Bacterial Antigen Preparation

A. Whole cell lysates

M. catarrhalis cells were either scraped from agar plates or centrifuged from a broth culture and suspended in 1 ml PBS. This very dense suspension was used to inoculate 5 ml PBS to obtain a suspension that yielded a reading of 300 Kletts. The bacteria in this latter suspension were pelleted by centrifugation and resuspended in 1 ml PBS. A 0.5 ml volume of 3X digestion buffer (0.1875 M Trizma base, 30% (v/v) glycerol, 6% (w/v) SDS, pyronin y for color, pH 6.8) was added, and the lysates were heated at 100°C for 10 min before being used in SDS-PAGE or stored at -20°C.

A 0.5 ml portion of an overnight culture of recombinant *E. coli* was used to inoculate 5 ml LB supplemented with chloramphenicol (15 µg/ml) and 5 µl CopyControl induction solution (Epicentre). This culture was grown at 37°C for 5 h with vigorous agitation. Bacteria were collected by centrifugation and suspended in 333 µl PBS and 167 µl 3X digestion buffer.

B. Preparation of extracts containing outer membrane vesicles

Outer membrane vesicles were isolated according to the broth culture supernatant method of Murphy and Loeb (221). A 10 ml culture of *M. catarrhalis* was grown in BHI for 4 h in a 125 ml Erlenmeyer flask. Four drops of this culture were added to 1 L BHI in a 2.8-

L Fernbach flask; this flask was incubated at 37°C overnight with aeration. The bacteria were collected by centrifugation and suspended in 30 ml EDTA buffer (0.05M Na₂HPO₄, 0.15 M NaCl, 0.01 M EDTA (ethylenediamine tetraacetic acid), pH 7.4). Bacteria were thoroughly suspended using a 15 ml glass homogenizer and poured into a 225 ml Erlenmeyer flask containing enough 3 mm diameter glass beads to cover the bottom of the flask. The centrifuge bottles were rinsed with a total of 30 ml EDTA buffer; this wash was also homogenized and added to the rest of the bacterial suspension. The flask was then agitated vigorously in a gyratory water bath at 55°C for 45 min before the suspension was transferred to 50 ml screw-cap centrifuge tubes. The flask and glass beads were washed 3 times with EDTA buffer, and all washes were also added to the centrifuge tubes. The suspension was centrifuged at 10,000 x *g* for 15 min to pull down whole cells and cell debris. The supernatant fluid was transferred to very clean screw-cap centrifuge tubes and centrifuged at 39,000 x *g* for 90 min. The supernatant was removed and the pellet containing the outer membrane vesicles was resuspended in PBS to a total volume of 150 µl. Protein content was measured using either the Bradford assay (Bio-Rad Protein Assay, Bio-Rad, Hercules, CA) or the NanoOrange Protein Quantification Kit (Molecular Probes, Eugene, OR) according to the manufacturer's instructions.

A similar protocol was followed to isolate outer membrane vesicles from Sorbarod-grown *M. catarrhalis*. Bacteria were grown as continuous-culture biofilms for 3 days, at which point the Sorbarod filter was forced from its silicone tubing, using a sterile P-1000 pipet tip into 5 ml EDTA buffer in a 15 ml snap-cap tube. The Sorbarod filter was vortexed vigorously until it disintegrated; the suspension was added to the flask with glass beads,

while care was taken to discard the bulk of the cellulose remnants. The remainder of the outer membrane vesicle isolation proceeded as above, except that an extra centrifugation at 10,000 x g for 10 min was performed to remove excess cellulose debris. Approximately 6-9 Sorbarod biofilms were used for each outer membrane vesicle isolation.

C. Lipooligosaccharide preparation

To prepare *M. catarrhalis* LOS for analysis, 10 μ l of proteinase K (10 mg/ml) was added to 75 μ l of a whole cell lysate and incubated at 56°C for 1 h. The lysate was then heated at 100°C for 5 min and stored at -20°C.

VI. SDS-PAGE

Samples for SDS-PAGE analysis were mixed with 3X digestion buffer (described above) and heated at 100°C for 10 min. Gels were cast and samples were separated using the Mini-PROTEAN 3 cell (Bio-Rad). Alternatively, for better separation of proteins, the larger Hoefer SE 600 gel electrophoresis unit (16 cm) (Amersham Pharmacia Biotech, Piscataway, NJ) or the PROTEAN II cell (20 cm) (Bio-Rad) were used. Polyacrylamide gels were made using a 30% acrylamide/bis solution, 37.5:1 (Bio-Rad). The stacking gel was composed of 4% (w/v) acrylamide, 0.125 M Tris-HCl (pH 6.8) and 0.1% (w/v) SDS. The separating gel consisted of 7.5% to 15% (w/v) acrylamide (depending on the application), 0.375 M Tris-HCl (pH 8.8), and 0.1% (w/v) SDS. All gels were polymerized with 0.1% (w/v) ammonium

persulfate (APS) and 0.1% (w/v) tetramethylethylenediamine (TEMED). The running buffer was composed of 0.025 M Tris-HCl (pH 8.3), 0.192 M glycine, and 0.1% (w/v) SDS.

All SDS-PAGE was conducted until the dye front was near the bottom of the gel, or had completely run off, depending on the application. Mini-gels were electrophoresed at 20 mA constant current per gel. Hoefer gels were electrophoresed at 40 mA until samples had entered the separating gel, at which point the current was increased to 55 mA. PROTEAN II gels were electrophoresed at 40 mA until the samples had entered the separating gel, after which the current was raised to 75 mA.

To visualize proteins, SDS-PAGE gels were soaked in Coomassie blue stain (0.1% (w/v) Coomassie brilliant blue, 10% (v/v) acetic acid, 25% (v/v) methanol) for at least 30 min. Gels were then placed in destain (10% (v/v) acetic acid, 10% (v/v) methanol, and 6% (v/v) glycerol) until the excess stain was released. Gels were dried using a Tut's Tomb gel drying frame (Research Products International Corp., Mount Prospect, IL), which encases the gel in cellophane.

VII. Separation and Detection of Lipooligosaccharides and Polysaccharides

A. Tricine SDS-PAGE

To determine the presence or the apparent mass of *M. catarrhalis* LOS or polysaccharides, samples were separated using tricine SDS-PAGE as published by Lesse *et al* (179). The stacking gel was prepared by the addition of 1 ml 49.5:3 acrylamide (49.5%

total acrylamide, 3% bisacrylamide), 3.1 ml gel buffer (3.0 M Tris base, 0.3% SDS, pH 8.45), and 8.4 ml water. The separating gel was made by mixing 16.6 ml 49.5:6 acrylamide (49.5% total acrylamide, 6% bisacrylamide), 16.6 ml gel buffer, 5.2 ml glycerol, and 11.5 ml water. Tricine SDS-PAGE gels were polymerized by using 0.1% APS and 0.1% TEMED. The anode buffer (0.2 M Tris base, pH 8.9) differed from the cathode buffer (0.1 M Tris base, 0.1 M tricine, 0.1% SDS, pH 8.25). Electrophoresis was performed at 30 V until samples entered the separating gel. Then, samples were electrophoresed at 102 V until the dye front was a few mm from the bottom of the gel. Alternatively, these samples were separated using 15% SDS-PAGE.

B. Silver stain

The method of Tsai and Frasch (305) was used to stain LOS and polysaccharides. These steps were all carried out in with gentle agitation using a rocker platform. Polyacrylamide gels were soaked for at least 1 h in fixative (40% (v/v) ethanol and 5% (v/v) glacial acetic acid) in a glass container. The gel was then placed in fixative containing freshly prepared 0.7% (w/v) periodic acid for 7 min. Following 3 washes with water lasting 15 min each, the gel was stained with a freshly prepared silver nitrate solution (0.019 M sodium hydroxide, 1.33% (w/v) ammonium hydroxide, and 0.67% (w/v) silver nitrate) for 10 min. The gel was washed again 3 times with water, for 10 min per wash. Then, the gel was soaked in developer (0.005% (v/v) citric acid and 0.019% formaldehyde (v/v)) until the desired intensity was achieved. This development process was halted by placing the gel in

1% (v/v) acetic acid for 10 min. To preserve the stained gel, the gel was placed in a solution of 20% methanol and 3% glycerol for at least 30 min. Gels were encased in cellophane for archiving as described above.

VIII. MAbs and Western Blot Analysis

Monoclonal antibody (MAb) 17C7, reactive with both the UspA1 and UspA2/UspA2H proteins (6), MAb 24B5, reactive with the UspA1 protein (174), MAb 10F3, reactive with the CopB protein of *M. catarrhalis* strain O35E (129), MAb 5D2, reactive with the Hag protein (235), and MAb 8E7, reactive with *M. catarrhalis* LOS (148), have been described. Human IgD κ chain myeloma protein (The Binding Site, San Diego, CA) was used as the source of IgD for the IgD binding assays. Western blot analysis was performed using either affinity-purified and radioiodinated goat anti-mouse IgG (174) or horseradish peroxidase-conjugated goat anti-human IgG (Jackson ImmunoResearch, West Grove, PA) as the secondary antibody to detect mouse MAbs. The goat anti-mouse IgG was obtained from Dr. Ellen S. Vitetta, Cancer Immunobiology Center, UT Southwestern. To detect human IgD, horseradish peroxidase-conjugated goat anti-human IgD (Biosource International, Camarillo, CA) was used as the secondary antibody. Horseradish peroxidase-antibody conjugates were detected by chemiluminescence with Western Lightning Chemiluminescence Reagent Plus (New England Nuclear, Boston, MA).

IX. DNA Preparation

A. Preparation of *M. catarrhalis* chromosomal DNA

For most experiments, *M. catarrhalis* DNA was isolated using the Easy-DNA kit (Invitrogen) and following the manufacturer's protocol. Chromosomal DNA for nucleotide sequencing was prepared using the UltraClean Microbial DNA Isolation Kit (MoBio Laboratories, Inc., Solana Beach, CA) according to the manufacturer's instructions, with minor exceptions. The amount of *M. catarrhalis* culture used per column was 2.5 ml, and at least two columns (5 ml culture) were needed to obtain sufficient DNA for sequencing. DNA was eluted into sterile, distilled water, and concentrated using a SpeedVac Concentrator (Savant/Scientific Resources Southwest, Inc., Stafford, TX), to a volume of approximately 25 μ l.

To obtain O35E chromosomal DNA containing transposon insertions for the purpose of transforming heterologous *M. catarrhalis* strains, approximately 5000 transposon insertion mutant colonies were pooled together into 500 ml TH broth and grown for 4 h. The bacteria were pelleted by centrifugation (3,800 x *g* for 10 min) and resuspended in 50 ml lysis buffer (40 mM Tris (pH 8.0), 20 mM sodium acetate, 1 mM EDTA, and 1% (w/v) SDS) before addition of 16.5 ml 5 M NaCl. This mixture was then centrifuged at 3,800 x *g* for 20 min. The supernatant was transferred to a 50 ml conical tube and incubated on ice for 30 min before centrifugation at 2,500 x *g* for 10 min. Four phenol/chloroform extractions were performed on the supernatant, followed by a single chloroform/isoamyl alcohol (IAA)

extraction. One volume of 100% ethanol was added to precipitate the DNA; this mixture was incubated at -20°C for two days. The precipitated chromosomal DNA was pelleted by centrifugation, washed once with 70% ethanol, and resuspended in water. This protocol was performed by Nikki Wagner, Department of Microbiology, UT Southwestern.

B. Plasmid isolation

Plasmids were isolated from *E. coli* using either the QIAprep Spin Miniprep Kit (Qiagen, Valencia, CA) or the Wizard *Plus* Minipreps DNA Purification System (Promega, Madison, WI) according to the manufacturer's instructions. Briefly, both methods relied on the alkaline lysis method of plasmid extraction followed by binding of the plasmid to a column and elution with water or Tris-HCl buffer.

X. Polysaccharide Analysis

A. Isolation of soluble polysaccharides from *M. catarrhalis* biofilms

Approximately 2 L of effluent from Sorbarod biofilms collected over the span of one week was centrifuged at 10,000 x g for 10 min to remove whole bacterial cells. A 0.1 M solution of Cetavlon (hexadecyltrimethylammonium bromide) was added to the supernatant to a final concentration of 0.005 M and this mixture was stirred overnight at 4°C. This mixture was then centrifuged at 10,000 x g for 10 min. The pellet was retained and mixed

with 40 ml 0.4 M NaCl vigorously for 20 min on ice. Following another centrifugation at 10,000 x *g* for 10 min, the supernatant was transferred to a clean flask. Two volumes of cold 95% ethanol were added to the supernatant, which was kept overnight at -20°C. This suspension was centrifuged at 10,000 x *g* for 30 min at 4°C; the supernatant was discarded and the pellet was dissolved in 40 ml distilled water and transferred to a clean flask. An equal volume of phenol was added; the mixture was stirred vigorously at room temperature for 30 min before being subjected to centrifugation at 10,000 x *g* for 10 min at 4°C. This phenol extraction was repeated until the phenol:aqueous phase interface was clean. The extracted aqueous phase was dialyzed (Spectra/Por 7 dialysis tubing, 10,000 MW cutoff, Spectrum Laboratories Inc., Rancho Dominguez, CA) against 4 L sterile, distilled water at 4°C for 2 days, with the water changed once after 24 h. The contents of the dialysis tubing were combined with NaCl to a final concentration of 0.1 M NaCl, then 2 vol ethanol was added. Following storage at -20°C overnight, the mixture was centrifuged at 10,000 x *g* for 30 min at 4°C. The A_{280} of the supernatant was determined to be less than 0.1 and it was discarded. The pellet was suspended in 8 ml distilled water and ultracentrifuged at 105,000 x *g* for 3 h to remove LOS. The majority of the supernatant was gently transferred to a 15 ml centrifuge tube, leaving the pellet intact. This supernatant was frozen at -20°C and lyophilized. Approximately 3 mg putative polysaccharide was obtained from this protocol.

B. Characterization of *M. catarrhalis* polysaccharide

M. catarrhalis polysaccharides were separated by tricine SDS-PAGE as described above. *H. ducreyi* LOS, provided by Dr. Joseph Nika, Department of Microbiology, UT Southwestern, was also included as a positive control. Polysaccharides and LOS were visualized using the Tsai-Frasch silver stain (described above). To determine whether the putative polysaccharide was actually DNA, 50 µg of polysaccharide (5 µg/µl) was treated with 2 µL of DNase (1 mg/ml). The treated polysaccharide was separated on a 2% (w/v) agarose gel, a 15% (w/v) polyacrylamide gel, or a 7.5% (w/v) polyacrylamide TBE gel with ethidium bromide incorporated. Nucleic acids were visualized using ultraviolet light, while polysaccharides were visualized using the Tsai-Frasch stain.

A 1 mg portion of the putative polysaccharide was sent to Dr. Roberta Merkle at the Complex Carbohydrate Research Center at the University of Georgia for glycosyl composition analysis. The sample was analyzed by Trina Abney for monosaccharide composition by preparing the trimethylsilyl (TMS) derivatives of the methyl glycosides followed by combined gas chromatography/mass spectrometry (GC/MS) analysis. TMS methyl glycosides were prepared from the sample (0.2 mg) by methanolysis in 1 M HCl in methanol at 80°C (18-22 h), followed by re-*N*-acetylation with pyridine and acetic anhydride (for detection of amino sugars). The sample was then treated with Tri-Sil. These procedures were accomplished as previously described (208, 337). GC/MS analysis of the TMS methyl glycosides was performed on an HP 5890 GC interfaced to a 5970 MSD, using a Supelco DB5 fused silica capillary column.

XI. Transformation Protocols

A. Electroporation of *M. catarrhalis*

Electroporation of *M. catarrhalis* was accomplished as in Helminen *et al* (131). A logarithmic-phase 20 ml culture of *M. catarrhalis* cells (125 Kletts; approximately $2-4 \times 10^8$ cfu/ml) was pelleted by centrifugation and washed three times with 10% (v/v) glycerol. The final pellet was suspended in 200 μ l 10% glycerol and kept on ice. A 20 μ l portion of this suspension was mixed with 5 μ l DNA (approximately 25-100 ng) and transferred into the microelectroporation chamber (Cel-Porator Electroporation System; GIBCO-BRL, Gaithersburg, MD). Electroporation was carried out using a field strength of 16.2 kV over a distance of 0.15 cm. A 1 mL volume of BHI broth was immediately added, and the suspension was incubated at 37°C for 1 h with aeration. Serial dilutions were plated on BHI or TH agar containing appropriate antibiotics as necessary.

B. Electroporation of *E. coli*

E. coli strains were grown in LB broth and washed with 10% (v/v) glycerol essentially as above. Aliquots of 50 μ l were stored at -70°C. A thawed aliquot was mixed with a 5 or 10 μ l portion of DNA (approximately 25-100 ng) and transferred to an Eppendorf Electroporation cuvette (Fisher Scientific). Bacteria were electroporated in the *E. coli* Pulser

(Bio-Rad) using a setting of 1.6 kV. Cells were immediately suspended in 0.5 ml SOC medium (Invitrogen) and incubated at 37°C for 1 hr before plating on LB agar containing appropriate antibiotics.

C. Chemical transformation of *E. coli*

Aliquots of commercially available chemically competent *E. coli* were thawed on ice. A 5 or 10 µl volume of DNA (approximately 25-100 ng), depending on the application, was gently mixed with the *E. coli* cells and allowed to sit on ice for 30 min. *E. coli* was heat-shocked at 42°C for 30 s and incubated on ice for 2 min before 0.5 ml room-temperature SOC broth was added. Bacteria were grown at 37°C for 1 hr and plated on LB medium with appropriate antibiotics.

D. Natural transformation of *M. catarrhalis*

This method was adapted from that described by Juni (155) for use with *Moraxella osloensis*. A 4 µl volume of *M. catarrhalis* chromosomal DNA (containing approximately 1 µg DNA) was spotted onto the surface of a BHI agar plate. A toothpick was then used to immediately transfer one or two *M. catarrhalis* colonies to the DNA spot. Using the same toothpick, the DNA and bacteria were spread over a circular area approximately 2 cm in diameter. Following incubation at 37°C with 95% air-5% CO₂ for 6 h, the bacterial growth was suspended in 300 µl BHI broth in a 1.5 ml Eppendorf centrifuge tube, diluted serially in

BHI broth, and spread onto BHI agar plates (containing an appropriate antibiotic supplement as necessary).

XII. Transposon Mutagenesis

Transposon mutagenesis of *M. catarrhalis* was accomplished using the EZ::TN<KAN-2> transposome kit (Epicentre) according to the manufacturer's protocol. Briefly, *M. catarrhalis* was grown in BHI broth to a density of 1×10^8 cfu/ml. The bacteria were washed three times with 10% (v/v) glycerol and resuspended in 1/100 volume of 10% glycerol. A 20 μ l portion of these *M. catarrhalis* cells was electroporated with 1 μ l of the transposome and then inoculated into 0.5 ml BHI broth. After 3 h incubation at 37°C, the cells were plated on BHI agar supplemented with kanamycin. Kanamycin-resistant transformants were screened for loss of biofilm formation ability by transferring a swatch of bacterial growth from a BHI-kanamycin agar plate into a 24-well tissue culture plate containing 2 ml BHI broth per well, and proceeding with the crystal violet-based assay.

To obtain transposon mutants of *M. catarrhalis* strains O46E and ETSU-9, which are not amenable to direct mutagenesis with the transposome kit, *M. catarrhalis* strain O35E was mutagenized as above. Transposon mutants were scraped together, and chromosomal DNA was isolated from these pooled mutants as described above in "Preparation of *M. catarrhalis* DNA". O46E and ETSU-9 were transformed using the agar plate technique with 10 μ l (approximately 1 μ g) of this pooled mutant DNA. Kanamycin-resistant transformants were screened for loss of the ability to form biofilms as above.

XIII. Recombinant DNA Techniques

A. DNA sequencing and analysis

Plasmids and PCR products were sequenced with a model 373A or model 377 automated DNA sequencer (Applied Biosystems, Foster City, CA). Chromosomal DNA was shipped on dry ice to Lone Star Labs, Inc. (Houston, TX) for automated direct sequencing. DNA sequence information was analyzed by using the MacVector analysis package (version 6.5, Oxford Molecular Group, Campbell, CA).

B. Southern blot analysis

M. catarrhalis chromosomal DNA was digested to completion with restriction endonucleases (New England Biolabs, Beverly, MA) and subjected to electrophoresis in a 0.7% (w/v) agarose gel. The gel was then immersed twice in denaturation solution (0.5 M NaOH, 1.5 M NaCl) for 15 minutes at room temperature, followed by two incubations in renaturation solution (1 M Tris (pH 7.4), 1.5 M NaCl) for 15 min each. A nitrocellulose (Schleicher & Schuell, Keene, NH) or positively-charged nylon membrane (Roche, Indianapolis, IN) was cut to fit the gel. Capillary transfer using 20X SSC (3 M NaCl, 300 mM sodium citrate) was used to transfer DNA from the gel to the membrane (262). After a 4 h-16 h transfer period, the gel was examined under ultraviolet light to ensure that transfer had

occurred. DNA was crosslinked to the membrane using a UV Stratalinker 1800 (Stratagene, La Jolla, CA) on the auto cross link setting.

Two different methods were employed for DNA probe labeling and hybridization. To prepare a radioactive probe, a PCR amplicon or gel-purified restriction digest was heated at 100°C for 5 min and quickly transferred to ice to denature the probe. The Random Primed DNA Labeling Kit (Roche) was used to label the probe with [$\alpha^{32}\text{P}$]-dCTP (PerkinElmer, Boston, MA) according to manufacturer's instructions. The membrane was immersed in 5 ml prehybridization solution (50X formamide, 5X Denhardts, 5X SSC, 0.1% SDS, 125 μl boiled salmon sperm DNA (2 mg/ml)) and incubated at 42°C for 30 min in a hybridization oven. The prehybridization solution was then removed, and 5 ml hybridization solution (prehybridization solution plus 0.5 g dextran sulfate and 1×10^7 CPM/min probe) was added to the nitrocellulose membrane. Hybridization was performed at 42°C overnight; then, the membrane was rinsed 3 times with 2X SSC for 15 min per wash. The membrane was dried and exposed to Fuji Medical X-ray film (Fujifilm/Diagnostic Imaging, Dallas, TX).

The DIG High Prime DNA Labeling and Detection Starter Kit II (Roche) was used to label DNA probes with digoxigenin (DIG) for chemiluminescent detection. Probes were labeled by the random priming method according to the manufacturer's instructions; alternatively, 1 μl DIG-dUTP was added to the PCR reaction to label the probe. The Southern blot was performed as specified by the manufacturer. Briefly, the nylon membrane was incubated with DIG Easy-Hyb granules (10 ml/100 cm^2 membrane). The melting temperature of the probe was calculated using the formula $T_m = 49.82 + 0.41(\%G+C) - (600/l)$, where l = the length of the probe in nucleotides. The hybridization temperature was

20 to 25°C below the melting temperature. The membrane was hybridized in DIG Easy-Hyb granules (3.5 ml/100 cm²) plus the denatured probe for at least 4 h. Two stringent washes were carried out at 65°C in 0.5X SSC for 15 min. The remaining steps were performed using reagents from the DIG Wash and Block Buffer Set (Roche). Chemiluminescence was initiated by addition of CSPD (disodium-3-(4-methoxyspiro(1,2-dioxetane-3,2'-(5'-chloro)tricyclo[3,3.1.1^{3,7}]decan)-4yl) phenyl phosphate). Blots were exposed to Fuji film as above.

XIV. Identification of the Site of the Transposon Insertion in Mutant 20A3

Rescue marker cloning was used to clone the transposon and its flanking chromosomal DNA from mutant 20A3. Southern blot analysis of 20A3 chromosomal DNA showed that the transposon was located in a *Nco*I fragment approximately 2000 nt in length. Agarose gel purification (GeneClean III Kit, Qbiogene, Carlsbad, CA) was used to isolate 20A3 chromosomal DNA *Nco*I fragments ranging from 1.6 to 3 kb in size. These fragments were ligated with the *Nco*I-linearized cloning vector pACYC184. The resulting ligation mixture was used to transform *E. coli* DH5 α , which was plated on LB agar supplemented with kanamycin. The presence of the transposon within the plasmid from the resulting kanamycin-resistant colonies was confirmed by PCR using the primers 5'-GGTTGATGAG AGCTTTGTTGTAGG-3' and 5'-CTCAAAATCTCTGATGTTACATTGC-3'. The DNA insert in one of these plasmids was subjected to nucleotide sequence analysis using the

primers 5'-GGCATCAGCACCTTGTCG-3' and 5'-TTCGTCTCAGCCAATCCC-3', which bind to pACYC184 on opposite sides of the *NcoI* restriction site.

XV. Tissue Culture Protocols

All cell lines used in these experiments were grown at 37°C under an atmosphere of 95% air-5% CO₂. All tissue culture media was supplemented with 10% (v/v) fetal calf serum and 1:100 GlutaMAX (GIBCO-BRL). Cells were passaged using trypsin-EDTA as necessary. Chang human conjunctival epithelial cells (Wong-Kilbourne derivative) were obtained from ATCC (CCL-20.2, clone 1-5c-4). Chang cells were grown in Medium 199. The 9HTEo- tracheal epithelial cell line (118), the 16HBE14o- bronchial epithelial cell line (118), and the NCI-H292 bronchial epithelial cell line (ATCC CRL 1848) were all generous gifts from Dr. Joseph St. Geme, Department of Molecular Microbiology, Washington University School of Medicine. MEM (minimal essential medium Eagle; Mediatech Cellgro/Fisher) tissue culture medium was used for growth of 9HTEo- and 16HBE14o- cells, and RPMI-1640 (Mediatech Cellgro/Fisher) was used for growth of NCI-H292 cells. HEP-2 human laryngeal carcinoma cells were purchased from ATCC (CCL-23) and were grown in DMEM media.

XVI. Attachment Assays

A. *M. catarrhalis*

The ability of *M. catarrhalis* to attach to human epithelial cells *in vitro* was measured as described previously (5). A 24-well tissue culture plate was seeded with $2-4 \times 10^5$ eukaryotic cells per well and was incubated overnight before use. *M. catarrhalis* strains were grown in 10 ml of BHI broth until mid-logarithmic phase was reached (approximately $2-4 \times 10^8$ cfu/ml, or 125 Klett units). Bacteria were collected by centrifugation and suspended in 5 ml PBS containing 0.15% (w/v) gelatin (PBS-G). This suspension was adjusted to a density of 210-230 Klett units by addition of PBS-G. Epithelial cell monolayers were inoculated with 25 μ l of this suspension; the tissue culture plate was then gently swirled to distribute the bacteria. The tissue culture plate was centrifuged for 5 min at 150 x g, then each well was gently washed 5 times with PBS-G to remove nonadherent bacteria. Epithelial cells were released by the addition of trypsin-EDTA and suspended in 0.5 ml PBS-G. This suspension was serially diluted in PBS-G and plated on BHI to determine the number of adherent *M. catarrhalis*. Adherence was calculated as the percentage of bacteria attached to the Chang cells relative to the initial inoculum.

B. *E. coli*

To measure attachment of recombinant *E. coli* to Chang cells, a 5 ml overnight broth culture was added to 20 ml fresh LB broth containing 25 μ l of CopyControl induction solution and this culture was grown at 37°C for 3 h with agitation at 300 rpm. A 10 ml portion of this induced culture was removed and the bacterial cells were pelleted by centrifugation, washed with PBS-G, and suspended in 1.5 ml PBS-G. This very dense suspension was used to inoculate a 5 ml volume of PBS-G to obtain a suspension that yielded a reading of 300 Klett units. A 25 μ l amount of this latter suspension was added in duplicate to a monolayer of Chang cells in fresh M-199 tissue culture medium in a 24-well tissue culture plate. The tissue culture plate was centrifuged for 5 min at 150 x g to promote bacterial attachment to the Chang cell monolayer. After 5 washes with PBS-G to remove nonadherent bacteria, the monolayer was detached by the addition of trypsin-EDTA, diluted, and spread onto LB agar plates. Adherence was determined as described above.

XVII. Hemagglutination Assays

Overnight 4-ml cultures of *M. catarrhalis* were centrifuged at 7,500 x g for 8 min and resuspended in PBS at room temperature to a density of 300 Klett units. A 50- μ l portion of this suspension and serial twofold dilutions of this suspension were added in triplicate to a 96-well U-bottom Costar polypropylene plate (Fisher Scientific). Citrated human blood (Rockland, Gilbertsville, PA) was centrifuged at 1,000 x g, and a 2% (v/v) suspension of

erythrocytes in PBS was prepared. A 50- μ l portion of the erythrocyte suspension was then added to each well, and the microtiter plate was gently agitated on a Vortex mixer for 30 s. Hemagglutination was recorded photographically after 15 min.

XVIII. Autoagglutination Assays

M. catarrhalis cells scraped from the surface of BHI agar plates were suspended in 1 ml of PBS (pH 7.3). Portions of this suspension were added to 4 ml of PBS to obtain a suspension that yielded a reading of 400 Klett units in a glass tube. Autoagglutination was measured as the decrease in Klett units over time.

XIX. Construction of and Enrichment for Biofilm-Forming Transformants

The biofilm-negative *M. catarrhalis* strain O35E was transformed with chromosomal DNA from the biofilm-positive *M. catarrhalis* strain O46E using the agar plate-based method described above. To enrich for biofilm-positive transformants, a 100 μ l portion of these bacteria (from the 300 μ l suspension) was added to a 24-well tissue culture plate containing 2 ml BHI broth and this plate was incubated overnight at 37°C. The broth was then removed by aspiration and each well was washed once with sterile BHI. Fresh BHI was added, and the plates were incubated for an additional 6 h at 37°C. After removing the broth again, adherent bacteria were scraped from the walls of each well, serially diluted, and spread onto BHI agar plates to obtain isolated colonies. Individual colonies were then grown as

patches on BHI agar and used to inoculate 24-well tissue culture plates to measure biofilm formation as described above.

XX. Cell Surface Expression Assay

M. catarrhalis strains were scraped from agar plates and suspended in 1 ml PBS plus 10% (v/v) FCS (PBS-FCS). This very dense suspension was used to inoculate 5 ml of PBS-FCS in a glass tube to obtain a suspension that yielded a reading of 105-115 Klett units. A 100 μ l portion of this suspension was transferred to a 1.5 ml tube in triplicate. A 1 ml portion of MAb 17C7 hybridoma culture supernatant was added to each tube and vortexed. These tubes were rocked for 1 hr at 4°C before pelleting the cells by centrifugation. The supernatant was carefully removed, and the pellet was washed once with 1 ml PBS-FCS; the bacteria were again collected by centrifugation before resuspension in 1 ml PBS-FCS. Radioiodinated goat anti-mouse IgG was added to each tube (10^6 CPM/tube), and all tubes were rocked for 1 hr at 4°C. A 25 μ l portion of a very dense suspension of *E. coli* DH5 α was added to each tube to increase pellet size. Tubes were centrifuged for 2 min to pellet the bacteria; pellets were washed 4 times with 1 ml PBS-FCS. The final pellet was suspended in 0.5 ml triple detergent (10 mM Tris-hydrochloride, pH 7.8, 1% (v/v) Triton X-100, 150 mM NaCl, 10 mM EDTA, 0.2% (w/v) sodium deoxycholate, and 0.1% (w/v) SDS) (122) and transferred to disposable glass tubes for measurement in a gamma counter (LS 6500 Multi-Purpose Scintillation Counter, Beckman Coulter, Fullerton, CA).

XXI. PCR

Polymerase chain reaction (PCR) amplification was achieved by use of *ExTaq* DNA polymerase (PanVera, Madison, WI) or *Taq* DNA polymerase (Promega) according to the manufacturer's instructions. PCR amplicons were generated in a Peltier-effect cyclor with a heated lid (MJ Research, Inc., Incline Village, NV) over 30 cycles of 94°C (denaturation) for 1 min, 50-55°C (annealing) for 1 min, and 72°C (extension) for 1 min/kb of the desired product. The final cycle included an extra 10 min extension period to ensure the production of complete amplicons with T/A overhangs. For cloning or site-directed mutagenesis, the high-fidelity proofreading *Pfu* DNA polymerase (Stratagene) was used. The same cycle parameters were used for *Pfu*, except that extension times were 3 min/kb, and the final extension generated blunt ends.

XXII. Analysis of Different Colony Phenotypes Arising from Sorbarod-Grown Biofilms

To confirm that different organisms isolated from Sorbarod biofilms and effluents were *M. catarrhalis*, portions of the *uspA1* and *hag* genes were amplified by PCR. Chromosomal DNA from 20 colonies of each different phenotype was isolated using the Easy-DNA kit as above, except that all reactions were carried out in one-third of the manufacturer's recommended volumes. A 450 nt portion of *uspA1* was amplified using the primers 5'-CCTTGGCAAAAGTAAGTG-3' and 5'-GGGATCCGACCATTGTGATAACCTGAACC-3', and a 500 nt portion of the *hag* gene was amplified using the primers 5'-TAG

CAGGTAAGCACTCTGG-3' and 5'-TTATCCGACAGCTTCGAC-3'. The presence of the expected amplicons, as detected by agarose gel electrophoresis, was indicative of *M. catarrhalis*.

General examination of colony phenotypes was conducted using a Bausch & Lomb dissecting microscope. Photographs of colonies on agar plates or in tissue culture plates were taken using the AlphaImager 2000 Documentation and Analysis System (Alpha Innotech Corporation, San Leandro, CA). Photographs of single colonies were taken under 10x objective lens magnification using an Olympus IMT-2 inverted microscope. Photographs of floating mats of *M. catarrhalis* in 24-well tissue culture plates were also taken using this same microscope.

XXIII. Molecular Genetic Techniques

A. Construction of isogenic mutants

(i) Construction of *uspA1* and *uspA2* mutants

Isogenic mutants of *uspA1* were constructed using either plasmid pUSPAKAN (confers kanamycin resistance) (5) or pELU1CAT (confers chloramphenicol resistance) (175) to transform the desired strain by either electroporation or plate transformation. These plasmids were constructed by Dr. Christoph Aebi and Dr. Eric Lafontaine, respectively, of the Department of Microbiology, UT Southwestern. Isogenic *uspA2* mutants were

constructed either using pELU244SPEC (confers spectinomycin resistance) (174) or pELU244ZEO (confers Zeocin resistance) (235). Both of these plasmids were constructed by Dr. Lafontaine. The only exception is the construction of strain ETSU-9.2H, which is detailed below.

(ii) Construction of *hag* mutants

With the working assumption that the 200 kDa protein of *M. catarrhalis* strain 4223 (265) was likely the same protein described phenotypically by Scott and co-workers (92), the nucleotide sequence of the gene from *M. catarrhalis* strain 4223 encoding the 200 kDa protein (264) was used to design oligonucleotide primers for the PCR-based amplification of the *hag* gene. The oligonucleotide primers 5'-ATTCTAGAGCTCAGGGTGATGCCTCGATTGCC-3' and 5'-ATTCTAGATGGAAGAAGCGGATACCTTGTTTC-3' (*Xba*I sites are underlined) were used together with *M. catarrhalis* strain P44 chromosomal DNA in PCR to amplify a 5.5 kb fragment from within the *hag* ORF which was subsequently cloned into the *Xba*I site in pUC19 (New England Biolabs). A spectinomycin resistance cartridge (329) was then ligated into the *Eco*RV site in the *hag* fragment to make the plasmid pELHGSPEC. The *uspA1 uspA2 hag* triple mutant O35E.ZCS was constructed by electroporating the *uspA1 uspA2* mutant O35E.ZC with pELHGSPEC and identifying a transformant resistant to chloramphenicol, Zeocin, and spectinomycin. The other *hag* mutants used in this study (Table 1) were constructed by electroporating wild-type and mutant strains of *M. catarrhalis* with pELHGSPEC. This plasmid was constructed by Dr. Eric Lafontaine, Department of

Microbiology, UT Southwestern.

(iii) Construction of a *corC* mutant

To construct an isogenic mutant unable to express the *corC* gene product, this gene and its flanking regions were amplified by PCR using the primers 5'-ATTTATGATGAATTGCGACC-3' and 5'-TGGTGAGCAGTTTTTACCG-3' and chromosomal DNA from *M. catarrhalis* transformant T14 as the template. This fragment was cloned using the TOPO TA Cloning Kit (Invitrogen); that is, the amplicon was ligated with pCR2.1 and used to transform *E. coli* strain INVαF'. The resulting plasmid, designated pMP14COR, was digested with *SphI* and *NdeI* to remove a fragment of approximately 200 nt from the *corC* ORF, and was blunt-end polished with *Pfu*. The promoterless *cat* cartridge from pCWn_{pcat}1 (constructed by Dr. Christine Ward, Department of Microbiology, UT Southwestern) was isolated by gel purification following digestion with *SmaI*, and ligated with the linearized pMP14COR plasmid. *E. coli* strain DH5α was electroporated with this ligation reaction mixture; the plasmid from a resultant chloramphenicol-resistant transformant was designated pMP14COR_{cat}. This plasmid was used to transform *M. catarrhalis* transformant T14 to obtain the isogenic mutant T14.COR.

(iv) Construction of an O35E strain expressing a hybrid UspA1 protein

To introduce the hybrid *uspA1* gene from transformant T14 into strain O35E, the *uspA1* gene from transformant T14 was amplified by PCR using the primers 5'-AGG GATCCACTGGCGTAAATGACTGATGAG-3' and 5'-AGGGATCCCCTGCCACCTAA AGCCTTG-3' and used to transform the *uspA1* mutant O35E.1 (which has a *kan* cartridge inserted in its *uspA1* gene) by plate transformation. Transformants were then screened for loss of kanamycin resistance to identify those in which allelic exchange had occurred. The presence of the entire hybrid *uspA1* gene in transformant O35E.14U1 was confirmed by nucleotide sequence analysis. Sarah Guinn, Department of Microbiology, UT Southwestern, constructed O35E.14U1.

(v) Construction of a mutant unable to express a putative phosphotransferase

To construct an isogenic mutant unable to express the product of the predicted phosphotransferase gene, a 2.5 kb fragment encompassing this gene was amplified by PCR using the primers 5'-TCCAGTTTTGGGGTGGTAGG-3' and 5'-TGATCTTGGACATAAGG CTTCG-3' and *M. catarrhalis* ETSU-9 chromosomal DNA as the template. This fragment was cloned using the TOPO TA Cloning Kit. The resulting plasmid, designated pMP714, was digested with *AccI*, which cuts within the predicted phosphotransferase ORF, and the ends were blunt-polished using *Pfu*. The promoterless *cat* cartridge from pSL33 (188) was

isolated by digestion of pSL33 with *Sma*I, followed by gel purification of the cartridge. The linearized pMP714 was ligated with the *cat* cartridge and used to transform *E. coli* strain DH5 α . Plasmid pMP714cat was purified from a chloramphenicol-resistant transformant and used to transform *M. catarrhalis* ETSU-9 to construct the isogenic mutant ETSU-9.714cat.

(vi) Construction of an *ampD* mutant

A 2.7 kb fragment encompassing the *ampD* gene was amplified by PCR using the primers 5'-CAATCGCCACACCAATGAGTC-3' and 5'-AAATCGCTGCAATGCGTGAGG G-3' and ETSU-9 chromosomal DNA as the template. This fragment was cloned using the TOPO TA Cloning Kit; the resulting plasmid, designated pMP988, was digested with *Acc*I, which cuts within the *ampD* ORF, and the ends were blunt-polished using *Pfu*. The promoterless *cat* cartridge from pCWnecat1 was isolated by gel electrophoresis following digestion with *Sma*I, and ligated with the linearized pMP988 plasmid. *E. coli* strain DH5 α was electroporated with this ligation reaction mixture; the plasmid from a resultant chloramphenicol-resistant transformant was designated pMP988cat. *M. catarrhalis* strain ETSU-9 was transformed with pMP988cat to generate the isogenic mutant ETSU-9.988cat.

(vii) Construction of a mutant lacking the ability to express a putative lytic murein transglycosylase D

Several attempts at cloning the entire putative lytic murein transglycosylase D gene and its flanking regions were unsuccessful; therefore, a fragment lacking the ATG translational start codon was amplified by PCR using the primers 5'-AAACACACCAAA TCTTCG-3' and 5'-TTATCGATTTGGTTCGGC-3' and ETSU-9 chromosomal DNA. This fragment was cloned using the TOPO TA Cloning Kit; the resulting plasmid, designated pMP222, was digested with *Nde*I, which cuts within the ORF, and the ends were blunt-polished using *Pfu*. The linearized vector was ligated to the gel-purified promoterless *cat* cartridge from pSL1 (189) and used to transform *E. coli* DH5 α . The plasmid from a resultant chloramphenicol-resistant transformant was designated pMP222cat and was used to transform ETSU-9 to obtain the isogenic mutant ETSU-9.222cat.

B. Enrichment for allelic exchange in *M. catarrhalis* by the use of congression

A streptomycin-resistant mutant of *M. catarrhalis* strain ETSU-9 was obtained by spreading 10^9 - 10^{10} CFU of this strain onto BHI agar supplemented with streptomycin and incubating overnight. The development of spontaneous streptomycin resistance in bacteria is frequently associated with a point mutation in the *rpsL* gene (223). To determine whether a mutation in the *M. catarrhalis* *rpsL* gene had occurred, a 0.8-kb fragment containing the entire *rpsL* gene was amplified by PCR using the primers 5'-GGAATTCACTCAAGTGA

AAATACGGAAAATC-3' and 5'-GAGGTACCGACGTCTTGGCATAATAGTT-3' together with chromosomal DNA from this streptomycin-resistant mutant. Nucleotide sequence analysis confirmed that a single nucleotide change at residue 128 in the *rpsL* gene resulted in a single altered amino acid (i.e., K43R). A 3-kb amplicon containing the mutated *rpsL* gene plus flanking sequence was generated by PCR using the oligonucleotide primers 5'-TGGCG AAGAACTCAAGCAAACAGC-3' and 5'-ACGCCACCAACAGCACAATAAACC-3'.

To replace the *hag* gene in transformant T14 or ETSU-9 with the *hag* gene from strain O35E, a 6.5-kb amplicon encompassing the O35E *hag* gene was amplified by PCR from O35E chromosomal DNA using the primers 5'-TTGCCCCATATCTGTACG-3' and 5'-GGTCATGGTGAAAGAGAATC-3'. A 5 µl portion of this PCR amplicon (approximately 0.5 µg DNA) was mixed with 0.5 µl of the 3-kb *rpsL* PCR amplicon (approximately 25 ng DNA) and was used to transform the spectinomycin-resistant strains T14.HG or ETSU-9.HG. These latter two strains have a *hag* gene that was inactivated by insertion of a spectinomycin resistance cartridge as described above. Transformants were selected on TH agar supplemented with streptomycin. Isolated colonies were then patched onto TH agar plates containing spectinomycin to identify those transformants in which the mutated *hag* gene had been replaced by all or part of the O35E wild-type *hag* gene. Nucleotide sequence analysis of the *hag* gene was used to confirm the occurrence of allelic exchange. The resultant transformants were designated T14.O35EHG and ETSU-9.O35EHG, respectively.

C. Insertional mutagenesis of *uspA2H*

Random 15 nt insertions in *uspA2H* were obtained by use of the GPS-LS Linker Scanning System (New England Biolabs). To accomplish this, a 2.7 kb fragment encompassing all of the ETSU-9 *uspA2H* open reading frame except the extreme 5' end was amplified by PCR using the primers 5'-AAATGCCGCAGGTCATTCGG -3' and 5'-CT TCTAGAGCTTTTATCCATCACTCAC-3' (*Xba*I site underlined). This amplicon was ligated and cloned using the Zero Blunt TOPO PCR cloning kit (Invitrogen) to obtain the plasmid pMPGTG3. The *uspA2H* nucleotide sequence was confirmed to be correct by sequencing the insert in pMPGTG3. Transposon insertions in pMPGTG3 were generated using the GPS-LS kit according to the manufacturer's instructions. Using the formula provided with the kit, it was determined that 27 insertions within the *uspA2H* gene should be analyzed to obtain transposon insertions approximately every 100 nt. After the transposition reaction, bacteria were plated on LB supplemented with chloramphenicol and kanamycin to select for both the transposon and the vector backbone. Resultant kanamycin- and chloramphenicol-resistant colonies were screened by PCR using the above primers to ascertain which clones possessed a transposon within the *uspA2H* gene. An insertion was visualized on an agarose gel as an apparent increase in PCR amplicon size from 2.7 kb to 4.1 kb, corresponding to the size of the transposon. Plasmids with an insertion in *uspA2H* were sequenced using the primer 5'-ATAATCCTTAAAACTCCATTTCCACCCCT-3' (Primer S, which comes with the kit), which binds to the 5' end of the transposon to determine the location of the insertion and whether the 15-nt insertion would be in frame with the *uspA2H*

ORF after transposon excision. The transposon was then excised by digestion with the restriction enzyme *PmeI*, leaving behind a 15-nt insertion. The plasmid was religated, transformed into electrocompetent DH5 α *E. coli*, and selected on LB agar containing kanamycin. Resultant colonies were patched onto both LB-kanamycin and LB-chloramphenicol plates; plasmids from transformants that were chloramphenicol-sensitive (and therefore had a successful excision of the transposon) were transformed into *M. catarrhalis* strain ETSU-9.2H (spectinomycin-resistant) using plate transformation. *M. catarrhalis* transformants possessing the 15-nt insertion in *uspA2H* were enriched by the technique of congression (described above) and were screened for loss of spectinomycin resistance. The presence of the 15 nt insertion was confirmed by sequence analysis; strains with the insertion were then tested for the ability to form biofilms using the crystal violet-based assay.

D. Site-directed mutagenesis of *uspA2H* and *uspA1*

Site-directed mutations were generated using the QuikChange site-directed mutagenesis kit (Stratagene) according to the manufacturer's instructions. Briefly, forward and reverse PCR primers were designed to recognize the site to be altered; these primers contained the desired altered sequence. To obtain the K34E mutation of ETSU-9 UspA2H, primers 5'-TATTAACAACGCCGAAGGCGATCGCTCTACCATC-3' and 5'-TGGTAGAGCGATCGCCTTCGGCGTTGTTAATAGCG-3' were used (altered nucleotide is underlined). To obtain the K34A mutation of ETSU-9 UspA2H, primers 5'-CGCTATTAACAACGCC

GCAGGCGATCGCTCTACC-3' and 5'-GGTAGAGCGATCGCCTGCGGCGTTGTTAAATAGCG-3' were used (altered nucleotides are underlined). The plasmid pMPGTG3 was PCR-amplified using these mutagenic primers. Unmutated parental DNA was then digested using the restriction enzyme *DpnI* (which only recognizes its restriction site when the site is methylated). Following transformation of chemically competent *E. coli* strain XL1-Blue with the mutated plasmid, the mutated sequence was confirmed by nucleotide sequence analysis. The mutated *uspA2H* gene was introduced into *M. catarrhalis* strain ETSU-9.2H by plate transformation. The desired transformants were enriched using the principle of congression with the *rpsL* gene as described above and screened for the loss of spectinomycin resistance. ETSU-9 with the K34E mutation was designated ETSU-9.K34E; likewise, the K34A mutant was designated ETSU-9.K34A. Both mutations were confirmed by nucleotide sequence analysis of PCR-amplified fragments of chromosomal DNA.

For site-directed mutagenesis of the O35E *uspA1* gene, a stable, nonexpressing clone of the *uspA1* gene was constructed. The *uspA1* gene from O35E was amplified by PCR using the primers 5'-ACGTCGAGAATAAAATTTATAAAGTGAAG-3' and 5'-AGGGATCCCCTGCCACCTAAAGCCTTG-3'; this DNA fragment lacked the ATG start codon of the *uspA1* ORF. This amplicon was ligated to pCR-Blunt II-TOPO and used in a transformation of chemically competent *E. coli* strain XL10-Gold. One clone, designated pMPUspA1, was confirmed to contain the correct insert by nucleotide sequence analysis. To obtain the E66K mutation of O35E UspA1, the primers 5'-GCGGTTATAACAAAGCCAAAGGCAGATAC TCTACCA-3' and 5'-TGGTAGAGTATCTGCCTTTGGCTTTGTTATAACCGC-3' were used (altered nucleotides are underlined). Mutagenic PCR was performed using pMPUspA1

as the template. Kanamycin-resistant *M. catarrhalis* strain O35E.1 was transformed with the mutated plasmid both with and without the use of congression to enrich for the desired transformants. Two transformants, designated O35E.E66K str^R (obtained using congression) and O35E.E66K, were obtained that had lost kanamycin resistance; the presence of the E66K mutation was confirmed by nucleotide sequence analysis.

E. Cloning and expression of *uspA1* in *E. coli*

The *uspA1* genes from *M. catarrhalis* strains O35E, O46E, and T14 were amplified by PCR using the primers 5'-AGGGATCCGGAGACCCCAGTCATTTATTAG-3' and 5'-AGGGATCCCCTGCCACCTAAAGCCTTG-3', ligated into the plasmid vector pCC1, and used to electroporate *E. coli* EPI300 from the CopyControl PCR Cloning Kit (Epicentre). Transformant colonies were inoculated into LB broth containing chloramphenicol and CopyControl induction solution to increase the plasmid copy number according to the manufacturer's instructions. The pCC1 plasmid is maintained as a single copy in EPI300 until the strain is grown in the presence of the induction solution. Western blot analysis of whole cell lysates was performed as described for *M. catarrhalis*, except that proteins were transferred to Immobilon-P PVDF membrane (Millipore Corp., Bedford, Mass.) instead of nitrocellulose. Western blots were probed with MAb 17C7 to detect UspA1. The recombinant plasmid expressing O35E UspA1 was designated pMP35U1, the plasmid expressing O46E UspA1 was designated pMP46U1, and the plasmid expressing T14 UspA1 was designated pMP14U1.

CHAPTER FOUR

The Sorbarod Continuous Culture Biofilm System

I. Introduction

Although biofilms have been a topic of increasing interest in the fields of medicine and microbiology, only a few pathogens have been studied in much detail with regard to their ability to form biofilms. There is a particular paucity of publications dealing with upper respiratory tract pathogens and biofilm formation. Although there have been reports in the literature of biofilm formation by *H. influenzae* (85, 218, 298), to date, there is only one biofilm study of *S. pneumoniae* at the molecular level (319) and only one *M. catarrhalis* biofilm manuscript was published before the initiation of this dissertation project. There is some indication that all three of these organisms can persist in the middle ear of otitis media patients, even after appropriate antibiotics have been administered (74, 240, 254), suggesting the occurrence of a biofilm mode of growth which could increase resistance to antibiotic treatment.

Budhani and Struthers (37) employed a modification of the Sorbarod method for growing biofilms originally devised by Gilbert and colleagues (140) for the purpose of analyzing the antimicrobial susceptibility of *S. pneumoniae* biofilms. Their preliminary study found that, although the strain of *S. pneumoniae* tested did not have greater resistance as a biofilm to antibiotic killing with the antibiotics tested, the bacteria grew to a very high

density in the biofilm within 24 h. In a subsequent study, this same group investigated biofilm growth of mixed cultures of *S. pneumoniae* and β -lactam sensitive or resistant strains of *M. catarrhalis* (38). Both organisms achieved a density of approximately 10^{13} cfu/Sorbarod, even when the ratios of the initial inocula were varied, or when either species was inoculated by itself. It was found that β -lactamase producing *M. catarrhalis* had a protective effect on β -lactam-sensitive *S. pneumoniae*. Surprisingly, the authors also found that β -lactamase-positive *M. catarrhalis* was frequently not found in the biofilm effluent when cocultured with *S. pneumoniae* at low antibiotic concentrations. It was suggested that interspecies communication could be causing *M. catarrhalis* to be retained within the biofilm (38). With this background, I endeavored to use the Sorbarod continuous culture biofilm method to investigate biofilm formation by *M. catarrhalis*.

II. Results

A. Growth dynamics

Initial determinations of viable numbers of *M. catarrhalis* strain O35E in Sorbarod biofilms indicated that the bacteria achieved a density of approximately 1×10^{12} to 1×10^{13} cfu/Sorbarod within 3 days (Fig. 4, squares). Bacterial densities in the biofilm effluents were approximately 1×10^{12} cfu/Sorbarod (Fig. 4, inverted triangles). Biofilms were maintained as long as 7 days, although the bacteria were not enumerated beyond 3 days. However, subsequent experiments consistently found that viable numbers of *M. catarrhalis* in 3-day-

old biofilms were $8-9 \times 10^8$ cfu/Sorbarod (Fig. 4, circle). The reason for this discrepancy remains unknown, as the overall appearance of these biofilms has not changed. *M. catarrhalis*-inoculated Sorbarods developed a pinkish color within 2 or 3 days, consistent with the color of *M. catarrhalis* cells grown in BHI broth. Furthermore, bacteria produced visible growth extending up and down the silicone tubing housing the Sorbarod; occasionally, the bacteria even formed a column that extended up to the BHI medium inlet drip. Bacteria within the effluent collection bottle frequently formed floating mats that sometimes adhered tenaciously to the sidewall of the bottle.

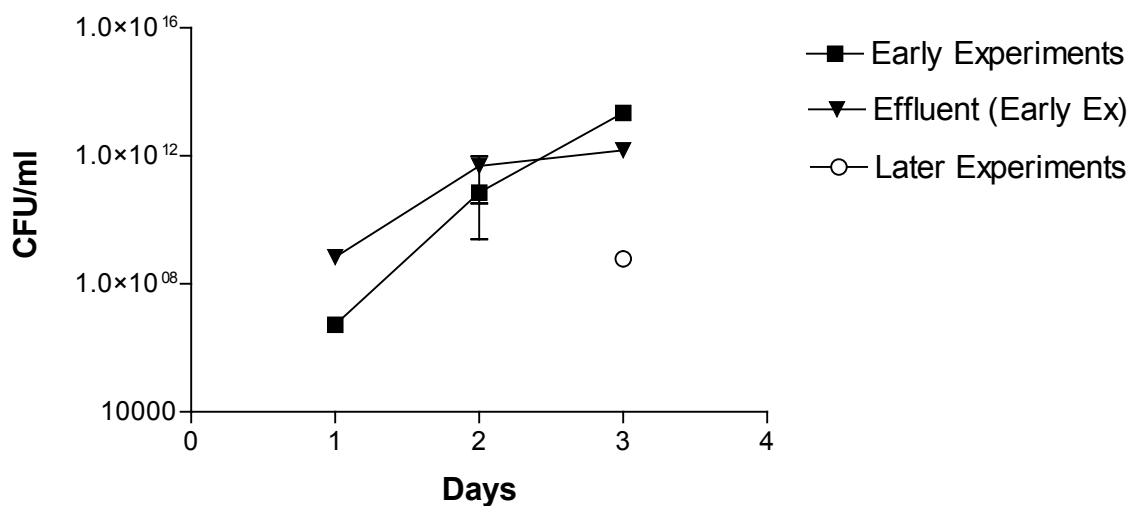


Fig. 4. Growth of *M. catarrhalis* in the continuous-culture biofilm system. Viability of *M. catarrhalis* in the Sorbarod biofilm system was determined at 1, 2, or 3 days following inoculation of the Sorbarod. During later biofilm experiments, viable numbers of *M. catarrhalis* were only enumerated after 3 days.

B. Outer membrane protein analysis

Outer membrane proteins from both broth- and biofilm-grown *M. catarrhalis* strains O35E and O46E were compared using SDS-PAGE (10% w/v polyacrylamide separating gel) and Coomassie staining. Proteins were separated using both minigels and 20-cm Protean II gels. The larger gel is shown in Fig. 5. Although there appeared to be a few differences between the broth- and biofilm-derived outer membrane proteins, none of these were very prominent. Two of these antigens, indicated by arrows in Fig. 5, were subjected to tryptic digestion and ion trap mass spectrometry by Dr. Clive Slaughter and Steve Afendis, Howard Hughes Medical Institute, Biopolymer Facility, UT Southwestern. The 60,000 Da protein was determined to be the heat-shock protein GroEL. No peptides were recovered following tryptic digestion of the 58,000 Da protein. As GroEL is supposed to be localized to the cytosol, the presence of this antigen in the outer membrane vesicle fraction was presumed to be the result of contamination with cytosolic protein. It should be noted that although these samples were not analyzed for purity of the outer membrane fraction, the protocol that was used to isolate outer membrane vesicles is well-established for *M. catarrhalis* (18, 221). The protein profile as seen in Fig. 5 closely resembles published *M. catarrhalis* outer membrane protein profiles, including the presence of the UspA2H and CopB proteins (data not shown). Proteins from these outer membrane vesicles were also separated on a 15% (w/v) polyacrylamide separating gel (Fig 6) to determine whether there was a difference in expression of low-molecular-weight antigens. Again, no major differences were seen between the two samples; one minor antigen (Fig. 6, arrow) was submitted for mass

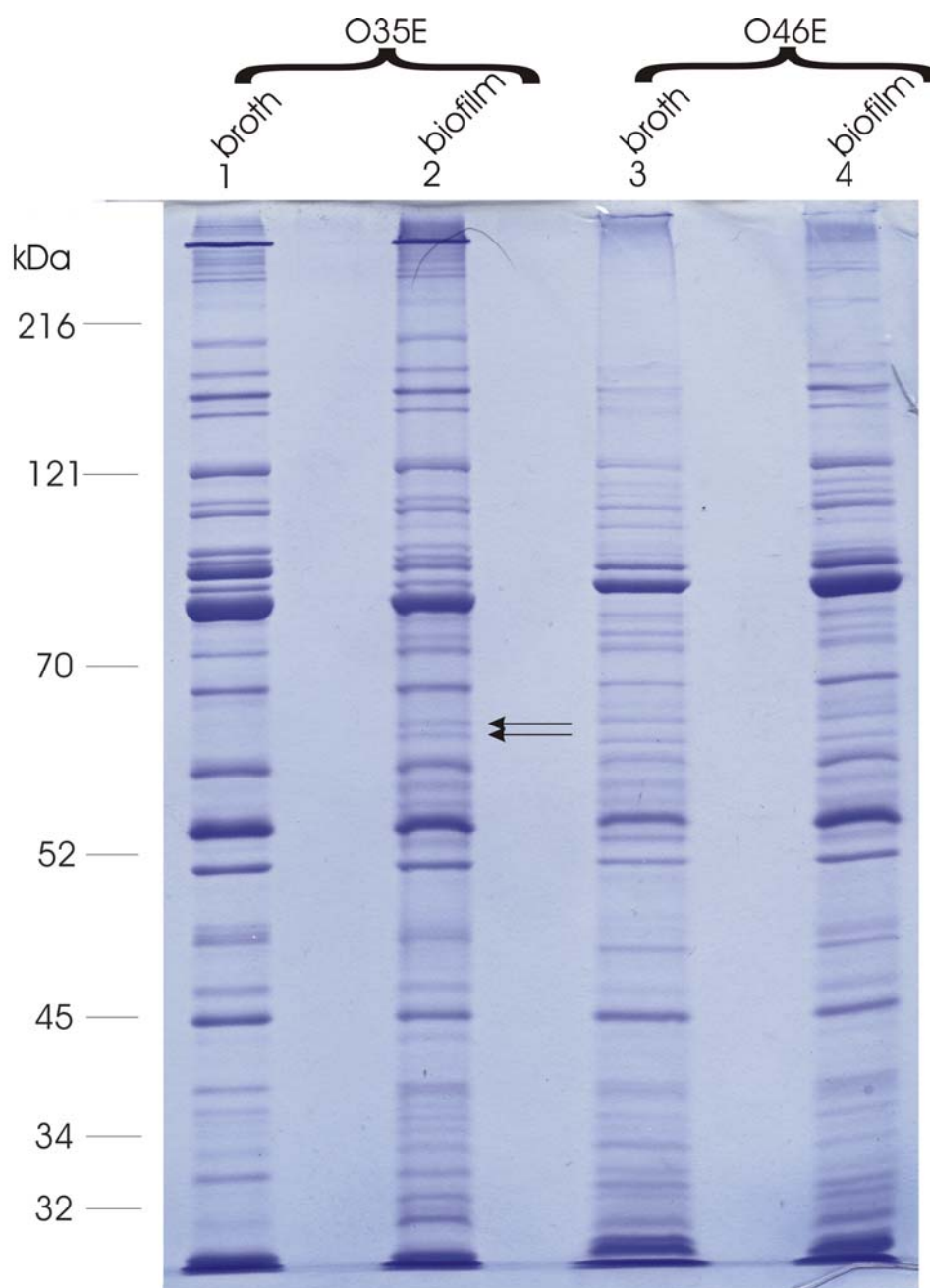


Fig. 5. SDS-PAGE comparison of outer membrane proteins. Outer membrane vesicles from broth- and biofilm-grown *M. catarrhalis* cells were isolated as described in “Materials and Methods” and the proteins in these vesicles separated by SDS-PAGE using a 10% (w/v) polyacrylamide separating gel. Lane 1, broth-grown strain O35E; Lane 2, biofilm-grown strain O35E; Lane 3, broth-grown strain O46E; Lane 4, biofilm-grown strain O46E. Arrows indicate the 60,000 Da and 58,000 Da proteins that were excised for analysis by mass spectrometry. Molecular weight position markers (in kDa) are present on the left side of this figure.

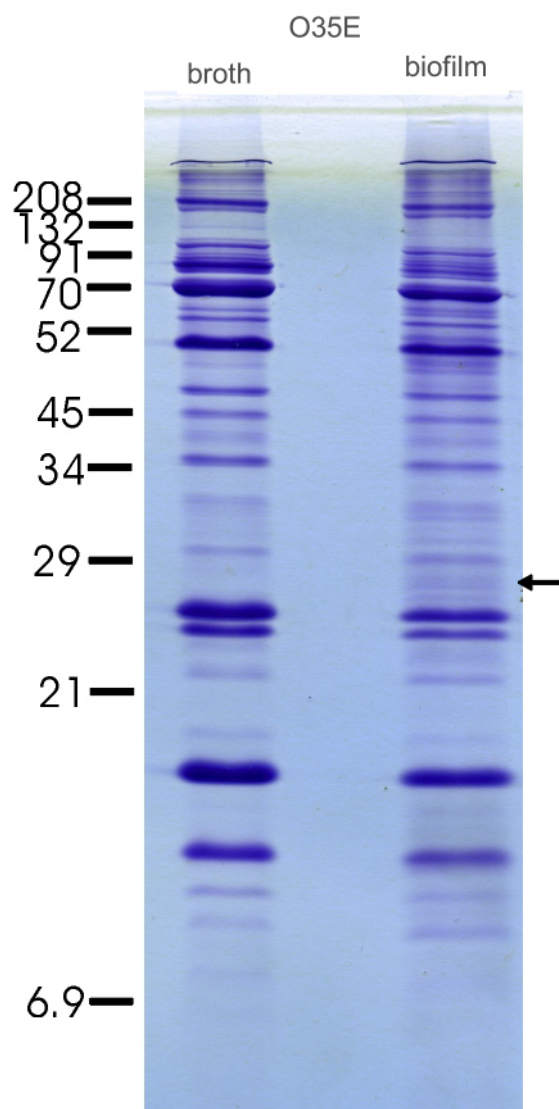


Fig. 6. 15% polyacrylamide gel analysis of broth- and biofilm-derived OMPs. Outer membrane vesicles were isolated as in Fig. 4. The proteins present in these vesicles were resolved by SDS-PAGE using a 15% (w/v) polyacrylamide separating gel, and stained with Coomassie blue. Arrow indicates an antigen that was excised for analysis by mass spectrometry. Molecular weight position markers (in kDa) are present on the left side of this figure.

spectrometry analysis and was found to be the 50S ribosomal protein L1, which is also localized to the cytosol. SDS-PAGE analysis of broth- and biofilm-grown cells of *M. catarrhalis* strain O12E revealed very similar outer membrane protein profiles, as did a comparison of O35E 3-day biofilms versus O35E 7-day biofilms (data not shown).

C. Isolation and characterization of a possible polysaccharide from *M. catarrhalis* biofilms

To ascertain whether *M. catarrhalis* biofilms produce an exopolysaccharide matrix, the polysaccharide capsule isolation protocol outlined in “Materials and Methods” was used. Following this procedure, approximately 3 mg of a white substance was obtained from biofilm culture supernatant. For the purpose of gel electrophoresis, 1 mg of the putative polysaccharide was suspended in 200 μ l of distilled water. Resolution of the sample using

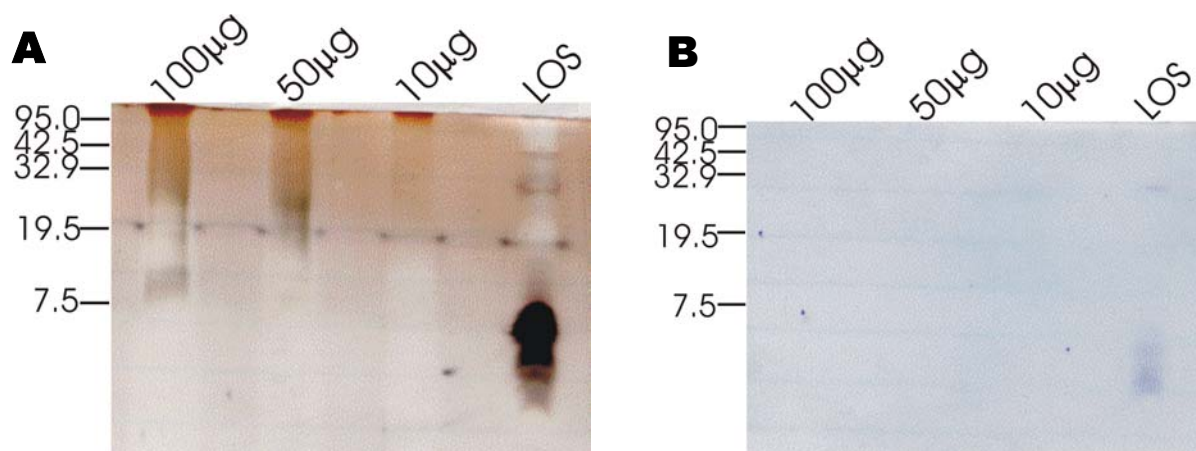


Fig. 7. Tricine SDS-PAGE comparison of silver- and Coomassie-stained putative polysaccharides. Samples of the putative polysaccharide (100 μ g, 50 μ g, or 10 μ g as indicated) or *H. ducreyi* LOS were separated by tricine SDS-PAGE as described in “Materials and Methods”. Panel A, Tsai-Frasch silver stain; Panel B, Coomassie stain.

tricine SDS-PAGE followed by silver staining using the Tsai-Frasch method revealed a very high molecular weight substance that barely entered the separating gel (Fig. 7A). In contrast, a *H. ducreyi* LOS control migrated as a series of bands with apparent molecular weights of less than 8000 Da. An equivalent tricine SDS-PAGE gel stained with Coomassie brilliant blue revealed no stain-reactive substances in the putative polysaccharide sample, even when 100 µg of the substance was stained (Fig. 7B). This indicated that the sample was likely not proteinaceous, whereas the LOS control had some faint Coomassie blue staining. Next, 50 µg of the substance was treated with DNase and separated on an agarose gel containing ethidium bromide; this resulted in a wide band of ethidium bromide-stained material that migrated with an apparent size of less than 100 bp (data not shown). However, the DNase-treated sample appeared exactly the same as the untreated sample (data not shown). Treatment of *M. catarrhalis* chromosomal DNA with DNase resulted in a similar very-low-molecular-weight staining pattern (data not shown). To ascertain whether the sample contained a substance in addition to nucleic acids, the sample was subjected to electrophoresis in a polyacrylamide TBE gel containing ethidium bromide. As seen in Fig 8A, the same low-molecular-weight ethidium bromide-stained material was again visible. However, when the same gel was stained using the Tsai-Frasch method, a high-molecular-weight substance is clearly visible at the top of the separating gel (Fig. 8B). Monosaccharide composition analysis of the substance (Table 3), performed by Trina Abney, Complex Carbohydrate Research Center, University of Georgia, indicated that the substance was composed of fucose, mannose, galactose, 2-acetamido-2-deoxy-glucose (GlcNAc), and possibly glucuronic acid. Xylose, glucose, and 2-acetamido-2-deoxy-galactose (GalNAc) were listed as likely contaminants.

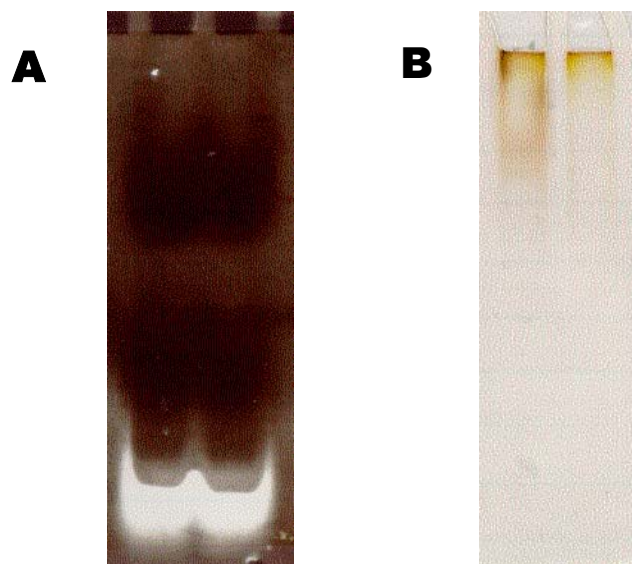


Fig. 8. Comparison of ethidium bromide and Tsai-Frasch silver staining of the putative polysaccharide. Panel A, polysaccharide samples were separated on a TBE gel and stained with ethidium bromide. Panel B, the same gel was silver stained according to the method of Tsai and Frasch (305). In both panels, the sample in the left lane was treated with DNase, while the sample in the right lane was not.

By far, the most abundant sugar component of the polysaccharide was ribose, consistent with nucleic acid contamination of this sample. Although it is possible that this polysaccharide was derived from the Sorbarod filter, this is unlikely given that the filter is composed of cellulose, which is a polymer of glucose.

D. Identification of colony morphology variants derived from biofilms:

“Lucky 4-leaf clovers”

M. catarrhalis cells from Sorbarod biofilm effluents were regularly plated on BHI agar to ensure that the biofilm being analyzed was a pure culture. Following a routine plating of strain ATCC 43617, it was observed that some of the resultant colonies had a shiny surface

Table 3. Glycosyl composition analysis

Glycosyl residue	Mass (μg)	Mole %¹
Ribose	10.0	28.5
Fucose	4.7	12.1
Xylose	1.1	3.1
Glucuronic acid	2.9	6.3
Mannose	6.9	16.4
Galactose	5.4	12.9
Glucose	2.2	5.3
GalNAc	0.8	1.5
GlcNAc	7.2	14.0

¹Values are expressed as mole percent of total carbohydrate. Carbohydrate represents approx. 20% of the mass of the sample, based on an approximate total sample weight of 1 mg. It is possible, however, that complete recovery of all carbohydrate mass was not achieved during this analysis.

whereas others had a matte surface, as viewed by the naked eye. When viewed under a low-power microscope, the shiny colonies resembled the usual phenotype for *M. catarrhalis*; that is, the colonies had round, smooth edges and were generally unremarkable (Fig 9A). However, the matte colonies, which were slightly smaller than the shiny colonies, were subdivided down the center into thirds and quarters, suggesting the appearance of three- and four-leaf clovers (Fig 9B). Some of these clover-type colonies even developed an apparent hole in the center of the colony. The identity of both colony types as *M. catarrhalis* was confirmed by PCR amplification of portions of the *uspA1* and *hag* genes. While selecting 20

colonies of each type for PCR analysis, it was noted that, when smooth-type colonies were touched with a bacteriological loop, the entire colony was lifted intact from the surface of the agar. However, clover-type colonies disintegrated when touched with a loop, leaving a granular appearance on the agar plate. Single colony passage of smooth-type colonies yielded only smooth colonies, while single colony passage of clover-type colonies resulted in mostly clover-type colonies but there were always some smooth colony revertants as well. Following this initial observation, it was noted that strain ATCC 43617 consistently formed both types of colonies after growth in Sorbarod biofilms. Bacteria from within the Sorbarod filter or the growth on the silicone tubing were a mixed population of both types. However, bacteria taken from the effluent broth were mostly smooth-type, while bacteria taken from floating mats in the effluent bottle were mostly clover-type. When 2 ml BHI in a 24-well

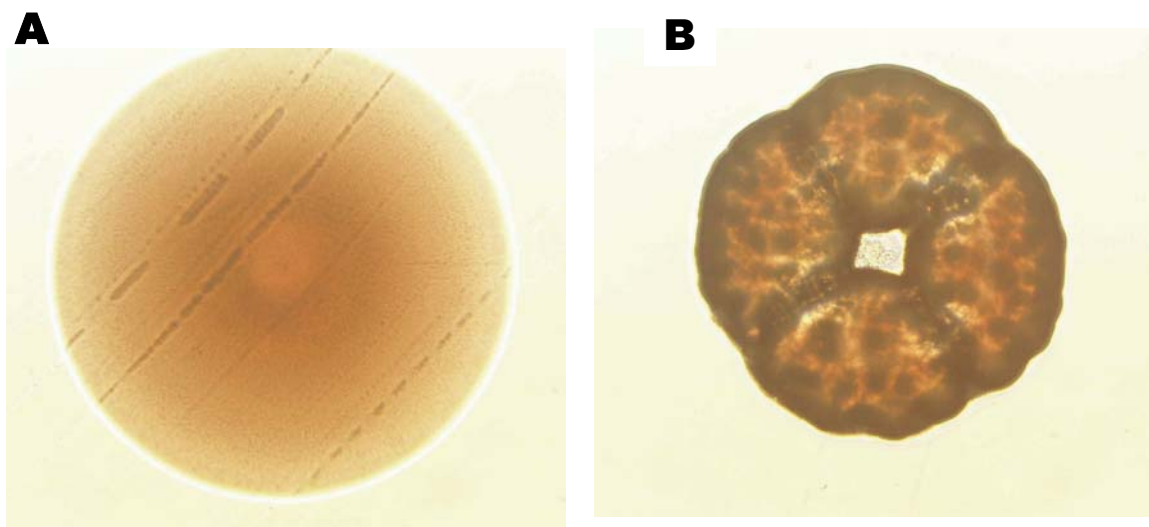


Fig. 9. Colony morphologies of strain ATCC 43617 grown in the Sorbarod continuous-culture biofilm system. A, smooth phenotype; B, clover phenotype.

tissue culture plate was inoculated with smooth-type colonies, the growth after overnight incubation was uniform in the broth, with very few or no floating mats of bacteria at the air-medium interface. In contrast, when the same experiment was performed using clover-type colonies, the bacteria grew both in a large mat on the surface and within the broth. It should be noted that when strain ATCC 43617 (that has not first been passaged as a biofilm is grown on agar plates or in aerated broth culture, only smooth-type colonies are observed.

To see whether other strains of *M. catarrhalis* produced similar colony phenotypes during growth in a biofilm, *M. catarrhalis* strains O35E and O46E were examined carefully after isolation from Sorbarod biofilms or effluents. Surprisingly, 4 different colony phenotypes were noted for strain O46E; none of these phenotypes, designated smooth, rough, flat, and cracked (Fig 10; cracked-type not shown), resembled the ATCC 43617 clover phenotype. It was observed that ATCC 43617 seemed to be producing a rough colony phenotype as well, which had a matte surface like the clover-type, but did not split down the center. In contrast, strain O35E colonies had similar appearances whether they were isolated from floating mats, biofilms, or effluent broth (data not shown). O35E floating mat isolates continued to produce floating mats when inoculated into static broth culture, whereas O35E broth isolates did not. The significance of these findings remains to be determined.

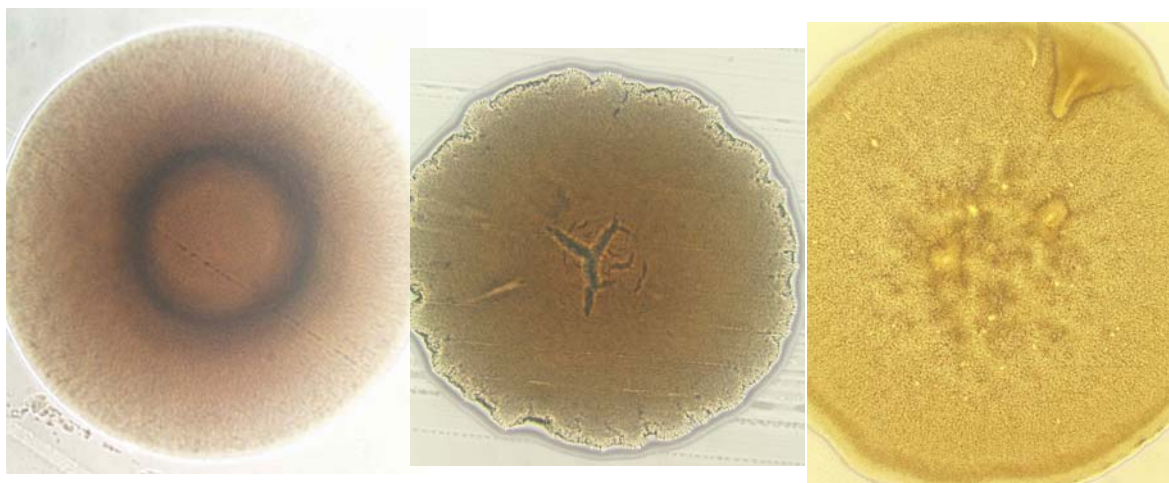


Fig. 10. Colony morphologies of strain O46E grown in the Sorbarod continuous-culture biofilm system. These colony types, from left to right, are designated as smooth, rough, and flat, respectively. The cracked colony phenotype is not shown.

III. Discussion

The definition of a biofilm has evolved over the years, and is still in some dispute. O'Toole *et al* (227) simply define a biofilm as a “community of microorganisms that are attached to a surface”. By this criterion, *M. catarrhalis* is clearly capable of forming a biofilm, as it not only grows upon the Sorbarod filter support but also spreads up and down the silicone tubing surrounding the Sorbarod. Perhaps the most detailed definition of a biofilm was given by Donlan and Costerton (76), who stated a biofilm is a “microbially derived sessile community” containing firmly attached cells (to a surface or each other) encased in a “matrix of extracellular polymeric substances that they have produced”, and exhibiting differential growth rate and gene expression. These criteria are more difficult to

fulfill with regard to *M. catarrhalis*, but the work outlined in this dissertation addresses at least some of these stipulations.

Comparison of the outer membrane protein profiles of biofilm- and broth-grown *M. catarrhalis* indicates that there is not much difference in protein expression between these two different modes of growth, at least at the level of detection achieved with Coomassie blue staining. Although some species of bacteria, such as *P. aeruginosa* (266) and *E. coli* (246), have widely divergent expression profiles when planktonic and biofilm cells are analyzed, it must be remembered that these species are able to grow in diverse niches. *M. catarrhalis*, on the other hand, grows exclusively within its human host. Thus, genes that are necessary for *M. catarrhalis* biofilm formation within the nasopharyngeal mucosa may not be subject to regulation. Indeed, a study by Murphy and Kirkham (218) found that *H. influenzae* outer membrane protein content is very similar in broth- and biofilm-grown organisms; in fact, the major antigens appeared identical in the two samples. Furthermore, Western blot analysis of several known *H. influenzae* antigens found that expression of these antigens was the same for broth- and biofilm-derived samples. Only LOS was found to have a different antigenic profile in the two samples (218). Swords *et al* (298) have confirmed the role of LOS in *H. influenzae* biofilm formation by finding that sialylated LOS promotes biofilm formation by this organism. It would be useful to examine LOS production by *M. catarrhalis* grown under different conditions as well. However, it may be premature to conclude that there are no differences in *M. catarrhalis* gene expression in biofilm versus planktonic growth. For instance, Coomassie staining of proteins resolved by SDS-PAGE of outer membrane vesicles does not detect all of the proteins in the outer membrane; UspA1

and Hag are two proteins which are very difficult if not impossible to detect by this method under normal conditions. Techniques such as two-dimensional gel electrophoresis and DNA microarray analysis may be able to detect subtle differences in gene expression. Although several attempts to analyze *M. catarrhalis* proteins in whole cell lysates by 2-D gel electrophoresis were unsuccessful, DNA microarray experiments are now ongoing in the laboratory.

GroEL is a member of the Hsp60 family of heat shock protein chaperonins (reviewed in (343)). It is usually described as a cytosolic protein, and therefore the discovery of GroEL in an outer membrane fraction of *M. catarrhalis* was quite surprising. It is quite possible that the presence of this antigen in the outer membrane was merely cytosolic contamination that occurred during the isolation procedure. GroEL lacks a signal peptide, and thus it is not clear how this protein could be transported to the bacterial cell surface. However, there have been several other reports in the literature of this protein being detected in outer membrane preparations (102, 106, 232, 299, 303). Vigh and colleagues (303) found that the association of *E. coli* GroEL with membranes was dependent on the presence of the C-terminal GroEL segment, and concluded that this highly conserved tail may be responsible for membrane targeting. In contrast, Mayrand and colleagues (114) reported that, while GroEL of *Actinobacillus actinomycetemcomitans* was found in association with outer membranes, it was mostly present in the extracellular material. By necessity, these studies were conducted using techniques such as ELISA, immunoelectron microscopy, or purified GroEL protein, as GroEL is essential for viability (91). Thus, elucidating the precise role of membrane-associated or extracellular GroEL in biofilm formation, if any, remains challenging.

Preliminary evidence presented here indicates that *M. catarrhalis* produces some sort of extracellular polysaccharide. It would be useful to repeat the polysaccharide isolation procedure on different strains of *M. catarrhalis* to ascertain whether this polysaccharide production is strain-dependent. In addition, it will be necessary to confirm that this polysaccharide is bacterially-derived by repeating the polysaccharide isolation procedure on BHI growth medium passed over uninoculated Sorbarod filters. It is also interesting that ribose was found in the polysaccharide sample. Mattick and colleagues (330) have reported that *P. aeruginosa* requires extracellular DNA for biofilm formation and that treatment of a young biofilm with DNase can cause biofilm dissolution. Thus, it is possible that DNA or RNA forms a component of the *M. catarrhalis* biofilm matrix. Perhaps a method more suitable to DNA isolation would reveal higher molecular weight or more abundant DNA. Another possibility is that *M. catarrhalis* produces matrix components that are tightly associated with the cell surface; such biopolymers would likely not be isolated using the culture supernatant-based method described above. There have been several recent reports about cellulose playing a role in biofilm formation (283, 286, 346). These groups identified the presence of cellulose by growing bacteria on agar supplemented with the fluorescent dye calcofluor white, which binds α , 1-4 linkages in glycans and polysaccharides (252). *M. catarrhalis* also fluoresces in the presence of calcofluor, although the biomolecule(s) responsible for this phenomenon has not been identified (data not shown).

The discovery of different colony morphologies arising from biofilm-derived cells has been reported before. Dowson and colleagues (319) found that growth of type 3 *S. pneumoniae* obtained from Sorbarod biofilms resulted in both large, capsular colonies and

smaller, acapsular colonies. Acapsular variants, which were not observed without prior biofilm growth, were caused by phase-variation due to random tandem duplications within the type 3 capsule locus. Spiers *et al* (286) recently reported that *P. fluorescens* produces a “wrinkly spreader” phenotype characterized by colonization of the air-broth interface. Wrinkly spreader colonies have a dry, wrinkled appearance and overproduce a cellulosic polymer. Interestingly, *M. catarrhalis* ATCC 43617 clover- and smooth-type colonies fluoresce equally well when grown in the presence of calcofluor, suggesting that differential cellulose production is not the cause of the different colony phenotypes. In addition, negative staining of both clover- and smooth-type colonies with Congo red yielded identical results (data not shown): single cells of both colony types appear to have a very narrow halo. Thus, there does not seem to be a capsule expressed by either colony type. Similarly, there are no data from other sources indicating that *M. catarrhalis* can produce a polysaccharide capsule.

CHAPTER FIVE

Characterization of Structures Extending from the *M. catarrhalis* Cell Surface

I. Introduction

Many portions of this chapter were reproduced directly from a published manuscript (235). This material was reproduced with permission from the American Society for Microbiology. Transmission electron microscopy (TEM) has proven very helpful in several biofilm studies. This technique is useful for observing cell-cell and cell-surface interactions in greater detail than is possible with other methods. Researchers have also found that extracellular structures such as capsules that may be involved in biofilm formation are often visible by TEM (63). In the present study, TEM was used to demonstrate that three proteins, UspA1, UspA2 (6), and Hag (discussed below) all form fibrillar projections on the *M. catarrhalis* cell surface.

Scott and colleagues (92, 93) correlated both hemagglutination activity and the expression of a 200 kDa protein by some *M. catarrhalis* isolates with the presence of a fibrillar surface array. In addition, Sasaki and colleagues reported that the 200 kDa protein expressed by *M. catarrhalis* strain 4223 was subject to phase variation *in vitro* (265) and determined the nucleotide sequence of the gene encoding this 200 kDa protein (264). Mutant analysis was used in the present study to show that this 200 kDa protein, designated herein as Hag (hemagglutinin), is involved not only in hemagglutination, but also in autoagglutination and the binding of human IgD by *M. catarrhalis* strain O35E.

II. Results

A. TEM analysis of *M. catarrhalis* grown in Sorbarod biofilms

To determine whether *M. catarrhalis* biofilms produced an extracellular matrix that could be visualized by TEM, a *M. catarrhalis* strain O35E biofilm was fixed for TEM analysis after growing for three days as described in “Materials and Methods”. Lysine was included in the prefixative solution to promote preservation of extracellular structures (90). When this sample was observed by TEM, it was noted that a dense layer of projections extended from the bacterial cell surface (Fig. 11, left). TEM of other *M. catarrhalis* wild-type strains revealed the presence of similar projections (Fig. 11, center and right). This layer did not have an appearance similar to that of polysaccharide capsules that have been observed in other bacterial species (63, 90). TEM observation of *M. catarrhalis* interactions with the cellulose fibers within the Sorbarod filter usually showed *M. catarrhalis* separated from the fiber surface by a distance of approximately 1 μm (data not shown). This uniform separation of *M. catarrhalis* from cellulose fibers was assumed to be an artifact of sample fixation for TEM. However, occasionally a pocket within a fiber was found that was packed completely full of *M. catarrhalis* cells and either extracellular material or cellular debris (Fig. 12).

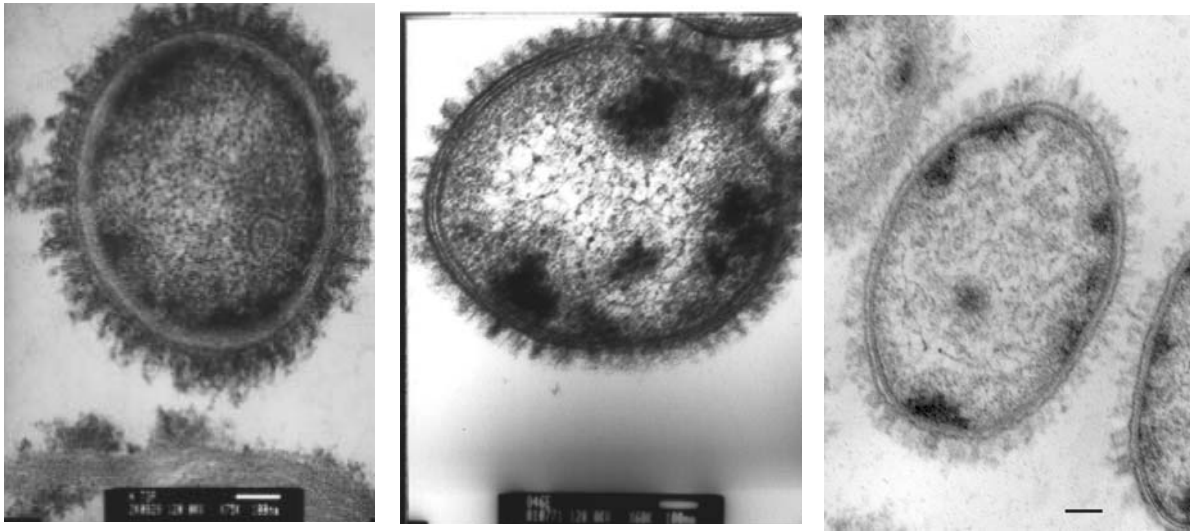


Fig. 11. TEM of biofilm-grown wild-type *M. catarrhalis* strains. From left to right, strains O35E, O46E, and ETSU-9. Bar, 100 nm.



Fig. 12. TEM of *M. catarrhalis* packed within a cellulose fiber pocket of the Sorbarod filter. Several individual *M. catarrhalis* cells can be seen within the pocket on the left. Bar represents 1 μ m.

B. Characterization of the *M. catarrhalis* strain O35E *hag* gene and its encoded protein product

The *hag* gene was amplified by PCR from *M. catarrhalis* strain O35E chromosomal DNA using oligonucleotide primers designed from the sequence of the gene encoding the 200 kDa surface protein from *M. catarrhalis* strain 4223 (264). The *hag* ORF contained 5,895 nt (GenBank Accession AY077637). The *hag* gene from strain O35E has at least two putative translational start sites separated by 45 nt, encoding predicted proteins with molecular masses of 201,566 Da and 199,700 Da, respectively. Inverted repeats that might function as transcriptional terminators were located 15 and 269 nt 3' from the end of the *hag* ORF. The N-terminal amino acid sequence of the predicted protein had properties consistent with the presence of a signal peptide, containing a short hydrophilic sequence followed by a longer hydrophobic region which contained a putative signal peptidase I cleavage site (i.e., AYA) at residues 64-66. It should be noted that the 5' end of this ORF contains a region with 6 consecutive G residues, similar to the 9 consecutive G residues observed in the 5' end of the ORF encoding the 200 kDa protein from *M. catarrhalis* strain 4223 (265). The deduced amino acid sequence of the Hag protein from strain O35E has several regions predicted to form coiled-coil structures (data not shown) and has homology with several bacterial surface proteins that are members of the autotransporter family (132, 134). In particular, the C-terminal domain of Hag has a predicted β -sheet structure very similar to that found in the well-characterized Hia autotransporter of *H. influenzae* (288, 289).

C. Construction of mutants deficient in expression of surface-exposed proteins

Previous studies from this laboratory had indicated that both UspA1 and UspA2 are present on the bacterial cell surface (5). The functional activity of the Hag protein (e.g., hemagglutination) indicated that this protein was also surface-exposed. In addition, purified Hag (MID) has been shown to bind human IgD, further confirming that this protein is on the cell surface (100). To determine whether the Hag, UspA1, and UspA2 proteins were present in the surface array on the wild-type strain O35E (Fig. 11), a mutant was constructed that was unable to express these three proteins. This *uspA1 uspA2 hag* triple mutant O35E.ZCS (Fig. 13, last lane) expressed none of these proteins at a detectable level whereas the wild-type parent strain expressed all three macromolecules as determined by Western blot analysis of whole cell lysates (Fig. 13, first lane). Transmission electron microscopy of biofilm-derived cells of this *uspA1 uspA2 hag* mutant (Fig. 14A) revealed that it appeared to possess no surface projections except for some bleb-like structures.

To determine the individual contributions of the Hag, UspA1 and UspA2 proteins to the wild-type surface layer, mutants of strain O35E were constructed that expressed each of these proteins in the absence of the other two. The *uspA2 hag* double mutant O35E.2HG (Fig. 13, lane 7) expressed only UspA1, and cells of this mutant (Fig. 14B) exhibited relatively long, thin projections that were sparsely distributed on the cell. The *uspA1 hag* double mutant O35E.1HG (Fig. 13, lane 6) that expressed UspA2 formed much shorter projections (Fig. 14C) that were very densely distributed on the cell surface.

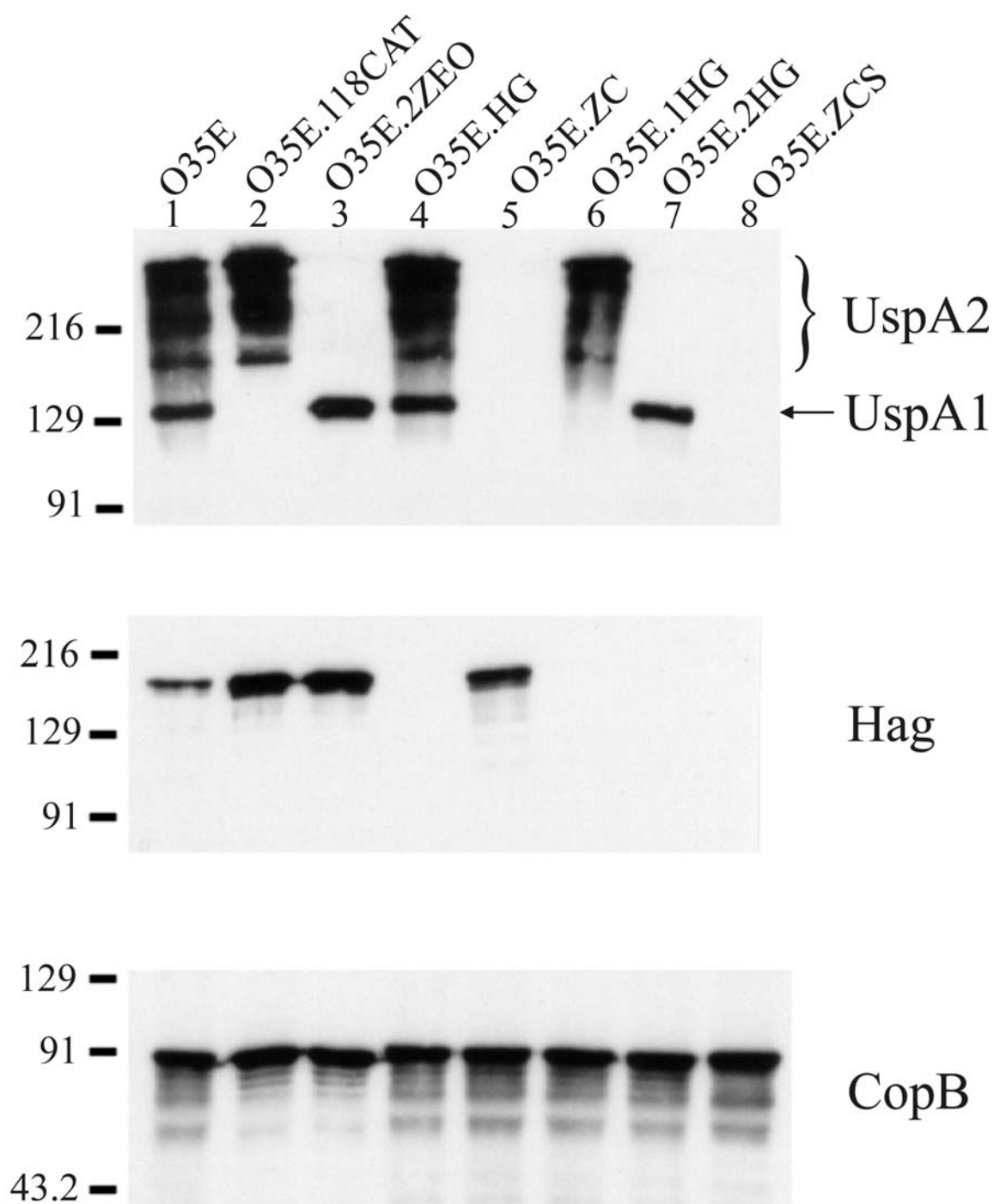


Fig. 13. Expression of Hag, UspA1, and UspA2 by wild-type and mutant strains of *M. catarrhalis* O35E. Whole-cell lysates were probed in Western blot analysis with the UspA1- and UspA2-reactive MAb 17C7 (top panel), with the Hag-specific MAb 5D2 (middle panel), and with the CopB-specific MAb 10F3. The UspA1 protein is indicated by an arrow and the UspA2 protein is indicated by a bracket in the top panel.

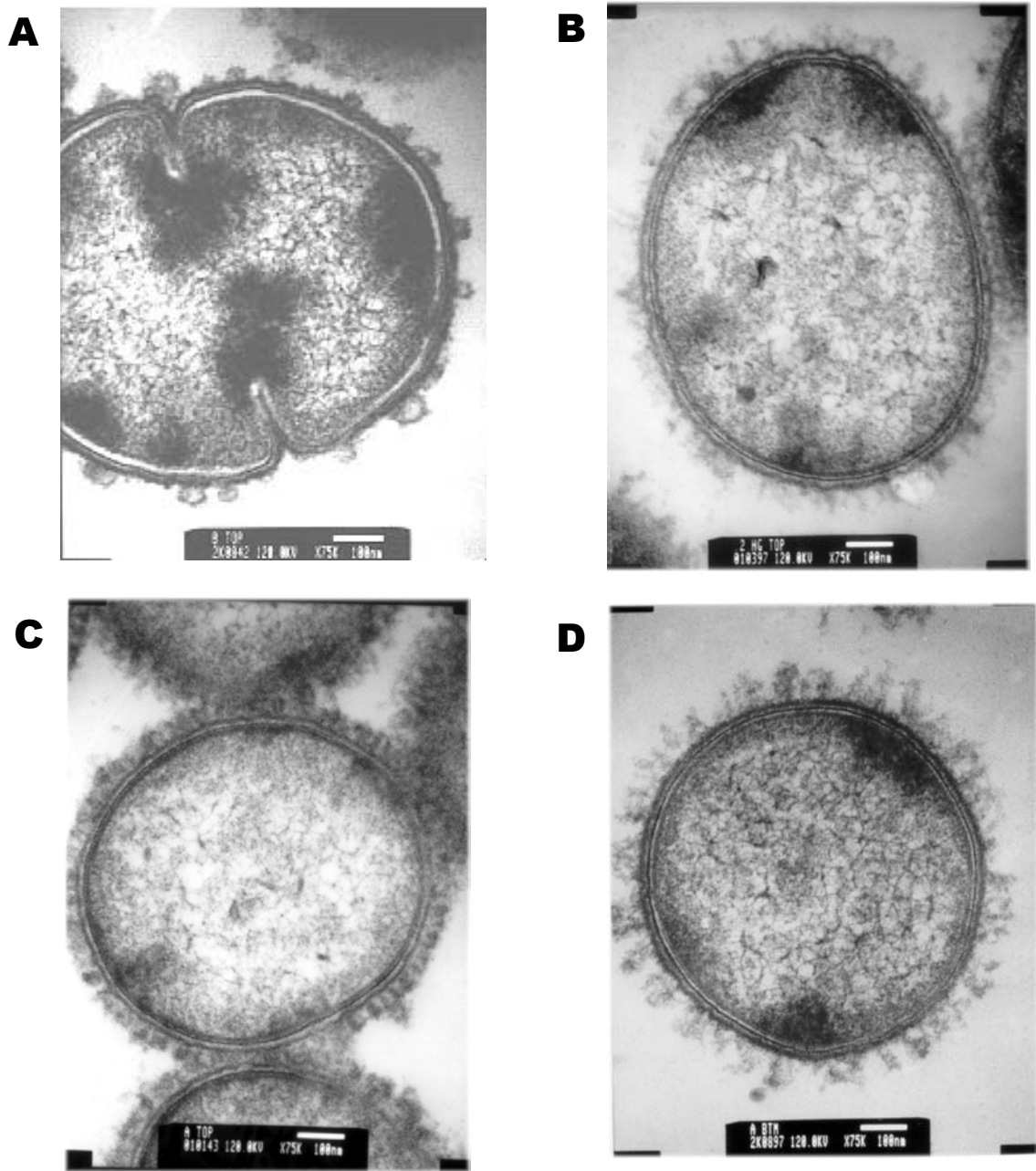


Fig. 14. Detection of projections on the surfaces of wild-type and mutant strains of *M. catarrhalis* by TEM. Each strain was grown as a biofilm for 3 days before being processed for TEM, as described in “Materials and Methods”. (A) *uspA1 uspA2 hag* triple mutant O35E.ZCS; (B) *uspA2 hag* double mutant O35E.2HG, expressing only the UspA1 protein; (C) *uspA1 hag* double mutant O35E.1HG expressing only the UspA2 protein; (D) *uspA1 uspA2* double mutant O35E.ZC expressing only the Hag protein. Compare these results with the TEM of wild-type O35E in Fig. 11.

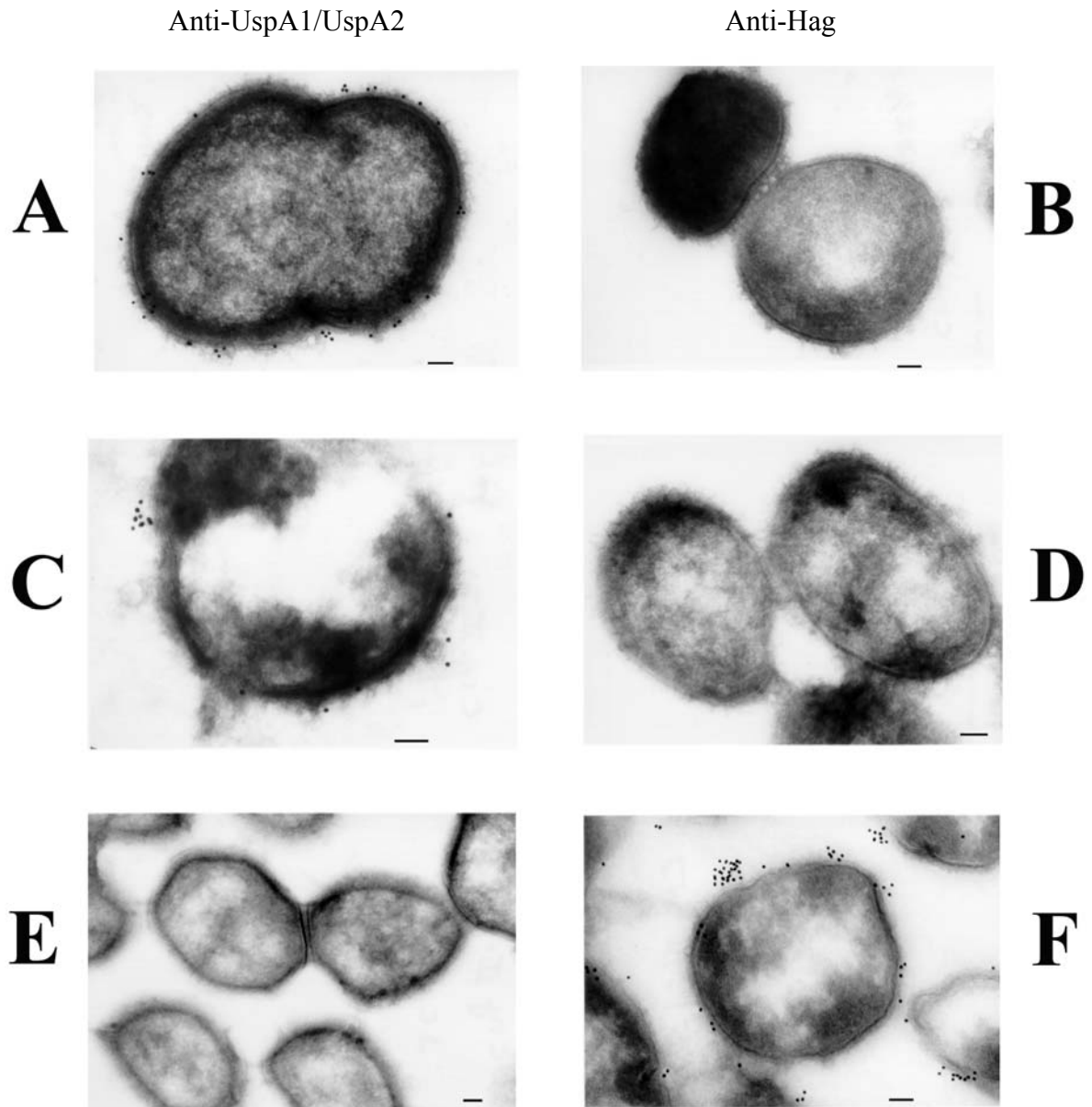


Fig. 15. Use of cryoimmunoelectron microscopy to detect UspA1, UspA2, and Hag on the *M. catarrhalis* cell surface. Biofilm-derived cells of *uspA2 hag* double mutant O35E.2HG, expressing only the UspA1 protein (A and B), *uspA1 hag* double mutant O35E.1HG, expressing only the UspA2 protein (C and D), and *uspA1 uspA2* double mutant O35E.ZC, expressing only the Hag protein (E and F) were probed with the UspA1- and UspA2-reactive MAb 17C7 (A, C, and E) and with the Hag-specific MAb 5D2 (B, D, and F) prior to incubation with gold particle-conjugated goat anti-mouse IgG. Bars (all panels), 100 nm.

The *uspA1 uspA2* double mutant O35E.ZC (Fig. 13, lane 5) that expressed only the Hag protein formed projections (Fig. 14D) that resembled those formed by the *uspA2 hag* mutant that expressed only UspA1.

Cryoimmunoelectron microscopy was used to confirm that all three of these proteins were expressed on the *M. catarrhalis* cell surface. The *uspA2 hag* double mutant O35E.2HG that expressed only the UspA1 protein bound the UspA1- and UspA2-reactive MAb 17C7 (Fig. 15A) and did not bind the Hag-specific MAb 5D2 (Fig. 15B). The *uspA1 hag* double mutant O35E.1HG that expressed only UspA2 also bound MAb 17C7 (Fig. 15C) and did not bind MAb 5D2 (Fig. 15D). Finally, the *uspA1 uspA2* double mutant O35E.ZC that expressed only the Hag protein bound the Hag-specific MAb 5D2 (Fig. 15F) but did not react with MAb 17C7 (Fig. 15E). In all cases, MAb-mediated binding of the antibody-conjugated gold particles was localized almost exclusively to the surface of the bacterial cell or to the area immediately exterior to the cell surface. The apparently punctuate staining may be due to the presence of membrane blebs.

D. Appearance of *M. catarrhalis* biofilms as revealed by SEM

When grown in Sorbarod filters as a biofilm, *M. catarrhalis* strain O35E forms grape-like clusters (Fig. 16). Thread-like structures that were observed in these images are possibly cellulose fibers from the Sorbarod filter or bacterial glycocalyx material that collapsed during the necessary dehydration procedure for SEM analysis. When the paper exterior of a Sorbarod filter was removed, a dense layer of *M. catarrhalis* was observed. At the

magnification used, no differences were seen when comparing wild-type strain O35E and its *uspA1 uspA2 hag* mutant O35E.ZCS (Fig 17). However, the resolution was insufficient at higher magnifications (i.e., 10,000x) to make definitive comparisons of mutant and wild-type morphologies.

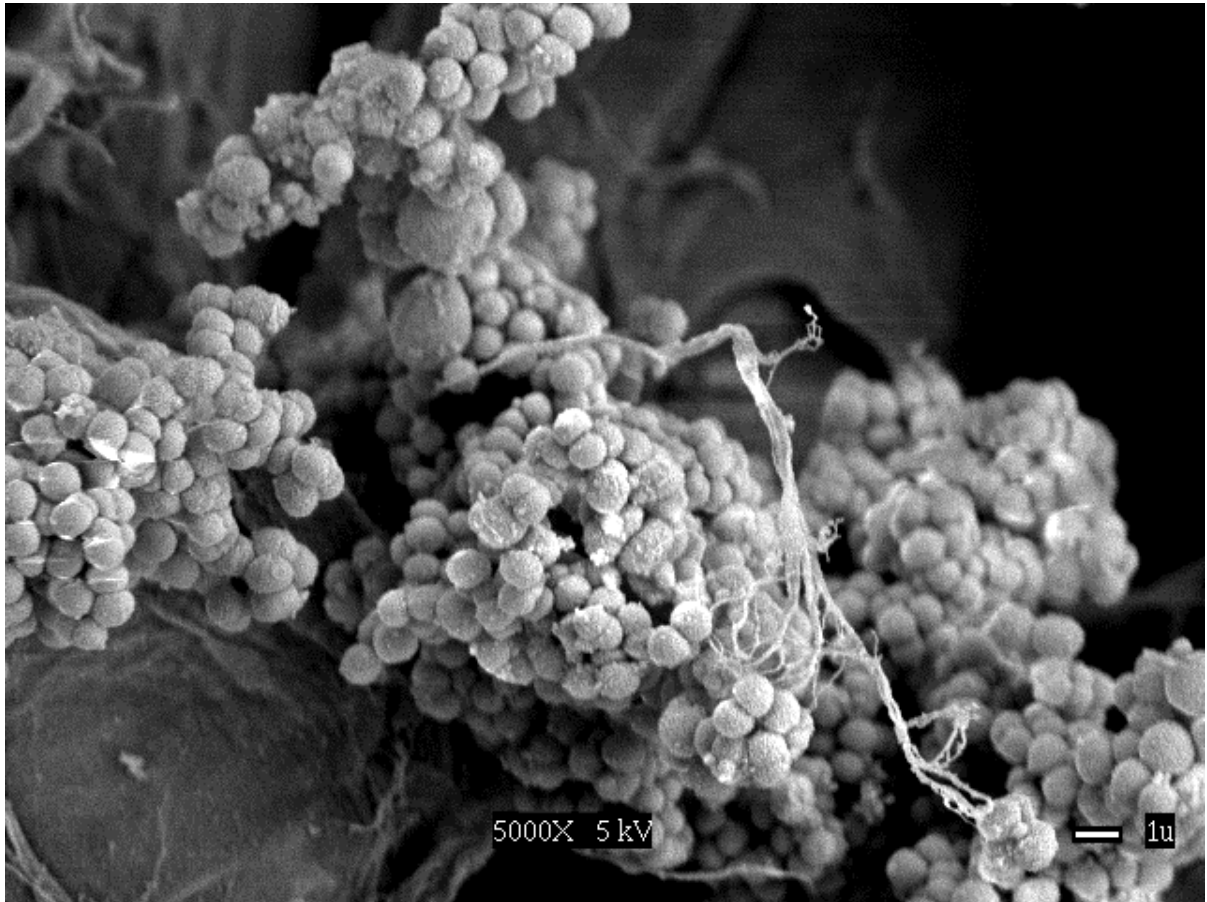


Fig. 16. SEM of wild-type O35E growing in a biofilm. Bar, 1 μm.

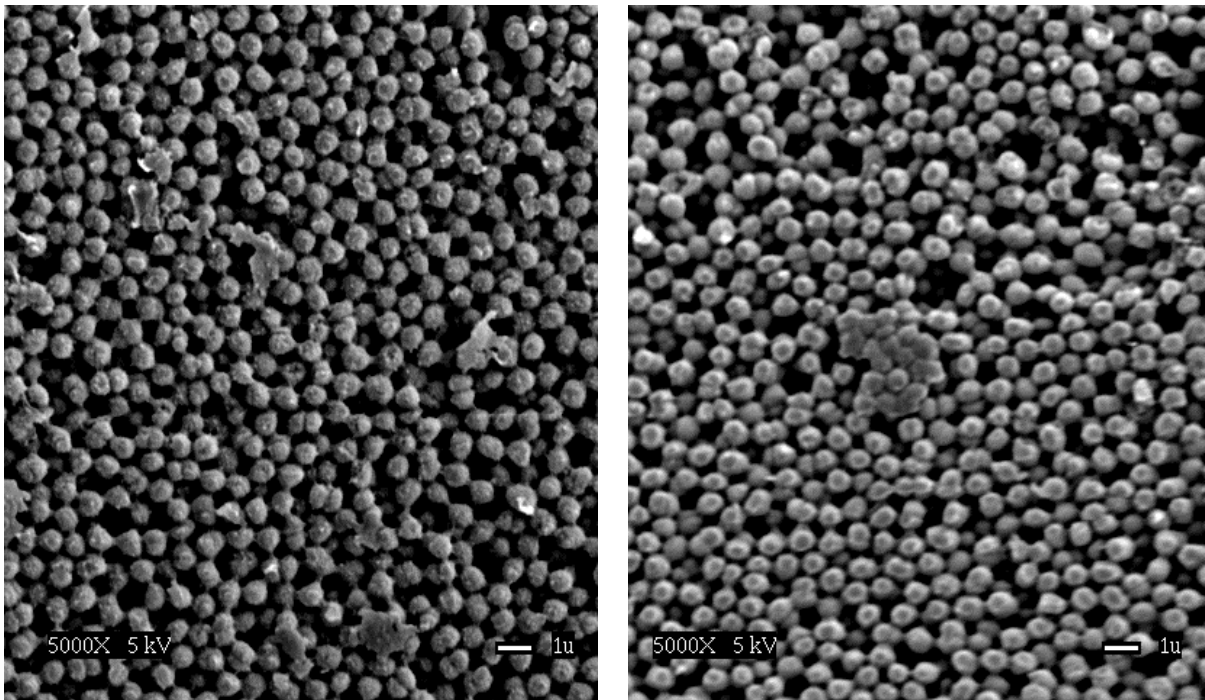


Fig. 17. SEM comparison of biofilm-grown O35E (left) and its isogenic *uspA1 uspA2 hag* triple mutant O35E.ZCS (right). Bar, 1 μ m.

E. Phenotype of the *M. catarrhalis* strain O35E *hag* mutant

(i) Effect of the *hag* mutation on hemagglutination ability

To determine whether the 200 kDa protein described by Scott and co-workers (213) as being associated with hemagglutination ability of some *M. catarrhalis* strains was encoded by the *hag* gene, an isogenic *hag* mutant of *M. catarrhalis* strain O35E was constructed. The *hag* mutant O35E.HG (Fig. 13B) did not express any detectable Hag protein whereas the wild-type parent strain O35E (Fig. 13B) expressed a readily detectable 200 kDa antigen that

bound the Hag-specific MAb 5D2. This *hag* mutant (Fig. 13A) also expressed wild-type levels of both UspA1 and UspA2. The wild-type parent strain (Fig. 18, first row) caused hemagglutination of human erythrocytes. In contrast, the *hag* mutant O35E.HG did not cause hemagglutination (Fig. 18, second row).

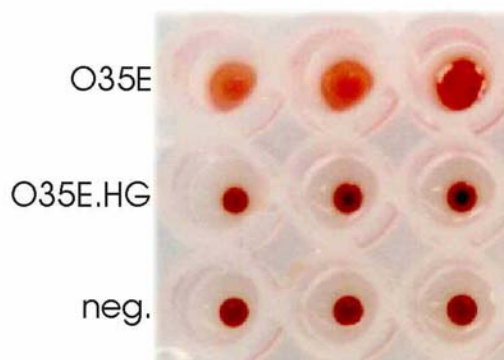


Fig. 18. Hemagglutination ability of wild-type and mutant strains of *M. catarrhalis* O35E. Cells of the wild-type parent strain, O35E, the *hag* mutant O35E.HG, and PBS (negative control) were mixed in triplicate with citrated human red blood cells and incubated at room temperature for 15 min.

(ii) Autoagglutination ability of the *hag* mutant

When dense bacterial suspensions were prepared, it was observed that the wild-type parent strain settled out of suspension more rapidly than did the *hag* mutant. To further investigate this phenomenon, the autoagglutination characteristics of both the wild-type parent strain and relevant mutants with altered expression of the Hag, UspA1, and UspA2 surface proteins were determined. The wild-type parent strain O35E, the *uspA1* mutant O35E.118CAT, and the *uspA2* mutant O35E.2ZEO (Fig. 19A) all exhibited the same rate and extent of autoagglutination in PBS. In contrast, the *hag* mutant O35E.HG exhibited little or

no tendency to autoagglutinate even after five hours in suspension (Fig. 19A). When double or triple mutant combinations of *uspA1*, *uspA2*, and *hag* were assayed for autoagglutination ability, a different pattern was observed (Fig. 19B). As expected given the above data, the *uspA1 uspA2* double mutant O35E.ZC autoagglutinated at the same rate as the wild-type parent strain. Also, the *uspA2 hag* double mutant O35E.2HG remained in suspension as well as the *hag* single mutant. However, the *uspA1 hag* double mutant O35E.1HG autoagglutinated at an intermediate rate (Fig. 19B). In addition, the *uspA1 uspA2 hag* triple mutant O35E.ZCS autoagglutinated almost as well as the wild-type parent strain O35E.

(iii) Effect of the *hag* mutation on attachment ability

Previous studies from this laboratory had indicated that *M. catarrhalis* readily attaches to Chang conjunctival epithelial cells *in vitro* and that the UspA1 protein is responsible for the observed attachment ability (5, 174). Because the Hag protein was involved in both hemagglutination and autoagglutination and therefore had the potential to interact directly with the surface of eukaryotic cells, the ability of the *hag* mutant to attach to Chang cells was tested. The wild-type strain O35E attached to these human cells at readily detectable levels (Fig. 20A, column 1) whereas, as expected, the *uspA1* mutant O35E.118CAT had little or no ability to attach to these same cells (Fig. 20A, column 2). In addition, the *uspA2* mutant O35E.2ZEO attached to the Chang cells at wild-type levels (Fig. 20A, column 3), consistent with previously published results obtained with an independently isolated *uspA2* mutant (5). The presence of the *hag* mutation had no detectable deleterious

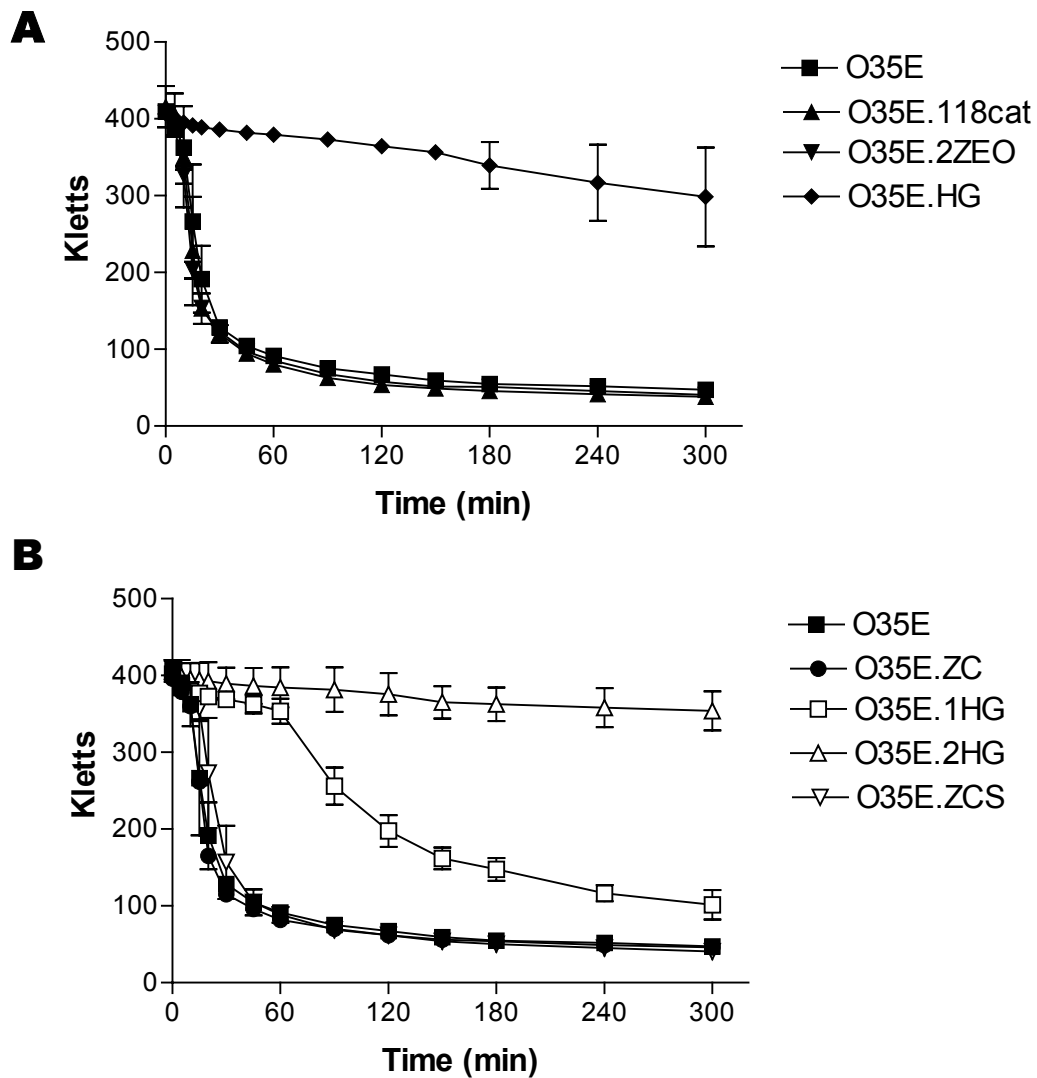


Fig. 19. Autoagglutination ability of wild-type and mutant strains of *M. catarrhalis* O35E. Cells grown on BHI agar plates overnight were suspended in PBS, and the change in turbidity over time was measured. Panel A, autoagglutination by wild-type O35E and single mutants; Panel B, autoagglutination by wild-type O35E and double and triple mutants.

effect on the attachment ability of *M. catarrhalis* strain O35E (Fig. 20A, column 4). Similarly, this *hag* mutant attached to several other human epithelial cell lines *in vitro* at levels similar or identical to those obtained with the wild-type parent strain (Fig. 20B-D). These cell lines included HEp-2 cells, 16HBE14o- bronchial epithelial cells, 9HTEo-tracheal cells (data not shown), and NCI-H292 epithelial cells. Although UspA1 is clearly an adhesin for Chang cells, it is apparent that it does not mediate attachment to the other cell lines tested (Fig. 20, B-D).

(iv) The Hag protein has IgD-binding activity

While the studies described above were in progress, Forsgren and colleagues (100) described the identification of a 200 kDa protein, designated MID, from *M. catarrhalis* strain Bc5 that possessed human IgD-binding activity. To determine whether the 200 kDa protein encoded by the *hag* gene of *M. catarrhalis* strain O35E was capable of binding IgD, both the wild-type parent strain and the *hag* mutant O35E.HG were tested in a Western blot assay for IgD binding activity. When a whole cell lysate of the wild-type O35E strain was incubated with human IgD, the majority of the IgD binding activity was associated with a band (Fig. 21A, lane 1, open arrow) that just entered the separating gel, together with a minor band (Fig. 21A, lane 1, closed arrow) that migrated to a point just below the 216 kDa standard. These two different binding activities were also described by Forsgren and co-workers in their studies of the MID protein (100). In contrast, there was no IgD-binding activity detected in the whole cell lysate of the *hag* mutant (Fig. 21A, lane 2) other than some minor reactive bands that

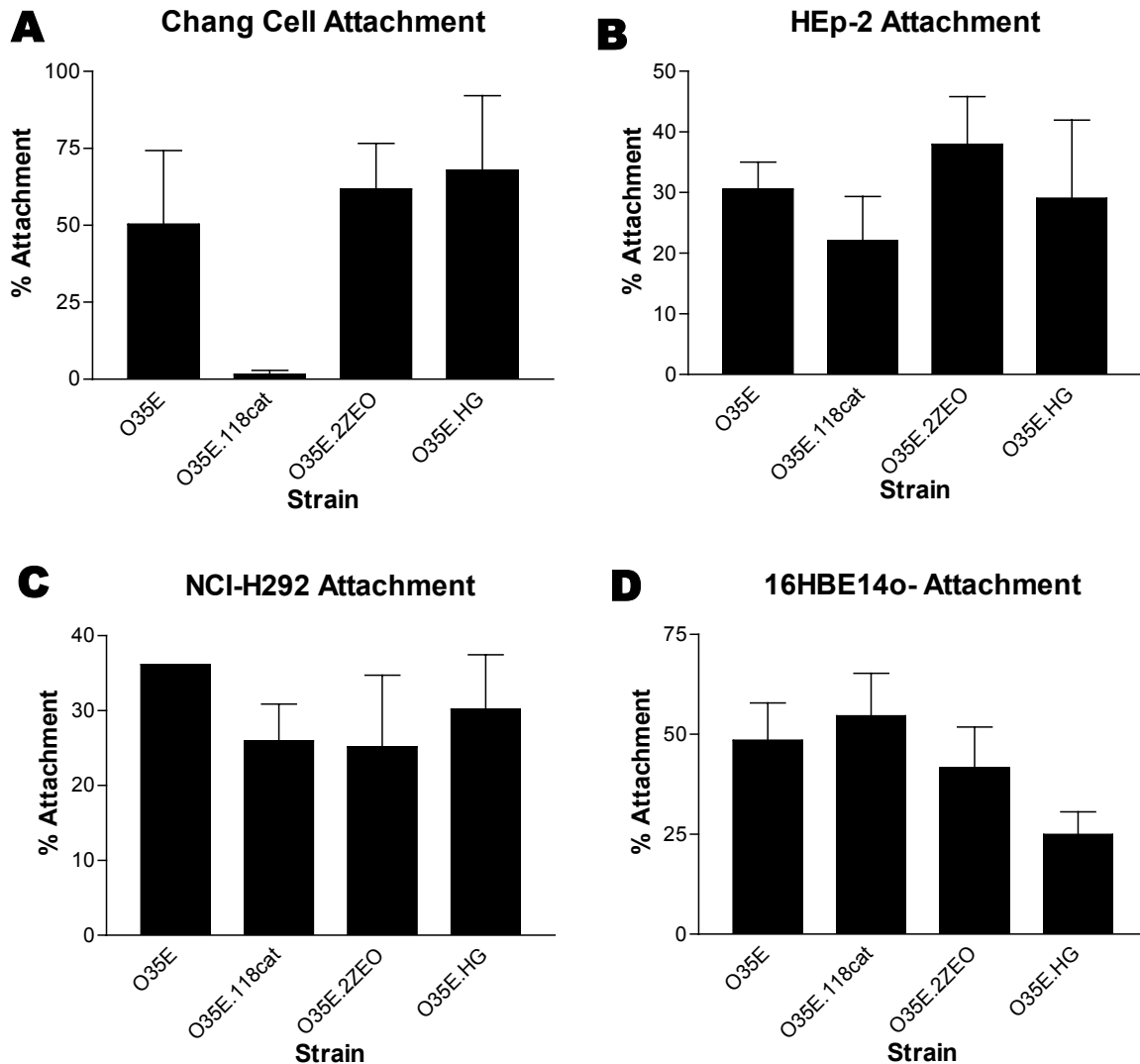


Fig. 20. Attachment of strain O35E, the *uspA1* mutant O35E.118cat, the *uspA2* mutant O35E.2ZEO, and the *hag* mutant O35E.HG to several different epithelial cell lines.

also appeared to be expressed by the wild-type parent strain. Western blot analysis of the whole cell lysate of the wild-type parent strain (Fig. 21B, lane 1) with the Hag-reactive MAb 5D2 indicated that this MAb bound an antigen that migrated to the same position as did the minor IgD-binding activity expressed by this strain (Fig. 21B, lane 1, closed arrow). In addition, this MAb also yielded weak reactivity with an antigen of the wild-type strain that migrated to the same position (i.e., near the top of the separating gel) (Fig. 21B, lane 1, open

arrow) as did the major IgD-binding activity present in the wild-type parent strain (Fig. 21A, lane 1). The CopB-specific MAb 10F3 (Fig. 21C) was used to ensure that equal protein loads were used in these Western blot experiments.

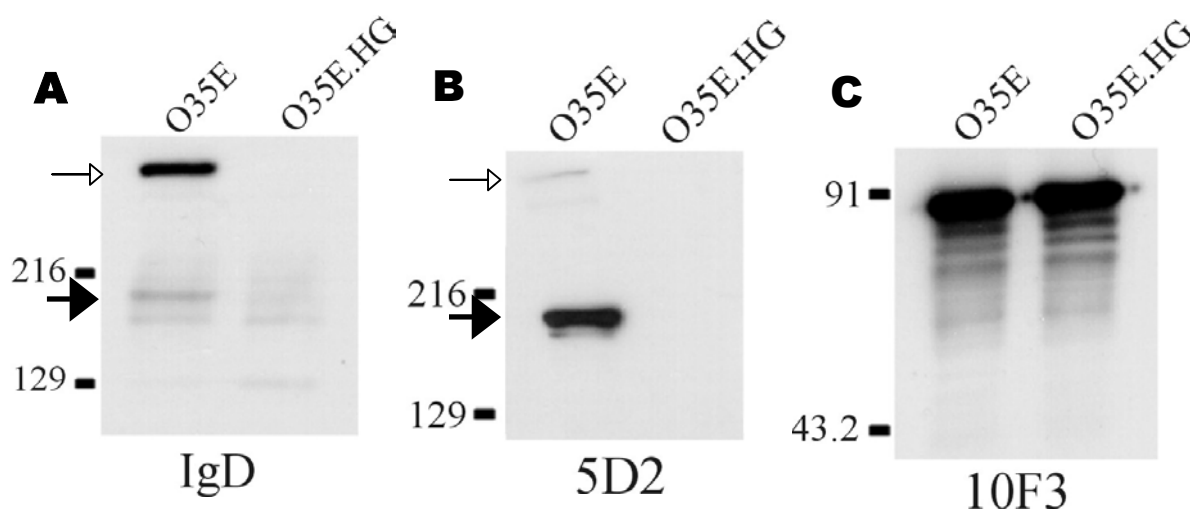


Fig. 21. Binding of human IgD by wild-type and mutant strains of *M. catarrhalis*. Whole cell lysates of wild-type strain O35E and *hag* mutant O35E.HG were probed in a Western blot analysis with human IgD (A), the Hag-reactive MAb 5D2 (B), and the CopB-specific MAb 10F3. In panels A and B, the open arrow indicates the position of the form of Hag that just barely enters the separating gel whereas the solid arrow indicates the position of the form that has an apparent molecular weight of approximately 200,000. Molecular size position markers (in kilodaltons) are shown on the left.

F. Conservation of a Hag antigenic determinant

Western blot analysis of twelve additional *M. catarrhalis* isolates revealed that ten of these twelve strains expressed a Hag protein that was readily detectable with MAb 5D2 in Western blot analysis (Fig. 22, lanes 2-13). The apparent molecular weight of these different

Hag proteins varied somewhat from strain to strain. In addition, the very large form of the Hag protein which barely entered the separating gel was readily apparent with a few of these strains (Fig. 22, lanes 2, 4, 8, 9). The lack of a detectable Hag protein with *M. catarrhalis* strains ATCC 25240 and ETSU-13 (Fig. 22, lanes 5 and 12, respectively) indicated that these two strains lacked a *hag* gene, possessed a non-functional *hag* gene, or expressed a Hag protein that lacked the epitope bound by MAb 5D2. To discriminate among these possibilities, we used PCR to amplify the 5' end of both strains' putative *hag* ORF; this is the region which contains the poly(G) tract. Nucleotide sequence analysis revealed that this region contained eight G residues in strain ATCC 25240 and eleven G residues in strain ETSU-13. In both cases, these numbers of G residues would result in premature termination of translation of the *hag* ORF, in the same manner as that postulated to occur in a spontaneous mutant of *M. catarrhalis* strain 4223 that had lost the ability to express the 200 kDa protein as the result of a change from nine to eight G residues in its poly(G) tract (265).

Nucleotide sequence analysis of the *hag* gene from *M. catarrhalis* strain O12E, which was reactive with MAb 5D2 (Fig. 22, lane 2), was also performed. The *hag* ORF from strain O12E contained 6,945 nt (GenBank Accession AY977638). The deduced amino acid sequence of the Hag protein from *M. catarrhalis* strain O35E was 60–76% identical to the Hag protein from strain O12E, the 200 kDa protein from strain 4223, and the MID protein from strain Bc5. The first 60 amino acids of these four proteins shared 96-100% identity, with the C-terminal 400 amino acids having 99% identity. All four proteins also possessed IAIGXXXXXXXXXXIAIG amino acid repeat motifs that tended to be clustered at the beginning and end of these macromolecules and which appear to be present in several other

large, surface-expressed bacterial proteins included in the autotransporter family (132).

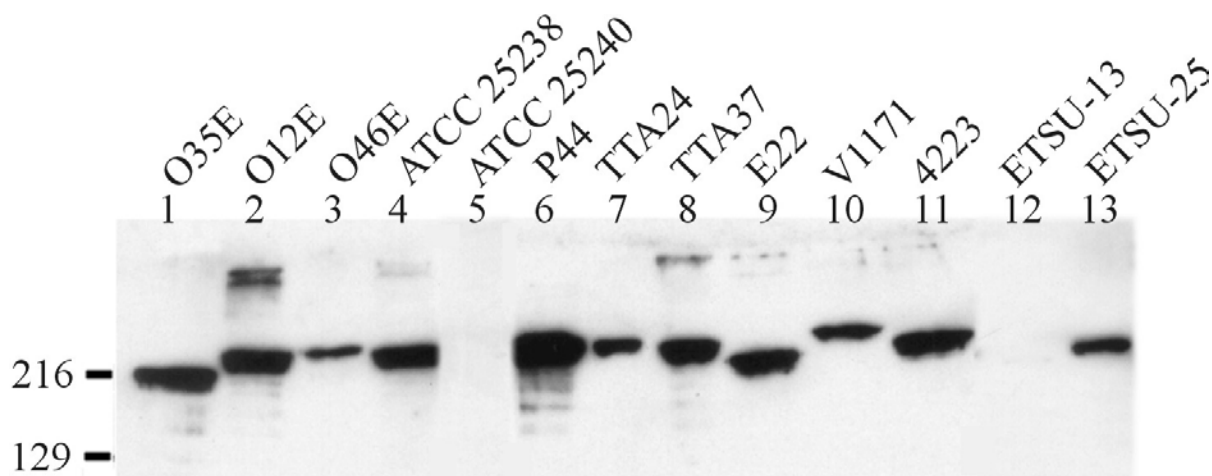


Fig. 22. Reactivity of 12 *M. catarrhalis* strains with Hag-specific MAb 5D2. Whole-cell lysates of these 12 strains were probed in Western blot analysis with Hag-reactive MAb 5D2. Molecular size position markers (in kilodaltons) are shown on the left.

G. Phenotypes of *hag* mutants of other *M. catarrhalis* strains

(i) Hemagglutination

Of the four *M. catarrhalis* strains tested for the ability to agglutinate erythrocytes, strain O12E possessed the most robust hemagglutination ability. This strain was capable of agglutinating both rabbit and human erythrocytes, whereas its isogenic *hag* mutant O12E.HG was not (data not shown). Strain O46E was inconsistent in its ability to agglutinate either human or rabbit erythrocytes. Strain P44 was weakly positive for hemagglutination; however, while the isogenic *hag* mutant P44.HG appeared to agglutinate erythrocytes, the *uspA1 uspA2 hag* triple mutant P44.12HG did not (data not shown).

(ii) Autoagglutination

The wild-type strain O46E expresses very little to undetectable levels of Hag because the poly(G) tract of its *hag* gene contains 10 G residues which result in premature termination of translation. Nevertheless, this strain autoagglutinated at a rate similar to that of the Hag-positive strain O35E (data not shown). Unexpectedly, the *uspA1* mutant of O46E and the *uspA1 hag* double mutant autoagglutinated extremely rapidly (within 5 min). The reason for this phenomenon is unknown; however, at the time that strain O46E was analyzed for autoagglutination, it was not recognized that the working stock of this organism (the 2001 stock; see Chapter 9 for more detail) contained a mixed population of UspA2H-positive and UspA2H-negative cells due to spontaneous phase variation. Although pure cultures of a UspA2H-positive O46E have not been rigorously tested, UspA2H-positive O46E also appears to exhibit the hyperautoagglutination phenotype. It is also possible that the 2001 O46E stock has a mixed population of Hag-positive and Hag-negative cells, which would explain why the O46E stock in Fig. 22 has some Hag reactivity while there is very little or no Hag expression in experiments in later chapters (which were conducted using the O46E 2001-1 isolate; see Chapter 9). The Hag-positive wild-type strain O12E and its isogenic *uspA1*, *uspA2*, and *hag* mutants O12E.1, O12E.2, and O12E.HG all autoagglutinate at the same rate (data not shown).

(iii) IgD-binding

Western blot-based analysis of two wild-type Hag-positive *M. catarrhalis* strains, O12E and 4223, for their IgD-binding ability gave different results (data not shown). Whereas the Hag protein from strain O12E appeared to bind human IgD, the Hag protein from strain 4223 did not, or bound IgD very weakly. Two Hag-negative strains, ETSU-13 and ATCC 25240, did not bind human IgD when analyzed by Western blot (data not shown).

III. Discussion

The existence of filamentous projections on the surface of *M. catarrhalis* was documented over three decades ago by Wistreich and Baker (334) who described the presence of putative fimbriae on the surface of a strain of *Neisseria (Moraxella) catarrhalis*. The ability of some *M. catarrhalis* strains to hemagglutinate different types of erythrocytes was also described by Wistreich and Baker (334) and then studied in some detail by several other laboratories (10, 161, 260). Some of these early workers differed on whether hemagglutination ability could be correlated with fimbriation (10, 260) or with the ability to attach to eukaryotic cells (161, 260). The more recent studies of Scott and co-workers (92, 93, 95, 213) showed that the hemagglutination ability of different strains of *M. catarrhalis* was associated with the expression of a 200 kDa protein which was present on the bacterial cell surface.

Previous studies from this laboratory had indicated that both UspA1 and UspA2 were

exposed on the surface of *M. catarrhalis* (5, 62) and that both of these proteins had regions that were likely to form coiled coils (62) which could project from the cell surface. The reported association of the 200 kDa protein with a fibrillar layer on some strains of *M. catarrhalis* (93) prompted an investigation as to whether the UspA1 and UspA2 proteins could also be involved in formation of this fibrillar layer. Examination by TEM of a triple mutant lacking the ability to express the Hag, UspA1, and UspA2 proteins (Fig. 14A) revealed that there were no detectable fibrillar projections on the surface of this strain. Next, the surface phenotype of double mutants which could express only one of each of these three proteins was examined. These studies revealed that a *uspA2 hag* mutant with a functional *uspA1* gene (Fig. 14B) and a *uspA1 uspA2* mutant with a functional *hag* gene (Fig. 14D) both expressed relatively long fibrillar structures that were sparsely distributed on the bacterial cell surface. In contrast, the *uspA1 hag* mutant that could express only UspA2 (Fig. 14C) had a much denser layer of shorter projections on its cell surface. Close inspection of the wild-type parent strain (Fig. 11, left) reveals the presence of two layers of projections. It is of interest to note that Wistreich and Baker (334) reported that the single fimbriate strain of *M. catarrhalis* used in their study expressed two fimbriae types, with one being much longer than the other.

A recent report from Hoiczky *et al.* (141), which appeared while the current study was in progress, indicated that a *uspA1 uspA2* mutant of strain O35E that had been constructed previously by our laboratory (5) lacked filamentous projections. There are two possible explanations for the reported absence of filamentous projections on this particular *uspA1 uspA2* mutant. The first is that the sparsely distributed surface projections associated

with expression of the *hag* gene may simply have been destroyed in the preparation of their samples for TEM. The second possibility would involve a mutation in the *hag* gene. Sasaki and co-workers (265) reported the presence of nine consecutive G residues near the 5' end of the ORF encoding the 200 kDa protein of *M. catarrhalis* strain 4223. A spontaneous change in the number of G residues from nine to eight, likely as the result of slipped-strand mispairing (136), caused lack of expression of the 200 kDa protein. This latter possibility seems less likely to have occurred in the *uspA1 uspA2* mutant O35E.12 (5), however, in view of the fact that the corresponding region of the *hag* gene of strain O35E has only six G residues and this shorter poly(G) tract would be less likely to undergo slipped-strand mispairing.

Inactivation of the *hag* gene in *M. catarrhalis* strain O35E resulted in the loss of both hemagglutination (Fig. 18) and autoagglutination (Fig. 19A) ability. This result confirmed that the Hag protein is responsible for hemagglutination by strain O35E. In addition, the propensity of this strain to form large aggregates (i.e., autoagglutination) was eliminated by the *hag* mutation. Interestingly, loss of the ability to express Hag was not associated with a decreased ability to attach to several human epithelial cell lines, including Chang conjunctival epithelial cells (Fig. 20A) and HEp-2 cells (Fig. 20B). This finding confirms an earlier report by Scott and colleagues (95) which indicated that the hemagglutination activity of *M. catarrhalis* isolates appeared to be independent of their ability to attach to HEp-2 cells *in vitro*. In contrast, Lafontaine and colleagues (144) found that the Hag protein mediates attachment of *M. catarrhalis* to A549 human lung cells and human middle ear epithelial (HMEE) cells. Forsgren *et al* (99) independently reported that Hag mediates adhesion of *M.*

catarrhalis to A549 cells. Thus, *M. catarrhalis* appears to employ different adhesins for different cell types.

The lack of autoagglutination by the O35E *hag* mutant (Fig. 19A) mimics that described for a spontaneous mutant or variant of *M. catarrhalis* strain 4223 that was isolated by Murphy and colleagues (173). These workers selected a non-clumping variant of strain 4223 by sequential passage in broth. This variant lacked detectable expression of a 200 kDa protein and also had reduced expression of the HMW-OMP (i.e., UspA2) as well as altered surface accessibility of some but not all of the surface epitopes of the outer membrane protein CD and its lipooligosaccharide molecule (173). It is likely that the 200 kDa protein missing from this variant is Hag, although this would need to be confirmed by Western blot analysis. The existence of a spontaneous frameshift mutant of strain 4223 that lacked the ability to express the 200 kDa protein (265) raises the possibility that the non-clumping variant isolated by broth passage (173) may have had the same type of mutation in the *hag* ORF. The other alterations in the phenotype of this non-clumping variant could have been the effect of the lack of expression of the 200 kDa protein on the surface architecture of the outer membrane. Alternatively, this variant of strain 4223 may have possessed additional genetic changes.

It was surprising to find that the *uspA1 hag* double mutant O35E.1HG and the triple mutant O35E.ZCS exhibit increased autoagglutination relative to the *hag* mutant O35E.HG (Fig. 19B). There are several possible explanations for this phenomenon. First, *M. catarrhalis* may possess a second factor capable of mediating autoagglutination that is only exposed when these other surface proteins are absent. TEM analysis indicates that the

UspA1 and Hag proteins form long projections extending from the cell surface, and the removal of both of these proteins may result in the ability to effect autoagglutination mediated by this other factor. The fact that strains O12E and O46E are able to autoagglutinate regardless of Hag expression seems to indicate that *M. catarrhalis* strains may possess more than one autoagglutinin. Another possibility is that the deletion of so much biomass from the *M. catarrhalis* cell surface results in altered membrane architecture. A change in hydrophobicity, for example, could cause increased interaction between bacteria which results in the clumping and settling of these cells. A third possibility is that O35E.1HG and O35E.ZCS each contain a secondary mutation that results in increased autoagglutination. This latter possibility seems rather unlikely because these mutants were constructed independently of each other.

It is of interest to note that the majority of the IgD-binding activity associated with the Hag protein (Fig. 21A) did not migrate to the same position in the separating gel as did the Hag antigen which bound the Hag-specific MAb 5D2 (Fig. 21B). Most of the MAb-reactive Hag protein migrated to a position just beneath the 216 kDa marker whereas the IgD-binding activity migrated much more slowly with an apparent molecular weight well in excess of 216 kDa. This behavior of the Hag protein in SDS-PAGE is similar to that described for UspA1 and UspA2, both of which form very large aggregates or complexes when analyzed by SDS-PAGE (62). It should also be noted that the IgD-binding activity of the MID protein described by Forsgren *et al.* (100) had two different forms in SDS-PAGE, with one form migrating near the 200 kDa marker and the other form barely entering the separating gel. It is possible that IgD preferentially binds to the multimeric form of the Hag

protein from strain O35E; the structural basis for this recognition remains to be determined.

The biological significance of two (i.e., hemagglutination and autoagglutination) of the three different phenotypes associated with expression of the Hag protein by *M. catarrhalis* strain O35E has been determined for a number of different organisms. Hemagglutination in Gram-negative bacteria is often associated with expression of pili or non-pilus adhesive proteins that promote attachment to and colonization of host mucosal surfaces (181, 184, 197, 271). The *hag* mutant of *M. catarrhalis* did not display any decrease in its ability to attach to a number of human cell lines *in vitro*, although lack of Hag expression was recently shown to affect attachment to cell types not included in the present study (99, 144). Autoagglutination, often caused either by certain types of pili or outer membrane proteins, has been used as a marker of virulence or attachment ability for several gram-negative pathogens including such diverse organisms as *Vibrio cholerae* (57), *Yersinia enterocolitica* (280), and *Fusobacterium nucleatum* (121). The lack of a relevant animal model for testing the virulence of *M. catarrhalis* precludes determination of whether the *hag* mutant is truly less virulent than its wild-type parent strain.

The biological relevance of IgD-binding activity is more difficult to ascertain. It has been known for many years that *M. catarrhalis* readily binds soluble human IgD (101) and Forsgren and colleagues have reported recently that the MID protein will bind IgD-expressing B cells (100). Soluble IgD is present in the nasopharynx of healthy children (284), thus providing the opportunity for this immunoglobulin to be bound by *M. catarrhalis*. Whether the interaction between IgD and the Hag protein might somehow augment the ability of *M. catarrhalis* to colonize the nasopharynx or cause otitis media remains to be

determined.

The N-terminal and C-terminal regions of the 200 kDa protein from strain 4223 (264), the Hag proteins of strains O35E and O12E, and the MID protein of strain Bc5 (100) have near perfect identity, with significant amino acid sequence differences being found in the more central regions of these proteins. This situation is similar to that described individually for the UspA1 and UspA2 proteins of *M. catarrhalis* where the N- and C-termini of each type of macromolecule are virtually identical among different strains (62). If the four 200 kDa proteins described immediately above are truly all Hag proteins, it would appear that there is a clustering of amino acid sequence polymorphisms between the highly conserved N- and C-termini. This would be similar to the mosaic structures of other surface-exposed proteins from different pathogens including *Neisseria gonorrhoeae* (120) and *N. meningitidis* (139) where mosaic genes have been proposed to result from horizontal genetic exchange. The fact that *M. catarrhalis* can be transformed *in vitro* (49) makes this latter possibility feasible.

Although an isogenic *mid* mutant has not been reported for strain Bc5, in which MID was originally described, Forsgren *et al* (99) have constructed *mid* mutants in two other strains of *M. catarrhalis*; these mutants were not able to agglutinate human erythrocytes. The IgD-binding activity of the Hag protein described in this study makes it likely that Hag and the MID protein described by Forsgren *et al.* (100) are the same macromolecule with strain-specific amino acid sequence differences.

CHAPTER SIX

Use of the Crystal Violet-Based Assay to Characterize Biofilm Formation by *M. catarrhalis*

I. Introduction

The previous chapter described the use of a continuous flow culture system for growing *M. catarrhalis* biofilms. While this system is very useful for detailed examinations of biofilms, it is difficult or impractical for use in screening many different *M. catarrhalis* strains or mutants for their ability to form biofilms. Thus, it became important to identify another method for biofilm study. The crystal violet-based assay, first reported as a tool for biofilm research by O'Toole and Kolter (229), seemed an ideal choice.

Initially, a large number of *M. catarrhalis* strains were tested for their biofilm formation ability. Isolates of this pathogen were found to vary in their ability to form biofilms *in vitro* and these biofilms were shown to sometimes differ in their gross appearance. *M. catarrhalis* strain O35E was found to form somewhat better biofilms when grown in richer growth media. Transposon insertion mutagenesis was performed on this strain to obtain mutants deficient in biofilm formation in this richer growth medium. One biofilm-deficient mutant, 20A3, had a transposon insertion in the gene encoding a putative S-adenosyl homocysteine hydrolase.

II. Results

A. Elucidation of the optimal conditions for *M. catarrhalis* biofilm formation

Because most laboratories utilizing the crystal violet-based assay for biofilm formation use 96-well polystyrene tissue culture plates as the surface for biofilm formation, this type of plate was also used in the preliminary biofilm studies in this laboratory. However, it was observed that biofilms were easier to visualize (as the presence of a pellicle at the air-medium interface or as a coating of bacteria on the sides or bottom of the well) when grown in the larger wells of a 24-well tissue culture plate (data not shown). The original protocol for this assay (229) did not require rinsing of the well before staining with crystal violet. In contrast, at the outset of this study, it was determined that the relatively rich BHI and TH growth media used to cultivate *M. catarrhalis* left a residue on the plastic well that stained with crystal violet. Therefore, it was necessary to rinse the wells of the tissue culture plate before staining. Several substances were tested as the rinse solution before M-199 tissue culture medium was chosen for its ability to give consistent results and maximal biofilm preservation. It was later recognized that it was possible to add M-199 to each well and then add crystal violet to the M-199 and obtain the same results. It is also important to note that biofilm incubations were always performed under a normal atmosphere; when incubations were carried out under an atmosphere of 95% air-5% CO₂, the amount of biofilm was much lower. This is possibly due to acidification of the growth medium due to the presence of dissolved CO₂.

B. *M. catarrhalis* strains vary in their ability to form biofilms

The crystal violet assay, modified from that described by O'Toole and Kolter (229) for use with *P. fluorescens*, was used to measure the ability of 88 wild-type *M. catarrhalis* strains to form biofilms in 24-well tissue culture plates (Table 4). These isolates comprised both strains isolated from persons with *M. catarrhalis* disease as well as strains obtained from the nasopharynx of healthy individuals (data not shown). The results of these assays indicated that *M. catarrhalis* strains have widely varying abilities to form biofilms, with most strains forming biofilms very poorly under these *in vitro* conditions. There was no apparent correlation between biofilm formation ability and the source of the strain. Figure 23 depicts the extent of biofilm formation by ten representative *M. catarrhalis* strains. In addition to the variation found in the amount of biofilm produced (i.e., as determined by crystal violet staining) among these strains, it was noted that the physical appearance of the biofilms also varied from strain to strain. For example, some strains formed biofilms that tightly adhered in an approximately uniform density to the tissue culture well whereas others formed very ragged-appearing biofilms that were easily detached from the plastic. Among the strains tested, strain O46E consistently yielded the highest level of staining in the crystal violet assay (Fig. 23). Accordingly, strain O46E was initially selected for subsequent analysis.

Table 4. Assessment of biofilm formation by 88 wild-type *M. catarrhalis* strains.

Strains that form biofilms well (A_{600} in crystal violet assay > 0.140)

O46E	ETSU-10	ETSU-W-1	Pt5P5
ETSU-1	ETSU-15	ETSU-13	FIN2341
ETSU-4	ETSU-19	ETSU-17	V1165
ETSU-9	V1119	B59504	7169
ATCC 43617			

Strains that form weak biofilms (A_{600} in crystal violet assay between 0.040 and 0.120)

FR2682	TTA1	B59911	FIN2404
URMC218:380	O12E	ETSU-7	2951
V1122	ATCC 25238	ETSU-12	FR2213
V1126	ATCC 25240	C20	179-3553
V1129	FIN2265	BC-1	B70287
V1153	FIN3423	V1168	

Strains that do not form biofilms (A_{600} in crystal violet assay < 0.040)

O35E	ETSU-5	C2	14P21
V1069	ETSU-6	C9	E22
V1118	ETSU-22	C16	4223
V1120	ETSU-23	M1	TTA24
V1121	ETSU-24	B59125	TTA37
V1127	ETSU-25	FIN2405	A221
V1130	ETSU-26	324.71	A225
V1145	FIN2284	FR2336	A238
V1156	FIN2344	FR3327	Pt5P16
V1165	FIN2406	B6	B59686
V1166	FIN2421	B21	P44
V1171	FIN6467	B22	P48
J-261			

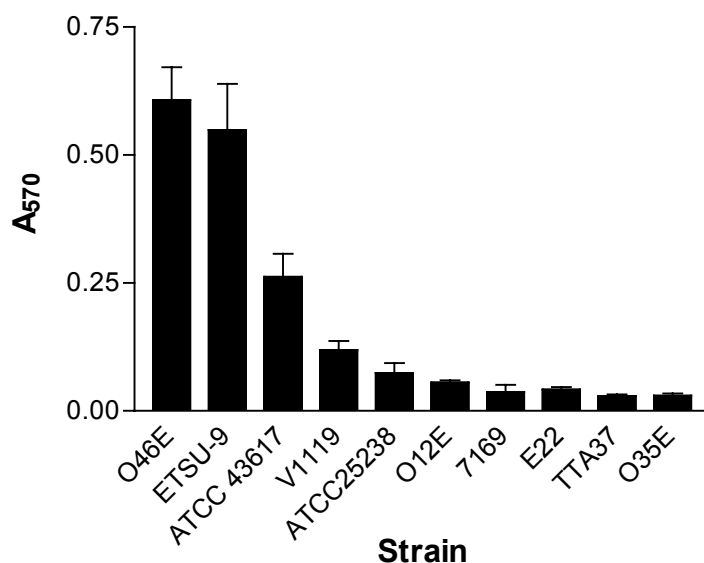


Fig. 23. Biofilm formation by wild-type *M. catarrhalis* strains. Bacteria were grown for 19 h in 24-well tissue culture plates. After rinsing, adherent bacteria were stained with crystal violet. Following extraction of the crystal violet with 95% ethanol, the absorbance of the ethanol extract was measured at 570 nm and was plotted on the vertical axis. Each assay was performed in triplicate and repeated three times.

C. Time course for O46E biofilm development

To determine the time of maximal biofilm development by strain O46E, this strain was grown in 24-well tissue culture plates and stained with crystal violet at different time points. Fig. 24 shows that the largest amount of biofilm formation had occurred 19 h after inoculation of the tissue culture plate wells with O46E. Thus, a 19 h incubation was used in all subsequent crystal violet-based assays in this study. After approximately 24 h, the growth

medium in the tissue culture plate wells was observed to evaporate significantly, especially in wells on the outer edge of the plate.

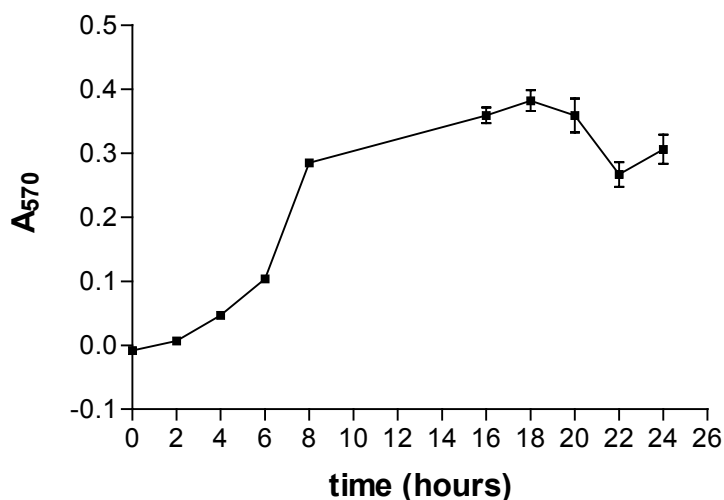


Fig. 24. Strain O46E reaches maximal biofilm formation by 19 h in a 24-well tissue culture plate. O46E was grown in 24-well tissue culture plates and stained with crystal violet at different time points. The absorbance at 570 nm was recorded following the extraction of crystal violet stain with ethanol.

D. Biofilm formation in different growth media

To test whether the nutritional content of the bacterial growth medium has an effect on biofilm formation, *M. catarrhalis* was grown in half-strength BHI. This BHI was supplemented with either PBS or NaCl to preserve osmolarity. *M. catarrhalis* biofilm formation was much weaker in half-strength BHI. However, when *M. catarrhalis* was grown in TH medium supplemented with 0.5% (w/v) yeast extract (THY.5), biofilm formation was improved for strain O35E. In contrast, strain O46E, which forms biofilms in BHI, did not

have increased biofilm formation in THY.5 medium (data not shown).

E. Transposon mutagenesis of strain O35E

Attempts were made to mutagenize several biofilm-positive strains (O46E, ETSU-9, and O12E). Unfortunately, none of these strains proved to be amenable to transposon mutagenesis. Because *M. catarrhalis* strain O35E formed biofilms moderately well in THY.5 medium and has been shown to be amenable to mutagenesis (144), it was used (instead of strain O46E) as the target for transposon mutagenesis with subsequent screening for loss of biofilm formation. A total of 425 kanamycin-resistant transposon mutants were patched onto BHI-kanamycin agar. Swatches of these patches were used to inoculate BHI in 24-well tissue culture plates; biofilms were measured using the crystal violet-based assay. One mutant, designated 20A3, was consistently deficient in biofilm formation compared to

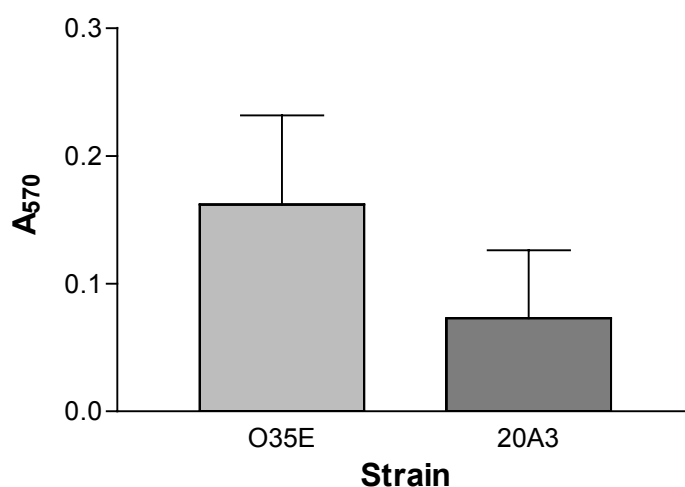


Fig. 25. Biofilm formation by transposon mutant 20A3. *M. catarrhalis* strain O35E and transposon mutant 20A3 were grown in THY.5 broth and measured for the ability to form biofilms using the crystal violet-based assay.

O35E (Fig. 25). Southern blot analysis of mutant 20A3, using the kanamycin gene from the transposon as a probe, confirmed that this mutant possessed a single transposon insertion (data not shown). A comparison of the growth in aerated broth culture of mutant 20A3 and the wild-type parent strain O35E showed that, although the mutant had a longer lag phase than the parent strain, both strains achieved the same final density (data not shown). The location of the transposon insertion was determined by rescue marker cloning. BLAST analysis (12) showed that the transposon was located within the ORF of the gene encoding a putative S-adenosyl homocysteine hydrolase (SAHH). This enzyme converts S-adenosylhomocysteine, which is a toxic metabolic intermediary, to adenosine and homocysteine (Fig. 26). All attempts to clone this gene for further analysis or construction of isogenic mutants were unsuccessful. To confirm the role of SAHH in biofilm formation, chromosomal DNA from mutant 20A3 was used to transform the biofilm-positive *M. catarrhalis* strains O46E and ETSU-9. Transformants were selected using kanamycin supplementation to obtain mutants that had incorporated the transposon in their chromosome. The presence of the transposon in the gene encoding SAHH was confirmed by PCR. Surprisingly, these O46E and ETSU-9 transformants grew poorly in static culture, even when they were grown in the richer THY.5 broth instead of BHI. As a result, they also formed biofilms poorly.

III. Discussion

This chapter details the first use of the crystal violet-based assay to measure biofilm formation by *M. catarrhalis*. It was found that *M. catarrhalis* strains exhibit a variety of biofilm phenotypes (Table 4), similar to the results obtained by Murphy and Kirkham (218) for nontypeable *H. influenzae*. Initial reports using the crystal violet-based assay allowed *P. fluorescens* or *E. coli* to grow in static culture for 10 h to form biofilms (229, 242). However, other investigators have used much longer incubation periods to measure biofilm formation in microtiter plates. For example, Klemm and colleagues (270) examined *E. coli* biofilm formation after 24 h. Watnick and Kolter (325) found that maximal biofilm formation by *V. cholerae* occurred after 29 h, while Murphy and Kirkham reported that *H. influenzae* biofilm formation plateaus after 16 h (218).

Nutrient composition of the growth medium has been shown to have an effect on biofilm growth and architecture. For example, the thickness of biofilms formed by oral streptococci is dependent on the amount of sucrose present. However, the base medium used for these experiments (TY) may be diluted up to four-fold with no effect on biofilm formation (40). Such differential biofilm formation under different conditions is not necessarily merely due to cellular metabolism; Kolter and colleagues (67) found that the surface-expressed protein Ag43 mediates biofilm formation of *E. coli* in glucose-minimal medium but not in Luria-Bertani broth. In contrast, flagellar-mediated motility is required for biofilm formation in both environments. It appears that *M. catarrhalis* forms biofilms best in richer growth media, at least when assayed using the crystal violet-based assay. It

would be interesting to examine *M. catarrhalis* biofilm thickness and architecture in biofilms obtained in different growth media. This objective would perhaps be best attained by the use of specialized flow cells to directly visualize biofilm formation by *M. catarrhalis*.

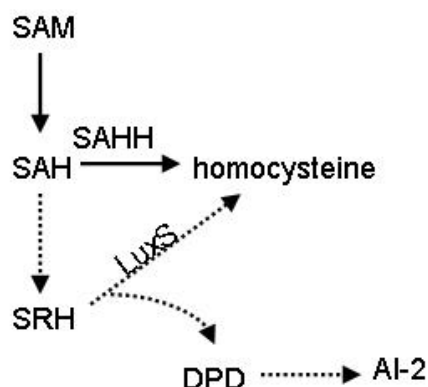


Fig. 26. Metabolism of S-adenosyl homocysteine (SAH). SAH is a toxic byproduct of S-adenosyl methionine (SAM). Eukaryotes and many prokaryotes convert SAH to homocysteine directly, catalyzed by SAHH (indicated by solid arrows). Some species of bacteria, however, convert SAH to homocysteine in two steps (indicated by dashed arrows). A byproduct of the conversion of S-ribosylhomocysteine (SRH) to homocysteine is 4,5-hydroxy 2,3 pentanedione (DPD), which is a precursor of AI-2.

Transposon-mediated mutagenesis of strain O35E resulted in the isolation of a mutant, 20A3, which was deficient in biofilm formation. Analysis of this mutant showed that the transposon was localized to a gene encoding a putative S-adenosyl homocysteine hydrolase. The highly conserved SAHH enzyme converts the toxic molecule S-adenosyl homocysteine (SAH) to adenosine and homocysteine, and is found in both prokaryotes and eukaryotes (Fig. 26, solid arrows). The apparent involvement of SAHH in biofilm formation by strain O35E is surprising, as SAHH would interfere with the synthesis of the quorum

sensing molecule autoinducer-2 (AI-2). In *E. coli*, SAH is converted to S-ribosylhomocysteine, which is in turn converted to homocysteine (Fig. 26, dashed arrows). A metabolic byproduct of this last step, catalyzed by LuxS, is 4,5-dihydroxy-2,3-pentanedione, which is a precursor to AI-2 (56, 296). AI-2 is a molecule involved in quorum sensing that is recognized to play a role in determination of biofilm architecture in other bacteria (206, 209, 248, 256). SAHH, however, removes SAH from the AI-2 pathway. In fact, there are no known examples of bacteria that possess the genes for both LuxS and SAHH (333). It is also interesting that mutation of the gene encoding SAHH apparently caused a more severe growth defect in the two biofilm-forming strains O46E and ETSU-9 than it did in strain O35E. The inability to construct an isogenic mutant of SAHH makes interpretation of these data more difficult. It would be illuminating to test *M. catarrhalis* strains with AI-2 indicator strains to see whether any *M. catarrhalis* strains produce AI-2. This latter possibility seems very unlikely however, given that the gene that encodes LuxS is not present in the mostly completed *M. catarrhalis* genome sequence (data not shown).

CHAPTER SEVEN

Use of the Crystal Violet-Based Assay to Characterize Biofilm Formation By *M. catarrhalis* Transformant Strains

I. Introduction

A major problem specific to *M. catarrhalis* research is the limited availability of genetic systems for use in this organism. While allelic exchange has been an option for more than a decade (131), plasmid complementation and transposon mutagenesis are not reliable options yet. In fact, only one strain, O35E, has been efficiently mutagenized (144), and only one transposon system has been shown to mutagenize the O35E chromosome. Unfortunately, O35E forms little or no biofilm in the crystal violet-based assay (unless grown in very rich media). Therefore, several methods were undertaken either to develop biofilm-positive *M. catarrhalis* strains that were amenable to transposon mutagenesis or to introduce transposon-mutagenized O35E chromosomal DNA into a biofilm-positive strain.

Using genetic transformation to introduce biofilm formation ability from a biofilm-forming strain into a non-biofilm-forming strain, we determined the identity of two genes (*uspA1* and *hag*) whose encoded protein products are involved, in different ways, in biofilm formation by *M. catarrhalis in vitro* in the crystal violet-based assay.

II. Results

A. Transformation of biofilm formation ability into strain O35E

Initial efforts to identify the gene products essential for biofilm formation by strain O46E involved the use of a transposon mutagenesis system. The EZ::TN<KAN-2> transposome system has been reported to be effective for introducing transposons into the chromosome of *M. catarrhalis* strain O35E (144, 185). However, all the biofilm-positive *M. catarrhalis* strains identified in the present study by use of the crystal violet assay could not be mutagenized using this system.

Many *M. catarrhalis* strains, including strain O35E, are naturally competent for transformation; therefore, experiments were initiated to construct a *M. catarrhalis* strain that was both able to form biofilms and amenable to transposon mutagenesis. Chromosomal DNA from the biofilm-positive strain O46E (Fig. 27A, well 1, and Fig. 27B, column 1) was used to transform the biofilm-negative strain O35E (Fig. 27A, well 2, and Fig. 27B, column 2) and transformants that were able to form biofilms were enriched for as described in Materials and Methods. From 365 colonies tested, three biofilm-positive transformants, designated T13, T14, and T84, were isolated by this method (Fig. 27B, columns 3-5, respectively). Biofilm formation by transformant T14 is depicted in Fig. 27A, well 3.

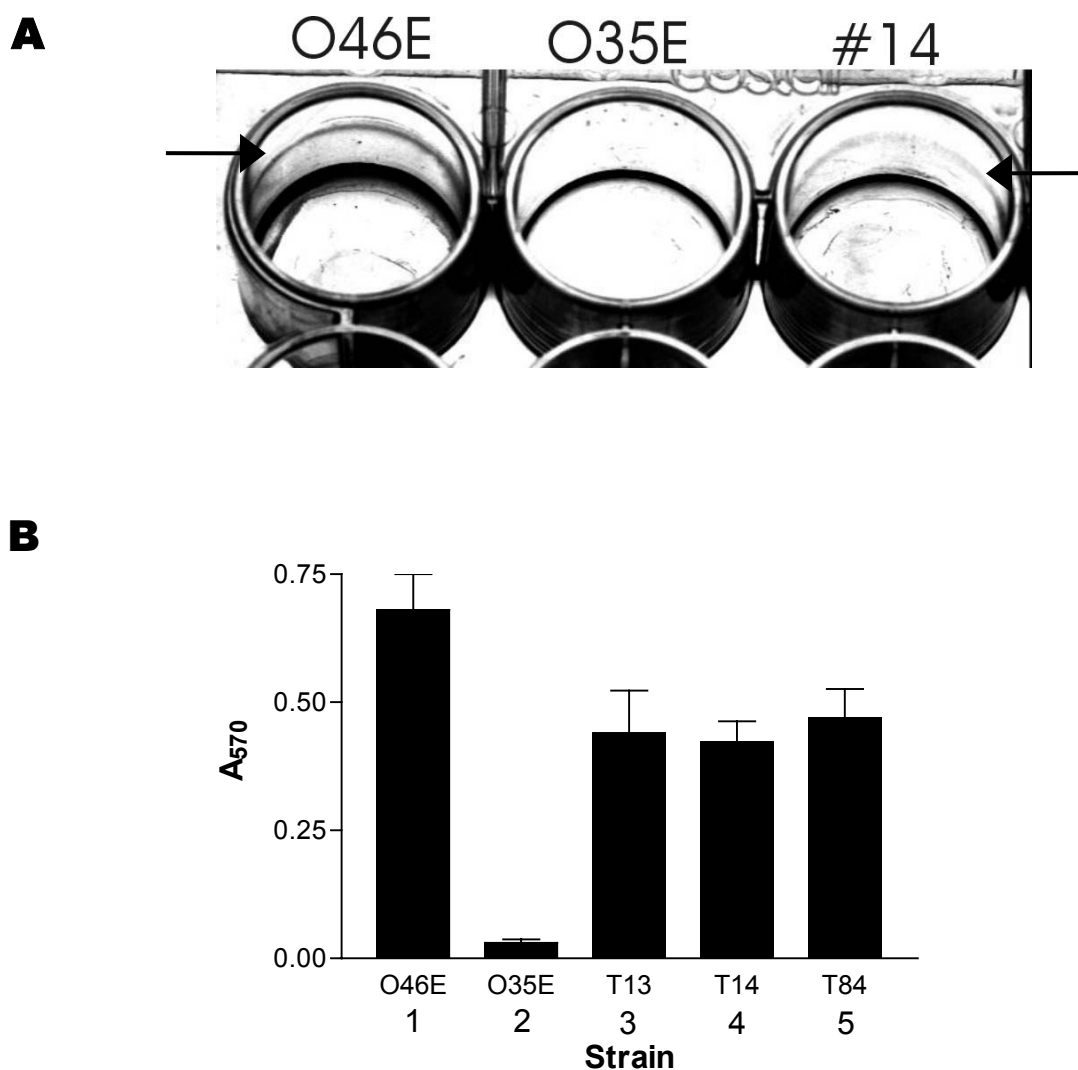


Fig. 27. Biofilm formation by wild-type and transformant strains of *M. catarrhalis*. Panel A, photograph of biofilm formation in a 24-well tissue culture plate. *M. catarrhalis* strains were grown in this 24-well plate, stained with crystal violet, and washed three times with deionized water. The arrows indicate biofilms that were formed at the air-medium interface. Panel B, Quantitative measurement of biofilm formation using the crystal violet assay. The absorbance (A_{570}) of the ethanol extract is plotted on the vertical axis. Each assay was performed in triplicate and repeated three times.

To ascertain whether the transformants T13, T14, or T84 had noticeable differences in their outer membrane protein composition when compared to strain O35E, outer membrane vesicles were isolated from each of these strains. Outer membrane proteins were separated by SDS-PAGE in a 10% (w/v) polyacrylamide gel and stained with Coomassie blue. As can be seen in Fig. 28, there were no obvious differences between O35E and transformants T13, T14, and T84. However, although the amounts of protein in each lane in the gel are not equivalent, it is apparent that the donor strain O46E has several differences in its protein profile compared to that of O35E.

To determine whether there was a difference in the LOS from the transformants and O35E, LOS from these strains was separated by SDS-PAGE in a 15% (w/v) polyacrylamide gel and silver-stained by the Tsai-Frasch method. Although O46E LOS has a larger apparent size than O35E LOS, the transformant strains all had LOS with the same apparent size as that of O35E (Fig. 29).

B. Isolation of biofilm-negative transposon insertion mutants

The transformants were next tested to ascertain whether they were amenable to transposon mutagenesis. Transformant strains T13 and T14 were subjected to transposon mutagenesis and a total of 398 kanamycin-resistant colonies were obtained. The occurrence of random transposon insertions was confirmed by using the kanamycin resistance gene as the probe in Southern blot analysis of chromosomal DNA from twenty of these kanamycin-resistant transformants (data not shown). All 398 of these putative transposon insertion mutants were

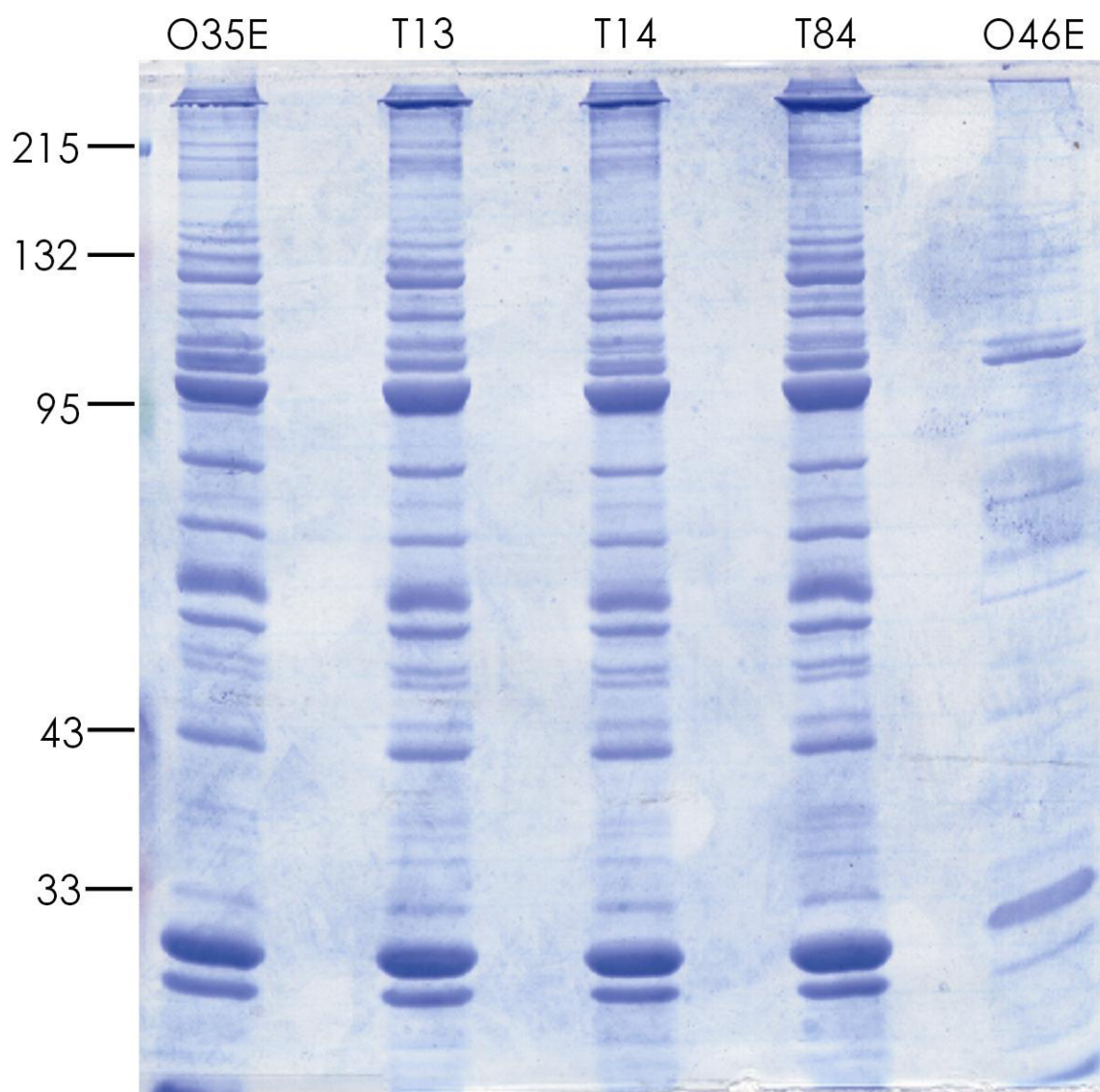


Fig. 28. Comparison of OMPs from strains O35E, O46E, and transformant strains. Outer membrane vesicles were isolated from wild-type strain O35E, transformant strains T13, T14, and T84, and wild-type strain O46E. OMPs were separated on a 10% (w/v) polyacrylamide gel and stained with Coomassie blue. Molecular weight markers (in kDa) are present on the left side of this figure.

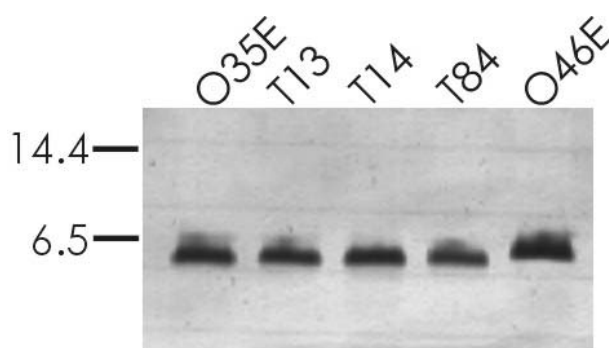


Fig. 29. Comparison of LOS from strains O35E, O46E, and transformant strains. LOS from wild-type strain O35E, transformant strains T13, T14, and T84, and wild-type strain O46E was separated on a 15% (w/v) polyacrylamide gel. The gel was silver stained using the Tsai-Frasch method. Molecular weight markers are shown on the left in kilodaltons.

screened for their ability to form biofilms using the crystal violet-based assay and three mutants deficient in biofilm formation ability were identified. These mutant strains were designated T13/38 (Fig. 30, column 4), T13/54 (Fig. 30, column 5), and T14/27 (Fig. 30, column 6). Initial attempts to use marker rescue cloning in *E. coli* (i.e., cloning of the transposon and immediately flanking chromosomal DNA) to identify the gene(s) disrupted by the transposon insertions in these three mutants were not successful.

Additional characterization of the original three biofilm-positive transformants T13, T14, and T84 included assessment of their ability to attach to Chang conjunctival epithelial cells *in vitro* (5, 174) because it was possible that the ability to form biofilms might be linked to or augment somehow the ability of *M. catarrhalis* to attach to human cells. Each of these three transformants exhibited an increased ability to attach to Chang cells relative to strain O35E (Fig. 31, columns 3, 5, 7). Because the UspA1 protein has been shown to be essential

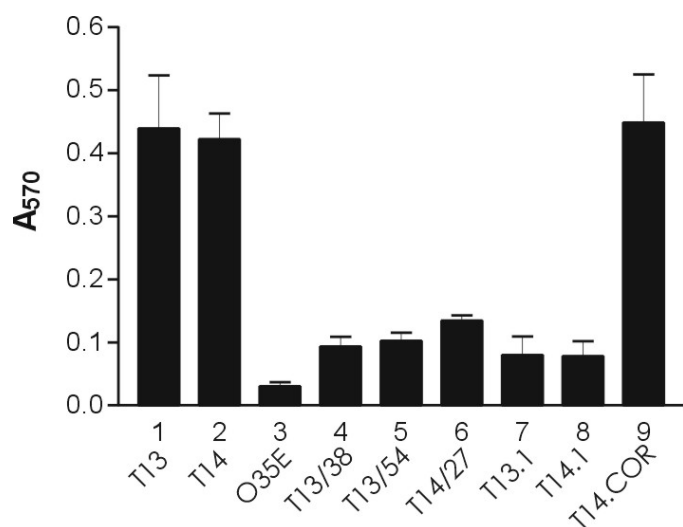


Fig. 30. Biofilm formation by transposon insertion mutants and isogenic mutants.

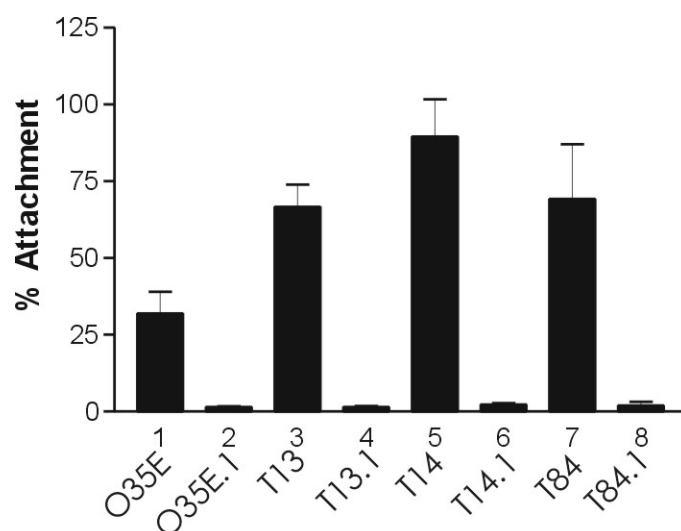


Fig. 31. Attachment of transformant strains and isogenic mutants to Chang cells.

for maximal attachment of *M. catarrhalis* strain O35E to these epithelial cells (174), isogenic *uspA1* mutants of transformant strains T13, T14, and T84 were constructed to confirm that elimination of the ability to express UspA1 adversely affected their attachment ability. Each of these *uspA1* mutants exhibited a greatly reduced ability to attach to Chang cells *in vitro* (Fig. 31, columns 4, 6, 8)). In addition, each of these *uspA1* mutants was found to be much less able to form biofilms than their immediate parent strains (Fig. 30, compare columns 1 and 7 and compare columns 2 and 8; data not shown for T84 and its *uspA1* mutant).

The fact that these isogenic *uspA1* mutants of transformants T13, T14, and T84 had all lost their ability to form biofilms prompted an investigation of whether any of the three original kanamycin-resistant transposon mutants might have had a transposon insertion in the *uspA1* gene. PCR-based amplification of the *uspA1* gene from transposon mutants T13/38 and T13/54 resulted in an amplicon that was approximately 1.2 kb larger than the *uspA1* gene in the wild-type strain O35E or O46E (data not shown); the size of this larger amplicon could be accounted for by the presence of the transposon within the *uspA1* gene. Therefore, both of these biofilm-negative mutants had transposon insertions in the *uspA1* gene; this was confirmed by nucleotide sequence analysis of the amplicons. Mutant T14/27, however, did not have a transposon insertion in its *uspA1* gene because its PCR-derived amplicon was the same size as that from the wild-type parent strain. Nucleotide sequence analysis of the *uspA1* gene from T14/27 was not performed, leaving open the possibility that there were secondary mutations present in this gene. The transposon-disrupted gene in T14/27 is discussed in a later section.

To assess the role of UspA1 in biofilm formation by the wild-type strain O46E (2001-1 stock; see Chapter 9 for more detail), this strain and its isogenic *uspA1* mutant O46E.1 were analyzed using the crystal violet-based assay. As seen in Fig. 32, biofilm formation is attenuated in O46E.1 compared to that obtained with O46E, confirming that expression of UspA1 by strain O46E is essential for normal biofilm formation by this strain. These data confirmed the relevance of the transformant strain model, and thus the *uspA1* gene from the transformant strains was investigated in more detail.

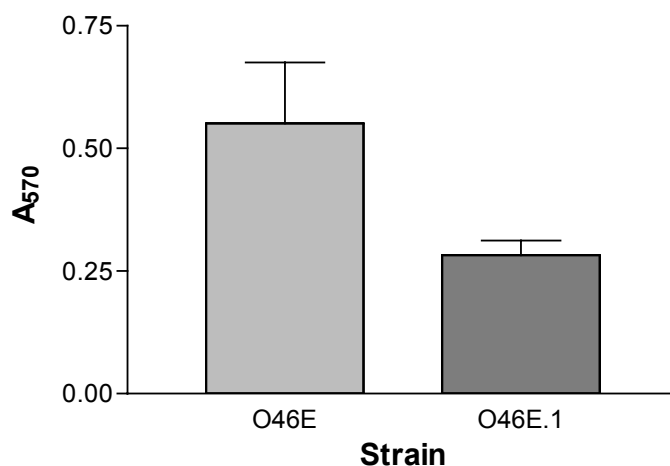


Fig. 32. Biofilm formation by strain O46E and its isogenic *uspA1* mutant O46E.1.

C. Transformant strains T13, T14, and T84 possess a hybrid *uspA1* gene

The fact that inactivation of the *uspA1* gene in the transformants T13 and T14 (Fig. 30, columns 7 and 8) adversely affected biofilm formation by these two strains raised the possibility that these O35E-derived transformants might express a hybrid UspA1 protein that

contained one or more segments from the O46E UspA1 protein. To investigate this possibility, the *uspA1* gene from transformant T14 was amplified by PCR and subjected to nucleotide sequence analysis. Comparison of the *uspA1* ORF from transformant strain T14 with the O35E *uspA1* and O46E *uspA1* ORFs revealed that this transformant possessed a hybrid *uspA1* sequence, with the 5' portion of the ORF corresponding to that of the O46E *uspA1* ORF and the remainder of the ORF matching O35E *uspA1* sequence (Fig. 33A). This hybrid gene encoded a predicted protein of 830 amino acids, with the first 155 amino acids being derived from strain O46E and the last 675 amino acids from strain O35E (Fig. 33B). Nucleotide sequence analysis of the *uspA1* genes from transformants T13 and T84 showed that these two strains also had the exact same hybrid *uspA1* sequence as that found in transformant T14 (data not shown).

D. Characterization of mutant T14/27

To determine the location of the transposon insertion in the biofilm-negative mutant T14/27 (which did not have a transposon insertion in its *uspA1* gene), chromosomal DNA from this strain was digested with *EcoRV* and probed in Southern blot analysis with the kanamycin resistance gene from the transposon. The transposon was localized to a 4.8 kb *EcoRV* fragment which was subsequently cloned into *E. coli* using the vector pACYC184. Nucleotide sequence and BLAST analyses of this DNA insert revealed that this transposon had inserted into an ORF with homology to the *E. coli corC* gene. The CorC protein of *E. coli* has been suggested to be involved in magnesium efflux (108). The wild- type *M.*

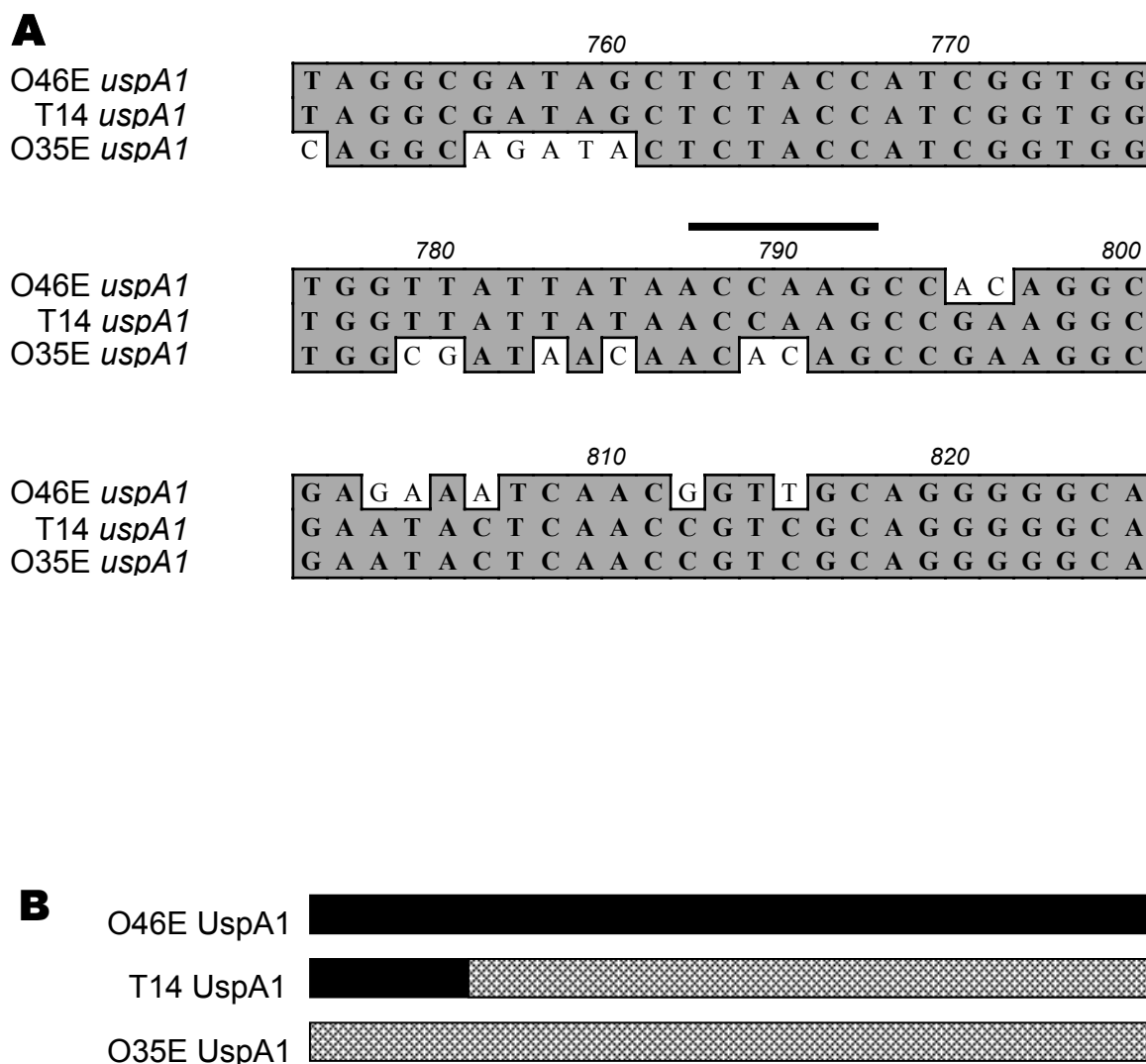
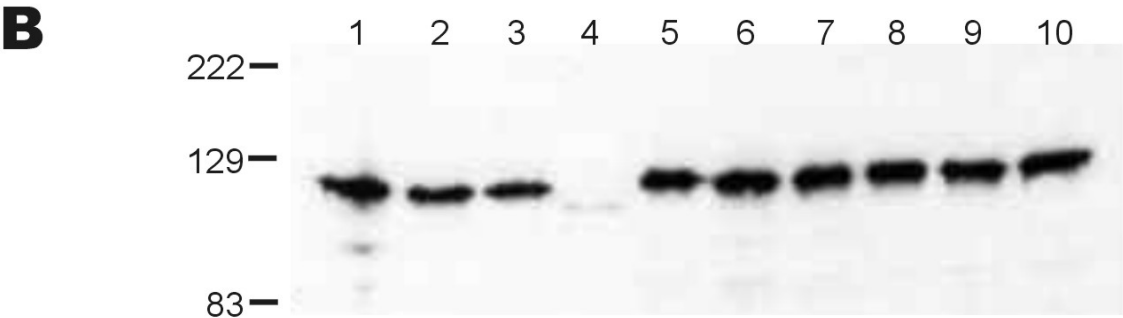
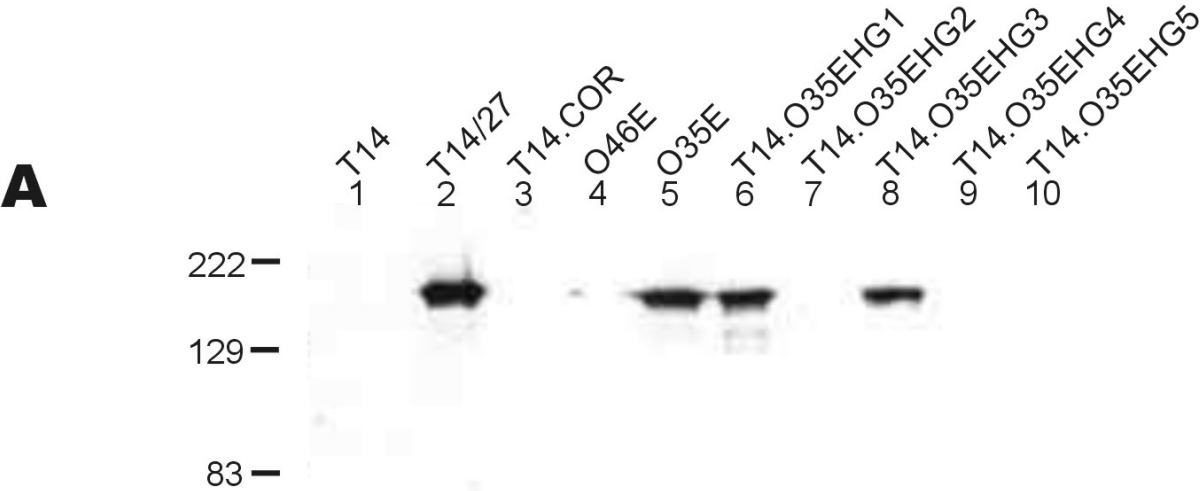


Fig. 33. Comparison of the nucleotide sequence of the *uspA1* ORFs from wild-type strain O46E, transformant T14, and wild-type strain O35E. (A) Nucleotide sequence of the 5' region of the *uspA1* ORF from the biofilm-positive wild-type strain O46E, the biofilm-positive transformant T14, and the biofilm-negative wild-type strain O35E. The black bar denotes the region in the T14 *uspA1* gene where crossover occurred between the O46E and O35E *uspA1* sequences. (B) Schematic of the T14 hybrid UspA1 protein relative to the UspA1 proteins from O46E and O35E.

catarrhalis corC gene together with flanking DNA was cloned from strain O35E, inactivated by insertion of a chloramphenicol acetyltransferase cartridge, and introduced into transformant strain T14 by transformation and allelic exchange. Unexpectedly, this isogenic *corC* mutant (T14.COR) formed biofilms as well as its parent strain T14 (Fig. 30, lane 9). This finding indicated that the lack of biofilm formation by strain T14/27 (Fig. 30, lane 6) was not the result of the transposon insertion in the *corC* gene but was caused by another as yet unidentified factor. The *uspA1* gene from this construct was not sequenced, leaving open the possibility that there was a secondary mutation in this gene.

E. Expression of Hag inhibits biofilm formation

Western blot analysis of the expression of the surface-exposed UspA1 and Hag proteins by the biofilm-positive transformant T14 (Fig. 34A and 34B, lane 1), the biofilm-negative transposon insertion mutant T14/27 (Fig. 34A and 34B, lane 2), and the biofilm-positive *corC* mutant of strain T14 (Fig. 34A and 34B, lane 3) revealed that transposon insertion mutant T14/27 differed from the other two strains in that it expressed the Hag protein whereas the others did not. Because the *hag* gene is known to undergo phase variation involving changes in a poly(G) tract located just within the 5' end of its ORF (210, 235, 265), the 5' end of the *hag* gene from transformant T14 was sequenced and its poly(G) tract was shown to contain 10 G residues (Fig. 34C). This resulted in the occurrence of a premature translational stop codon immediately following the poly(G) tract (data not shown).



C *hag* poly(G) 10 9 10 10 6 6 10 6 10 10

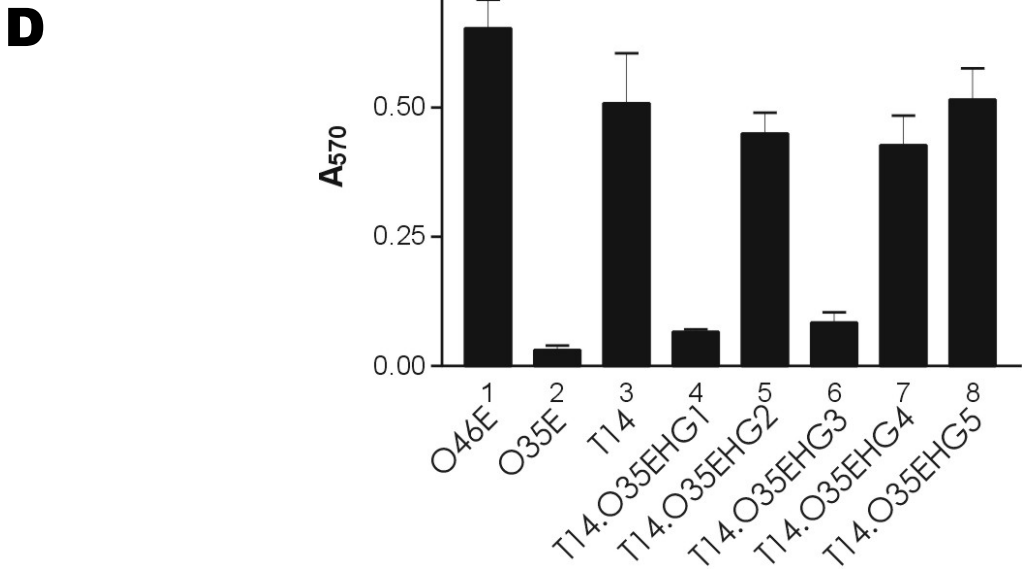


Fig. 34. Effect of Hag expression on biofilm formation by transformant T14. Western blot analysis of whole cell lysates was accomplished using the Hag-specific MAb 5D2 (panel A) and the UspA1-specific MAb 24B5 (panel B) as the primary antibody probes. Molecular weight position markers are present on the left side of each panel. The number of G residues contained in the *hag* poly(G) tract of each strain is listed in panel C. The very low level of expression of UspA1 by strain O46E (panel B, lane 4) is the result of phase variation of the poly(G) tract in the 5'-untranslated region of the *uspA1* gene and has been described previously (175). Biofilm formation was measured by means of the crystal violet-based assay (panel D).

Additional nucleotide sequence analysis of the 5' end of the *hag* gene in transformant T14 revealed that it was identical to that of the *hag* gene from strain O46E (Fig. 35). This result indicated that transformant T14 was likely derived from transformation and allelic exchange of at least two separate fragments of O46E DNA – one containing the 5' end of the *uspA1* ORF and the other containing the 5' end of the *hag* gene. It should be noted that the *uspA1* and *hag* genes are not physically adjacent to each other in the *M. catarrhalis* genome (data not shown).

Additional Western blot analyses showed that the biofilm-negative wild-type O35E strain did express Hag (Fig. 34A, lane 5) whereas the biofilm-positive, wild-type strain O46E either did not express its Hag protein or expressed only a very low level of this macromolecule (Fig. 34A, lane 4). Taken together with the Hag expression data derived from the biofilm-positive transformant T14 (Fig. 34A, lane 1) and the biofilm-negative transposon mutant T14/27 (Fig. 34A, lane 2), these results raised the possibility that expression of the Hag protein might inhibit or prevent biofilm formation by these strains in this crystal violet-based model system.

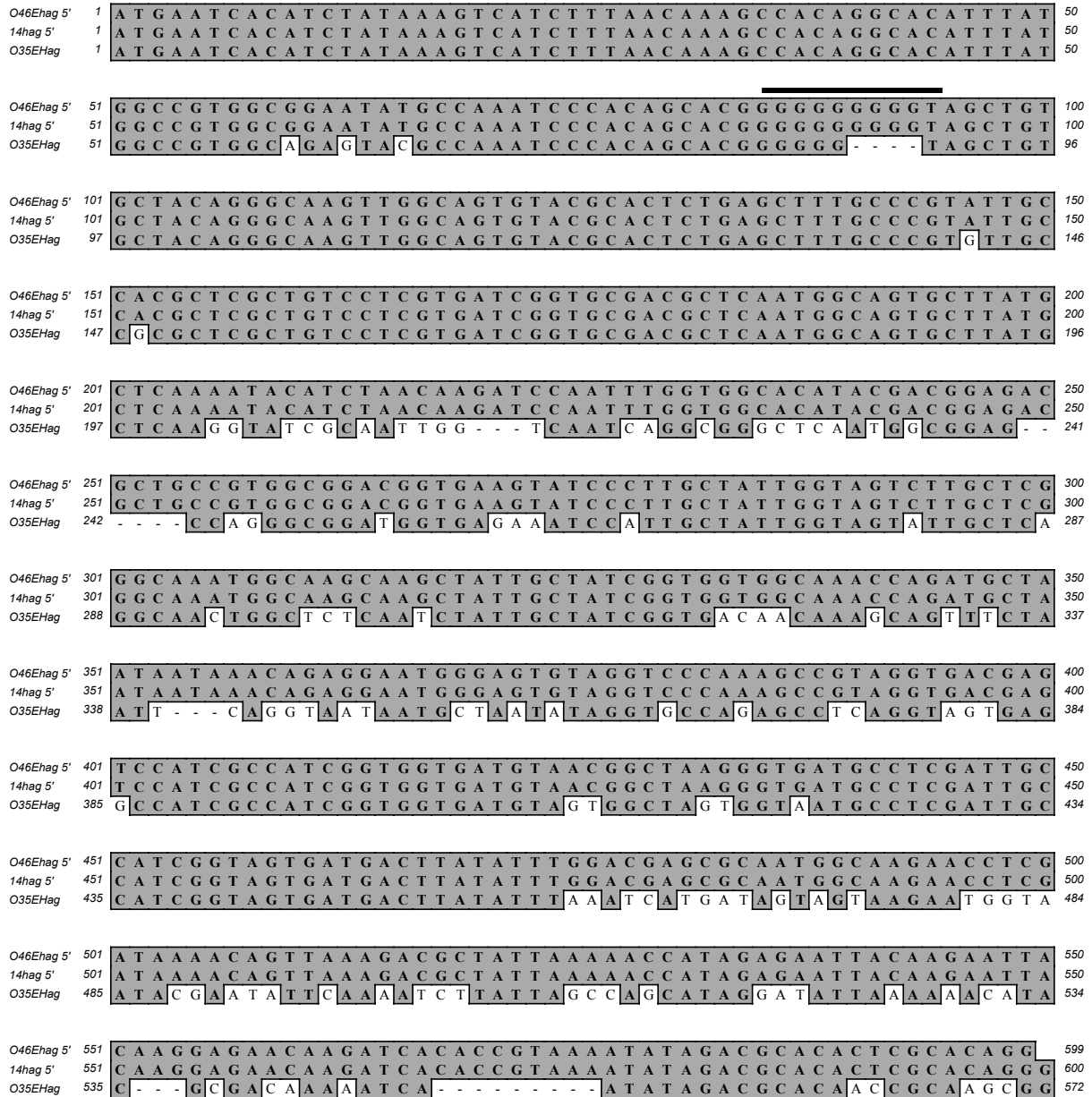


Fig. 35. Alignment of the first 600 nt of the *hag* ORFs from strains O46E, T14, and O35E. The Hag protein is not expressed in strain O46E or transformant strain T14 due to the presence of a frameshift mutation in the poly(G) tract, indicated with a bar.

To determine directly whether Hag expression adversely affected biofilm formation by transformant T14, an isogenic *hag* mutant of transformant T14 (T14.HG) was constructed by inserting a spectinomycin resistance cartridge into the *hag* ORF. While the original transformant T14 was unable to express Hag, it was still necessary to insert an antibiotic resistance cartridge into the T14 *hag* gene to facilitate the identification of new transformants in which this mutated *hag* gene had been replaced by a functional *hag* gene. To accomplish this, the wild-type *hag* gene from strain O35E was amplified by PCR and used to transform T14.HG; congression was used to facilitate identification of transformants containing the O35E *hag* gene or some portion thereof. Five transformants that were spectinomycin-sensitive were analyzed by Western blot for Hag expression (Fig. 34A, lanes 6-10) and were tested for their ability to form biofilms (Fig. 34D, lanes 4-8). The two transformants (T14.O35EHG1 and T14.O35EHG3) that possessed 6 G residues in their *hag* poly(G) tract (Fig. 34C) were both positive for Hag expression (Fig. 34A, lanes 6 and 8) and markedly impaired in biofilm formation (Fig. 34D, lanes 4 and 6).

F. Hag expression in ETSU-9 in relation to biofilm formation

In addition, Western blot analysis of the biofilm-positive wild-type strain ETSU-9 (Fig. 36, lane 2) showed that this strain also did not express Hag (Fig. 36A, lane 1). Nucleotide sequence analysis of the 5' end of the ETSU-9 *hag* ORF revealed that the poly(G) tract of this gene contained 10 G residues (Fig. 36B), resulting in a premature translational stop codon in the *hag* ORF (data not shown). To enable ETSU-9 to express a Hag protein,

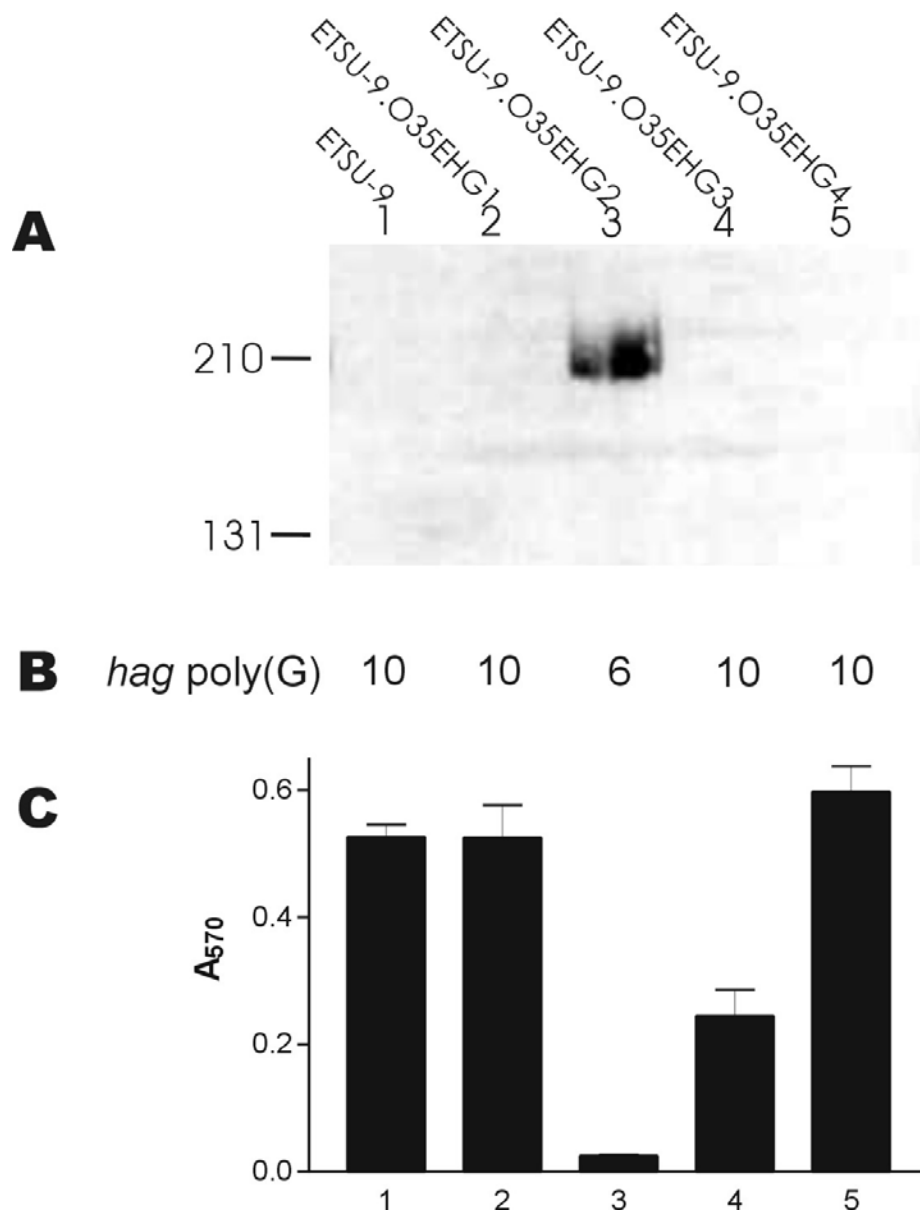


Fig. 36. Effect of Hag expression on biofilm formation by *M. catarrhalis* strain ETSU-9. Western blot analysis of whole cell lysates was accomplished using the Hag-specific MAb 5D2 (panel A). Molecular weight position markers (in kDa) are present on the left side of this panel. The number of G residues contained in the *hag* poly(G) tract of each strain is listed in panel B. Biofilm formation was measured by means of the crystal violet-based assay (panel C). Wild-type ETSU-9 is Hag-negative as a result of the presence of 10 G residues in the poly(G) tract of its *hag* gene.

the ETSU-9 *hag* gene was marked by insertion of a spectinomycin resistance cartridge (as described above with transformant T14) and then this isogenic *hag* mutant was transformed with the wild-type, functional O35E *hag* gene (in the form of a PCR amplicon). Four spectinomycin-sensitive transformants were obtained from this experiment and screened for their expression of Hag and ability to form biofilms. The single Hag-expressing transformant (Fig. 36A, lane 3) was found to possess six G residues in its poly(G) tract (derived from the O35E *hag* gene) and to have lost the ability to form a biofilm in the crystal violet assay (Fig. 36C, column 3). The three Hag-negative transformants (Fig. 36A, lanes 2, 4, and 5) still possessed 10 G residues in their poly(G) tract, likely because the cross-over that eliminated the spectinomycin cartridge occurred downstream from the poly(G) tract. These same three Hag-negative transformants still retained the ability to form biofilms (Fig. 36C, lanes 2, 4, and 5), although one of these was reduced relative to that obtained with wild-type.

G. Biofilm formation by strain O35E

Because the hybrid UspA1 protein in transformant T14 was necessary for biofilm formation by that strain, we sought to determine whether expression of this hybrid UspA1 protein by the biofilm-negative wild-type strain O35E would be sufficient to confer biofilm formation ability on strain O35E. Therefore, the hybrid *uspA1* gene from transformant T14 was amplified by PCR and used to transform the kanamycin-resistant *uspA1* mutant O35E.1 (5). Putative transformants were screened for loss of kanamycin resistance and one of these, designated O35E.14U1 (Fig. 37A, lane 5), was found to contain the entire *uspA1* gene from

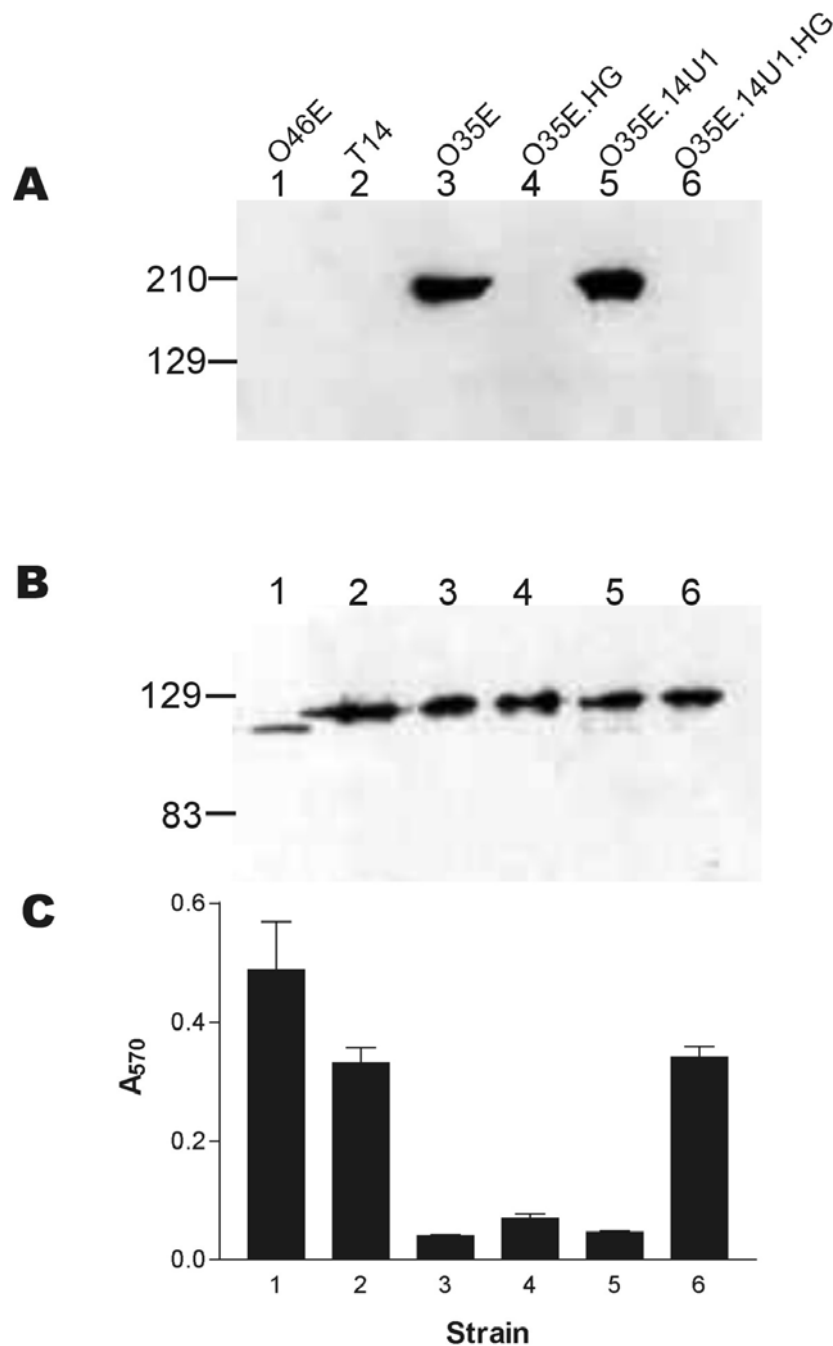


Fig. 37. Effect of UspA1 and Hag expression on biofilm formation by *M. catarrhalis* strain O35E and related strains. Expression of Hag (panel A) and UspA1 (panel B) was detected by Western blot analysis of whole cell lysates using MAb 5D2 and 24B5, respectively, as the primary antibody probes. Molecular weight position markers are present on the left side of the panel. Biofilm formation (panel C) was assessed using the crystal violet-based assay. It should be noted that the UspA1 protein from strain O46E migrates more rapidly than the O35E UspA1 protein.

transformant T14. When tested in the crystal violet assay for biofilm formation, strain O35E.14U1 was unable to form a biofilm (Fig. 37C, lane 5). As noted above, however, the wild-type strain O35E expressed the Hag protein (Fig. 34A and Fig. 37A, lane 3) which apparently adversely affected biofilm formation by transformant T14. Therefore, the *hag* gene in O35E.14U1 was inactivated by insertion of a spectinomycin cartridge. The resultant isogenic *hag* mutant O35E.14U1.HG (Fig. 37A, lane 6) was able to form a biofilm (Fig. 37C, lane 6). In contrast, an isogenic *hag* mutant of strain O35E (O35E.HG) (Fig. 37A, lane 4) was shown to be unable to form a biofilm (Fig. 37C, lane 4). Taken together, these results indicated that expression of the hybrid T14 UspA1 protein by strain O35E was necessary but not sufficient to allow biofilm formation. The biofilm-forming potential of this hybrid UspA1 protein can only be expressed in this model system in the absence of Hag protein production.

H. Biofilm formation by recombinant *E. coli* expressing UspA1

To ascertain whether the hybrid UspA1 protein from transformant T14 was sufficient to confer the ability to form biofilms on a heterologous organism, we expressed the UspA1 proteins from *M. catarrhalis* strains O35E and T14 in a biofilm-negative strain of *E. coli*. To accomplish this, the PCR-amplified *uspA1* genes from O35E and T14 were cloned into *E. coli* strain EPI300 as described in Materials and Methods. Two recombinant plasmids, designated pMP35U1 (expressing O35E UspA1) and pMP14U1 (expressing the hybrid T14 UspA1) were selected for further analysis. When analyzed by Western blot, it was found that

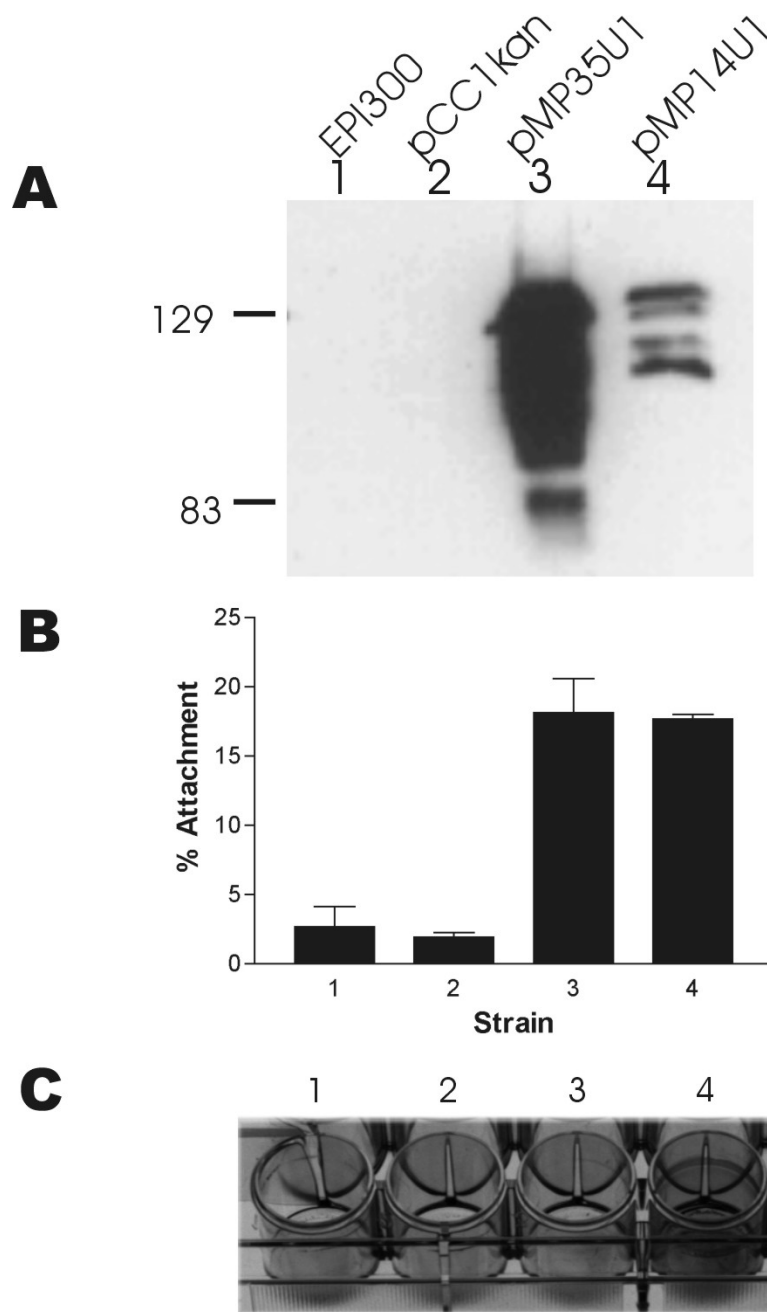


Fig. 38. Biofilm formation by recombinant *E. coli* strains expressing UspA1 proteins. Expression of UspA1 was detected by Western blot analysis of whole cell lysates using MAb 17C7 as the primary antibody probe (panel A). Attachment of recombinant *E. coli* strains to Chang conjunctival epithelial cells was measured as described in Materials and Methods (panel B). Panel C is a photograph of biofilm formation in a 24-well tissue culture plate. Recombinant *E. coli* were grown in this 24-well plate, stained with crystal violet, and washed three times with deionized water.

E. coli EPI300(pMP35U1) (Fig. 38A, lane 3) expressed much higher levels of UspA1 than did *E. coli*(pMP14U1) (Fig. 38A, lane 4).

To confirm that both constructs were producing a functional, cell surface-expressed protein, these recombinant strains were evaluated for their ability to attach to Chang conjunctival epithelial cells. *E. coli* EPI300 (Fig. 38B, lane 1) and EPI300(pCC1kan) containing only a cloned *kan* gene (Fig. 38B, lane 2) both attached at very low levels to Chang cells. However, strains EPI300(pMP35U1) (Fig. 38B, lane 3) and EPI300(pMP14U1) (Fig. 38B, lane 4), expressing O35E UspA1 and T14 UspA1 respectively, both attached at much higher but similar levels to Chang cells, confirming that the UspA1 proteins produced by these two strains were functional. When tested for the ability to form biofilms using the crystal violet-based assay, *E. coli* EPI300 (Figs. 38C and 39, lane 1) was found to be biofilm-negative as was EPI300(pCC1kan) (Figs. 38C and 39, lane 2). EPI300(pMP35U1) (Figs. 38C and 39, lane 3) was found to be biofilm-negative whereas EPI300(pMP14U1) (Figs. 38C and 39, lane 4) was positive for biofilm formation. Thus, expression of the T14 hybrid UspA1 protein was sufficient to confer the ability to form biofilms on *E. coli* strain EPI300.

To confirm whether the UspA1 protein from wild-type strain O46E conferred upon *E. coli* the ability to form biofilms, the O46E *uspA1* gene was also cloned into *E. coli* EPI300. Western blot analysis of whole cell lysates from EPI300(pMPU146) indicated that this strain was producing levels of UspA1 comparable to the levels for EPI300(pMPU135) (Fig. 38A, lane 1) (data not shown). A single Chang cell attachment assay indicated that EPI300(pMPU146) attached to Chang conjunctival cells at a similar level to that observed for EPI300(pMPU135) and EPI300(pMPU114) (data not shown). When tested for the ability

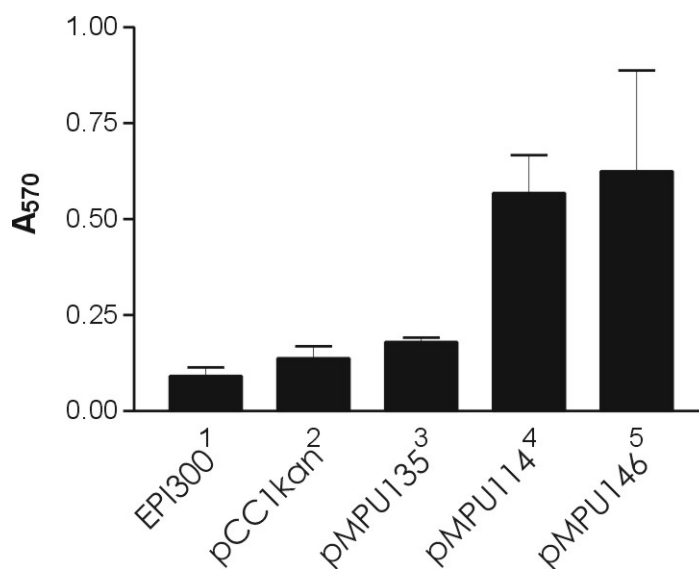


Fig. 39. Biofilm formation by *E. coli* strains expressing *M. catarrhalis* UspA1. Quantitative measurement of biofilm formation was determined using the crystal violet assay. The absorbance (A₅₇₀) of the ethanol extract is plotted on the vertical axis. Each assay was performed in triplicate and repeated once.

to form biofilms in the crystal violet-based assay, EPI300(pMPU146) formed a similar amount of biofilm as EPI300(pMPU114) (Fig. 39, lane 5). Surprisingly, however, EPI300(pMPU146) did not form a pellicle after growth in 24-well plates, in contrast to either *E. coli* EPI300(pMPU114) (Fig. 38C) or wild-type *M. catarrhalis* strain O46E (data not shown).

III. Discussion

In the present study, genetic transformation was used to construct *M. catarrhalis* strains that were both able to form biofilms and amenable to transposon mutagenesis. Subsequent analysis revealed that these transformant strains (T13, T14, and T84) all

possessed a hybrid *uspA1* gene, with the 5' end of the gene being derived from strain O46E and the remainder of the gene derived from strain O35E (Fig. 33). It could be inferred from these data that the UspA1 protein of strain O46E was involved in biofilm formation *in vitro* by this strain. Accordingly, inactivation of the *uspA1* gene in O46E resulted in a 50% decrease in biofilm formation as measured in the crystal violet-based assay (Fig. 32). It is important to note that these data were obtained using O46E isolate 2001-1, which does not express the UspA2H protein (discussed in detail in the next chapter). The hybrid *uspA1* genes from these strains all had the O46E-O35E sequence crossover within the same four-nucleotide region (Fig. 33), indicating that these three transformants were likely the progeny of a single transformant. Although the hybrid UspA1 protein from transformant T14 was able to confer biofilm formation ability on both strain O35E (Fig. 37) and an *E. coli* strain (Fig. 38), the native UspA1 protein from O35E does not permit development of this phenotype. Interestingly, the UspA1 proteins from both strain O35E and transformant T14 function as adhesins for Chang conjunctival epithelial cells. These results indicate that UspA1-dependent epithelial cell attachment ability and biofilm formation by these *M. catarrhalis* strains are separate and distinguishable activities.

Subsequent nucleotide sequence analysis showed that transformant T14 also had a hybrid *hag* gene, with the 5' portion of the gene coming from O46E and the 3' end of the gene originating from O35E. This hybrid *hag* gene has a premature translational stop codon in the 5' end of the ORF which resulted in a lack of expression of the Hag protein by transformant T14. This premature translational stop codon is also present in the wild-type O46E strain used in this study and is likely the result of slipped-strand mispairing in the

poly(G) tract located in the 5' end of the *hag* ORF (210, 235, 265). Western blot analyses of additional biofilm-positive and biofilm-negative strains and transformants used in this study revealed a negative correlation between expression of Hag and biofilm development in the crystal violet-based assay. Subsequent construction of isogenic *hag* mutants from transformant strain T14 (Fig. 34) and the wild-type strain ETSU-9 (Fig. 36) and testing of these mutants in the crystal violet-based assay confirmed that expression of Hag had a negative effect on biofilm development by these strains. It could be inferred from these results that the UspA1 and Hag proteins play different and apparently opposing roles in biofilm formation in the crystal violet-based assay by the *M. catarrhalis* strains used in this study. It would prove interesting to isolate Hag-positive phase variants of strains ETSU-9, O46E, and T14 to ascertain whether a specific portion of the O35E Hag sequence interferes with biofilm formation, or if the native Hag protein from each of these strains interferes with biofilm formation.

The UspA1 adhesin has been proposed to be a member of the autotransporter protein family (134, 135) and the C-terminal 250 amino acids of the Hag protein from *M. catarrhalis* strain O35E have 44% identity with the C-terminal region of the *H. influenzae* Hia adhesin, a well-characterized autotransporter protein (288). Proteins in the autotransporter family contain all the necessary information for transport into the outer membrane of gram-negative bacteria and can be either surface-expressed or released extracellularly following proteolytic cleavage. Thus far, only two other autotransporter proteins have been implicated in biofilm formation. Expression of the Ag43 protein of *E. coli* was shown to be necessary to allow biofilm formation in minimal media (67). Similarly, the calcium-binding autotransporter

Cah, an Ag43 homolog found in *E. coli* O157:H7, has been found to play a role in biofilm formation (304). Ag43 is known to undergo a type of phase variation (72, 133, 322); this is a characteristic shared with both the UspA1 (175) and Hag proteins (210, 235, 265). It is of interest to note that Ag43 is also implicated in autoaggregation of *E. coli* (72). In contrast, the Hag protein of *M. catarrhalis* strain O35E is an autoaggregation (autoagglutination) factor (235) but expression of Hag by strains O35E and T14 appeared to block or prevent biofilm formation in the crystal violet-based assay.

It should be noted that protein structures that contribute to biofilm formation under one circumstance may play no role at all or even have an inhibitory effect on biofilm formation under a different set of experimental conditions. A paradigm for this dichotomy can be found with *E. coli* expressing type 1 fimbriae. These proteins consist of rod-like structures with an adhesin encoded by the *fimH* gene located at the tips. Type 1 fimbriae are required for biofilm formation by *E. coli* in complex media (242). Conversely, type 1 fimbriae are not required for biofilm formation in minimal media; instead, Ag43 is important for biofilm formation under these conditions (67). However, both spontaneous and isogenic *fimH* mutants have been isolated that have a reduced ability to form biofilms and exhibit increased autoaggregation compared to wild-type (67, 269). This inhibition of biofilm formation occurs during growth both in complex and minimal media (67). Finally, expression of wild-type type 1 fimbriae abolishes Ag43-mediated autoaggregation (126). Therefore, it is possible that the Hag protein of *M. catarrhalis* may play a role in biofilm formation or maintenance under conditions other than those examined in this study. In fact, preliminary studies using a different *in vitro* system (39) to measure biofilm formation

indicate that Hag-expressing *M. catarrhalis* strains may have a selective advantage in this other model system (discussed in the next chapter). In addition, at least one *M. catarrhalis* strain (ATCC 43617) that readily forms biofilms in the crystal violet-based assay (Fig. 23) expresses a Hag protein. The differential ability of given mutants to form biofilms under different experimental conditions may also explain why strain O35E, which is negative for biofilm formation in the crystal violet assay, appears to form biofilms quite well in the Sorbarod continuous culture biofilm system. It should also be noted that the physical characteristics of the Sorbarod filter-based system are very different from those in the crystal violet-based assay and that the strands of the cellulose filter provide a very different environment from that found in a 24-well tissue culture plate.

CHAPTER EIGHT

Hag Expression in Biofilms

I. Introduction

The TEM and IEM analysis presented in Chapter 5 indicated that the Hag protein forms projections that extend from the bacterial cell surface. BLAST analysis indicated that this protein might belong to the autotransporter family. Another putative autotransporter protein, Ag43, has been implicated in both autoagglutination and biofilm formation by *E. coli* (67). The data presented in the previous chapter, however, suggest that expression of the Hag protein interferes with biofilm formation in the wells of tissue culture plates. Therefore, the expression of Hag in both Sorbarod- and tissue culture well-derived biofilms was investigated.

II. Results

A. Hag expression in Sorbarod biofilms

M. catarrhalis recovered from 3-day-old Sorbarod biofilms was streaked on agar plates for isolation of single colonies. The bacteria from the Sorbarod biofilms were obtained from diverse sites, including the bacterial growth on the silicone tubing surrounding

the Sorbarod filter, the broth effluent, and the floating mats within the effluent collection bottles. Selected single colonies were grown on agar plates; whole cell lysates were made from these isolates and probed with Hag-specific MAb 5D2 in Western blot analysis. Surprisingly, *M. catarrhalis* strain O46E, which does not normally express Hag, was found to be expressing Hag in Sorbarod biofilms (Fig. 40). Notably, all four colony types were found in two separate experiments to be expressing Hag. In addition, Hag from the flat-type colony had a different appearance in Western blot analysis from the appearance of Hag from the other colony types. That is, instead of appearing as a single band with an apparent molecular weight of approximately 200,000, the Hag protein from flat-type colonies appeared as a smear beginning at the top of the gel and ending at approximately 200,000 Da (Fig. 40). *M. catarrhalis* strain ATCC 43617, which expresses Hag, was found to be expressing Hag in Sorbarod biofilms as well (data not shown). Interestingly, Hag from ATCC 43617 smooth isolates appears as a single band in Western blot while Hag from clover-type isolates has the same appearance in Western blot as Hag from O46E flat-type colonies does. Similarly, *M. catarrhalis* strain O35E, which also expresses Hag, was found to express Hag in Sorbarod biofilms (data not shown).

B. Hag expression in tissue culture plate biofilms

To investigate whether strain O46E (2001-1 stock; see Chapter 9 for more detail) that is forming biofilms in the wells of a tissue culture plate is expressing Hag, this strain was grown for 19 h in a tissue culture plate. Two wells of the 24-well plate were gently rinsed

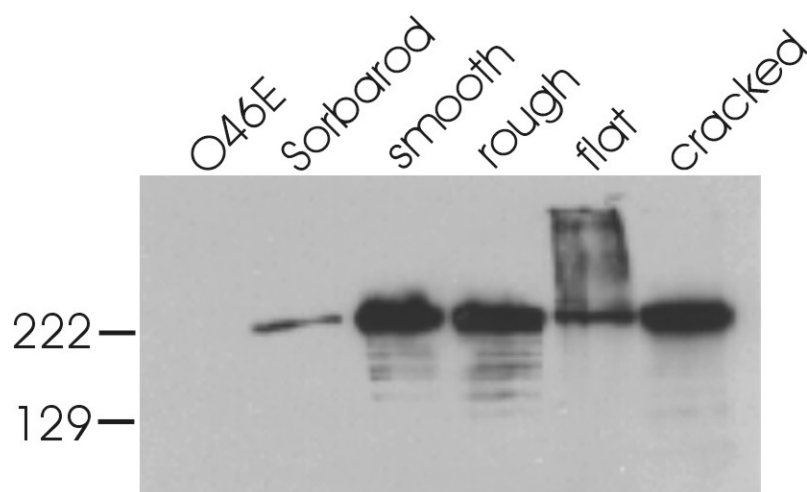


Fig. 40. Hag expression by Sorbarod biofilm-grown strain O46E. *M. catarrhalis* strain O46E was grown in aerated broth culture. A 3 ml portion of this culture was used to inoculate a Sorbarod filter, while a whole cell lysate was made from the remainder of the culture (O46E lane on the above Western blot). After O46E was grown for 3 days in the Sorbarod continuous culture biofilm system, the Sorbarod filter was vortexed vigorously. A whole cell lysate was made from this suspension (Sorbarod lane). Four different colony morphologies were identified among isolates obtained from various locations in the biofilm system (smooth, rough, flat, and cracked). Whole cell lysates were made from each colony type and analyzed by Western blot for Hag expression using MAb 5D2.

with M-199; then, the pellicle region from each well was scraped with a sterile toothpick. A third well was stained with crystal violet to confirm that biofilm formation had occurred. Bacteria on the toothpick were suspended in broth, serially diluted, and plated for obtain isolated colonies. These isolates were grown in sufficient quantity to prepare whole cell lysates for Western blot analysis. In two separate experiments, none of the pellicle-derived O46E colonies expressed the Hag protein (data not shown).

III. Discussion

This study contains the first report of apparent differential protein expression by *M. catarrhalis* grown under different conditions (i.e., in Sorbarod biofilms and in the wells of tissue culture plates). Several *M. catarrhalis* genes are known to be phase-variable, including UspA1 (175), Hag (235, 265), and UspA2H (Chapter 9). However, this phase variation is believed to be random. That is, isolates that express UspA1 at a relatively high level can be obtained from a laboratory stock that expresses this protein at a very low level, and vice versa. It seems likely that the expression of Hag in Sorbarod by strain O46E is the result of a positive selection for Hag-expressing *M. catarrhalis* (arising from slipped-strand mispairing) in these continuous-culture biofilms. Slipped-strand mispairing may occur due to the presence of nucleotide repeats (i.e., the poly(G) tract in *hag*). These repeats cause a transient mispairing during DNA replication that occasionally results in the addition or deletion of one or more repeat units (reviewed in (136)).

The expression of Hag by *M. catarrhalis* strain O46E grown in continuous culture biofilms but not in biofilms formed in tissue culture plates was surprising. In fact, the results of the previous chapter suggested that expression of the Hag protein by *M. catarrhalis* strains interfered with biofilm formation in tissue culture plates. These results emphasize the differences between the Sorbarod filter and tissue culture plate methods for growing biofilms. To begin to address the possible roles of Hag in biofilm formation, it would be interesting to clone the *hag* genes from O35E (where Hag expression seems to interfere with biofilm formation in the crystal violet-based assay) and ATCC 43617 (where Hag expression

seems to have no effect in the crystal-violet based assay) into *E. coli*. These constructs could be used to express UspA1 and Hag simultaneously (in a background that would not have interference from other, unknown phase-variable *M. catarrhalis* genes) and would be tested for their ability to form biofilms.

CHAPTER NINE

Analysis of Biofilm Formation by *M. catarrhalis* Strain O46E

I. Introduction

The previous chapter detailed the ability of certain *M. catarrhalis* transformants to form biofilms. Transposon insertion mutagenesis of these transformant strains led to the discovery that the UspA1 protein is involved in biofilm formation by *M. catarrhalis* strain O46E. However, a *uspA1* mutant of O46E still forms a modest amount of biofilm that can be measured by the crystal violet assay; therefore, this strain apparently possesses other genes that encode products which suffice for some degree of biofilm formation. This chapter discusses attempts to analyze biofilm formation by strain O46E and describes phase variation of the O46E *uspA2H* gene.

II. Results

A. Attempts to analyze *M. catarrhalis* strain O46E transposon insertion mutants

Because *M. catarrhalis* strain O46E was not amenable to transposon mutagenesis, a pool of O35E chromosomal DNA containing random transposon insertions was constructed. Nikki Wagner, Department of Microbiology, UT Southwestern used this transposon-

containing DNA to transform O46E; approximately 1000 kanamycin-resistant transformants were obtained. The crystal violet-based assay was used to screen 636 of these transformants for biofilm formation. Surprisingly, many of these transformants did not grow well in broth culture and formed biofilms poorly. Southern blot analysis using the kanamycin resistance gene from the transposon as a probe showed that the transposon insertions were random (data not shown). However, transposon mutants that did not grow well or formed biofilms poorly also had many different transposon insertion sites, suggesting that the presence of the transposon in these different loci was not responsible for the lack of biofilm formation. Instead, Western blot analysis indicated that the expression of the UspA2H protein could be correlated with poor biofilm formation. In addition, several of these transformants autoagglutinated extremely rapidly in suspension; these transformants also expressed a UspA2H protein whose Western blot reactivity (i.e., the pattern of antibody-reactive bands) was different than that observed with biofilm-negative transformants with normal autoagglutination (data not shown). Further confounding the analysis of these data was the realization that some of these biofilm-negative putative O46E transposon insertion mutants had O35E protein profiles as seen by Coomassie blue staining of whole cell lysates (data not shown), suggesting that O35E had been present as a contaminant in the O46E cells used in the transformation system.

B. Characterization of laboratory stocks of strain O46E

Routine Western blot analysis of *M. catarrhalis* strain O46E revealed that the amount of UspA2H protein produced by subcultures of this strain varied from experiment to experiment, from robust expression to no detectable protein. Therefore, the *uspA2H* genes from a UspA2H-positive O46E strain and an O46E strain with no detectable UspA2H expression were subjected to nucleotide sequence analysis by Dr. Wei Wang, Department of Microbiology, UT Southwestern. It was found that the *uspA2H* gene has a poly(A) tract at the 5' end of the ORF; UspA2H-positive strains had 8A residues in this poly(A) tract whereas strains with no UspA2H expression had 7A residues in the poly(A) tract. The presence of 7 A residues in this poly(A) tract caused the occurrence of a premature translational stop codon in the *uspA2H* ORF. Laboratory stocks with intermediate UspA2H expression were found to be a mixed population of strains with either 8A or 7A poly(A) tracts. An assessment of biofilm formation by these different strains or variants revealed that only strains with 7A poly(A) tracts or mixed populations of 7A and 8A strains were positive for biofilm formation using the crystal violet-based assay. Strains of O46E with 8A residues in the *uspA2H* poly(A) tract were negative for biofilm formation and settled out of broth suspension very rapidly. The growth rate and the serum resistance of these different strains were assessed by Ahmed Attia, Department of Microbiology, UT Southwestern. A summary of these data is presented in Table 5.

It should be noted that all of these O46E stocks possess a *uspA1* gene with 9G in their poly(G) tract; that is, they all express low levels of UspA1 (175). To obtain an O46E isolate

with high UspA1 expression, 300 colonies of O46E were patched onto agar plates and screened by colony blot using MAb 24B5. One isolate of O46E that had high expression of UspA1 (i.e., possesses 10G residues in its poly(G) tract) was designated O46E.149. Unfortunately, it was derived from the O46E 2002 stock, and therefore O46E.149 also lacked UspA2H expression.

Stock Date/Name	Poly(A) tract	UspA2H Western blot	Serum Resistance	Autoagglutination	Hag Western blot	Biofilm	Growth Rate
1990	8A	++	ND	+++	(-)	-	Slow
2001	7 & 8A	+	40%	++	(-)	+	Normal
2001-1	7A	-	2.10%	+	(-)	+	Normal
2001-2	8A	++	94.50%	+++	(-)	-	Slow
2001-3	8A	++	127%	+++	+	-	Intermed
2001-4	8A	++	126%	+++	(-)	ND	Slow
2002 (MP2*)	7A	-	ND	+	(-)	+	Normal

Table 5. Characteristics of laboratory stocks of strain O46E. Stocks and isolates were analyzed for the number of A residues in the poly(A) tract of the *uspA2H* gene, the amount of UspA2H protein as visualized by Western blot analysis, serum resistance, autoagglutination, expression of Hag, biofilm formation using the crystal violet-based assay, and growth rate. ND, not determined.

III. Discussion

In this chapter, the natural competence for transformation of *M. catarrhalis* strain O46E was used to transform this strain with transposon-mutagenized chromosomal DNA from strain O35E. This technique resulted in over 1000 kanamycin-resistant O46E transformants. Although the results of this particular study were difficult to interpret due to

several confounding variables, this basic method would be useful for mutagenesis of other genetically competent *M. catarrhalis* strains.

In retrospect, it appears that there are several explanations for the unexpected results obtained from the mutagenesis of strain O46E. First, the stock of O46E that was used in these studies was the 2001 stock, which contains a mixed population of UspA2H-positive and UspA2H-negative O46E cells. Expression of UspA2H by strain O46E apparently leads to a hyperautoagglutination phenotype. UspA2H-positive O46E does not grow to the same density as UspA2H-negative O46E (data not shown), and can even be seen to settle out of suspension in an agitated broth culture. UspA2H-positive O46E also does not form biofilms as measured by the crystal violet assay. Therefore, any UspA2H-positive bacteria in the O46E 2001 stock that received a transposon insertion would be negative for biofilm formation regardless of the location of the transposon insertion in the chromosome. Nevertheless, this study represents the first report of phase variation of the *uspA2H* gene.

A second potential difficulty in the interpretation of data from this study is the negative role of the Hag protein in biofilm formation, as reported in the last chapter. This Hag-related phenotype had not been identified at the time the experiments in this chapter were conducted, but it is likely that many biofilm-negative transposon mutants actually were *hag* phase variants that were expressing the Hag protein. A third issue with the results of these experiments is that some of the putative O46E transposon insertion mutants possessed whole cell lysate profiles that appeared identical to an O35E whole cell lysate, as seen on a Coomassie blue-stained 10% (w/v) polyacrylamide gel. The simplest explanation for this

result is that both O35E and O46E were present during the mutagenesis, or that the O35E transposon-mutagenized chromosomal DNA was contaminated with live O35E bacteria.

Phase variation of surface antigens appears to be fairly common in *M. catarrhalis*. The *uspA1* (175) and *hag* (210, 235, 265) genes are known to vary their expression by changes in the number of nucleotides in poly(G) tracts, presumably due to slipped-strand mispairing (136). Ongoing studies by Ahmed Attia in this laboratory are investigating the role of a tetranucleotide (i.e. AGAT) repeat upstream of the *uspA2* ORF in possible phase variation by this gene. Thus, it was interesting to find that the *uspA2H* gene of strain O46E undergoes phase variation as well. In addition, it appears that the UspA2H protein is involved in the hyperautoagglutination phenotype of this strain.

With the knowledge gained from the experiments in this dissertation, it would be reasonable to conduct another mutagenesis of strain O46E. To prevent the variables described above from occurring again, the O46E 2001-1 stock (containing only a UspA2H-negative population) would be used as the parent strain. All resulting transposon mutants would need to be tested by Western blot for both UspA2H and Hag expression as well. Finally, the sterility of the transforming chromosomal DNA should be confirmed; the use of the single-colony passaged O46E 2001-1 stock should also lessen the likelihood of transformation of a mixed population.

CHAPTER TEN

Analysis of the Ability of *M. catarrhalis* Strain ETSU-9 to Form Biofilms

I. Introduction

The previous chapter described attempts to mutagenize the wild-type *M. catarrhalis* strain O46E. Although those studies were not reproducible, it was still important to analyze biofilm formation in a wild-type strain background, as it was apparent that, at least in strain O46E, more than one gene product was necessary for maximum biofilm formation. Also, *M. catarrhalis* can have very different phenotypes from strain to strain. An excellent example of this would be serum resistance. Virtually all *M. catarrhalis* strains express a UspA2 or UspA2H protein, and expression of this protein is necessary to confer resistance to killing by normal human serum. However, a few strains of *M. catarrhalis* are not serum resistant even though they express either UspA2 or UspA2H. Similarly, although the UspA1 protein mediates attachment of *M. catarrhalis* strain O35E to Chang conjunctival epithelial cells, not all UspA1-expressing *M. catarrhalis* strains are able to attach to Chang cells. Further examples of strain-to-strain variation are found in Chapter 5 of this dissertation in the studies of the *hag* mutants. Thus, in this chapter, biofilm formation by the wild-type ETSU-9 strain was characterized.

II. Results

A. Screening for biofilm-negative transposon insertion mutants of ETSU-9

A total of 3000 kanamycin-resistant transposon insertion mutants were screened for loss of the ability to form biofilms using the crystal violet assay. These transposon mutants were obtained by transforming *M. catarrhalis* strain ETSU-9 with chromosomal DNA from strain O35E that contained random transposon insertions as discussed previously. In this screen, 105 mutants either lacked or had noticeably less biofilm formation compared to wild-type ETSU-9. Chromosomal DNA from these mutants was used to transform ETSU-9 to confirm the relevance of the transposon insertion; these backcross experiments led to the isolation of 6 kanamycin-resistant mutants that were consistently biofilm-negative or attenuated for biofilm formation.

Because the UspA1 protein had been identified as having a role in biofilm formation by *M. catarrhalis* strain O46E, initial experiments were designed to determine whether either the UspA1 protein or the related UspA2H protein of strain ETSU-9 was involved in biofilm formation. To accomplish this, whole cell lysates of these six biofilm-negative mutants were evaluated for expression of the UspA1 and UspA2H proteins by Western blot analysis. Three of the six transposon insertion mutants, designated ETSU-9.698, ETSU-9.714, and ETSU-9.2311 lacked expression of UspA2H (Fig. 41). The involvement of UspA2H in biofilm formation was confirmed by examining biofilm formation by ETSU-9, its isogenic *uspA1* mutant ETSU-9.1, and its isogenic *uspA2H* mutant ETSU-9.2 (Fig. 42). The other

three transposon insertions (mutants ETSU-9.222, ETSU-9.724, and ETSU-9.988) are discussed in a later section. Since mutations in LOS have been shown to have an effect on biofilm formation by other bacterial species (218, 298), LOS was isolated from the six biofilm-negative transformants. When separated on a 15% (w/v) polyacrylamide gel and silver stained, there was no difference observed between LOS from the transposon insertion mutants compared to LOS from wild-type ETSU-9 (data not shown).

The vast majority of the 105 biofilm-negative mutants produced inconsistent results when chromosomal DNA from these mutants was used to transform wild-type ETSU-9. Typically, when 10 transformants from a backcross experiment were tested for the ability to form biofilms, half of the transformants were biofilm-positive while the other half were biofilm-negative. To further investigate these perplexing results, whole cell lysates were made from selected transformants obtained by backcrossing chromosomal DNA from mutants ETSU-9.1315 and ETSU-9.1441 into ETSU-9. When these whole cell lysates were analyzed by Western blot for Hag expression, it was found that Hag-negative backcrossed transformants were biofilm-positive and that Hag-positive backcrossed transformants were biofilm-negative (Fig. 43). Fig. 43, lane 1 shows Hag expression by wild-type ETSU-9. Fig. 43, lanes 2 and 3, shows Hag expression by two isolates obtained by transforming ETSU-9 with chromosomal DNA from ETSU-9.1315. Fig. 43, lanes 4 and 5, shows Hag expression by two isolates obtained by transforming ETSU-9 with chromosomal DNA from ETSU-9.1441

When other biofilm-negative transposon mutants and their backcrossed transformants were analyzed, it was observed that biofilm-negative mutants had a different UspA2H

reactivity in Western blot analysis compared to biofilm-positive mutants or wild-type ETSU-9 (data not shown). One of these transposon mutants, ETSU-9.327, was sequenced to determine the location of the transposon insertion. This mutant had an insertion in the *metR* gene, which is located immediately downstream from the *uspA2H* gene and which is oriented in the opposite direction as *uspA2H* (data not shown). Further sequence analysis showed that ETSU-9.327 possessed the *uspA2* gene from O35E instead of the *uspA2H* gene from ETSU-9, a result which indicates that this mutant acquired the *uspA2* gene from the transposon-mutagenized DNA (from O35E).

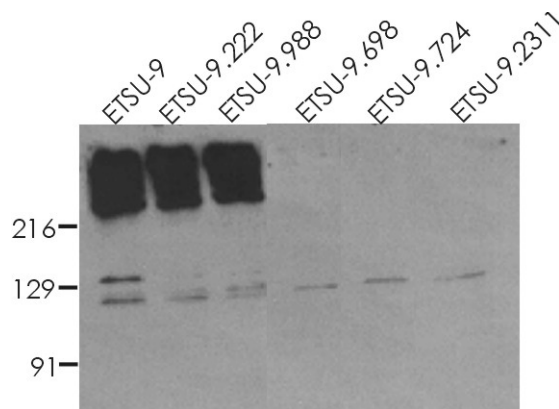


Fig. 41. UspA2H expression by biofilm-negative ETSU-9 transposon mutants. Whole cell lysates were made of five of the six biofilm-negative transposon mutants and analyzed for UspA2H expression using MAb 17C7 as the primary antibody probe. The sixth biofilm-negative transposon mutant, ETSU-9.724, is not shown but expresses UspA2H. The faintly visible antigen that is present in all 6 lanes near the 129 kDa molecular weight marker is the UspA1 protein.

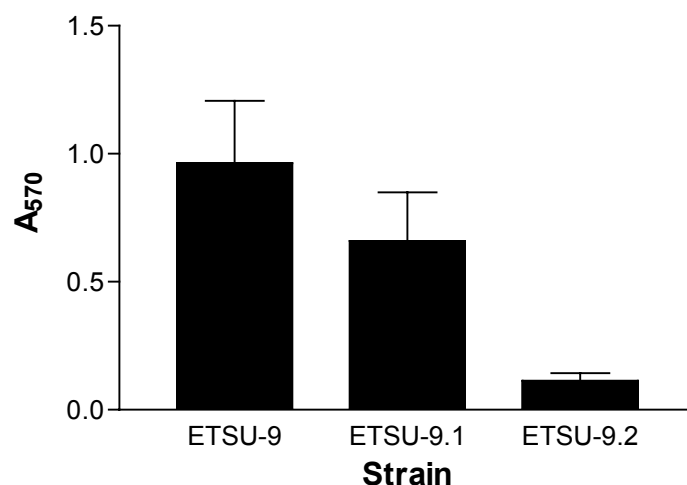


Fig. 42. Biofilm formation by ETSU-9, the isogenic *uspA1* mutant ETSU-9.1, and the isogenic *uspA2H* mutant ETSU-9.2. Biofilm formation was measured using the crystal violet-based assay.

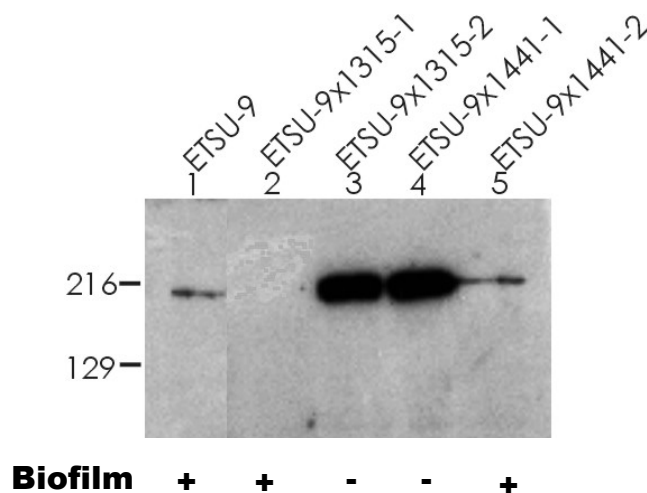


Fig. 43. Hag expression by biofilm-positive and biofilm-negative backcrossed transposon mutants. Whole cell lysates of ETSU-9 and backcross strains were analyzed by Western blot using MAb 5D2 as the primary antibody probe. ETSU-9x1315-1 and ETSU-9x1315-2 were obtained by transforming ETSU-9 with DNA from biofilm-negative transposon mutant ETSU-9.1315. Similarly, ETSU-9x1441-1 and ETSU-9x1441-2 were obtained by transforming ETSU-9 with DNA from biofilm-negative transposon mutant ETSU-9.1441.

B. Insertional mutagenesis of the ETSU-9 *uspA2H* gene

In order to identify the domain(s) of the ETSU-9 UspA2H protein that might be necessary for biofilm formation, random 15 nt insertions were introduced into the cloned *uspA2H* gene by means of a transposon-based insertion/excision system. These insertions were introduced to strain ETSU-9 by plate transformation. Since there is no selectable marker in the 15 nt insertion after the transposon is excised, the chances of obtaining the desired transformants were enhanced by employing the technique of congression using a streptomycin-resistant *rpsL* gene as described in Materials and Methods. Thus, all 15 nt insertion mutants were also streptomycin-resistant, and a streptomycin-resistant isolate of ETSU-9, designated ETSU-9.str^R, was used as a positive control in subsequent experiments. All mutated *uspA2H* genes were sequenced to confirm the presence of the 15-nt insertion and to confirm that no premature translational stop codons had been introduced. The position of each of these 5 aa (15 nt) insertions within the UspA2H protein is depicted in Fig. 44. Each of these mutant strains was tested for the ability to form biofilms using the crystal violet-based assay. Surprisingly, the majority of the mutants were biofilm-negative (Fig. 45). In addition, two mutants that retained the ability to form biofilms (ETSU-9.mut92 and ETSU-9.mut81) did not form biofilms as well as ETSU-9 str^R. To confirm that all of these insertional mutants were producing UspA2H protein, Western blot analysis was conducted on all mutants. Most of these mutants were positive for UspA2H protein production as detectable by Western blot (Fig. 46) except ETSU-9.mut3 and ETSU-9.mut92. ETSU-9.mut86, which also did not express UspA2H, had a 15 nt insertion near the 3' end of the



Fig. 44. Position of 5 aa insertions in the ETSU-9 UspA2H protein. A region of the protein consisting of a sequence repeated six times is colored blue. Three insertions actually resulted in in-frame deletions; the extent of each deletion is denoted with brackets with the mutant number posted above each bracket. Mutant ETSU-9.mut20 contains a 15 nt insertion in the DNA 3' of the translational stop codon of the *uspA2H* gene; it is noted with a “20” after the C-terminal amino acid of UspA2H.

uspA2H gene which resulted in a premature stop codon. ETSU-9.mut3 was found to have a 15 nt insertion at the very end of the *uspA2H* ORF (Fig. 44). The ETSU-9.mut92 mutant has a large in-frame deletion in the middle of its *uspA2H* gene, resulting in the loss of 418 of the 875 aa in the mutant protein, including the epitope recognized by the primary antibody used

in the Western blot, MAb 17C7. To determine whether ETSU-9.mut92 was actually making any UspA2H protein, the *uspA2H* gene in ETSU-9.mut92 was inactivated by insertional mutagenesis. Outer membrane vesicles were isolated from ETSU-9.mut92 and its *uspA2H* null mutant, and the outer membrane proteins were separated by SDS-PAGE and stained with Coomassie brilliant blue. As can be seen in Fig 47, mut92 produced a smaller form of UspA2H than wild-type ETSU-9, consistent with the internal deletion in the *uspA2H* gene of the former strain. This smaller band was absent when the *uspA2H* mutant of ETSU-9.mut92, designated ETSU-9.mut92.2, was analyzed (Fig. 47). Interestingly, ETSU-9.mut81 also has an in-frame deletion of its *uspA2H* gene, although this deletion is not as extensive as the deletion in ETSU-9.mut92 (Fig. 44).

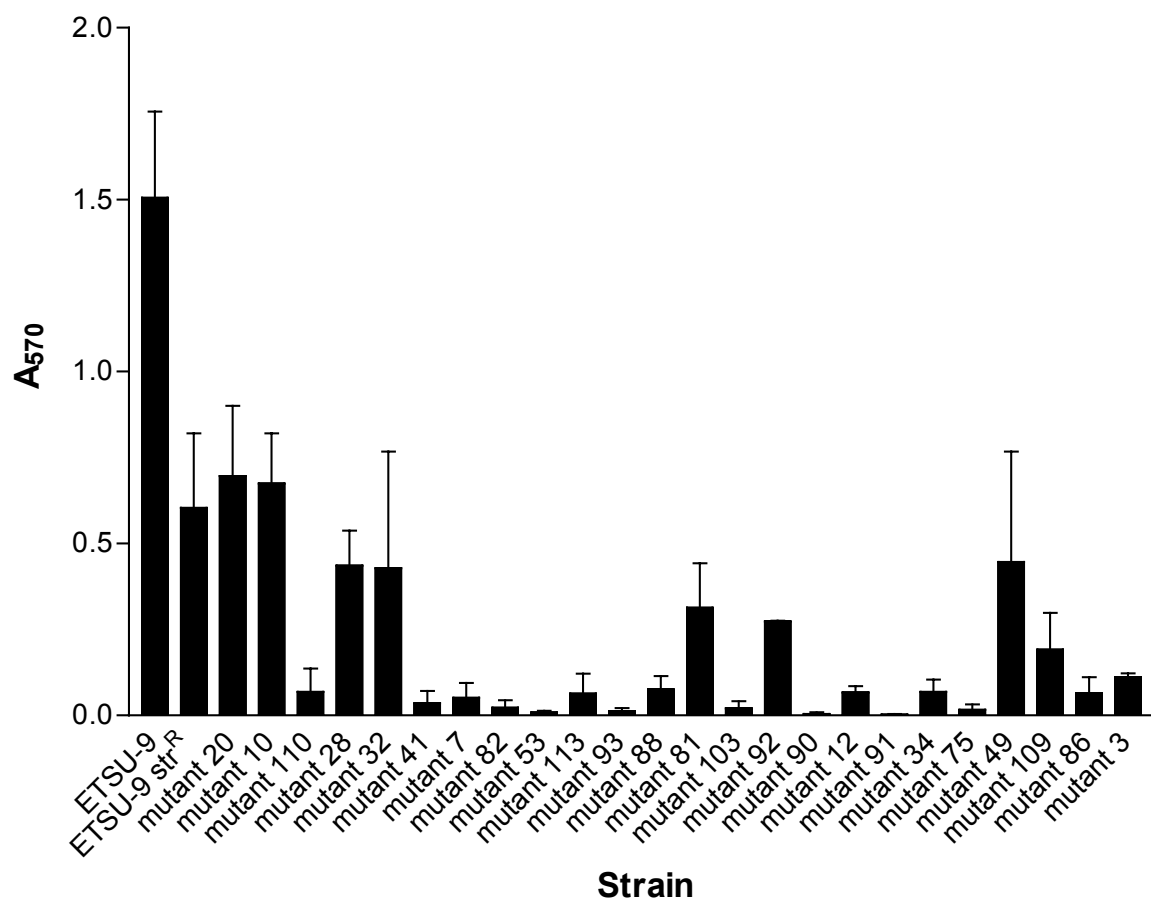


Fig. 45. Biofilm formation by *uspA2H* insertion mutants. ETSU-9.mut20 is an insertion mutant containing the 15 nt insertion downstream of the *uspA2H* ORF. The remaining *uspA2H* insertion mutants are listed in order of the site of the insertion, 5' to 3' in the *uspA2H* ORF. ETSU-9.mut86 possesses an insertion that caused a premature translational stop codon, leading to a deletion of the final 5 aa of UspA2H.

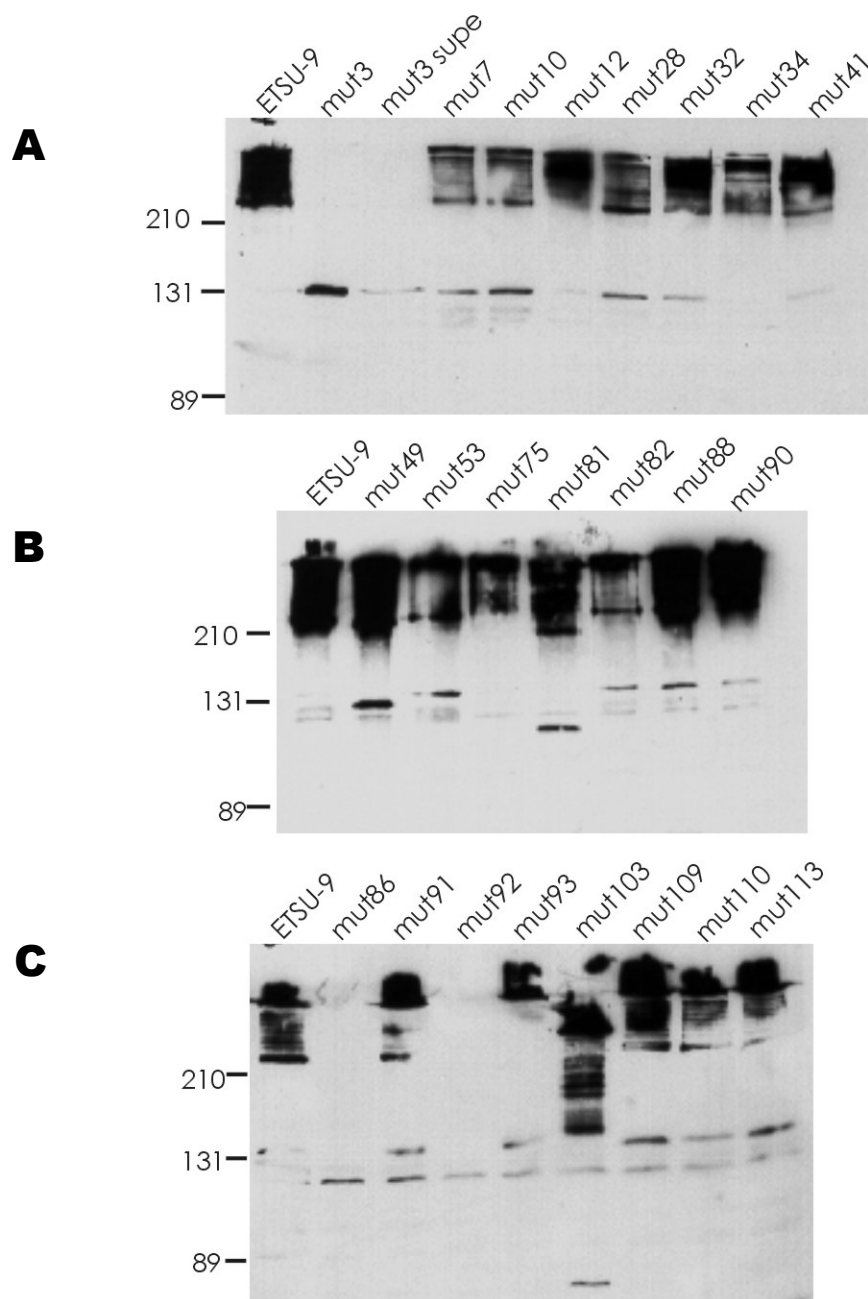


Fig. 46. Expression of UspA2H by *uspA2H* insertion mutants. Whole cell lysates were analyzed by Western blot using MAb 17C7 as the primary antibody probe. In lane 3 of panel A, concentrated culture supernatant from ETSU-9.mut3 was examined for the presence of UspA2H. ETSU-9.mut86 has an insertion resulting in a premature truncation resulting in the loss of the last 5 aa of the UspA2H protein (panel C, lane 2).

The Chang conjunctival epithelial cell attachment assay was used to test for functional, surface-expressed UspA2H protein in the biofilm-negative insertion mutants. The *uspA1* gene was first inactivated by insertion of a *kan* cartridge, since both the UspA1 and UspA2H proteins are adhesins (Fig. 48). Surprisingly, all of these mutants except two (ETSU-9.mut41.1 and ETSU-9.mut28.1) attached to Chang cells (Fig 48). These two mutants had levels of attachment that were equal to or lower than the negative control, the *uspA1 uspA2H* mutant ETSU-9.12 str^R. The cell surface expression assay was used to confirm that mutant ETSU-9.mut41.1 had surface expressed UspA2H (Fig 49).

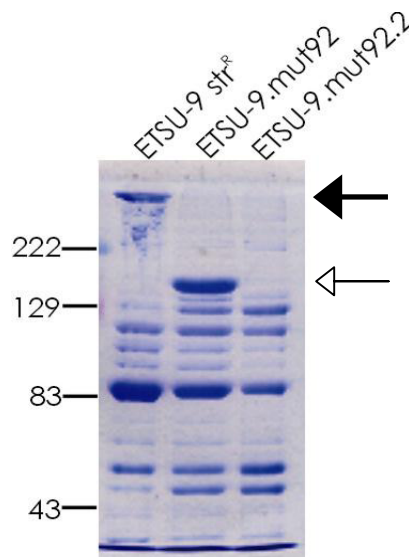


Fig. 47. Expression of UspA2H by ETSU-9.mut92. Outer membrane vesicles were isolated from ETSU-9.str^R, ETSU-9.mut92, and the *uspA2H* null mutant ETSU-9.mut92.2. OMPs were separated on a 10% (w/v) polyacrylamide gel and stained with Coomassie blue. Wild-type UspA2H is indicated with a solid arrow, and the smaller form of UspA2H expressed by ETSU-9.mut92 is indicated with a hollow arrow. Molecular weight markers (in kDa) are indicated to the left of the figure.

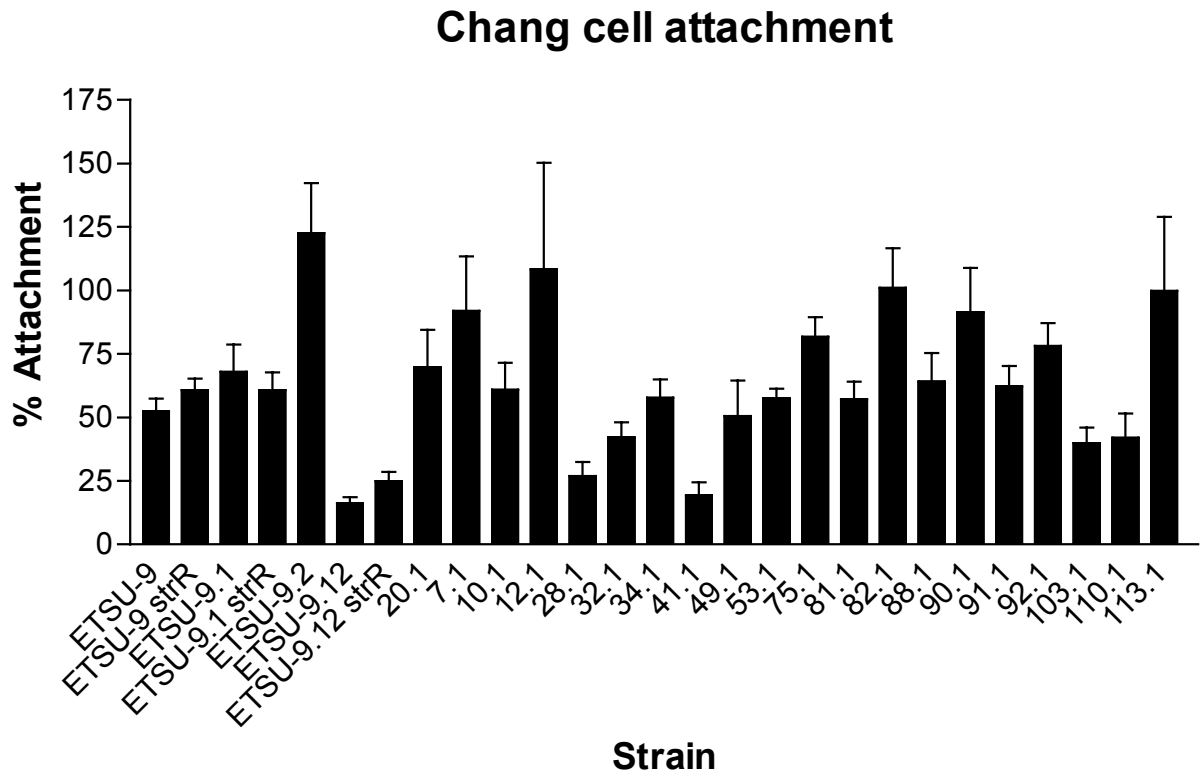


Fig. 48. Attachment of ETSU-9 *uspA2H* insertion mutants to Chang conjunctival epithelial cells. All insertion mutants in this experiment are streptomycin resistant and do not express UspA1. ETSU-9.mut20.1 is both streptomycin resistant and a *uspA1* mutant that possesses a 15 nt insertion downstream of the *uspA2H* ORF; it is also included as a positive control.

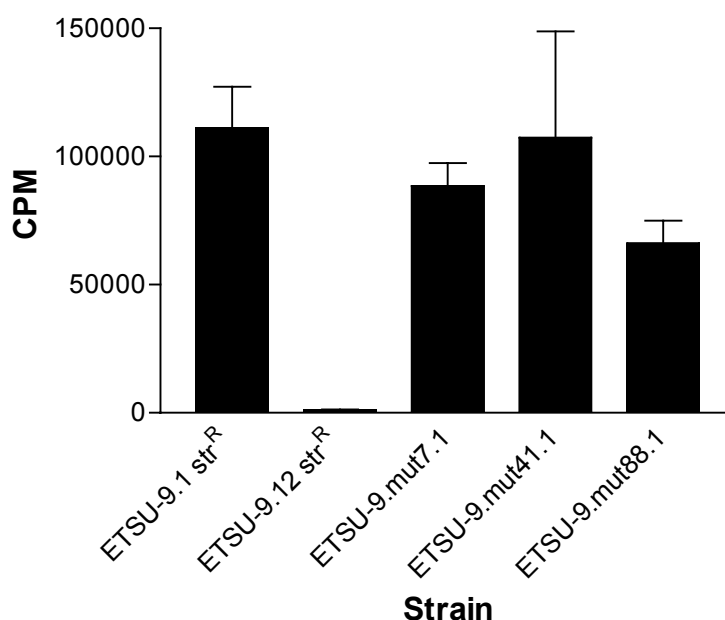


Fig. 49. Cell surface expression assay for UspA2H. The *uspA1* mutant ETSU-9.1 str^R and the *uspA1 uspA2H* mutant ETSU-9.12 str^R are included as positive and negative controls, respectively. ETSU-9.mut7.1 and ETSU-9.mut88.1 are mutants that attach to Chang cells and are included as positive controls. ETSU-9.mut41.1 does not attach to Chang cells but has surface-expressed UspA2H. The vertical axis indicates CPM of radioiodinated goat anti-mouse IgG bound to MAb 17C7 on the bacterial cell surface.

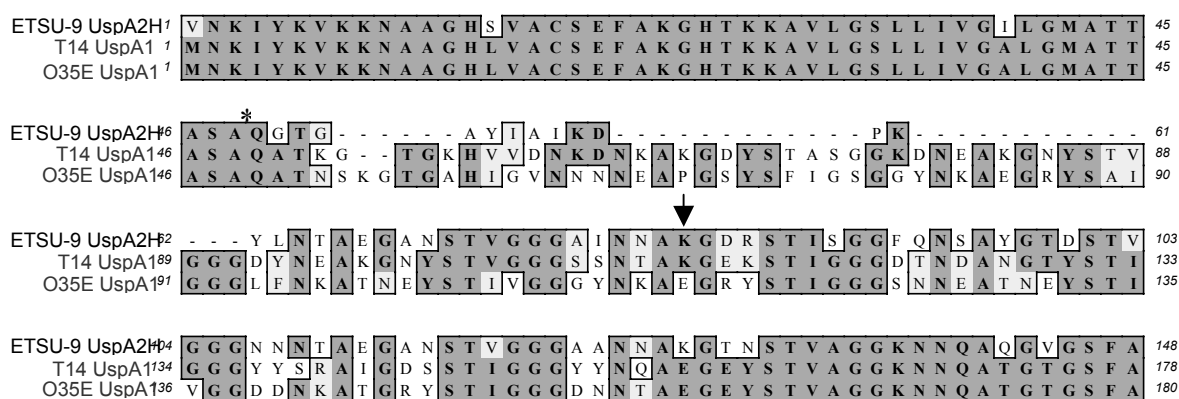


Fig. 50. Alignment of the N-termini of ETSU-9 UspA2H, T14 UspA1, and O35E UspA1. The asterisk indicates the putative cleavage site of the signal peptide. The arrow indicates the amino acid (K) of ETSU-9 UspA2H that was mutated (i.e., K34E and K34A).

C. Site-directed mutagenesis of the *uspA2H* gene

Because UspA2H-dependent biofilm formation appeared to be exquisitely sensitive to insertions in the UspA2H sequence, the ability of mutants with single amino acid changes in UspA2H to form biofilms was analyzed next. To find candidate amino acid residues for mutagenesis, we compared the sequence of ETSU-9 UspA2H with UspA1 from the biofilm-negative strain O35E and the biofilm-positive transformant strain T14 (from chapter 7). This sequence alignment revealed several amino acids that were conserved in the proteins from the biofilm-positive strains but different in O35E UspA1 (Fig. 50). We chose amino acid K34 of the mature ETSU-9 UspA2H, which corresponds to a glutamate residue in O35E UspA2, for further analysis. The K34E mutation was introduced into strain ETSU-9.2H by plate transformation; desired mutants were enriched by using the congression technique. Testing of the ETSU-9 K34E mutant showed that this mutant was completely negative for biofilm formation (Fig. 51). An ETSU-9 K34A mutant, however, formed biofilms about half as well as wild-type ETSU-9. Expression of UspA2H by both of these mutants was confirmed by Western blot analysis.

D. Site-directed mutagenesis of the O35E *uspA1* gene

Since the K34E mutation of ETSU-9 UspA2H eliminated the ability of ETSU-9 to form biofilms, we wanted to determine whether the opposite mutation in O35E UspA1 (i.e., E66K) would allow this strain to form biofilms. Because strain O35E produces a Hag

protein, which is known to interfere with biofilm formation by some strains of *M. catarrhalis* (Chapter 7), the E66K mutation was tested in both a Hag-positive and a *hag* mutant background. However, the E66K mutation did not confer the ability to form biofilms regardless of Hag expression (data not shown).

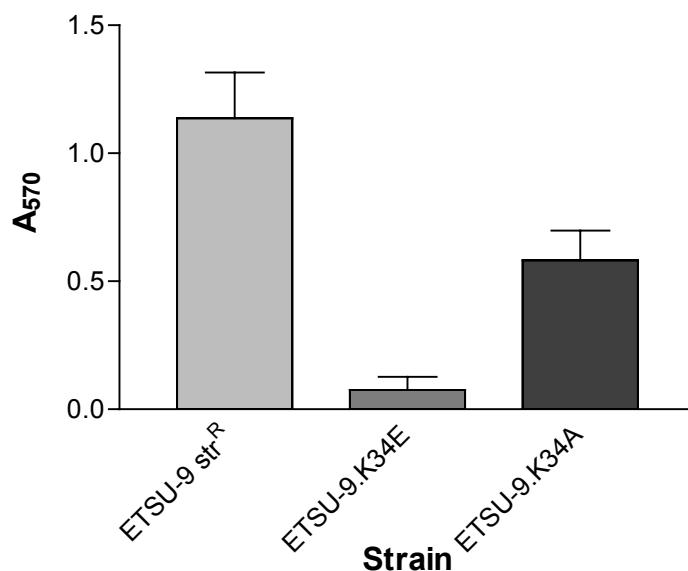


Fig. 51. Biofilm formation by ETSU-9 containing site-directed mutations in *uspA2H*.

E. Characterization of other biofilm-negative transposon mutants

Transposon insertions in three other genes in addition to *uspA2H* were found to cause a loss of biofilm formation by strain ETSU-9. Direct sequencing of the transposon insertion from the chromosomal DNA indicated that all 3 mutants had insertions in ORFs. ETSU-9.222 had an insertion in a putative lytic murein transglycosylase D gene, ETSU-9.714 had an insertion in a predicted phosphotransferase gene, and ETSU-9.988 had an insertion in the

ampD gene. All three of these genes are predicted to play a role in bacterial cell wall metabolism. Isogenic *M. catarrhalis* mutants were constructed by insertion of a promoterless *cat* gene into each of these ORFs; all three of these mutants were found to be attenuated for biofilm formation (Fig. 52) when a broth culture was used as the inoculum in the 24-well tissue culture plate. However, when a swatch of growth from an agar plate was used as the inoculum, the defect in biofilm formation was much less pronounced. Analysis of the ability of these three mutants to grow in broth culture compared to growth of wild-type ETSU-9 revealed that all three of these mutants have a slight growth defect (Fig. 53).

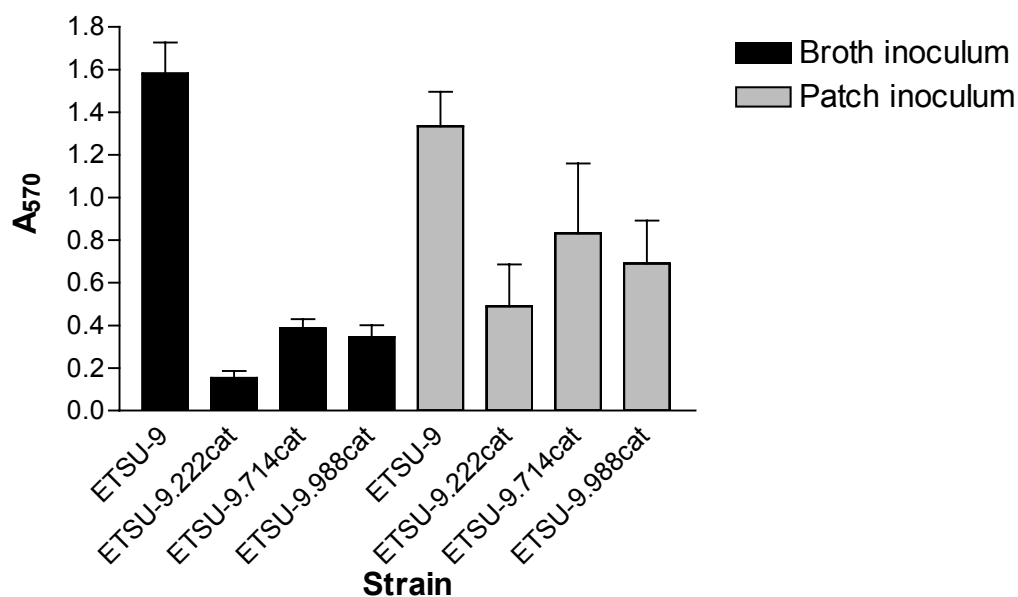


Fig. 52. Biofilm formation by the isogenic mutants ETSU-9.222cat, ETSU-9.714cat, and ETSU-9.988cat. The black bars on the left represent biofilm formation following inoculation of a 24-well plate with a broth culture. The grey bars on the right represent biofilm formation following inoculation of a 24-well plate with a swatch of bacterial growth from an agar plate.

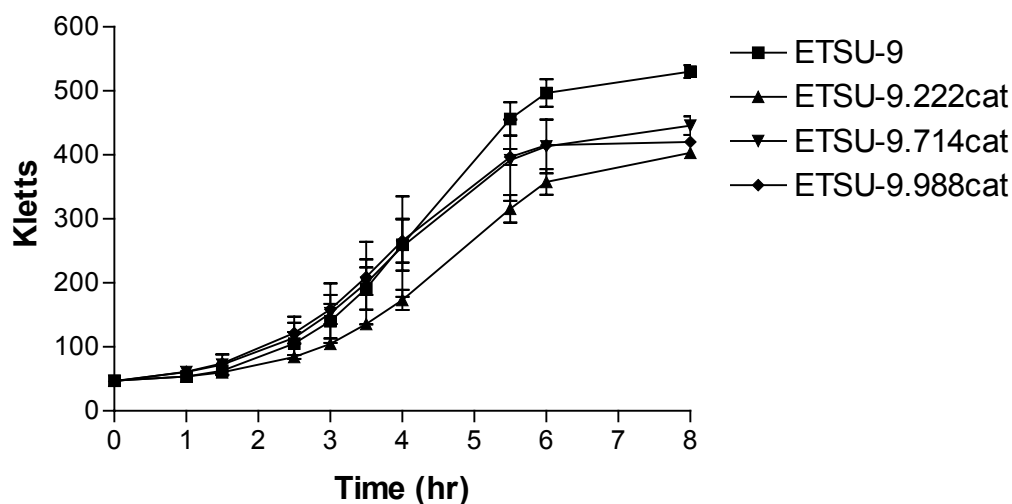


Fig. 53. Growth curve of ETSU-9 and the three isogenic mutants. Strains were grown in sidarm flasks in TH broth, and bacterial density was recorded over time.

III. Discussion

In this chapter, it was shown that the UspA2H protein plays a role in biofilm formation by *M. catarrhalis* strain ETSU-9, as evaluated using the crystal violet-based assay. In contrast to the data obtained from a genetic analysis of biofilm formation by strain O46E, it appears that expression of the UspA1 protein does not enhance biofilm formation by strain ETSU-9 (Fig. 42).

It was surprising that the introduction of 15 nt insertions in-frame into the *uspA2H* gene of strain ETSU-9 had such a negative effect on the ability of the UspA2H protein to mediate biofilm formation. This technique was intended to identify domains within the UspA2H protein that are directly involved in biofilm formation. Instead, it appears that insertion of this five amino acid sequence at almost any site in the UspA2H protein results in

loss of function, at least with regard to biofilm formation. Interestingly, these mutated UspA2H proteins were still able to mediate attachment to Chang conjunctival epithelial cells (Fig. 48), indicating that the insertions were likely not causing a gross conformational change. In addition, at least one of the insertions that caused a loss of the ability to attach to Chang cells (ETSU-9.mut41) allowed the UspA2H protein to still be expressed on the bacterial cell surface (Fig. 49).

As noted previously, the UspA2H protein has some homology to the YadA protein of *Yersinia* species. Heesemann and colleagues (141) aligned the sequences of YadA, UspA1, and UspA2 and examined both *Y. enterocolitica* and *M. catarrhalis* by TEM. They found that the YadA protein appears to have a “lollipop” shape as revealed by TEM and proposed a structure for YadA consisting of an N-terminal head, a stalk region consisting of coiled coils, and C-terminal β strands that anchor the protein to the bacterial outer membrane. This group also suggested that UspA1 and UspA2 might have the same organization (141). The data presented in the current study suggest that this might be the case for ETSU-9 UspA2H. Computer analysis indicates a high probability for coiled-coil formation in the amino acid repeat region of ETSU-9 UspA2H (highlighted in blue in Fig. 44), corresponding to the stalk region in the lollipop model. In addition, the data presented in Fig. 50 suggest that the region of UspA1 or UspA2H involved in biofilm formation is near the N-terminus of these proteins.

The majority of the *uspA2H* genes with 15 nt insertions in this study were not capable of mediating biofilm formation. Comparison with the lollipop model may indicate why this occurred. In this model, it is possible that the N-terminal head domain is the domain that is actually mediating biofilm formation. Any perturbations in this region might alter the

configuration of the protein. Similarly, any insertions in the stalk region might introduce a “kink” into the protein structure, so that the head domain is not in the proper position to mediate biofilm formation. However, an in-frame deletion of the stalk would lead to a functional protein with a shorter stalk. This could be the case for mutants ETSU-9.mut81 and ETSU-9.mut92, which contain deletions in the repeat region yet still form biofilms. It is possible that positioning of the head domain is not as important for mediating attachment to Chang conjunctival epithelial cells as it is for mediating biofilm development in the plastic wells of a tissue culture plate. Finally, an insertion in the C-terminus of UspA2H would, according to the lollipop model, interfere with the anchoring of the protein to the outer membrane. This is possibly the reason why ETSU-9.mut3, which has a 5 aa insertion near the C-terminus of UspA2H, does not express a UspA2H protein detectable in either whole cell lysates (Fig. 46A).

The finding that 105 of 3000 transposon mutants (3.5%) were deficient in biofilm formation relative to the wild-type strain ETSU-9 was initially surprising. However, this experiment was performed before the apparent inhibitory role of Hag in biofilm formation (as measured by the crystal violet-based assay) was elucidated. In retrospect, the unexpectedly high percentage of biofilm-negative transposon insertion mutants, most of which appeared to be biofilm-negative due to some other factor than the transposon insertion, can probably be explained by phase variation of the *hag* gene. The wild-type strain ETSU-9 expresses very little or undetectable levels of the Hag protein (Fig. 43). In contrast, at least some of the biofilm-negative transposon mutants were Hag-positive. Transformation of ETSU-9 with the chromosomal DNA from these Hag-positive transposon mutants resulted in

both biofilm-positive and biofilm-negative transformants, regardless of the presence of the transposon. Instead, expression of the Hag protein could be correlated with a lack of biofilm formation (Fig. 43). The *uspA1* gene is known to undergo phase variation from high to low levels of expression at a frequency of 3.7×10^{-2} (or from low to high levels at a frequency of 9.7×10^{-3}) (175). If the *hag* gene undergoes phase variation at a similar rate, this could help explain the high percentage (3.5%) of biofilm-negative transposon mutants obtained in this study. It should be noted that at least one of the 105 biofilm-negative transposon mutants had a *uspA2* gene derived from strain O35E instead of the *uspA2H* gene from strain ETSU-9. This O35E gene was derived from the transposon-mutagenized O35E chromosomal DNA. Incorporation of certain O35E genes (O35E is a biofilm-negative strain when measured using the crystal violet-based assay) into the ETSU-9 chromosomal DNA could also explain why some transposon mutants are biofilm-negative.

Insertional mutagenesis and domain swapping have also been used to study the surface-expressed autotransporter protein Ag43 (163). Just as the UspA1 and UspA2H proteins have different properties in different *M. catarrhalis* isolates with regard to biofilm formation, epithelial cell attachment, or serum resistance, the Ag43 protein from diverse *E. coli* subtypes confers different abilities in autoaggregation. Exchange of the α -subunits of Ag43 proteins with different autoaggregation characteristics suggested that the portion of the protein responsible for this phenotype resides within the α -subunit of Ag43. In contrast with the current study, Klemm and colleagues (163) were able to use insertional mutagenesis to localize regions of Ag43 that were important for autoaggregation. This is possibly explained by the fact that the linker insertions used in the Ag43 study resulted in the insertion of 2 aa

(i.e., RS), while the technique employed in the current study resulted in the insertion of 5 aa. Alternatively, Ag43-mediated autoaggregation may be less sensitive to perturbations in protein structure than UspA2H-mediated biofilm formation. The results of the insertional mutagenesis of Ag43 were used to construct hybrid proteins from autoaggregating and nonaggregating Ag43 wild-type proteins. The data obtained from the hybrid proteins suggested that the portion of Ag43 that was necessary for autoaggregation could be localized to the first 47 aa of the α -subunit. These results for the Ag43 protein are similar to some of the data presented in this chapter for the UspA2H protein; that is, it appears that at least one residue (i.e. K34) of the UspA2H protein that is necessary for biofilm formation is located within the first 76 aa of the mature protein (Fig. 50).

Site-directed mutagenesis of the UspA2H protein indicated that the lysine residue at position 34 may be involved in biofilm formation. Unfortunately, mutation of the corresponding glutamate residue in O35E UspA1 to the lysine residue found in ETSU-9 UspA2H did not result in biofilm formation by strain O35E, even in a Hag-negative background. Interestingly, Klemm and colleagues (163) found that Ag43-mediated autoaggregation is greatly diminished between pH 9 and pH 10, suggesting that a lysine residue may also be involved in this phenotype. It is noteworthy that there are at least two other charged amino acids near K34 in UspA2H that are the same in T14 UspA1 but different in O35E UspA1 (Fig. 50, ETSU-9 residues D36, R37). It would be interesting to mutate these corresponding residues in O35E UspA1 to ascertain whether this would be sufficient to allow O35E to form biofilms.

Three of the transposon insertion mutants identified in this study, ETSU-9.222, ETSU-9.714, and ETSU-9.988, possess insertions in genes that putatively encode proteins involved in bacterial cell wall metabolism. Although there have been no reports of these proteins having a role in biofilm formation by other organisms, it is known that *E. coli* recycles almost 50% of its murein in each generation (112). As is the case for *M. catarrhalis*, *E. coli* cell wall recycling mutants grow normally. Although the role of murein recycling has not yet been elucidated, Park (233) has suggested that this function may be a method for sensing the condition of the cell wall. Possibly, the status of the cell wall may act as an indicator of the exterior cell environment. This in turn may be necessary for bacterial biofilm formation.

One unexpected finding from this study was that the ability of the isogenic mutants ETSU-9.222cat, ETSU-9.714cat, and ETSU-9.988cat to form biofilms was affected by the method of tissue culture plate inoculation (i.e., broth inoculum or a swatch of growth from an agar plate; Fig. 52). It has been suggested that inoculating tissue culture plate wells with a patch of growth is akin to inoculating these wells with pre-formed biofilms (J. W. Costerton, personal communication). This could explain why different results were obtained when ETSU-9 isogenic mutants were tested for biofilm formation using these two different methods of inoculation (Fig. 52). The initial screen of 3000 transposon mutants was conducted using the agar plate swatch method. In retrospect, some biofilm-attenuated mutants may have been missed in the initial screen due to the use of this method of inoculation. Thus, any future *M. catarrhalis* biofilm studies should be carried out using broth inocula.

CHAPTER ELEVEN

Summary and Conclusions

M. catarrhalis is the third-most prevalent cause of otitis media, sinusitis, and exacerbations of COPD. Biofilm formation is now commonly implicated in recurrent or chronic infections caused by several species of bacteria, and has been directly visualized on tympanostomy tubes from otitis media patients. The experiments within this dissertation were designed to characterize biofilm formation by *M. catarrhalis* and identify gene products that were necessary for biofilm formation to occur.

Biofilm formation by *M. catarrhalis* is dependent, at least *in vitro*, on the method used to grow the bacteria. The Sorbarod continuous-culture biofilm system appears to permit robust biofilm growth by all strains that have been grown in this system thus far. In contrast, the majority of *M. catarrhalis* strains form biofilms poorly in the tissue culture plate-based (crystal violet) method. In addition, expression of the Hag protein prevents biofilm formation in tissue culture plates whereas Hag-expressing cells appear to be selected for in the continuous-culture biofilm system. While these results are perhaps not intuitive, they are consistent with the results of other biofilm researchers, who have found that many different factors can contribute to biofilm formation. For example, *Enterococcus faecalis* strains vary in their ability to form biofilms in microtiter plates. In addition, *E. faecalis* biofilm formation can have different dynamics depending on the growth medium used (170). Similarly, *Vibrio*

cholerae is known to use different gene products for biofilm formation on borosilicate glass surfaces versus chitin (324). As discussed previously, in *E. coli*, type I fimbriae are required for biofilm formation in rich media (242) whereas Ag43 is required for biofilm formation in minimal medium (67). Furthermore, the expression of a polysaccharide capsule by *E. coli* can block biofilm formation by Ag43 (270).

The UspA1 and UspA2H proteins were found to mediate biofilm formation, in a strain-dependent manner, by *M. catarrhalis* grown in tissue culture plates. These two proteins have also been shown to act as adhesins for Chang conjunctival epithelial cells *in vitro* (174). The UspA2H protein can also confer resistance to killing by normal human serum. However, the ability of the UspA1 and UspA2H proteins to mediate attachment to Chang cells appears to be independent of their ability to mediate biofilm formation. Whereas the majority of UspA1 and UspA2H proteins that have been analyzed confer the ability to attach to Chang cells, only a very few strains form UspA1- or UspA2H-dependent biofilms in tissue culture plates.

The results summarized above allow for the development of a model for *M. catarrhalis* biofilm formation that encompasses the data from both the Sorbarod continuous-culture and the tissue culture plate-based methods for growing biofilms. It should be noted that this model is based on the results presented within this dissertation; more recent data that were obtained following the defense of this dissertation potentially conflict with this model and will be discussed below. I propose that the UspA1 (or UspA2H) protein is responsible for initiating biofilm formation by *M. catarrhalis*. The UspA1 or UspA2H protein mediates firm attachment of the bacterial cell to the surface upon which the biofilm is being formed.

However, if *M. catarrhalis* is expressing the Hag protein, the bacteria will autoaggregate and fall out of suspension (in a tissue culture plate) or be washed away (from the nasopharyngeal mucosa) instead of forming an attachment to a surface (Fig. 54A). Thus, the tissue culture plate method for growing biofilms likely measures the early events in biofilm formation. In contrast, the Sorbarod continuous-culture system, which is used to grow *M. catarrhalis* biofilms over a period of three days, allows the formation of mature biofilms. Once a *M. catarrhalis* biofilm has become established, the Hag protein plays a beneficial or positive role in biofilm maintenance. Hag expression allows *M. catarrhalis* cells to adhere to other *M. catarrhalis* cells as the biofilm grows away from the surface (Fig. 54B). Self-recognition of Hag could contribute to the spacing of *M. catarrhalis* cells within a biofilm, thus contributing to the architecture of the mature biofilm. Hag expression may even allow *M. catarrhalis* to bind to other bacterial species that are already established as a biofilm *in vivo*. This autoaggregation property might then aid in propagation of the biofilm. In the respiratory tract, clusters of preformed *M. catarrhalis* biofilm could break away and infect a new location, such as the lungs of a COPD patient or the middle ear of an infant. The Hag protein would help the detached fragment of biofilm remain intact as it transited to a new site of infection.

Clearly, there are alternate possibilities for the overall mechanism of biofilm formation by *M. catarrhalis*. Expression of the Hag protein prevents biofilm formation by most *M. catarrhalis* strains in the wells of tissue culture plates. However, at least one *M. catarrhalis* strain, ATCC 43617, is both Hag-positive and forms biofilms in tissue culture plates. This observation raises the concern that perhaps Hag plays a different role *in vivo*:

perhaps its role in eukaryotic cell attachment is more relevant, and its apparent antagonistic role in biofilm formation *in vitro* is not important. Alternatively, Hag may block UspA1- or UspA2H-mediated biofilm formation by steric hindrance. This latter possibility seems unlikely, however, given that UspA1 mediates attachment to Chang cells regardless of Hag expression, and UspA2H confers serum resistance whether or not Hag is expressed. Also, TEM analysis indicates that Hag and UspA1 form cell surface projections of similar length. It is not clear how the surface projections formed by UspA1 and Hag might interact in intact bacteria. An intriguing alternative possibility is that UspA1 and Hag could form heteroligomers, and that the composition of these projections determines their functions.

Instead of keeping a biofilm intact, Hag could function as a dispersion factor that causes *M. catarrhalis* to break away from the biofilm as a planktonic cell. It appears that, at least for strain O46E, variants that express Hag are selected in the continuous-culture model for biofilm formation. This was the case whether these variants were obtained from the growth on the silicone tubing, in the broth effluent, or from the floating mat of bacteria within the effluent bottle. As with some determinants of biofilm formation in several other bacterial species (for example, Ag43 (72) or capsule (319)), the UspA1, UspA2H and Hag proteins are all subject to phase variation. Thus, it seems quite possible that these three different proteins could be necessary at different stages of biofilm formation.

After the Results section of this dissertation had been completed and after the dissertation defense, I isolated a phase variant of O46E 2001-1 that expresses the Hag protein (O46E.24). New data obtained by Dr. Wei Wang in this laboratory at about the same time suggested that the Hag protein from *M. catarrhalis* strain O46E may not mediate

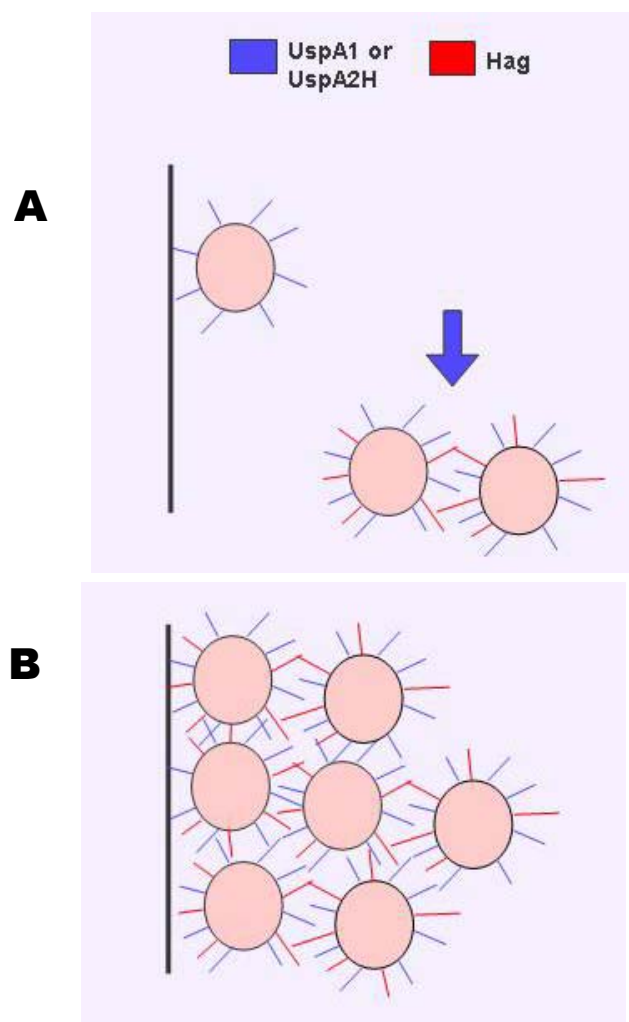


Fig. 54. Model for biofilm formation by *M. catarrhalis*. Panel A, expression of the UspA1 or UspA2H proteins allows some strains of *M. catarrhalis* to initiate biofilm formation. Expression of Hag at this stage prevents biofilm formation, possibly by causing the bacteria to autoagglutinate and settle out of suspension. In an established biofilm (Panel B), expression of the Hag protein may help to maintain biofilm architecture, perhaps through self-recognition of other Hag-expressing cells.

autoagglutination. However, I have found that the Hag-positive O46E.24 variant is still unable to form biofilms in tissue culture plates using the crystal violet-based assay. Furthermore, a *hag* null mutant of O46E.24 is again able to form biofilms (data not shown). Taken together, these data indicate that, at least with strain O46E, Hag may not cause autoagglutination that interferes with biofilm formation in the crystal violet-based assay.

Therefore, it seems likely that Hag interferes with initial biofilm formation by strain O46E in the crystal violet-based assay by some other mechanism which remains to be determined. It will be necessary to examine numerous other *M. catarrhalis* strains to determine the relative importance and contribution of Hag to biofilm formation by these strains.

The ability of most *M. catarrhalis* strains to take up *M. catarrhalis* DNA from other strains was used to construct *M. catarrhalis* transformant and transposon insertion mutant strains for the purpose of studying biofilm formation. In one case, transformant strains were obtained that were both amenable to transposon mutagenesis and able to form biofilms in the wells of tissue culture plates (Chapter 7). Although study of such transformant strains was useful, this approach also had some shortcomings. Specifically, it appears that more than one gene product is necessary for maximum biofilm formation by wild-type strain O46E. Because it is unknown exactly how much of the transformant strains' (i.e., T13, T14, and T84) chromosomal DNA was derived from O46E, it is impossible to know whether these transformant strains could be used to identify the remaining gene(s) necessary for biofilm formation by O46E. Experiments performed in Chapters 9 and 10 used wild-type strains of *M. catarrhalis* (i.e. strains O46E and ETSU-9) that had been transformed with transposon-mutagenized DNA from strain O35E. These studies led to the identification of several gene products that are involved in biofilm formation by ETSU-9. However, there are also aspects to this experimental design that are undesirable. For example, transformation of ETSU-9 with O35E chromosomal DNA may result in multiple crossovers within the ETSU-9 chromosome. O35E-derived genes that are flanking any given transposon insertion may be incorporated into ETSU-9 in this process. In at least one case, this resulted in the removal of

one gene necessary for biofilm formation (i.e., *uspA2H*) and its replacement with another gene that apparently does not play a role in *M. catarrhalis* biofilm formation (i.e., *uspA2*). In addition, this mutagenesis strategy would not allow the identification of ETSU-9 genes that are necessary for biofilm formation if those specific genes are not also present in the O35E chromosome. Thus, the studies in this dissertation were limited somewhat by the current lack of genetic systems for working with *M. catarrhalis*. Thus, future efforts to develop direct mutagenesis strategies that are effective in more than one *M. catarrhalis* strain are warranted.

To address some of the concerns that have been discussed, it will be necessary to examine the process of biofilm formation in more detail. For example, although O35E appears to form biofilms well in the continuous-culture model but not in the tissue culture plate model, it is possible that there are considerable differences in biofilm architecture in the continuous-culture model-derived O35E biofilms compared to O46E or ETSU-9 biofilms. Ideally, a method would be devised to allow microscopic observation of living *M. catarrhalis* biofilms in both tissue culture plates (which may be more useful for studying initial events in biofilm formation) and in the continuous-culture system. Confocal laser scanning microscopy has been used extensively by other researchers to examine the architecture of living biofilms. Immunofluorescence studies might indicate which bacteria in a biofilm population were expressing the Hag protein. If the development of methods to view living biofilms with the tissue culture plate or continuous-culture models is unsuccessful, it may be illuminating to pursue additional SEM analysis of different *M. catarrhalis* strains and isogenic *uspA1*, *uspA2H*, or *hag* mutants. Another option for direct visualization of living

biofilms would be to try growing *M. catarrhalis* as a biofilm in flow cells. These may now be purchased directly, and thus no longer have to be made by hand in the laboratory.

In summary, *M. catarrhalis* is able to form biofilms *in vitro*. However, there are many aspects of *M. catarrhalis* biofilm formation that have yet to be examined. It is hoped that there might be a relevant animal model developed to study *M. catarrhalis* disease so that *M. catarrhalis* biofilm formation might be studied *in vivo*. These studies could contribute to new methods to prevent *M. catarrhalis* colonization and, ultimately, *M. catarrhalis* disease.

Reference List

1. 1981. Dorland's Illustrated Medical Dictionary. W.B. Saunders Company, Philadelphia.
2. 1995. Standards for the diagnosis and care of patients with chronic obstructive pulmonary disease. American Thoracic Society. Am.J.Respir.Crit Care Med. **152**:S77-121.
3. **Adams, G. A., T. G. Tornabene, and M. Yaguchi.** 1969. Cell wall lipopolysaccharides from *Neisseria catarrhalis*. Can.J.Microbiol. **15**:365-374.
4. **Aebi, C., L. D. Cope, J. L. Latimer, S. E. Thomas, C. A. Slaughter, G. H. McCracken, Jr., and E. J. Hansen.** 1998. Mapping of a protective epitope of the CopB outer membrane protein of *Moraxella catarrhalis*. Infect.Immun. **66**:540-548.
5. **Aebi, C., E. R. Lafontaine, L. D. Cope, J. L. Latimer, S. R. Lumbley, G. H. McCracken, Jr., and E. J. Hansen.** 1998. Phenotypic effect of isogenic *uspA1* and *uspA2* mutations on *Moraxella catarrhalis* O35E. Infect.Immun. **66**:3113-3119.
6. **Aebi, C., I. Maciver, J. L. Latimer, L. D. Cope, M. K. Stevens, S. E. Thomas, G. H. McCracken, Jr., and E. J. Hansen.** 1997. A protective epitope of *Moraxella catarrhalis* is encoded by two different genes. Infect.Immun. **65**:4367-4377.
7. **Aebi, C., B. Stone, M. Beucher, L. D. Cope, I. Maciver, S. E. Thomas, G. H. McCracken, Jr., P. F. Sparling, and E. J. Hansen.** 1996. Expression of the CopB outer membrane protein by *Moraxella catarrhalis* is regulated by iron and affects iron acquisition from transferrin and lactoferrin. Infect.Immun. **64**:2024-2030.
8. **Ahmed, K., H. Masaki, T. C. Dai, A. Ichinose, Y. Utsunomiya, M. Tao, T. Nagatake, and K. Matsumoto.** 1994. Expression of fimbriae and host response in *Branhamella catarrhalis* respiratory infections. Microbiol.Immunol. **38**:767-771.
9. **Ahmed, K., K. Matsumoto, N. Rikitomi, T. Nagatake, T. Yoshida, and K. Watanabe.** 1990. Effect of ampicillin, cefmetazole and minocycline on the adherence of *Branhamella catarrhalis* to pharyngeal epithelial cells. Tohoku J.Exp.Med. **161**:1-7.
10. **Ahmed, K., N. Rikitomi, and K. Matsumoto.** 1992. Fimbriation, hemagglutination and adherence properties of fresh clinical isolates of *Branhamella catarrhalis*. Microbiol.Immunol. **36**:1009-1017.

11. **Ahmed, K., N. Rikitomi, T. Nagatake, and K. Matsumoto.** 1990. Electron microscopic observation of *Branhamella catarrhalis*. *Microbiol.Immunol.* **34**:967-975.
12. **Altschul, S. F., W. Gish, W. Miller, E. W. Myers, and D. J. Lipman.** 1990. Basic local alignment search tool. *J.Mol.Biol.* **215**:403-410.
13. **Anwar, H., J. L. Strap, and J. W. Costerton.** 1992. Eradication of biofilm cells of *Staphylococcus aureus* with tobramycin and cephalexin. *Can.J.Microbiol.* **38**:618-625.
14. **Archibald, F. S. and I. W. DeVoe.** 1979. Removal of iron from human transferrin by *Neisseria meningitidis*. *FEMS Microbiol.Lett.* **6**:159-162.
15. **Azghani, A. O., S. Idell, M. Bains, and R. E. Hancock.** 2002. *Pseudomonas aeruginosa* outer membrane protein F is an adhesin in bacterial binding to lung epithelial cells in culture. *Microb.Pathog.* **33**:109-114.
16. **Bakaletz, L. O., D. M. Murwin, and J. M. Billy.** 1995. Adenovirus serotype 1 does not act synergistically with *Moraxella (Branhamella) catarrhalis* to induce otitis media in the chinchilla. *Infect.Immun.* **63**:4188-4190.
17. **Barenkamp, S. J. and J. W. St.Geme, III.** 1996. Identification of a second family of high-molecular-weight adhesion proteins expressed by non-typable *Haemophilus influenzae*. *Mol.Microbiol.* **19**:1215-1223.
18. **Bartos, L. C. and T. F. Murphy.** 1988. Comparison of the outer membrane proteins of 50 strains of *Branhamella catarrhalis*. *J.Infect.Dis.* **158**:761-765.
19. **Beaulieu, D., M. Ouellette, M. G. Bergeron, and P. H. Roy.** 1988. Characterization of a plasmid isolated from *Branhamella catarrhalis* and detection of plasmid sequences within the genome of a *B. catarrhalis* strain. *Plasmid* **20**:158-162.
20. **Berk, S. L.** 1990. From Micrococcus to Moraxella. The reemergence of *Branhamella catarrhalis*. *Arch.Intern.Med.* **150**:2254-2257.
21. **Beucher, M. and P. F. Sparling.** 1995. Cloning, sequencing, and characterization of the gene encoding FrpB, a major iron-regulated, outer membrane protein of *Neisseria gonorrhoeae*. *J.Bacteriol.* **177**:2041-2049.
22. **Bhushan, R., R. Craige, and T. F. Murphy.** 1994. Molecular cloning and characterization of outer membrane protein E of *Moraxella (Branhamella) catarrhalis*. *J.Bacteriol.* **176**:6636-6643.

23. **Bhushan, R., C. Kirkham, S. Sethi, and T. F. Murphy.** 1997. Antigenic characterization and analysis of the human immune response to outer membrane protein E of *Branhamella catarrhalis*. *Infect.Immun.* **65**:2668-2675.
24. **Black, P. N.** 1991. Primary sequence of the *Escherichia coli fadL* gene encoding an outer membrane protein required for long-chain fatty acid transport. *J.Bacteriol.* **173**:435-442.
25. **Bliska, J. B., M. C. Copass, and S. Falkow.** 1993. The *Yersinia pseudotuberculosis* adhesin YadA mediates intimate bacterial attachment to and entry into HEp-2 cells. *Infect.Immun.* **61**:3914-3921.
26. **Boel, E., E. Bootsma, J. Dekruif, M. Jansze, K. L. Klingman, H. van Dijk, and T. Logtenberg.** 1998. Phage antibodies obtained by competitive selection of a complement-resistant *Moraxella (Branhamella) catarrhalis* recognize the high-molecular-weight outer membrane protein. *Infect.Immun.* **66**:83-88.
27. **Bonnah, R. A., H. Wong, S. M. Loosmore, and A. B. Schryvers.** 1999. Characterization of *Moraxella (Branhamella) catarrhalis lbpB*, *lbpA*, and lactoferrin receptor *orf3* isogenic mutants. *Infect.Immun.* **67**:1517-1520.
28. **Bonnah, R. A., R. H. Yu, H. Wong, and A. B. Schryvers.** 1998. Biochemical and immunological properties of lactoferrin binding proteins from *Moraxella (Branhamella) catarrhalis*. *Microb.Pathog.* **24**:89-100.
29. **Bonnah, R. A., R.-H. Yu, and A. B. Schryvers.** 1995. Biochemical analysis of lactoferrin receptors in the Neisseriaceae: identification of a second bacterial lactoferrin receptor protein. *Microb.Pathog.* **19**:285-297.
30. **Bootsma, H. J., H. G. Der Heide, P. S. van De, L. M. Schouls, and F. R. Mooi.** 2000. Analysis of *Moraxella catarrhalis* by DNA Typing: Evidence for a Distinct Subpopulation Associated with Virulence Traits. *J.Infect.Dis.* **181**:1376-1387.
31. **Bosma, M. J. and A. M. Carroll.** 1991. The SCID mouse mutant: definition, characterization, and potential uses. *Annu.Rev.Immunol.* **9**:323-350.
32. **Bovre, K.** 1965. Studies on transformation in *Moraxella* and organisms assumed to be related to *Moraxella*. 4. Streptomycin resistance transformation between asaccharolytic *Neisseria* strains. *Acta Pathol.Microbiol.Scand.* **64**:229-242.
33. **Bovre, K.** 1967. Transformation and DNA base composition in taxonomy, with special reference to recent studies in *Moraxella* and *Neisseria*. *Acta Pathol.Microbiol.Scand.* **69**:123-144.

34. **Bovre, K.** 1979. Proposal to divide the genus *Moraxella* Lwoff 1939 emend. Henriksen and Bovre 1968 into two subgenera, subgenus *Moraxella* (Lwoff 1939) Bovre 1979 and subgenus *Branhamella* (Catlin 1970) Bovre 1979. *Int.J.Syst.Bacteriol.* **29**:403-406.
35. **Bowers, L. C., J. E. Purcell, G. B. Plauche, P. A. Denoel, Y. Lobet, and M. T. Philipp.** 2002. Assessment of the nasopharyngeal bacterial flora of rhesus macaques: *Moraxella*, *Neisseria*, *Haemophilus*, and other genera. *J.Clin.Microbiol* **40**:4340-4342.
36. **Brorson, J. E. and B. E. Malmvall.** 1981. *Branhamella catarrhalis* and other bacteria in the nasopharynx of children with longstanding cough. *Scand.J.Infect.Dis.* **13**:111-113.
37. **Budhani, R. K. and J. K. Struthers.** 1997. The use of Sorbarod biofilms to study the antimicrobial susceptibility of a strain of *Streptococcus pneumoniae*. *J.Antimicrob.Chemother.* **40**:601-602.
38. **Budhani, R. K. and J. K. Struthers.** 1998. Interaction of *Streptococcus pneumoniae* and *Moraxella catarrhalis*: investigation of the indirect pathogenic role of beta-lactamase-producing Moraxellae by use of a continuous-culture biofilm system. *Antimicrob.Agents Chemother.* **42**:2521-2526.
39. **Budhani, R. K. and J. K. Struthers.** 1998. Interaction of *Streptococcus pneumoniae* and *Moraxella catarrhalis*: investigation of the indirect pathogenic role of beta-lactamase-producing Moraxellae by use of a continuous-culture biofilm system. *Antimicrob.Agents Chemother.* **42**:2521-2526.
40. **Burne, R. A., R. G. Quivey, Jr., and R. E. Marquis.** 1999. Physiologic homeostasis and stress responses in oral biofilms. *Methods Enzymol.* **310**:441-460.
41. **Calder, M. A., M. J. Croughan, D. T. McLeod, and F. Ahmad.** 1986. The incidence and antibiotic susceptibility of *Branhamella catarrhalis* in respiratory infections. *Drugs* **31 Suppl 3**:11-16.
42. **Campagnari, A. A., T. F. Ducey, and C. A. Rebmann.** 1996. Outer membrane protein B1, an iron-repressible protein conserved in the outer membrane of *Moraxella (Branhamella) catarrhalis*, binds human transferrin. *Infect.Immun.* **64**:3920-3924.
43. **Campagnari, A. A., K. L. Shanks, and D. W. Dyer.** 1994. Growth of *Moraxella catarrhalis* with human transferrin and lactoferrin: Expression of iron-repressible proteins without siderophore production. *Infect.Immun.* **62**:4909-4914.

44. **Carter, G., M. Wu, D. C. Drummond, and L. E. Bermudez.** 2003. Characterization of biofilm formation by clinical isolates of *Mycobacterium avium*. J.Med.Microbiol. **52**:747-752.
45. **Catlin, B. W.** 1964. Reciprocal genetic transformation between *Neisseria catarrhalis* and *Moraxella nonliquefaciens*. J.Gen.Microbiol. **37**:369-379.
46. **Catlin, B. W.** 1970. Transfer of the organism named *Neisseria catarrhalis* to Branhamella gen. nov. Int.J.Syst.Bacteriol. **20**:155-159.
47. **Catlin, B. W.** 1990. *Branhamella catarrhalis*: an organism gaining respect as a pathogen. Clin.Microbiol.Rev. **3**:293-320.
48. **Catlin, B. W. and L. S. Cunningham.** 1961. Transforming activities and base contents of deoxyribonucleate preparations from various neisseriae. J.Gen.Microbiol. **26**:303-312.
49. **Catlin, B. W. and L. S. Cunningham.** 1964. Genetic transformation of *Neisseria catarrhalis* by deoxyribonucleate preparations having different average base compositions. J.Gen.Microbiol. **37**:341-352.
50. **Caye-Thomasen, P. and M. Tos.** 2004. Eustachian tube gland tissue changes are related to bacterial species in acute otitis media. Int.J.Pediatr.Otorhinolaryngol. **68**:101-110.
51. **Ceri, H., M. E. Olson, C. Stremick, R. R. Read, D. Morck, and A. Buret.** 1999. The Calgary Biofilm Device: new technology for rapid determination of antibiotic susceptibilities of bacterial biofilms. J.Clin.Microbiol. **37**:1771-1776.
52. **Chang, A. C. Y. and S. N. Cohen.** 1978. Construction and characterization of amplifiable multicopy DNA cloning vehicles derived from the P15A cryptic miniplasmid. J.Bacteriol. **134**:1141-1156.
53. **Chen, D., V. Barniak, K. R. VanDerMeid, and J. C. McMichael.** 1999. The levels and bactericidal capacity of antibodies directed against the UspA1 and UspA2 outer membrane proteins of *Moraxella (Branhamella) catarrhalis* in adults and children. Infect.Immun. **67**:1310-1316.
54. **Chen, D., J. C. McMichael, K. R. van der Meid, D. Hahn, T. Mininni, J. Cowell, and J. Eldridge.** 1996. Evaluation of purified UspA from *Moraxella catarrhalis* as a vaccine in a murine model after active immunization. Infect.Immun. **64**:1900-1905.
55. **Chen, D., J. C. McMichael, K. R. VanDerMeid, A. W. Masi, E. Bortell, J. D. Caplan, D. N. Chakravarti, and V. L. Barniak.** 1999. Evaluation of a 74-kDa

- transferrin-binding protein from *Moraxella (Branhamella) catarrhalis* as a vaccine candidate. *Vaccine* **18**:109-118.
56. **Chen, X., S. Schauder, N. Potier, A. Van Dorsselaer, I. Pelczer, B. L. Bassler, and F. M. Hughson.** 2002. Structural identification of a bacterial quorum-sensing signal containing boron. *Nature* **415**:545-549.
 57. **Chiang, S. L., R. K. Taylor, M. Koomey, and J. J. Mekalanos.** 1995. Single amino acid substitutions in the N-terminus of *Vibrio cholerae* TcpA affect colonization, autoagglutination, and serum resistance. *Mol.Microbiol.* **17**:1133-1142.
 58. **Christensen, J. J., J. Ursing, and B. Bruun.** 1994. Genotypic and phenotypic relatedness of 80 strains of *Branhamella catarrhalis* of worldwide origin. *FEMS Microbiol.Lett.* **119**:155-160.
 59. **Chung, M., R. Enrique, D. J. Lim, and T. F. DeMaria.** 1994. *Moraxella (Branhamella) catarrhalis*-induced experimental otitis media in the chinchilla. *Acta Otolaryngol.* **114**:415-422.
 60. **Collazos, J., J. de Miguel, and R. Ayarza.** 1992. *Moraxella catarrhalis* bacteremic pneumonia in adults: two cases and review of the literature. *Eur.J.Clin.Microbiol.Infect.Dis.* **11**:237-240.
 61. **Cook, G. S., J. W. Costerton, and R. J. Lamont.** 1998. Biofilm formation by *Porphyromonas gingivalis* and *Streptococcus gordonii*. *J.Periodontal Res.* **33**:323-327.
 62. **Cope, L. D., E. R. Lafontaine, C. A. Slaughter, C. A. Hasemann, Jr., C. Aebi, F. W. Henderson, and G. H. McCracken, Jr.** 1999. Characterization of the *Moraxella catarrhalis* *uspA1* and *uspA2* genes and their encoded products. *J.Bacteriol.* **181**:4026-4034.
 63. **Costerton, J. W.** 1979. The role of electron microscopy in the elucidation of bacterial structure and function. *Annu.Rev.Microbiol.* **33**:459-479.
 64. **Costerton, J. W., K. J. Cheng, G. G. Geesey, T. I. Ladd, J. C. Nickel, M. Dasgupta, and T. J. Marrie.** 1987. Bacterial biofilms in nature and disease. *Annu.Rev.Microbiol.* **41**:435-464.
 65. **Costerton, J. W., P. S. Stewart, and E. P. Greenberg.** 1999. Bacterial biofilms: a common cause of persistent infections. *Science* **284**:1318-1322.
 66. **Cramton, S. E., C. Gerke, N. F. Schnell, W. W. Nichols, and F. Gotz.** 1999. The intercellular adhesion (*ica*) locus is present in *Staphylococcus aureus* and is required for biofilm formation. *Infect.Immun.* **67**:5427-5433.

67. **Danese, P. N., L. A. Pratt, S. L. Dove, and R. Kolter.** 2000. The outer membrane protein, antigen 43, mediates cell-to-cell interactions within *Escherichia coli* biofilms. *Mol.Microbiol* **37**:424-432.
68. **Davies, D. G., A. M. Chakrabarty, and G. G. Geesey.** 1993. Exopolysaccharide production in biofilms: substratum activation of alginate gene expression by *Pseudomonas aeruginosa*. *Appl.Environ.Microbiol.* **59**:1181-1186.
69. **Davies, D. G., M. R. Parsek, J. P. Pearson, B. H. Iglewski, J. W. Costerton, and E. P. Greenberg.** 1998. The involvement of cell-to-cell signals in the development of a bacterial biofilm. *Science* **280**:295-298.
70. **DeMaria, T. F., B. R. Briggs, D. J. Lim, and N. Okazaki.** 1984. Experimental otitis media with effusion following middle ear inoculation of nonviable *H. influenzae*. *Ann.Otol.Rhinol.Laryngol.* **93**:52-56.
71. **Dickinson, D. P. and D. M. Dryja.** 1988. Restriction fragment mapping of *Branhamella catarrhalis*: A new tool for studying the epidemiology of the middle ear pathogen. *J.Infect.Dis.* **158**:205-208.
72. **Diderichsen, B.** 1980. *flu*, a metastable gene controlling surface properties of *Escherichia coli*. *J.Bacteriol.* **141**:858-867.
73. **DiGiovanni, C., T. V. Riley, G. F. Hoyne, R. Yeo, and P. Cooksey.** 1987. Respiratory tract infections due to *Branhamella catarrhalis*: epidemiological data from Western Australia. *Epidemiol.Infect.* **99**:445-453.
74. **Dingman, J. R., M. G. Rayner, S. Mishra, Y. Zhang, M. D. Ehrlich, J. C. Post, and G. D. Ehrlich.** 1998. Correlation between presence of viable bacteria and presence of endotoxin in middle-ear effusions. *J.Clin.Microbiol* **36**:3417-3419.
75. **Djordjevic, D., M. Wiedmann, and L. A. McLandsborough.** 2002. Microtiter plate assay for assessment of *Listeria monocytogenes* biofilm formation. *Appl.Environ.Microbiol.* **68**:2950-2958.
76. **Donlan, R. M. and J. W. Costerton.** 2002. Biofilms: survival mechanisms of clinically relevant microorganisms. *Clin.Microbiol Rev.* **15**:167-193.
77. **Dorrell, N., M. C. Martino, R. A. Stabler, S. J. Ward, Z. W. Zhang, A. A. McColm, M. J. Farthing, and B. W. Wren.** 1999. Characterization of *Helicobacter pylori* PldA, a phospholipase with a role in colonization of the gastric mucosa. *Gastroenterol.* **117**:1098-1104.
78. **Doyle, W. J.** 1989. Animal models of otitis media: other pathogens. *Pediatr.Infect.Dis.J.* **8**:S45-S47.

79. **Du, R. P., Q. J. Wang, Y.-P. Yang, A. B. Schryvers, P. Chong, M. H. Klein, and S. M. Loosmore.** 1998. Cloning and expression of the *Moraxella catarrhalis* lactoferrin receptor genes. *Infect.Immun.* **66**:3656-3665.
80. **Dunn, R. A. and M. H. Gordon.** 1905. Remarks on the clinical and bacteriologic aspects of an epidemic simulating influenza. *BMJ* 420-427.
81. **Dunne, W. M., Jr.** 2002. Bacterial adhesion: seen any good biofilms lately? *Clin.Microbiol Rev.* **15**:155-166.
82. **Edebrink, P., P. E. Jansson, M. M. Rahman, G. Widmalm, T. Holme, and M. Rahman.** 1995. Structural studies of the O-antigen oligosaccharides from two strains of *Moraxella catarrhalis* serotype C. *Carbohydr.Res.* **266**:237-261.
83. **Edebrink, P., P. E. Jansson, G. Widmalm, T. Holme, and M. Rahman.** 1996. The structures of oligosaccharides isolated from the lipopolysaccharide of *Moraxella catarrhalis* serotype B, strain CCUG 3292. *Carbohydr.Res.* **295**:127-146.
84. **Edebrink, P., P.-E. Jansson, M. M. Rahman, G. Widmalm, T. Holme, M. Rahman, and A. Weintraub.** 1994. Structural studies of the O-polysaccharide from the lipopolysaccharide of *Moraxella (Branhamella) catarrhalis* serotype A (strain ATCC 25238). *Carbohydrate Research* **257**:269-284.
85. **Ehrlich, G. D., R. Veeh, X. Wang, J. W. Costerton, J. D. Hayes, F. Z. Hu, B. J. Daigle, M. D. Ehrlich, and J. C. Post.** 2002. Mucosal biofilm formation on middle-ear mucosa in the chinchilla model of otitis media. *JAMA* **287**:1710-1715.
86. **Elkins, C., K. J. Morrow, Jr., and B. Olsen.** 2000. Serum resistance in *Haemophilus ducreyi* requires outer membrane protein DsrA. *Infect.Immun.* **68**:1608-1619.
87. **Elvers, K. T., K. Leeming, and H. M. Lappin-Scott.** 2002. Binary and mixed population biofilms: time-lapse image analysis and disinfection with biocides. *J.Ind.Microbiol.Biotechnol.* **29**:331-338.
88. **Enright, M. C., P. E. Carter, I. A. MacLean, and H. McKenzie.** 1994. Phylogenetic relationships between some members of the genera *Neisseria*, *Acinetobacter*, *Moraxella*, and *Kingella* based on partial 16S ribosomal DNA sequence analysis. *Int.J.Syst.Bacteriol.* **44**:387-391.
89. **Faden, H. S., Y. Harabuchi, J. J. Hong, and Tonawanda/Williamsburg Pediatrics.** 1994. Epidemiology of *Moraxella catarrhalis* in children during the first 2 years of life: Relationship to otitis media. *J.Infect.Dis.* **169**:1312-1317.

90. **Fassel, T. A. and C. E. Edmiston.** 2000. Evaluating adherent bacteria and biofilm using electron microscopy, p. 235-248. *In* Y. H. An and R. J. Friedman (eds.), Handbook of Bacterial Adhesion: Principles, Methods, and Applications. Humana Press, Totowa.
91. **Fayet, O., T. Ziegelhoffer, and C. Georgopoulos.** 1989. The groES and groEL heat shock gene products of *Escherichia coli* are essential for bacterial growth at all temperatures. *J.Bacteriol.* **171**:1379-1385.
92. **Fitzgerald, M., R. Mulcahy, S. Murphy, C. Keane, D. Coakley, and T. Scott.** 1997. A 200 kDa protein is associated with haemagglutinating isolates of *Moraxella (Branhamella) catarrhalis*. *FEMS Immunol.Med.Microbiol.* **18**:209-216.
93. **Fitzgerald, M., R. Mulcahy, S. Murphy, C. Keane, D. Coakley, and T. Scott.** 1999. Transmission electron microscopy studies of *Moraxella (Branhamella) catarrhalis*. *FEMS Immunol.Med.Microbiol.* **23**:57-66.
94. **Fitzgerald, M., S. Murphy, R. Mulcahy, C. Keane, D. Coakley, and T. Scott.** 1996. Haemagglutination properties of *Moraxella (Branhamella) catarrhalis*. *Br.J.Biomed.Sci.* **53**:257-262.
95. **Fitzgerald, M., S. Murphy, R. Mulcahy, C. Keane, D. Coakley, and T. Scott.** 1999. Tissue culture adherence and haemagglutination characteristics of *Moraxella (Branhamella) catarrhalis*. *FEMS Immunol.Med.Microbiol.* **24**:105-114.
96. **Fletcher, M.** 1977. The effects of culture concentration and age, time, and temperature on bacterial attachment to polystyrene. *Can.J.Microbiol.* **23**:1-6.
97. **Flieger, A., S. Gongab, M. Faigle, H. A. Mayer, U. Kehrer, J. Mussotter, P. Bartmann, and B. Neumeister.** 2000. Phospholipase A secreted by *Legionella pneumophila* destroys alveolar surfactant phospholipids. *FEMS Microbiol.Lett.* **188**:129-133.
98. **Fomsgaard, J. S., A. Fomsgaard, N. Hoiby, B. Bruun, and C. Galanos.** 1991. Comparative immunochemistry of lipopolysaccharides from *Branhamella catarrhalis* strains. *Infect.Immun.* **59**:3346-3349.
99. **Forsgren, A., M. Brant, M. Karamehmedovic, and K. Riesbeck.** 2003. The immunoglobulin D-binding protein MID from *Moraxella catarrhalis* is also an adhesin. *Infect.Immun.* **71**:3302-3309.
100. **Forsgren, A., M. Brant, A. Mollenkvist, A. Muyombwe, H. Janson, N. Woin, and K. Riesbeck.** 2001. Isolation and characterization of a novel IgD-binding protein from *Moraxella catarrhalis*. *J.Immunol.* **167**:2112-2120.

101. **Forsgren, A. and A. O. Grubb.** 1979. Many bacterial species bind human IgD. *J.Immunol.* **122**:1468-1472.
102. **Frisk, A., C. A. Ison, and T. Lagergard.** 1998. GroEL heat shock protein of *Haemophilus ducreyi*: Association with cell surface and capacity to bind to eukaryotic cells. *Infect.Immun.* **66**:1252-1257.
103. **Fulghum, R. S. and H. G. Marrow.** 1996. Experimental otitis media with *Moraxella (Branhamella) Catarrhalis*. *Ann.Otol.Rhinol.Laryngol.* **105**:234-241.
104. **Furano, K. and A. A. Campagnari.** 2003. Inactivation of the *Moraxella catarrhalis* 7169 ferric uptake regulator increases susceptibility to the bactericidal activity of normal human sera. *Infect.Immun.* **71**:1843-1848.
105. **Gander, S. and P. Gilbert.** 1997. The development of a small-scale biofilm model suitable for studying the effects of antibiotics on biofilms of gram-negative bacteria. *J.Antimicrob.Chemother.* **40**:329-334.
106. **Garduno, R. A., G. Faulkner, M. A. Trevors, N. Vats, and P. S. Hoffman.** 1998. Immunolocalization of Hsp60 in *Legionella pneumophila*. *J.Bacteriol.* **180**:505-513.
107. **Gaynor, E. C., N. Ghor, and S. Falkow.** 2001. Bile-induced 'pili' in *Campylobacter jejuni* are bacteria-independent artifacts of the culture medium. *Mol.Microbiol.* **39**:1546-1549.
108. **Gibson, M. M., D. A. Bagga, C. G. Miller, and M. E. Maguire.** 1991. Magnesium transport in *Salmonella typhimurium*: the influence of new mutations conferring Co²⁺ resistance on the CorA Mg²⁺ transport system. *Mol.Microbiol* **5**:2753-2762.
109. **Giebink, G. S., E. E. Payne, E. L. Mills, S. K. Juhn, and P. G. Quie.** 1976. Experimental otitis media due to *Streptococcus pneumoniae*: immunopathogenic response in the chinchilla. *J.Infect.Dis.* **134**:595-604.
110. **Gilbert, P., D. G. Allison, D. J. Evans, P. S. Handley, and M. R. Brown.** 1989. Growth rate control of adherent bacterial populations. *Appl.Environ.Microbiol.* **55**:1308-1311.
111. **Goldenhersh, M. J., G. S. Rachelefsky, J. Dudley, J. Brill, R. M. Katz, A. S. Rohr, S. L. Spector, S. C. Siegel, P. Summanen, E. J. Baron, and .** 1990. The microbiology of chronic sinus disease in children with respiratory allergy. *J.Allergy Clin.Immunol.* **85**:1030-1039.
112. **Goodell, E. W.** 1985. Recycling of murein by *Escherichia coli*. *J.Bacteriol.* **163**:305-310.

113. **Gordon, J. E.** 1921. The gram-negative cocci in colds and influenza. *J.Infect.Dis.* **29**:463-494.
114. **Goulhen, F., A. Hafezi, V. J. Uitto, D. Hinode, R. Nakamura, D. Grenier, and D. Mayrand.** 1998. Subcellular localization and cytotoxic activity of the GroEL-like protein isolated from *Actinobacillus actinomycetemcomitans*. *Infect.Immun.* **66**:5307-5313.
115. **Govan, J. R. and V. Deretic.** 1996. Microbial pathogenesis in cystic fibrosis: mucoid *Pseudomonas aeruginosa* and *Burkholderia cepacia*. *Microbiol.Rev.* **60**:539-574.
116. **Gray-Owen, S. D. and A. B. Schryvers.** 1993. The interaction of primate transferrins with receptors on bacteria pathogenic to humans. *Microb.Pathog.* **14**:389-398.
117. **Griffiths, G., A. McDowall, R. Back, and J. Dubochet.** 1984. On the preparation of cryosections for immunocytochemistry. *J.Ultrastruct.Res.* **89**:65-78.
118. **Gruenert, D. C., C. B. Basbaum, M. J. Welsh, M. Li, W. E. Finkbeiner, and J. A. Nadel.** 1988. Characterization of human tracheal epithelial cells transformed by an origin-defective simian virus 40. *Proc.Natl.Acad.Sci.U.S.A* **85**:5951-5955.
119. **Gu, X.-X., J. Chen, S. J. Barenkamp, J. B. Robbins, C.-M. Tsai, D. J. Lim, and J. Battey.** 1998. Synthesis and characterization of lipooligosaccharide-based conjugates as vaccine candidates for *Moraxella (Branhamella) catarrhalis*. *Infect.Immun.* **66**:1891-1897.
120. **Halter, R., J. Pohlner, and T. F. Meyer.** 1989. Mosaic-like organization of IgA protease genes in *Neisseria gonorrhoeae* generated by horizontal genetic exchange *in vivo*. *EMBO J.* **8**:2737-3744.
121. **Han, Y. W., W. Shi, G. T. Huang, H. S. Kinder, N. H. Park, H. Kuramitsu, and R. J. Genco.** 2000. Interactions between periodontal bacteria and human oral epithelial cells: *Fusobacterium nucleatum* adheres to and invades epithelial cells. *Infect.Immun.* **68**:3140-3146.
122. **Hansen, E. J., C. F. Frisch, R. L. McDade, Jr., and K. H. Johnston.** 1981. Identification of immunogenic outer membrane proteins of *Haemophilus influenzae* type b in the infant rat model system. *Infect.Immun.* **32**:1084-1092.
123. **Harabuchi, Y., H. Murakata, M. Goh, H. Kodama, A. Kataura, H. Faden, and T. F. Murphy.** 1998. Serum antibodies specific to CD outer membrane protein of *Moraxella catarrhalis*, P6 outer membrane protein of non-typeable *Haemophilus influenzae* and capsular polysaccharides of *Streptococcus pneumoniae* in children with otitis media with effusion. *Acta Otolaryngol.* **118**:826-832.

124. **Harkness, R. E., M.-J. Guimond, B.-A. McBey, M. H. Klein, D. H. Percy, and B. A. Croy.** 1993. *Branhamella catarrhalis* pathogenesis in SCID and SCID/beige mice. *APMIS* **101**:805-810.
125. **Hart, V. K.** 1927. The bacteriology of acute ears. *Laryngoscope* **37**:56-61.
126. **Hasman, H., T. Chakraborty, and P. Klemm.** 1999. Antigen-43-mediated autoaggregation of *Escherichia coli* is blocked by fimbriation. *J.Bacteriol.* **181**:4834-4841.
127. **Hays, J. P., S. C. van der, A. Loogman, K. Eadie, C. Verduin, H. Faden, H. Verbrugh, and A. Van Belkum.** 2003. Total genome polymorphism and low frequency of intra-genomic variation in the *uspA1* and *uspA2* genes of *Moraxella catarrhalis* in otitis prone and non-prone children up to 2 years of age. Consequences for vaccine design? *Vaccine* **21**:1118-1124.
128. **Heesemann, J. and L. Gruter.** 1987. Genetic evidence that the outer membrane protein YOP1 of *Yersinia enterocolitica* mediates adherence and phagocytosis resistance to human epithelial cells. *FEMS Microbiol.Lett.* **40**:37-41.
129. **Helminen, M. E., I. Maciver, J. L. Latimer, L. D. Cope, G. H. McCracken, Jr., and E. J. Hansen.** 1993. A major outer membrane protein of *Moraxella catarrhalis* is a target for antibodies that enhance pulmonary clearance of the pathogen in an animal model. *Infect.Immun.* **61**:2003-2010.
130. **Helminen, M. E., I. Maciver, J. L. Latimer, J. Klesney-Tait, L. D. Cope, M. M. Paris, G. H. McCracken, Jr., and E. J. Hansen.** 1994. A large, antigenically conserved protein on the surface of *Moraxella catarrhalis* is a target for protective antibodies. *J.Infect.Dis.* **170**:867-872.
131. **Helminen, M. E., I. Maciver, J. L. Latimer, S. R. Lumbley, L. D. Cope, G. H. McCracken, Jr., and E. J. Hansen.** 1993. A mutation affecting expression of a major outer membrane protein of *Moraxella catarrhalis* alters serum resistance and survival of this organism in vivo. *J.Infect.Dis.* **168**:1194-1201.
132. **Henderson, I. R., R. Cappello, and J. P. Nataro.** 2000. Autotransporter proteins, evolution and redefining protein secretion. *Trends Microbiol.* **8**:529-532.
133. **Henderson, I. R., M. Meehan, and P. Owen.** 1997. A novel regulatory mechanism for a novel phase-variable outer membrane protein of *Escherichia coli*. *Adv.Exp.Med.Biol.* **412**:349-355.
134. **Henderson, I. R. and J. P. Nataro.** 2001. Virulence functions of autotransporter proteins. *Infect.Immun.* **69**:1231-1243.

135. **Henderson, I. R., F. Navarro-Garcia, and J. P. Nataro.** 1998. The great escape: structure and function of the autotransporter proteins. *Trends Microbiol.* **6**:370-378.
136. **Henderson, I. R., P. Owen, and J. P. Nataro.** 1999. Molecular switches--the ON and OFF of bacterial phase variation. *Mol.Microbiol.* **33**:919-932.
137. **Henriksen, S. D. and K. Bovre.** 1968. The Taxonomy of the genera *Moraxella* and *Neisseria*. *J.Gen.Microbiol.* **51**:387-392.
138. **Hill, D. J. and M. Virji.** 2003. A novel cell-binding mechanism of *Moraxella catarrhalis* ubiquitous surface protein UspA: specific targeting of the N-domain of carcinoembryonic antigen-related cell adhesion molecules by UspA1. *Mol.Microbiol.* **48**:117-129.
139. **Hobbs, M. M., A. Seiler, M. Achtman, and J. G. Cannon.** 1994. Microevolution within a clonal population of pathogenic bacteria: recombination, gene duplication and horizontal genetic exchange in the *opa* gene family of *Neisseria meningitidis*. *Mol.Microbiol.* **12**:171-180.
140. **Hodgson, A. E., S. M. Nelson, M. R. Brown, and P. Gilbert.** 1995. A simple in vitro model for growth control of bacterial biofilms. *J.Appl.Bacteriol.* **79**:87-93.
141. **Hoiczky, E., A. Roggenkamp, M. Reichenbecher, A. Lupas, and J. Heesemann.** 2000. Structure and sequence analysis of *Yersinia* YadA and *Moraxella* UspAs reveal a novel class of adhesins. *EMBO J.* **19**:5989-5999.
142. **Hol, C., C. Schalen, C. M. Verduin, E. van Dijke, J. Verhoef, A. Fleer, and H. van Dijk.** 1996. *Moraxella catarrhalis* in acute laryngitis: infection or colonization? *J.Infect.Dis.* **174**:636-638.
143. **Holm, M. M., S. L. Vanlerberg, I. M. Foley, D. D. Sledjeski, and E. R. Lafontaine.** 2004. The *Moraxella catarrhalis* Porin-Like Outer Membrane Protein CD Is an Adhesin for Human Lung Cells. *Infect.Immun.* **72**:1906-1913.
144. **Holm, M. M., S. L. Vanlerberg, D. D. Sledjeski, and E. R. Lafontaine.** 2003. The Hag protein of *Moraxella catarrhalis* strain O35E is associated with adherence to human lung and middle ear cells. *Infect.Immun.* **71**:4977-4984.
145. **Hoyle, B. D., L. J. Williams, and J. W. Costerton.** 1993. Production of mucoid exopolysaccharide during development of *Pseudomonas aeruginosa* biofilms. *Infect.Immun.* **61**:777-780.
146. **Hsiao, C. B., S. Sethi, and T. F. Murphy.** 1995. Outer membrane protein CD of *Branhamella catarrhalis* - Sequence conservation in strains recovered from the human respiratory tract. *Microb.Pathog.* **19**:215-225.

147. **Hu, W. G., J. Chen, J. F. Battey, and X. X. Gu.** 2000. Enhancement of clearance of bacteria from murine lungs by immunization with detoxified lipooligosaccharide from *Moraxella catarrhalis* conjugated to proteins. *Infect.Immun.* **68**:4980-4985.
148. **Hu, W. G., J. Chen, J. C. McMichael, and X. X. Gu.** 2001. Functional characteristics of a protective monoclonal antibody against serotype A and C lipooligosaccharides from *Moraxella catarrhalis*. *Infect.Immun.* **69**:1358-1363.
149. **Hu, W.-G., J. Chen, F. M. Collins, and X.-X. Gu.** 1999. An aerosol challenge mouse model for *Moraxella catarrhalis*. *Vaccine* **18**:799-804.
150. **Ioannidis, J. P. A., M. Worthington, J. K. Griffiths, and D. R. Snyderman.** 1995. Spectrum and significance of bacteremia due to *Moraxella catarrhalis*. *Clin.Infect.Dis.* **21**:390-397.
151. **Jackson, D. W., K. Suzuki, L. Oakford, J. W. Simecka, M. E. Hart, and T. Romeo.** 2002. Biofilm formation and dispersal under the influence of the global regulator CsrA of *Escherichia coli*. *J.Bacteriol.* **184**:290-301.
152. **Johnson, K. G., I. J. McDonald, and M. B. Perry.** 1976. Studies on the cellular and free lipopolysaccharides from *Branhamella catarrhalis*. *Can.J.Microbiol.* **22**:460-467.
153. **Jordan, K. L., S. H. Berk, and S. L. Berk.** 1990. A comparison of serum bactericidal activity and phenotypic characteristics of bacteremic, pneumonia-causing strains, and colonizing strains of *Branhamella catarrhalis*. *Am.J.Med.* **88(5A)**:28S-32S.
154. **Jousimies-Somer, H. R., S. Savolainen, and J. S. Ylikoski.** 1989. Comparison of the nasal bacterial floras in two groups of healthy subjects and in patients with acute maxillary sinusitis. *J.Clin.Microbiol.* **27**:2736-2743.
155. **Juni, E.** 1974. Simple genetic transformation assay for rapid diagnosis of *Moraxella osloensis*. *Applied Microbiol.* **27**:16-24.
156. **Juni, E. and K. Bovre.** 2004. Family: Moraxellaceae, *In* D. J. Brenner, N. R. Krieg, and J. T. Staley (eds.), *The Proteobacteria*. Springer-Verlag, New York.
157. **Juni, E., G. A. Heym, and M. Avery.** 1986. Defined medium for *Moraxella (Branhamella) catarrhalis*. *Appl.Environ.Microbiol.* **52**:546-551.
158. **Kamme, C., M. Vang, and S. Stahl.** 1983. Transfer of beta-lactamase production in *Branhamella catarrhalis*. *Scand.J.Infect.Dis.* **15**:225-226.
159. **Kamme, C., M. Vang, and S. Stahl.** 1984. Intrgeneric and intergeneric transfer of *Branhamella catarrhalis* B-lactamase production. *Scand.J.Infect.Dis.* **16**:153-155.

160. **Karalus, R. and A. Campagnari.** 2000. *Moraxella catarrhalis*: a review of an important human mucosal pathogen. *Microbes.Infect.* **2**:547-559.
161. **Kellens, J., M. Persoons, M. Vaneechoutte, F. van Tiel, and E. Stobberingh.** 1995. Evidence for lectin-mediated adherence of *Moraxella catarrhalis*. *Infection* **23**:37-41.
162. **Klein, J. O.** 1994. Otitis media. *Clin.Infect.Dis.* **19**:823-833.
163. **Klemm, P., L. Hjerrild, M. Gjermansen, and M. A. Schembri.** 2004. Structure-function analysis of the self-recognizing Antigen 43 autotransporter protein from *Escherichia coli*. *Mol.Microbiol* **51**:283-296.
164. **Klingman, K. L. and T. F. Murphy.** 1994. Purification and characterization of a high-molecular-weight outer membrane protein of *Moraxella (Branhamella) catarrhalis*. *Infect.Immun.* **62**:1150-1155.
165. **Klingman, K. L., A. Pye, T. F. Murphy, and S. L. Hill.** 1995. Dynamics of respiratory tract colonization by *Branhamella catarrhalis* in bronchiectasis. *Am.J.Respir.Crit.Care Med.* **152**:1072-1078.
166. **Knobloch, J. K., K. Bartscht, A. Sabottke, H. Rohde, H. H. Feucht, and D. Mack.** 2001. Biofilm formation by *Staphylococcus epidermidis* depends on functional RsbU, an activator of the sigB operon: differential activation mechanisms due to ethanol and salt stress. *J.Bacteriol.* **183**:2624-2633.
167. **Koch, C. and N. Hoiby.** 1993. Pathogenesis of cystic fibrosis. *Lancet* **341**:1065-1069.
168. **Kolenbrander, P. E.** 2000. Oral microbial communities: biofilms, interactions, and genetic systems. *Annu.Rev.Microbiol.* **54**:413-437.
169. **Kostiala, A. A. and T. Honkanen.** 1989. *Branhamella catarrhalis* as a cause of acute purulent pericarditis. *J.Infect.* **19**:291-292.
170. **Kristich, C. J., Y. H. Li, D. G. Cvitkovitch, and G. M. Dunny.** 2004. Esp-independent biofilm formation by *Enterococcus faecalis*. *J.Bacteriol.* **186**:154-163.
171. **Kuehn, M., M. Hausner, H. J. Bungartz, M. Wagner, P. A. Wilderer, and S. Wuertz.** 1998. Automated confocal laser scanning microscopy and semiautomated image processing for analysis of biofilms. *Appl.Environ.Microbiol.* **64**:4115-4127.
172. **Kyd, J., A. John, A. Cripps, and T. F. Murphy.** 1999. Investigation of mucosal immunisation in pulmonary clearance of *Moraxella (Branhamella) catarrhalis*. *Vaccine* **18**:398-406.

173. **Kyd, J. M., A. W. Cripps, and T. F. Murphy.** 1998. Outer-membrane antigen expression by *Moraxella (Branhamella) catarrhalis* influences pulmonary clearance. *J.Med.Microbiol.* **47**:159-168.
174. **Lafontaine, E. R., L. D. Cope, C. Aebi, J. L. Latimer, G. H. McCracken, Jr., and E. J. Hansen.** 2000. The UspA1 protein and a second type of UspA2 protein mediate adherence of *Moraxella catarrhalis* to human epithelial cells in vitro. *J.Bacteriol.* **182**:1364-1373.
175. **Lafontaine, E. R., N. J. Wagner, and E. J. Hansen.** 2001. Expression of the *Moraxella catarrhalis* UspA1 protein undergoes phase variation and is regulated at the transcriptional level. *J.Bacteriol.* **183**:1540-1551.
176. **Lambert, M. A., D. G. Hollis, D. W. Moss, R. E. Weaver, and M. L. Thomas.** 1971. Cellular fatty acids of nonpathogenic *Neisseria*. *Can.J.Microbiol.* **17**:1491-1502.
177. **Lamont, R. J., A. El Sabaeny, Y. Park, G. S. Cook, J. W. Costerton, and D. R. Demuth.** 2002. Role of the *Streptococcus gordonii* SspB protein in the development of *Porphyromonas gingivalis* biofilms on streptococcal substrates. *Microbiology* **148**:1627-1636.
178. **Lawrence, J. R., D. R. Korber, B. D. Hoyle, J. W. Costerton, and D. E. Caldwell.** 1991. Optical sectioning of microbial biofilms. *J.Bacteriol.* **173**:6558-6567.
179. **Lesse, A. J., A. A. Campagnari, W. E. Bittner, and M. A. Apicella.** 1990. Increased resolution of lipopolysaccharides and lipooligosaccharides utilizing tricine-sodium dodecyl sulfate- polyacrylamide gel electrophoresis. *J.Immunol.Methods* **126**:109-117.
180. **Lewis, V. J., R. E. Weaver, and D. G. Hollis.** 1968. Fatty acid composition of *Neisseria* species as determined by gas chromatography. *J.Bacteriol.* **96**:1-5.
181. **Li, X., D. E. Johnson, and H. L. Mobley.** 1999. Requirement of MrpH for mannose-resistant *Proteus*-like fimbria-mediated hemagglutination by *Proteus mirabilis*. *Infect.Immun.* **67**:2822-2833.
182. **Li, X., Z. Yan, and J. Xu.** 2003. Quantitative variation of biofilms among strains in natural populations of *Candida albicans*. *Microbiology* **149**:353-362.
183. **Liu, L. and E. J. Hansen.** 1999. Structural analysis of plasmid pLQ510 from *Moraxella catarrhalis* E22. *Plasmid* **42**:150-153.

184. **Locht, C., P. Bertin, F. D. Menozzi, and G. Renauld.** 1993. The filamentous haemagglutinin, a multifaceted adhesin produced by virulent *Bordetella* spp. *Mol.Microbiol.* **9**:653-660.
185. **Luke, N. R., S. Allen, B. W. Gibson, and A. A. Campagnari.** 2003. Identification of a 3-deoxy-D-manno-octulosonic acid biosynthetic operon in *Moraxella catarrhalis* and analysis of a KdsA-deficient isogenic mutant. *Infect.Immun.* **71**:6426-6434.
186. **Luke, N. R. and A. A. Campagnari.** 1999. Construction and characterization of *Moraxella catarrhalis* mutants defective in expression of transferrin receptors. *Infect.Immun.* **67**:5815-5819.
187. **Luke, N. R., T. A. Russo, N. Luther, and A. A. Campagnari.** 1999. Use of an isogenic mutant constructed in *Moraxella catarrhalis* to identify a protective epitope of outer membrane B1 defined by monoclonal antibody 11C6. *Infect.Immun.* **67**:681-687.
188. **Lukomski, S., N. P. Hoe, I. Abdi, J. Rurangirwa, P. Kordari, M. Liu, S. J. Dou, G. G. Adams, and J. M. Musser.** 2000. Nonpolar inactivation of the hypervariable streptococcal inhibitor of complement gene (sic) in serotype M1 *Streptococcus pyogenes* significantly decreases mouse mucosal colonization. *Infect.Immun.* **68**:535-542.
189. **Lukomski, S., R. A. Hull, and S. I. Hull.** 1996. Identification of the O antigen polymerase (*rfc*) gene in *Escherichia coli* O4 by insertional mutagenesis using a nonpolar chloramphenicol resistance cassette. *J.Bacteriol.* **178**:240-247.
190. **Lundgren, K. and L. Ingvarsson.** 1986. Acute otitis media in Sweden. Role of *Branhamella catarrhalis* and the rationale for choice of antimicrobial therapy. *Drugs* **31 Suppl 3**:125-131.
191. **Maciver, I., M. Unhanand, G. H. McCracken, Jr., and E. J. Hansen.** 1993. Effect of immunization on pulmonary clearance of *Moraxella catarrhalis* in an animal model. *J.Infect.Dis.* **168**:469-472.
192. **Mack, D., H. Rohde, S. Dobinsky, J. Riedewald, M. Nedelmann, J. K. Knobloch, H. A. Elsner, and H. H. Feucht.** 2000. Identification of three essential regulatory gene loci governing expression of *Staphylococcus epidermidis* polysaccharide intercellular adhesin and biofilm formation. *Infect.Immun.* **68**:3799-3807.
193. **Mack, D. H., J. Heesemann, and R. Laufs.** 1994. Characterization of different oligomeric species of the *Yersinia enterocolitica* outer membrane protein YadA. *Med.Microbiol.Immunol.* **183**:217-227.

194. **Mackey, L.** 1919. The bacteriology of chronic nasal catarrh and its treatment by autogenous vaccines. *BMJ* **160**:3058-3059.
195. **Macasai, M. S., D. S. Hillman, and J. B. Robin.** 1988. *Branhamella* keratitis resistant to penicillin and cephalosporins. Case report. *Arch.Ophthalmol.* **106**:1506-1507.
196. **Marrs, C. F. and S. Weir.** 1990. Pili (fimbriae) of *Branhamella* species. *Am.J.Med.* **88(5A)**:36S-40S.
197. **Marsh, J. W. and R. K. Taylor.** 1999. Genetic and transcriptional analyses of the *Vibrio cholerae* mannose-sensitive hemagglutinin type 4 pilus gene locus. *J.Bacteriol.* **181**:1110-1117.
198. **Martin, D. W., M. J. Schurr, H. Yu, and V. Deretic.** 1994. Analysis of promoters controlled by the putative sigma factor AlgU regulating conversion to mucoidy in *Pseudomonas aeruginosa*: relationship to sigma E and stress response. *J.Bacteriol.* **176**:6688-6696.
199. **Masoud, H., M. B. Perry, and J. C. Richards.** 1994. Characterization of the lipopolysaccharide of *Moraxella catarrhalis*. Structural analysis of the lipid A from *M. catarrhalis* serotype A lipopolysaccharide. *Eur.J.Biochem.* **220**:209-216.
200. **Masson, P. L., J. F. Heremans, J. J. Prignot, and G. Wauters.** 1966. Immunohistochemical localization and bacteriostatic properties of an iron-binding protein from bronchial mucus. *Thorax* **21**:538-544.
201. **Mathers, K., M. Leinonen, and D. Goldblatt.** 1999. Antibody response to outer membrane proteins of *Moraxella catarrhalis* in children with otitis media. *Pediatr.Infect.Dis.J.* **18**:982-988.
202. **Mathers, K. E., D. Goldblatt, C. Aebi, R. Yu, A. B. Schryvers, and E. J. Hansen.** 1997. Characterisation of an outer membrane protein of *Moraxella catarrhalis*. *FEMS Immunol.Med.Microbiol.* **19**:231-236.
203. **McCoy, W. F. and J. W. Costerton.** 1982. Fouling biofilm development of tubular flow systems. *Developments in Industrial Microbiology* **23**:551-558.
204. **McMichael, J. C.** 2001. Vaccines for *Moraxella catarrhalis*. *Vaccine* **19**:S101-S107.
205. **McMichael, J. C., M. J. Fiske, R. A. Fredenburg, D. N. Chakravarti, K. R. VanDerMeid, V. Barniak, J. Caplan, E. Bortell, S. Baker, R. Arumugham, and D. Chen.** 1998. Isolation and characterization of two proteins from *Moraxella catarrhalis* that bear a common epitope. *Infect.Immun.* **66**:4374-4381.

206. **McNab, R., S. K. Ford, A. El Sabaeny, B. Barbieri, G. S. Cook, and R. J. Lamont.** 2003. LuxS-based signaling in *Streptococcus gordonii*: autoinducer 2 controls carbohydrate metabolism and biofilm formation with *Porphyromonas gingivalis*. J.Bacteriol. **185**:274-284.
207. **Meier, P. S., R. Troller, I. N. Grivea, G. A. Syrogiannopoulos, and C. Aebi.** 2002. The outer membrane proteins UspA1 and UspA2 of *Moraxella catarrhalis* are highly conserved in nasopharyngeal isolates from young children. Vaccine **20**:1754-1760.
208. **Merkle, R. K. and I. Poppe.** 1994. Carbohydrate composition analysis of glycoconjugates by gas-liquid chromatography/mass spectrometry. Methods Enzymol. **230**:1-15.
209. **Merritt, J., F. Qi, S. D. Goodman, M. H. Anderson, and W. Shi.** 2003. Mutation of luxS affects biofilm formation in *Streptococcus mutans*. Infect.Immun. **71**:1972-1979.
210. **Mollenkvist, A., T. Nordstrom, C. Hallden, J. J. Christensen, A. Forsgren, and K. Riesbeck.** 2003. The *Moraxella catarrhalis* immunoglobulin D-binding protein MID has conserved sequences and is regulated by a mechanism corresponding to phase variation. J.Bacteriol. **185**:2285-2295.
211. **Molstad, S., I. Eliasson, B. Hovelius, C. Kamme, and C. Schalen.** 1988. Beta-lactamase production in the upper respiratory tract flora in relation to antibiotic consumption: a study in children attending day nurseries. Scand.J.Infect.Dis. **20**:329-334.
212. **Morgan, M. G., H. McKenzie, M. C. Enright, M. Bain, and F. X. Emmanuel.** 1992. Use of molecular methods to characterize *Moraxella catarrhalis* strains in a suspected outbreak of nosocomial infection. Eur.J.Clin.Microbiol.Infect.Dis. **11**:305-312.
213. **Murphy, S., M. Fitzgerald, R. Mulcahy, C. Keane, D. Coakley, and T. Scott.** 1997. Studies on haemagglutination and serum resistance status of strains of *Moraxella catarrhalis* isolated from the elderly. Gerontology **43**:277-282.
214. **Murphy, T. F.** 1996. *Branhamella catarrhalis* : Epidemiology, surface antigenic structure, and immune response. Microbiol.Rev. **60**:267.
215. **Murphy, T. F. and L. C. Bartos.** 1989. Surface exposed and antigenically conserved determinants of outer membrane proteins of *Branhamella catarrhalis*. Infect.Immun. **57**:2938-2941.

216. **Murphy, T. F., A. L. Brauer, N. Yuskiw, and T. J. Hiltke.** 2000. Antigenic structure of outer membrane protein E of *Moraxella catarrhalis* and construction and characterization of mutants . Infect.Immun. **68**:6250-6256.
217. **Murphy, T. F., A. L. Brauer, N. Yuskiw, E. R. McNamara, and C. Kirkham.** 2001. Conservation of outer membrane protein E among strains of *Moraxella catarrhalis*. Infect.Immun. **69**:3576-3580.
218. **Murphy, T. F. and C. Kirkham.** 2002. Biofilm formation by nontypeable *Haemophilus influenzae*: strain variability, outer membrane antigen expression and role of pili. BMC.Microbiol **2**:7.
219. **Murphy, T. F., C. Kirkham, and A. J. Lesse.** 1993. The major heat-modifiable outer membrane protein CD is highly conserved among strains of *Branhamella catarrhalis*. Mol.Microbiol. **10**:87-97.
220. **Murphy, T. F., J. M. Kyd, A. John, C. Kirkham, and A. W. Cripps.** 1998. Enhancement of pulmonary clearance of *Moraxella (Branhamella) catarrhalis* following immunization with outer membrane protein CD in a mouse model. J.Infect.Dis. **178**:1667-1675.
221. **Murphy, T. F. and M. R. Loeb.** 1989. Isolation of the outer membrane of *Branhamella catarrhalis*. Microb.Pathog. **6**:159-174.
222. **Myers, L. E., Y.-P. Yang, R. P. Du, Q. J. Wang, R. E. Harkness, A. B. Schryvers, M. H. Klein, and S. M. Loosmore.** 1998. The transferrin binding protein B of *Moraxella catarrhalis* elicits bactericidal antibodies and is a potential vaccine antigen. Infect.Immun. **66**:4183-4192.
223. **Nair, J., D. A. Rouse, G. H. Bai, and S. L. Morris.** 1993. The *rpsL* gene and streptomycin resistance in single and multiple drug-resistant strains of *Mycobacterium tuberculosis*. Mol.Microbiol **10**:521-527.
224. **Neumayer, U., H. K. Schmidt, K. P. Mellwig, and G. Kleikamp.** 1999. *Moraxella catarrhalis* endocarditis: report of a case and literature review. J.Heart Valve Dis. **8**:114-117.
225. **Nickel, J. C., I. Ruseska, J. B. Wright, and J. W. Costerton.** 1985. Tobramycin resistance of *Pseudomonas aeruginosa* cells growing as a biofilm on urinary catheter material. Antimicrob.Agents Chemother. **27**:619-624.
226. **Nordstrom, T., A. Forsgren, and K. Riesbeck.** 2002. The immunoglobulin D-binding part of the outer membrane protein MID from *Moraxella catarrhalis* comprises 238 amino acids and a tetrameric structure. J.Biol.Chem. **277**:34692-34699.

227. **O'Toole, G., H. B. Kaplan, and R. Kolter.** 2000. Biofilm formation as microbial development. *Annu.Rev.Microbiol.* **54**:49-79.
228. **O'toole, G. A. and R. Kolter.** 1998. Flagellar and twitching motility are necessary for *Pseudomonas aeruginosa* biofilm development. *Mol.Microbiol.* **30**:295-304.
229. **O'toole, G. A. and R. Kolter.** 1998. Initiation of biofilm formation in *Pseudomonas fluorescens* WCS365 proceeds via multiple, convergent signalling pathways: a genetic analysis. *Mol.Microbiol* **28**:449-461.
230. **Oishi, K., H. Tanaka, F. Sonoda, S. Borann, K. Ahmed, Y. Utsunomiya, K. Watanabe, T. Nagatake, M. Vaneechoutte, G. Verschraegen, and K. Matsumoto.** 1996. A monoclonal antibody reactive with a common epitope of *Moraxella (Branhamella) catarrhalis* lipopolysaccharides. *Clin.Diagn.Lab Immunol.* **3**:351-354.
231. **Onofrio, J. M., A. N. Shulkin, P. J. Heidbrink, G. B. Toews, and A. K. Pierce.** 1981. Pulmonary clearance and phagocytic cell response to normal pharyngeal flora. *Am.Rev.Respir.Dis.* **123**:222-225.
232. **Paju, S., F. Goulhen, S. Asikainen, D. Grenier, D. Mayrand, and V. Uitto.** 2000. Localization of heat shock proteins in clinical *Actinobacillus actinomycetemcomitans* strains and their effects on epithelial cell proliferation. *FEMS Microbiol.Lett.* **182**:231-235.
233. **Park, J. T.** 1996. The murein sacculus, p. 48-57. *In* F. C. Neidhardt (ed.), *Escherichia coli* and *Salmonella*: Cellular and Molecular Biology. ASM Press, Washington, D.C.
234. **Patterson, T. F., J. E. Patterson, B. Z. Masecar, G. E. Barden, W. J. Heirholzer, Jr., and M. J. Zervos.** 1988. A nosocomial outbreak of *Branhamella catarrhalis* confirmed by restriction endonuclease analysis. *J.Infect.Dis.* **157**:996-1001.
235. **Pearson, M. M., E. R. Lafontaine, N. J. Wagner, J. W. St.Geme, III, and E. J. Hansen.** 2002. A *hag* mutant of *Moraxella catarrhalis* strain O35E is deficient in hemagglutination, autoagglutination, and immunoglobulin D-binding activities. *Infect.Immun.* **70**:4523-4533.
236. **Pelton, S. I.** 2003. Otitis media, p. 190-198. *In* S. S. Long, L. K. Pickering, and C. G. Prober (eds.), *Principles and Practice of Pediatric Infectious Diseases*. Churchill Livingstone, Philadelphia.
237. **Pettersson, A., A. Maas, D. van Wassenaar, P. van der Ley, and J. Tommassen.** 1995. Molecular cloning of FrpB, the 70-kilodalton iron-regulated outer membrane protein of *Neisseria meningitidis*. *Infect.Immun.* **63**:4181-4184.

238. **Pettersson, B., A. Kodjo, M. Ronaghi, M. Uhlen, and T. Tonjum.** 1998. Phylogeny of the family Moraxellaceae by 16S rDNA sequence analysis, with special emphasis on differentiation of *Moraxella* species. *Int.J.Syst.Bacteriol.* **48 Pt 1**:75-89.
239. **Pilz, D., T. Vocke, J. Heesemann, and V. Brade.** 1992. Mechanism of YadA-mediated serum resistance of *Yersinia enterocolitica* serotype O3. *Infect.Immun.* **60**:189-195.
240. **Post, J. C., R. A. Preston, J. J. Aul, M. Larkins-Pettigrew, J. Rydquist-White, K. W. Anderson, R. M. Wadowsky, D. R. Reagan, E. S. Walker, L. A. Kingsley, A. E. Magit, and G. D. Ehrlich.** 1995. Molecular analysis of bacterial pathogens in otitis media with effusion. *JAMA* **273**:1598-1604.
241. **Prasadaraao, N. V., A. M. Blom, B. O. Villoutreix, and L. C. Linsangan.** 2002. A novel interaction of outer membrane protein A with C4b binding protein mediates serum resistance of *Escherichia coli* K1. *J.Immunol.* **169**:6352-6360.
242. **Pratt, L. A. and R. Kolter.** 1998. Genetic analysis of *Escherichia coli* biofilm formation: roles of flagella, motility, chemotaxis and type I pili. *Mol.Microbiol* **30**:285-293.
243. **Pratten, J. and M. Wilson.** 1999. Antimicrobial susceptibility and composition of microcosm dental plaques supplemented with sucrose. *Antimicrob.Agents Chemother.* **43**:1595-1599.
244. **Pratten, J., M. Wilson, and D. A. Spratt.** 2003. Characterization of in vitro oral bacterial biofilms by traditional and molecular methods. *Oral Microbiol.Immunol.* **18**:45-49.
245. **Prigent-Combaret, C., G. Prensier, T. T. Le Thi, O. Vidal, P. Lejeune, and C. Dorel.** 2000. Developmental pathway for biofilm formation in curli-producing *Escherichia coli* strains: role of flagella, curli and colanic acid. *Environ.Microbiol.* **2**:450-464.
246. **Prigent-Combaret, C., O. Vidal, C. Dorel, and P. Lejeune.** 1999. Abiotic surface sensing and biofilm-dependent regulation of gene expression in *Escherichia coli*. *J.Bacteriol.* **181**:5993-6002.
247. **Prosser, B. L., D. Taylor, B. A. Dix, and R. Cleeland.** 1987. Method of evaluating effects of antibiotics on bacterial biofilm. *Antimicrob.Agents Chemother.* **31**:1502-1506.
248. **Prouty, A. M., W. H. Schwesinger, and J. S. Gunn.** 2002. Biofilm formation and interaction with the surfaces of gallstones by *Salmonella* spp. *Infect.Immun.* **70**:2640-2649.

249. **Raad, I., W. Costerton, U. Sabharwal, M. Sacilowski, E. Anaissie, and G. P. Bodey.** 1993. Ultrastructural analysis of indwelling vascular catheters: a quantitative relationship between luminal colonization and duration of placement. *J.Infect.Dis.* **168**:400-407.
250. **Rahman, M. and T. Holme.** 1996. Antibody response in rabbits to serotype-specific determinants in lipopolysaccharides from *Moraxella catarrhalis*. *J.Med.Microbiol.* **44**:348-354.
251. **Rahman, M., T. Holme, I. Jonsson, and A. Krook.** 1995. Lack of serotype-specific antibody response to lipopolysaccharide antigens of *Moraxella catarrhalis* during lower respiratory tract infection. *Eur.J.Clin.Microbiol.Infect.Dis.* **14**:297-304.
252. **Ramaswamy, S., M. Dworkin, and J. Downard.** 1997. Identification and characterization of *Myxococcus xanthus* mutants deficient in calcofluor white binding. *J.Bacteriol.* **179**:2863-2871.
253. **Ratledge, C. and L. G. Dover.** 2000. Iron metabolism in pathogenic bacteria. *Annu.Rev.Microbiol* **54**:881-941.
254. **Rayner, M. G., Y. Zhang, M. C. Gorry, Y. Chen, J. C. Post, and G. D. Ehrlich.** 1998. Evidence of bacterial metabolic activity in culture-negative otitis media with effusion. *JAMA* **279**:296-299.
255. **Reddy, M. S., T. F. Murphy, H. S. Faden, and J. M. Bernstein.** 1997. Middle ear mucin glycoprotein; purification and interaction with nontypeable *Haemophilus influenzae* and *Moraxella catarrhalis*. *Otolaryngol.Head Neck Surg.* **116**:175-180.
256. **Reisner, A., J. A. Haagenzen, M. A. Schembri, E. L. Zechner, and S. Molin.** 2003. Development and maturation of *Escherichia coli* K-12 biofilms. *Mol.Microbiol.* **48**:933-946.
257. **Retzer, M. D., R. H. Yu, and A. B. Schryvers.** 1999. Identification of sequences in human transferrin that bind to the bacterial receptor protein, transferrin-binding protein B. *Mol.Microbiol.* **32**:111-121.
258. **Richards, S. J., A. P. Greening, M. C. Enright, M. G. Morgan, and H. McKenzie.** 1993. Outbreak of *Moraxella catarrhalis* in a respiratory unit. *Thorax* **48**:91-92.
259. **Riedel, K., M. Hentzer, O. Geisenberger, B. Huber, A. Steidle, H. Wu, N. Hoiby, M. Givskov, S. Molin, and L. Eberl.** 2001. N-acylhomoserine-lactone-mediated communication between *Pseudomonas aeruginosa* and *Burkholderia cepacia* in mixed biofilms. *Microbiology* **147**:3249-3262.

260. **Rikitomi, N., B. Andersson, K. Matsumoto, R. Lindstedt, and C. Svanborg.** 1991. Mechanism of adherence of *Moraxella (Branhamella) catarrhalis*. *Scand.J.Infect.Dis.* **23**:559-567.
261. **Roychoudhury, S., N. A. Zielinski, J. D. DeVault, J. Kato, D. L. Shinabarger, T. B. May, R. Maharaj, K. Kimbara, T. K. Misra, and A. M. Chakrabarty.** 1991. *Pseudomonas aeruginosa* infection in cystic fibrosis: biosynthesis of alginate as a virulence factor. *Antibiot.Chemother.* **44**:63-67.
262. **Sambrook, J., E. F. Fritsch, and T. Maniatis.** 1989. Molecular cloning - a laboratory manual, 2nd Edition. Cold Spring Harbor Laboratory Press, Cold Spring Harbor, N.Y.
263. **Sarwar, J., A. A. Campagnari, C. Kirkham, and T. F. Murphy.** 1992. Characterization of a antigenically conserved heat-modifiable major outer membrane protein of *Branhamella catarrhalis*. *Infect.Immun.* **60**:804-809.
264. **Sasaki, K., R. E. Harkness, and M. H. Klein.** 1998. Nucleic acids encoding high molecular weight major outer membrane protein of *Moraxella*. U.S.Patent Publication **5808024**.
265. **Sasaki, K., L. Myers, S. M. Loosmore, and M. H. Klein.** 1999. Control mechanism of the 200 kD protein gene expression in *Moraxella (Branhamella) catarrhalis*. Abstracts of the 99th general meeting of the American Society for Microbiology **B/D-306**:89.
266. **Sauer, K., A. K. Camper, G. D. Ehrlich, J. W. Costerton, and D. G. Davies.** 2002. *Pseudomonas aeruginosa* displays multiple phenotypes during development as a biofilm. *J.Bacteriol.* **184**:1140-1154.
267. **Schalen, L., P. Christensen, I. Eliasson, S. Fex, C. Kamme, and C. Schalen.** 1985. Inefficacy of penicillin V in acute laryngitis in adults. Evaluation from results of double-blind study. *Ann.Otol.Rhinol.Laryngol.* **94**:14-17.
268. **Schalen, L., P. Christensen, C. Kamme, H. Miorner, K. I. Pettersson, and C. Schalen.** 1980. High isolation rate of *Branhamella catarrhalis* from the nasopharynx in adults with acute laryngitis. *Scand.J.Infect.Dis.* **12**:277-280.
269. **Schembri, M. A., G. Christiansen, and P. Klemm.** 2001. FimH-mediated autoaggregation of *Escherichia coli*. *Mol.Microbiol.* **41**:1419-1430.
270. **Schembri, M. A., D. Dalsgaard, and P. Klemm.** 2004. Capsule shields the function of short bacterial adhesins. *J.Bacteriol.* **186**:1249-1257.

271. **Scheuerpflug, I., T. Rudel, R. Ryll, J. Pandit, and T. F. Meyer.** 1999. Roles of PilC and PilE proteins in pilus-mediated adherence of *Neisseria gonorrhoeae* and *Neisseria meningitidis* to human erythrocytes and endothelial and epithelial cells. *Infect.Immun.* **67**:834-843.
272. **Schryvers, A. B. and B. C. Lee.** 1989. Comparative analysis of the transferrin and lactoferrin binding proteins in the family *Neisseriaceae*. *Can.J.Microbiol.* **35**:409-415.
273. **Sethi, S., S. L. Hill, and T. F. Murphy.** 1995. Serum antibodies to outer membrane proteins (OMPs) of *Moraxella (Branhamella) catarrhalis* in patients with bronchiectasis: Identification of OMP B1 as an important antigen. *Infect.Immun.* **63**:1516-1520.
274. **Sethi, S. and T. F. Murphy.** 2001. Bacterial infection in chronic obstructive pulmonary disease in 2000: a state-of-the-art review. *Clin.Microbiol Rev.* **14**:336-363.
275. **Sethi, S., J. M. Surface, and T. F. Murphy.** 1997. Antigenic heterogeneity and molecular analysis of CopB of *Moraxella (Branhamella) catarrhalis*. *Infect.Immun.* **65**:3666-3671.
276. **Shurin, P. A.** 1986. General discussion: Section 1. *Drugs* **31**:38-39.
277. **Shurin, P. A., S. I. Pelton, A. Donner, and J. O. Klein.** 1979. Persistence of middle-ear effusion after acute otitis media in children. *N.Engl.J.Med.* **300**:1121-1123.
278. **Sims, K. L. and A. B. Schryvers.** 2003. Peptide-peptide interactions between human transferrin and transferrin-binding protein B from *Moraxella catarrhalis*. *J.Bacteriol.* **185**:2603-2610.
279. **Singh, P. K., A. L. Schaefer, M. R. Parsek, T. O. Moninger, M. J. Welsh, and E. P. Greenberg.** 2000. Quorum-sensing signals indicate that cystic fibrosis lungs are infected with bacterial biofilms. *Nature* **407**:762-764.
280. **Skurnik, M., I. Bolin, H. Heikkinen, S. Piha, and H. Wolf-Watz.** 1984. Virulence plasmid-associated agglutination in *Yersinia* spp. *J.Bacteriol.* **158**:1033-1036.
281. **Slot, J. W. and H. J. Geuze.** 1998. Localization of macromolecular components by application of the immunogold technique on cryosectioned bacteria. *Methods Microbiol* **20**:211-236.

282. **Slot, J. W., H. J. Geuze, S. Gigengack, G. E. Lienhard, and D. E. James.** 1991. Immuno-localization of the insulin regulatable glucose transporter in brown adipose tissue of the rat. *J.Cell Biol.* **113**:123-135.
283. **Solano, C., B. Garcia, J. Valle, C. Berasain, J. M. Ghigo, C. Gamazo, and I. Lasa.** 2002. Genetic analysis of *Salmonella enteritidis* biofilm formation: critical role of cellulose. *Mol.Microbiol* **43**:793-808.
284. **Sorensen, C. H. and P. L. Larsen.** 1988. IgD in nasopharyngeal secretions and tonsils from otitis-prone children. *Clin.Exp.Immunol.* **73**:149-154.
285. **Soto-Hernandez, J. L., S. Holtsclaw-Berk, L. M. Harvill, and S. L. Berk.** 1989. Phenotypic characteristics of *Branhamella catarrhalis* strains. *J.Clin.Microbiol.* **27**:903-908.
286. **Spiers, A. J., J. Bohannon, S. M. Gehrig, and P. B. Rainey.** 2003. Biofilm formation at the air-liquid interface by the *Pseudomonas fluorescens* SBW25 wrinkly spreader requires an acetylated form of cellulose. *Mol.Microbiol* **50**:15-27.
287. **St.Geme, J. W., III and D. Cutter.** 1995. Evidence that surface fibrils expressed by *Haemophilus influenzae* type b promote attachment to human epithelial cells. *Mol.Microbiol.* **15**:77-85.
288. **St.Geme, J. W., III and D. Cutter.** 2000. The *Haemophilus influenzae* Hia adhesin is an autotransporter protein that remains uncleaved at the C terminus and fully cell associated. *J.Bacteriol.* **182**:6005-6013.
289. **St.Geme, J. W., III, D. Cutter, and S. J. Barenkamp.** 1996. Characterization of the genetic locus encoding *Haemophilus influenzae* type b surface fibrils. *J.Bacteriol.* **178**:6281-6287.
290. **Steeghs, L., R. den Hartog, A. den Boer, B. Zomer, P. Roholl, and P. van der Ley.** 1998. Meningitis bacterium is viable without endotoxin. *Nature* **392**:449-450.
291. **Stefanou, J., A. V. Agelopoulou, N. V. Sipsas, N. Smilakou, and A. Avlami.** 2000. *Moraxella catarrhalis* endocarditis: case report and review of the literature. *Scand.J.Infect.Dis.* **32**:217-218.
292. **Stepanovic, S., D. Vukovic, I. Dakic, B. Savic, and M. Svabic-Vlahovic.** 2000. A modified microtiter-plate test for quantification of staphylococcal biofilm formation. *J.Microbiol.Methods* **40**:175-179.
293. **Stoodley, P., D. deBeer, and H. M. Lappin-Scott.** 1997. Influence of electric fields and pH on biofilm structure as related to the bioelectric effect. *Antimicrob.Agents Chemother.* **41**:1876-1879.

294. **Stoodley, P., K. Sauer, D. G. Davies, and J. W. Costerton.** 2002. Biofilms as complex differentiated communities. *Annu.Rev.Microbiol.* **56**:187-209.
295. **Strom, M. S. and S. Lory.** 1993. Structure-function and biogenesis of the type IV pili. *Annu.Rev.Microbiol.* **47**:565-596.
296. **Surette, M. G. and B. L. Bassler.** 1998. Quorum sensing in *Escherichia coli* and *Salmonella typhimurium*. *Proc.Natl.Acad.Sci.USA* **95**:7046-7050.
297. **Suzuki, K. and L. O. Bakaletz.** 1994. Synergistic effect of adenovirus type 1 and nontypeable *Haemophilus influenzae* in a chinchilla model of experimental otitis media. *Infect.Immun.* **62**:1710-1718.
298. **Swords, W. E., M. L. Moore, L. Godzicki, G. Bukofzer, M. J. Mitten, and J. VonCannon.** 2004. Sialylation of lipooligosaccharides promotes biofilm formation by nontypeable *Haemophilus influenzae*. *Infect.Immun.* **72**:106-113.
299. **Tang, S. W., S. Abubakar, S. Devi, S. Puthucherry, and T. Pang.** 1997. Induction and characterization of heat shock proteins of *Salmonella typhi* and their reactivity with sera from patients with typhoid fever. *Infect.Immun.* **65**:2983-2986.
300. **Timpe, J. M., M. M. Holm, S. L. Vanlerberg, V. Basrur, and E. R. Lafontaine.** 2003. Identification of a *Moraxella catarrhalis* outer membrane protein exhibiting both adhesin and lipolytic activities. *Infect.Immun.* **71**:4341-4350.
301. **Tokuyasu, K. T.** 1980. Immunocytochemistry on ultrathin frozen sections. *Histochem.J.* **12**:381-403.
302. **Tomlin, K. L., O. P. Coll, and H. Ceri.** 2001. Interspecies biofilms of *Pseudomonas aeruginosa* and *Burkholderia cepacia*. *Can.J.Microbiol.* **47**:949-954.
303. **Torok, Z., I. Horvath, P. Goloubinoff, E. Kovacs, A. Glatz, G. Balogh, and L. Vigh.** 1997. Evidence for a lipochaperonin: association of active protein-folding GroESL oligomers with lipids can stabilize membranes under heat shock conditions. *Proc.Natl.Acad.Sci.U.S.A* **94**:2192-2197.
304. **Torres, A. G., N. T. Perna, V. Burland, A. Ruknudin, F. R. Blattner, and J. B. Kaper.** 2002. Characterization of Cah, a calcium-binding and heat-extractable autotransporter protein of enterohaemorrhagic *Escherichia coli*. *Mol.Microbiol* **45**:951-966.
305. **Tsai, C.-M. and C. E. Frasch.** 1982. A sensitive silver stain for detecting lipopolysaccharide in polyacrylamide gels. *Anal.Biochem.* **119**:115-119.

306. **Turner, H. R., M. R. Taylor, and W. R. Lockwood.** 1985. *Branhamella catarrhalis* endocarditis in a patient receiving hemodialysis. *South.Med.J.* **78**:1021-1022.
307. **Unhanand, M., I. Maciver, O. Ramilo, O. Arencibia-Mireles, J. C. Argyle, G. H. McCracken, Jr., and E. H. Hansen.** 1992. Pulmonary clearance of *Moraxella catarrhalis* in an animal model. *J.Infect.Dis.* **165**:644-650.
308. **Van Belkum, A., s. Scherer, L. van Alphen, and H. Verbrugh.** 1998. Short-sequence DNA repeats in prokaryotic genomes. *Microbiol.Mol.Biol.Rev.* **62**:275-293.
309. **VandeWoude, S. J. and M. B. Luzarraga.** 1991. The role of *Branhamella catarrhalis* in the "bloody-nose syndrome" of cynomolgus macaques. *Lab Anim Sci.* **41**:401-406.
310. **Vaneechoutte, M., G. Verschraegen, G. Claeys, and A. M. van den Abeele.** 1990. Respiratory tract carrier rates of *Moraxella (Branhamella catarrhalis)* in adults and children and interpretation of the isolation of *M. catarrhalis* from sputum. *J.Clin.Microbiol.* **28**:2674-2680.
311. **Vaneechoutte, M., G. Verschraegen, G. Claeys, and A. M. van den Abeele.** 1990. Serological typing of *Branhamella catarrhalis* strains on the basis of lipopolysaccharide antigens. *J.Clin.Microbiol.* **28**:182-187.
312. **Varon, E., C. Levy, R. F. De La, M. Boucherat, D. Deforche, I. Podglajen, M. Navel, and R. Cohen.** 2000. Impact of antimicrobial therapy on nasopharyngeal carriage of *Streptococcus pneumoniae*, *Haemophilus influenzae*, and *Branhamella catarrhalis* in children with respiratory tract infections. *Clin.Infect.Dis.* **31**:477-481.
313. **Verduin, C. M., C. Hol, A. FLeer, H. van Dijk, and A. Van Belkum.** 2002. *Moraxella catarrhalis*: from emerging to established pathogen. *Clin.Microbiol.Rev.* **15**:125-144.
314. **Verduin, C. M., M. Kools-Sijmons, P. J. van der, J. Vlooswijk, M. Tromp, H. van Dijk, J. Banks, H. Verbrugh, and A. Van Belkum.** 2000. Complement-resistant *Moraxella catarrhalis* forms a genetically distinct lineage within the species. *FEMS Microbiol.Lett.* **184**:1-8.
315. **Vergheze, A., E. Berro, J. Berro, and B. W. Franzus.** 1990. Pulmonary clearance and phagocytic cell response in a murine model of *Branhamella catarrhalis* infection. *J.Infect.Dis.* **162**:1189-1192.
316. **Virji, M., D. Evans, A. Hadfield, F. Grunert, A. M. Teixeira, and S. M. Watt.** 1999. Critical determinants of host receptor targeting by *Neisseria meningitidis* and *Neisseria gonorrhoeae*: identification of Opa adhesiotopes on the N-domain of CD66 molecules. *Mol.Microbiol.* **34**:538-551.

317. **Vu-Thien, H., C. Dulot, D. Moissenet, and B. Fauroux.** 1999. Comparison of randomly amplified polymorphic DNA analysis and pulsed-field gel electrophoresis for typing of *Moraxella catarrhalis* strains. *J.Clin.Microbiol.* **37**:450-452.
318. **Vuong, C., H. L. Saenz, F. Gotz, and M. Otto.** 2000. Impact of the agr quorum-sensing system on adherence to polystyrene in *Staphylococcus aureus*. *J.Infect.Dis.* **182**:1688-1693.
319. **Waite, R. D., J. K. Struthers, and C. G. Dowson.** 2001. Spontaneous sequence duplication within an open reading frame of the pneumococcal type 3 capsule locus causes high-frequency phase variation. *Mol.Microbiol.* **42**:1223-1232.
320. **Wald, E. R.** 1998. Sinusitis. *Pediatr.Ann.* **27**:811-818.
321. **Walker, E. S., R. A. Preston, J. C. Post, G. D. Ehrlich, J. H. Kalbflesch, and K. L. Klingman.** 1998. Genetic diversity among strains of *Moraxella catarrhalis* : Analysis using multiple DNA probes and a single-locus PCR-restriction fragment length polymorphism method. *J.Clin.Microbiol.* **36**:1977-1983.
322. **Warne, S. R., J. M. Varley, G. J. Boulnois, and M. G. Norton.** 1990. Identification and characterization of a gene that controls colony morphology and auto-aggregation in *Escherichia coli* K12. *J.Gen.Microbiol* **136 (Pt 3)**:455-462.
323. **Watnick, P. and R. Kolter.** 2000. Biofilm, city of microbes. *J.Bacteriol.* **182**:2675-2679.
324. **Watnick, P. I., K. J. Fullner, and R. Kolter.** 1999. A role for the mannose-sensitive hemagglutinin in biofilm formation by *Vibrio cholerae* El Tor. *J.Bacteriol.* **181**:3606-3609.
325. **Watnick, P. I. and R. Kolter.** 1999. Steps in the development of a *Vibrio cholerae* El Tor biofilm. *Mol.Microbiol.* **34**:586-595.
326. **Weinberg, E. D.** 1978. Iron and infection. *Microbiol.Rev.* **42**:45-66.
327. **Westman, E., A. Melhus, S. Hellstrom, and A. Hermansson.** 1999. *Moraxella catarrhalis*-induced purulent otitis media in the rat middle ear. Structure, protection, and serum antibodies. *APMIS* **107**:737-746.
328. **Whipple, G. C.** 1901. Changes that take place in the bacterial contents of waters during transportation. *Technical Quarterly* **14**:21.
329. **Whitby, P. W., D. J. Morton, and T. L. Stull.** 1998. Construction of antibiotic resistance cassettes with multiple paired restriction sites for insertional mutagenesis of *Haemophilus influenzae*. *FEMS Microbiol.Lett.* **158**:57-60.

330. **Whitchurch, C. B., T. Tolker-Nielsen, P. C. Ragas, and J. S. Mattick.** 2002. Extracellular DNA required for bacterial biofilm formation. *Science* **295**:1487.
331. **Whiteley, M., M. G. Banger, R. E. Bumgarner, M. R. Parsek, G. M. Teitzel, S. Lory, and E. P. Greenberg.** 2001. Gene expression in *Pseudomonas aeruginosa* biofilms. *Nature* **413**:860-864.
332. **Wingren, A. G., R. Hadzic, A. Forsgren, and K. Riesbeck.** 2002. The novel IgD binding protein from *Moraxella catarrhalis* induces human B lymphocyte activation and Ig secretion in the presence of Th2 cytokines. *J.Immunol.* **168**:5582-5588.
333. **Winzer, K., K. R. Hardie, N. Burgess, N. Doherty, D. Kirke, M. T. Holden, R. Linforth, K. A. Cornell, A. J. Taylor, P. J. Hill, and P. Williams.** 2002. LuxS: its role in central metabolism and the in vitro synthesis of 4-hydroxy-5-methyl-3(2H)-furanone. *Microbiology* **148**:909-922.
334. **Wistreich, G. A. and R. F. Baker.** 1971. The presence of fimbriae (pili) in three species of *Neisseria*. *J.Gen.Microbiol.* **65**:167-173.
335. **Wong, H. and A. B. Schryvers.** 2003. Bacterial lactoferrin-binding protein A binds to both domains of the human lactoferrin C-lobe. *Microbiology* **149**:1729-1737.
336. **Yang, Y.-P., L. E. Myers, U. McGuinness, P. Chong, Y. Kwok, M. H. Klein, and R. E. Harkness.** 1997. The major outer membrane protein, CD, extracted from *Moraxella (Branhamella) catarrhalis* is a potential vaccine antigen that induces bactericidal antibodies. *FEMS Immunol.Med.Microbiol.* **17**:187-199.
337. **York, W. S., A. G. Darvill, M. McNeil, T. T. Stevenson, and P. Albersheim.** 1985. Isolation and characterization of plant cell walls and cell-wall components. *Methods Enzymol.* **118**:3-40.
338. **Yoshimura, F., L. S. Zalman, and H. Nikaido.** 1983. Purification and properties of *Pseudomonas aeruginosa* porin. *J.Biol.Chem.* **258**:2308-2314.
339. **Yu, R. H., R. A. Bonnah, S. Ainsworth, and A. B. Schryvers.** 1999. Analysis of the immunological responses to transferrin and lactoferrin receptor proteins from *Moraxella catarrhalis*. *Infect.Immun.* **67**:3793-3799.
340. **Yu, R.-H. and A. B. Schryvers.** 1993. Regions located in both the N-lobe and C-lobe of human lactoferrin participate in the binding interaction with bacterial lactoferrin receptors. *Microb.Pathog.* **14**:343-353.
341. **Yu, R.-H. and A. B. Schryvers.** 1993. The interaction between human transferrin and transferrin binding protein 2 from *Moraxella (Branhamella) catarrhalis* differs from that of other human pathogens. *Microb.Pathog.* **15**:433-445.

342. **Zaleski, A., N. K. Scheffler, P. Densen, F. K. Lee, A. A. Campagnari, B. W. Gibson, and M. A. Apicella.** 2000. Lipooligosaccharide P(k) (Gal α 1-4Gal β 1-4Glc) epitope of *Moraxella catarrhalis* is a factor in resistance to bactericidal activity mediated by normal human serum . *Infect.Immun.* **68**:5261-5268.
343. **Zeilstra-Ryalls, J., O. Fayet, and C. Georgopoulos.** 1991. The universally conserved GroE (Hsp60) chaperonins. *Annu.Rev.Microbiol.* **45**:301-325.
344. **ZoBell, C. E.** 1943. The effect of solid surfaces upon bacterial activity. *J.Bacteriol.* **46**:39-56.
345. **ZoBell, C. E. and D. Q. Anderson.** 1936. Observations on the multiplication of bacteria in different volumes of stored sea water and the influence of oxygen tension and solid surfaces. *Biol.Bull.* **71**:324-342.
346. **Zogaj, X., M. Nimtz, M. Rohde, W. Bokranz, and U. Romling.** 2001. The multicellular morphotypes of *Salmonella typhimurium* and *Escherichia coli* produce cellulose as the second component of the extracellular matrix. *Mol.Microbiol* **39**:1452-1463.

VITA

Melanie Michelle Pearson was born on August 8, 1975 in Rockford, Illinois, the daughter of Mary Kathryn Davis Pearson and Roy Levan Pearson. After alternately living in Missouri and Michigan, she graduated from Sturgis High School in Sturgis, Michigan in 1993 and began study at Western Michigan University in Kalamazoo, Michigan. In 1995, she spent a semester at Sunway College in Petaling Jaya, Malaysia. She received her Bachelor of Science degree in biomedical sciences *magna cum laude* from Western Michigan University in 1997. Since 1998 she has been enrolled at the University of Texas Southwestern Medical Center. She currently lives in Dallas, Texas with her “significant other”, Daniel Naruta.

Permanent address: 5225 Fleetwood Oaks Ave. Apt 426
Dallas, Texas 75235